Missouri S&T Library and Learning Resources

Scholars' Mine

Doctoral Dissertations | Student Theses and Dissertations

1966

# Turbulence measurements in polymer solutions using hot-film anemometry

Gary Kent Patterson
*Missouri University of Science and Technology*

Follow this and additional works at: https://scholarsmine.mst.edu/doctoral_dissertations

 Part of the Chemical Engineering Commons

Department: Chemical and Biochemical Engineering

## Recommended Citation

Patterson, Gary Kent, "Turbulence measurements in polymer solutions using hot-film anemometry" (1966). *Doctoral Dissertations*. 459.
https://scholarsmine.mst.edu/doctoral_dissertations/459

This thesis is brought to you by Scholars' Mine, a service of the Missouri S&T Library and Learning Resources. This work is protected by U. S. Copyright Law. Unauthorized use including reproduction for redistribution requires the permission of the copyright holder. For more information, please contact scholarsmine@mst.edu.

# TURBULENCE MEASUREMENTS IN POLYMER SOLUTIONS USING HOT-FILM ANEMOMETRY

BY

GARY KENT PATTERSON

---

A

DISSERTATION

submitted to the faculty of the

UNIVERSITY OF MISSOURI AT ROLLA

in partial fulfillment of the work required for the

Degree of

Doctor of Philosophy

Rolla, Missouri

January, 1966

THE UNIVERSITY OF MISSOURI AT ROLLA

GRADUATE SCHOOL

Graduate Form Ph.D. IV
(Final Ph.D. Thesis Examination)

The Final Ph.D. Thesis Examination of Gary Kent Patterson

candidate for the degree of Doctor of Philosophy in

Chemical Engineering

has been conducted in accordance with the regulations of the Graduate School. The undersigned, appointed to conduct this examination, agree that the candidate has successfully passed this examination.

Respectfully submitted,

Jacques L. Zakin (Chairman)

Frank H. Conrad

W. J. James

Ralph E. Lee

D. T. Miller

M. R. Strunk

Noted:

Wouter Bosch

Wouter Bosch, ~~EXECUTIVE~~ Dean
Graduate School

Date: 24 January 1966

ABSTRACT

Hot-film anemometry was used to study the detailed structure of turbulence (intensities, energy spectra, and auto-correlations) in Newtonian solvents, non-drag reducing polymer solutions, and drag reducing polymer solutions. This was done in two smooth wall tubes with diameters of 1.0 inch and 2.0 inches. A probe traversing mechanism was used for measurements at radial positions from the center to as near the wall as possible for both the film probes ($r/a=0.85$ in the 2-inch tube) and the impact tubes ($r/a=0.98$). The impact tubes were used to measure velocities for film probe calibration.

The solvents used in this investigation were toluene, cyclohexane, and benzene. Three concentrations of a medium molecular weight polyisobutylene (Vistanex L-80, molecular weight about 720,000) in cyclohexane, two concentrations of the same polymer in benzene, two concentrations of a high molecular weight polymethyl methacrylate (Plexiglas, molecular weight about 1,500,000) in toluene, one concentration of a low molecular weight polymethyl methacrylate (V-100 molding powder, molecular weight about 110,000) in toluene, three concentrations of a high molecular weight polyisobutylene (Vistanex L-200, molecular weight about 4,700,000) in toluene, and one concentration of the same polymer in cyclohexane were used.

In the liquids not showing drag reduction a viscous and/or elastic effect was found for both turbulence intensities and energy spectra. Turbulence intensities were higher and energy spectrum

frequencies were lower for the polymer solutions of high viscosity. Unfortunately the most viscous solutions were also elastic, so purely viscous liquid studies will be necessary to distinguish between elastic and viscous effects.

During drag reduction it was found that the energy spectra changed little from purely viscous solvents. The turbulence intensities, however, showed very unusual effects. The intensities relative to friction velocity increased at low drag ratio values (high drag reduction), rather than remain constant as expected from mixing length considerations. This behavior was dependent upon the degree of mechanical polymer degradation, lower intensities occurring for fresh than for degraded solutions during drag reduction.

Normal stress differences ($P_{11} - P_{22}$) were measured for two of the solutions used in this investigation, one showing drag reduction at attainable flow rates in the 1-inch tube, the other showing drag reduction only in 0.5-inch and smaller tubes. Both solutions yielded normal stress differences of about the same level.

A quantitative viscoelastic mechanism of drag reduction was tested using the viscosity and normal stress data for the two solutions discussed above. The drag reduction mechanism demonstrated the relative effects of elasticity and viscosity on drag reduction. The adequate prediction of drag ratios for two solutions at two flow rates in each of two tube sizes demonstrated the validity of the mechanism and the reasonableness of the assumptions made.

TABLE OF CONTENTS

# LIST OF FIGURES

Page

Page

Page

Page

# LIST OF TABLES

# SUMMARY

The turbulent flow velocity profiles and friction factors in pipes for Newtonian and non-Newtonian purely viscous fluids have been well characterized using pressure drop and impact tube measurements. Completely general phenomenological relationships have not yet been developed, but the velocity profiles and pressure drops of these fluids in pipe flow can be predicted with little error.

This cannot be said for the polymer solutions which exhibit drag reduction in turbulent flow. The mechanism of drag reduction has not been adequately defined to permit predictions of turbulent pressure drop from measureable solution properties. The phenomenon has also presented great experimental difficulty because of its gradual disappearance while the solution is being pumped. Reliable velocity profiles have not been measured, because impact tube data are biased and yield low flow rates when integrated over the pipe area.

In this investigation hot film anemometry was used to study the detailed structure of turbulence (intensities, energy spectra, and autocorrelations) in Newtonian solvents, non-drag reducing polymer solutions, and drag reducing polymer solutions. This was done in two smooth wall tubes with diameters of 1.0 inch and 2.0 inches. A probe traversing mechanism was used for measurements at radial positions from the center to as near the wall as possible for both the film probes ($r/a=0.85$ in the 2-inch tube) and the impact tubes ($r/a=0.98$). The impact tubes were used to measure velocities for film probe calibration.

The solvents used in this investigation were toluene, cyclohexane, and benzene. Three concentrations of a medium molecular weight poly-

isobutylene (Vistanex L-80, molecular weight about 720,000) in cyclohexane, two concentrations of the same polymer in benzene, two concentrations of a high molecular weight polymethyl methacrylate (Plexiglas, molecular weight about 1,500,000) in toluene, one concentration of a low molecular weight polymethyl methacrylate (V-100 molding powder, molecular weight about 110,000) in toluene, three concentrations of a high molecular weight polyisobutylene (Vistanex L-200, molecular weight about 4,700,000) in toluene, and one concentration of the same polymer in cyclohexane were used.

In the liquids not showing drag reduction a viscous and/or elastic effect was found for both turbulence intensities and energy spectra. Turbulence intensities were higher and energy spectrum frequencies were lower for the polymer solutions of high viscosity. Unfortunately the most viscous solutions were also elastic, so purely viscous liquid studies will be necessary to distinguish between elastic and viscous effects.

During drag reduction it was found that the energy spectra changed little from purely viscous solvents. The turbulence intensities, however, showed very unusual effects. The intensities relative to friction velocity increased at low drag ratio values (high drag reduction), rather than remain constant as expected from mixing length considerations. This behavior was dependent upon the degree of mechanical polymer degradation, lower intensities occurring for fresh than for degraded solutions during drag reduction.

Normal stress differences ($P_{zz} - P_{rr}$) were measured for two of the solutions used in this investigation, one showing drag reduction at attainable flow rates in the 1-inch tube, the other showing drag reduction only in 0.5-inch and smaller tubes. Both solutions yielded normal stress differences of about the same level.

A quantitative viscoelastic mechanism of drag reduction was tested using the viscosity and normal stress data for the two solutions discussed above. The mechanism predicts the turbulent energy dissipation reduction for viscoelastic fluids. From this result the drag reduction was calculated using a relation between the turbulent energy dissipation and the wall shear stress derived from the Nikuradse friction factor correlation for turbulent pipe flow. The energy spectra measured for the two fluids tested were used for the dissipation reduction calculations.

The drag reduction mechanism demonstrated the relative effects of elasticity and viscosity on drag reduction. The adequate prediction of drag ratios for two solutions at two flow rates in each of two tube sizes demonstrated the validity of the mechanism and the reasonableness of the assumptions made.

# INTRODUCTION

Hershey (33) has made a comprehensive study of the effects of polymer type and molecular weight, concentration, solvent type, tube size, and flow rate on the turbulent flow pressure drop of organic polymer solutions. That investigation showed the general polymer-solvent properties which cause drag reduction and led to a means of predicting the possibility of drag reduction for a given system and the flow rates required for incipient drag reduction.

This investigation was conducted to determine the detailed structure of turbulence for the tube flow of organic solvents and polymer solutions--with and without drag reduction. The results of the investigation provide a clearer picture of turbulent behavior during drag reduction flow of polymer solutions, and a viscoelastic mechanism which predicts the amount of drag reduction from viscosity and normal stress data.

# LITERATURE REVIEW

## 1. Phenomenological Equations of Turbulent Pipe Flow

### 1.1. The turbulent mixing length

The turbulent flow of fluids is characterized by a stochastic fluctuation of velocity and pressure at each point in the flow field. The seemingly random nature of the velocity fluctuations was observed directly by Reynolds (76) and many others in streamline marker experiments using dye injection. These experiments showed visually that the straight streamlines of laminar flow in a pipe became sinuous, or turbulent, at a Reynolds number somewhere above 2100. Reynolds also observed the presence of eddies by illuminating his dye tracer with light from a spark. This irregular, eddying motion brings about a much higher shear stress for a given velocity gradient, and the heat and mass transfer rates are much higher than for laminar flow.

Early considerations of turbulent flow stressed the similarity between molecular diffusion as described by the kinetic theory and the larger scale turbulent diffusion of mass, momentum, and heat. The mixing length in molecular diffusion is the mean free path of the molecules. Prandtl (74) reasoned that in turbulent flow the magnitudes of $u'$ and $v'$, the fluctuating velocity components in the x and y directions respectively, were both proportional to $\ell \left| \frac{d\bar{u}}{dy} \right|$, a mixing length times the velocity gradient. As will be shown later, the turbulent shear stress, known as the Reynolds stress, is given by:

$$\tau_{rz} = \rho \overline{u'v'} \qquad (1)$$

Prandtl concluded, therefore, that the stress may be given by:

$$\tau_{rz} = \rho \, \ell^2 (\frac{d\bar{u}}{dy})^2 \tag{2}$$

In order to use this analogy to obtain a velocity profile equation, a value for the length, $\ell$, must be assumed. Prandtl let $\ell = k_p y$ and used the model to derive the logarithmic velocity distribution for turbulent pipe flow:

$$\bar{u} = \bar{u}_{max} + \frac{u^*}{k_p} \ln(\frac{a-r}{a}) \tag{3}$$

where $k_p = 0.40$, $u^* = \sqrt{\tau_w/\rho}$, and a is pipe radius. The derivation of this equation involves the assumption that:

$$\tau_{rz} = \tau_w(\frac{r}{a}) \approx \tau_w$$

which is valid only near the wall. If this assumption is not made (10):

$$\bar{u} = \bar{u}_{max} - \frac{u^*}{k_p} \left(\ln(\frac{1 + \sqrt{r/a}}{1 - \sqrt{r/a}}) - 2\sqrt{r/a}\right) \tag{4}$$

where a is the pipe radius. This equation, however, does not agree as well with the experimental data as the simplified form. This indicates that for a cylindrical pipe the mixing length should have been defined as $\ell = k_p y \sqrt{r/a}$ (10). The velocity profile data of Nikuradse, which is generally accepted as the best available, fit the simplified logarithmic form very well away from the wall (65).

1.2. Universal velocity profile equation

In order to more nearly fit the velocity profile data near the wall the so called "universal" velocity profile equation was derived. The equation may be obtained by substituting the equation for the velocity profile in the laminar layer at the wall,

$$\frac{\bar{u}}{u^*} = \frac{y \, u^*}{\nu} \, , \tag{5}$$

into the Prandtl logarithmic velocity profile to obtain:

$$\frac{\bar{u}}{u^*} = \frac{\bar{u}_{max}}{u^*} - 2.5 \ln \frac{a\, u^{*2}}{\bar{u}\, \nu} \tag{6}$$

Where the laminar profile intersects the turbulent profile:

$$\frac{\bar{u}_{max}}{u^*} = \frac{\overline{u_\delta}}{u^*} + 2.5 \ln \frac{a\, u^{*2}}{\overline{u_\delta}\, \nu} \tag{7}$$

Substituting 7 into 3 and letting $\frac{\bar{u}}{u^*} = u^+$ and $\frac{u^* y}{\nu} = y^+$ ,

$$u^+ = A + 2.5 \ln y^+ \tag{8}$$

A best fit of Nikuradse's data is given (65) by A = 5.5.

1.3. Comparisons with velocity profile data

The universal velocity profile equation fits the turbulent velocity profile data very well near the wall (except in the transition region below $y^+ = 50$). There is a consistent lack of fit, however, near the center of the pipe. The data of Hershey (33), Bunch (7), Tao (91), Bogue (4), and to some degree that of Nikaradse (65) and Deissler (12) show a positive deviation from equation 8 at the points near the pipe center. Figure 1 illustrates this deviation using the data of Tao. In the data of Bogue, Hershey, Bunch, and Tao the values of $y^+$ corresponding to the tube center are easily distinguished by their characteristic rise. An attempt to improve the $u^+ - y^+$ equation by an additive term as a function of y/a was made by Bogue. His equation was of the form:

$$u^+ - G(y/a)\sqrt{2/f} = 2.42 \ln y^+ + 5.57 \tag{9}$$

The correction term is purely empirical. The above equation suitably correlated velocity profiles for the turbulent flow of both Newtonian fluids (water and air) and some non-Newtonian fluids (water solutions of Carbopol and clay suspensions). No significant differences were found

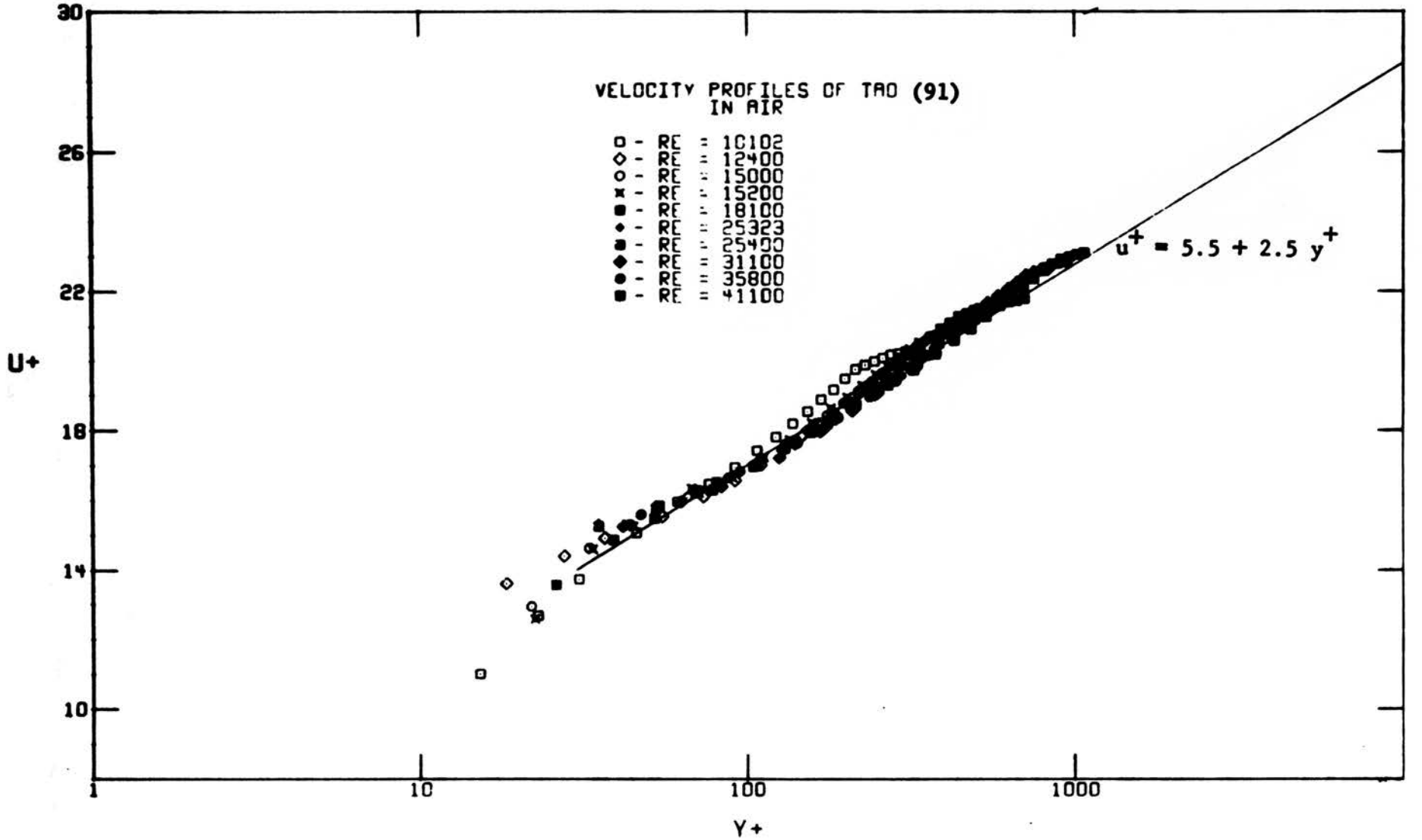


PLOT OF UNIVERSAL VELOCITY DISTRIBUTION FOR TURBULENT FLOW

FIGURE 1

between Newtonian and non-Newtonian velocity profile data by Bogue or Clapp (9) who also studied water solutions of Carbopol. Non-Newtonian rheological relations are summarized in Appendix VII.

Hershey (33) measured velocity profiles in the turbulent flow of the following solvents and solutions: toluene, cyclohexane, polyisobutylene L-80[1] in cyclohexane, polyisobutylene L-80 in benzene, and polymethyl methacrylate G[2] in toluene. The profiles for all these solutions were almost identical to previously reported Newtonian profiles when plotted either as $\bar{u}/\bar{u}_{max}$ vs. y/a or as $u^+$ vs. $y^+$. All of Hershey's solutions were Newtonian except for the highest concentration polyisobutylene (PIB) L-80 in cyclohexane.

1.4. Recent inovations in velocity profile equations

Mention should be made of other recent improvements in the representation of turbulent velocity profiles. These will not be discussed at length because the data of interest here have been presented in terms of the universal equation. A significant improvement over the universal velocity profile is the use of two equations to describe the near wall and center regions. Ross (80) has recommended the use of the von Karman velocity profile equation based on the similarity theory in the region $0 < r/a < 0.85$. The equation is:

$$\bar{u} = \bar{u}_{max} + \frac{u^*}{k_k} \left(\sqrt{1-y/a} + \ln \left(1-\sqrt{1-y/a}\right)\right) + b \qquad (10)$$

Goldstein (27) recommended that $k_k = 0.295$ and $b = 0.172$. This equation is used for pipe flow, but is actually derived for flow between flat plates. Ross recommended the use of the universal equation for $0.85 < r/a < 1.0$.

---

1 Enjay MM Vistanex; grade L-80; lot B40828 code 230; molecular weight approximately 720,000.

2 Rohm and Haas 1/4-inch plexiglas sheet; molecular weight approximately 1,500,000.

Efforts to more nearly represent the velocity profile in one equation lead to the use of longer equations with more constants. Gill and Scher (26) modified the Prandtl mixing length as follows:

$$\ell = k_p y(1 - \exp(-\phi y/a))$$

Using this length, they obtained the following equation for the velocity profile:

$$u^+ = \int_o^{y^+} ((-1 + \sqrt{1 + 4cd})/2c)\,dy^+$$

$$\text{where} \quad c = k_p^2 (a^+)^2 (1 - \exp(-\phi y^{+2}/a^+)) \qquad (11)$$

$$d = 1 - y^+/a^+$$

$$\phi = (a^+ - a')/b$$

$$a^+ = a u^* \rho/\mu$$

The added constants are a' and b. a' is set to be 60 to force $\ell$=0 at Re=1800, and b is 22 for best fit to the velocity profile data. This equation reduces to $u^+ = y^+$ near the wall and near the center the experimentally observed deviation from the universal equation is reproduced.

Pai (68) obtained a series solution of the Reynold's equations[1] for turbulent flow in a pipe. The equation applied to the entire profile is as follows:

$$\frac{\bar{u}}{u^*} = \frac{u_{max}}{u^*}\left(1 + \frac{s-n}{n-1}(r/a)^2 + \frac{1-s}{n-1}(r/a)^{2n}\right) \qquad (12)$$

$$\text{where} \quad s = u^{*2} a\rho/(\mu\, u_{max})$$

n is an adjustable constant which Pai set at 16. This equation has not been adequately tested to determine its generality. When s=1 the equation reduces to the laminar flow velocity profile.

---

[1] To be discussed later.

## 1.5. Velocity profiles for "drag reducing" solutions

Shaver (85) measured turbulent velocity profiles for solutions of carboxymethylcellulose (CMC) which were very non-Newtonian[1] (n=0.54 to 0.85) some showing lower than normal pressure drop. These solutions, in contrast to those mentioned previously, yielded higher slopes for $\bar{u}/u^*$ versus ln y as the fluids became more non-Newtonian. Bogue (4) attributed this phenomenon to the elasticity[2] of CMC solutions, which possibly suppresses the turbulent fluctuations thereby producing a lower turbulent shear stress for a given shear rate. This means that $\frac{d\bar{u}}{dr}/u^*$ from equation 3, will be larger. Some evidence of suppression for the largest scale fluctuations was directly observed by Shaver in a dye injection experiment. It should be noted, however, that when plotted simply as $\bar{u}/\bar{u}_{max}$ versus y/a, Shaver's data look the same as Newtonian data (33).

Ernst (18) measured velocity profiles in 0.05 per cent CMC solutions, and found a parallel shift (higher $u^+$) in the velocity profile when plotted as $u^+$ versus ln $y^+$ using the apparent wall viscosity to calculate $y^+$. Wells (98) found an upward shift plus an increase in slope for CMC and guar gum solutions when he attempted to correlate his velocity profiles using a generalized $u^+ - y^+$ diagram where:

$$u^+ = \bar{u}/u^*$$

$$y^+ = \rho(u^*)^{2-n}\, y^n/K \qquad (13)$$

---

1 See Appendix I for a summary of non-Newtonian rheological relations.

2 Shear elasticity is discussed in detail in section 4, "Viscoelastic Theories of Drag Reduction".

This procedure is identical to the use of an apparent wall viscosity for $y^+ = \rho u^* y/\mu_w$ when the fluid considered follows the power law. As shown in Figures 2 and 3, even though Wells' $u^+ - y^+$ slopes are higher than for Newtonian fluids for his concentrated solutions, his profiles appear more blunt[1] when plotted as $\bar{u}/\bar{u}_{max}$ versus $y/a$.

Newtonian fluids (air, water, organic solvents and solutions) and some non-Newtonian fluids (carbopol-water solutions and clay suspensions) seem to be adequately correlated if the apparent wall viscosity for the fluid is used to calculate $y^+$ in the $u^+ - y^+$ correlation. This is not the case, however, for the water solutions of CMC and guar gum discussed above. The profiles of Ernst showed a parallel displacement from the Newtonian $u^+ - y^+$ curve, but the data of Wells and Shaver demonstrated higher $u^+ - y^+$ slopes in the turbulent core with about the same $u^+$ intercepts at $\ln y^+=0$ as for Newtonian fluids.

The data for the Shaver, Ernst, and Wells profiles can be partially reconciled. The universal correlation can be written (after Bogue (4)):

$$u^+ = \frac{\bar{u}}{u^*} = 5.57 + 2.42 \ln y u^* \rho/\mu_w \qquad (14)$$

where $\mu_w$ is the apparent viscosity at the wall. The upward parallel shift of Ernst can be correlated by increasing the constant from 5.57 to some higher value. For a given wall shear rate this amounts to increasing the viscous layer thickness. Since Ernst mentions that his flow rates are about seven per cent below his integrated velocity profiles the shift might not actually be so great. In order to cause a steeper turbulent velocity profile for a given wall shear stress (or wall shear rate), the

---

[1] This does not necessarily indicate slip at the wall, because an infinite number of velocity profiles are possible with zero wall velocity.

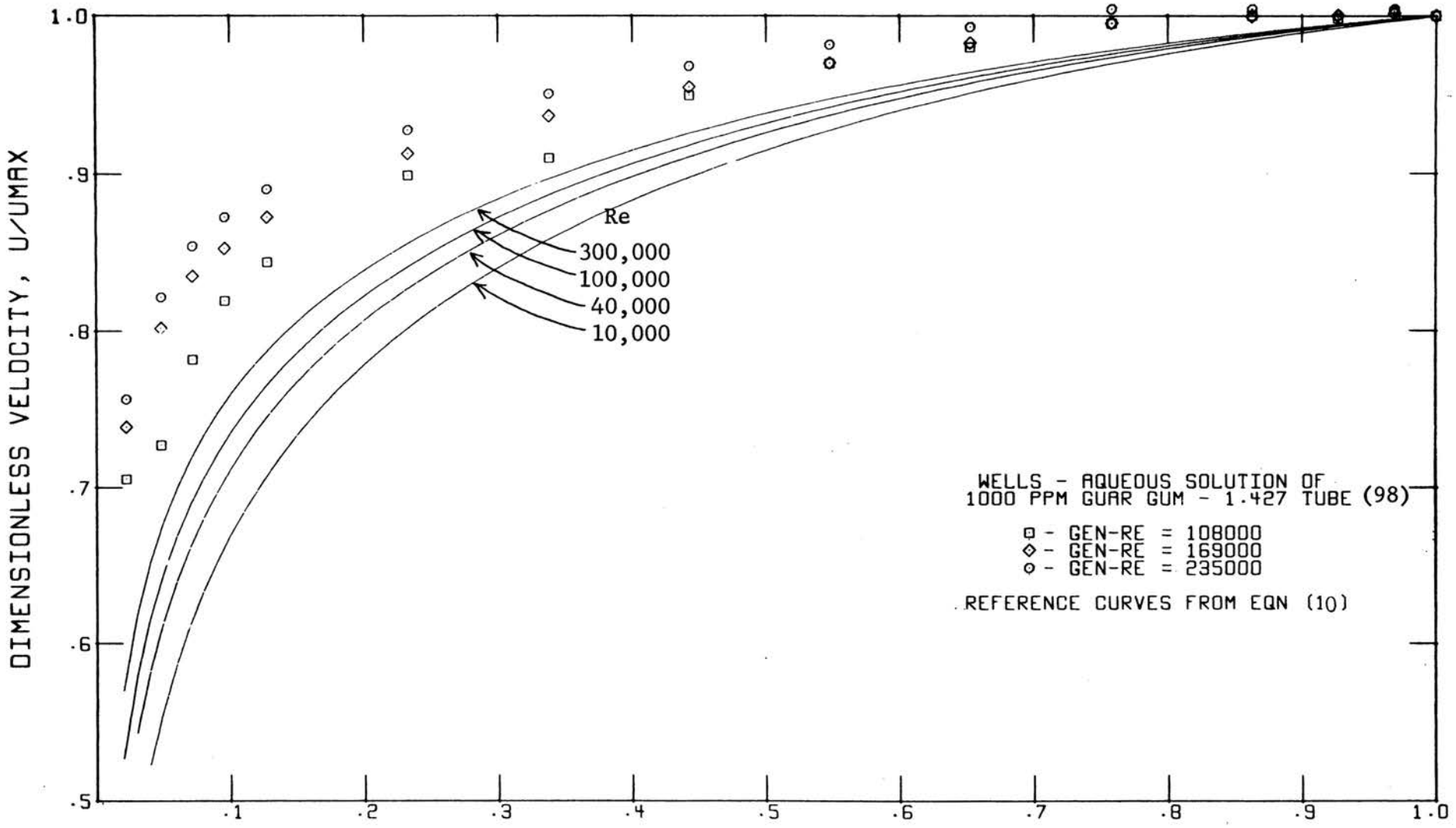


PLOT OF DIMENSIONLESS VELOCITY VERSUS DIMENSIONLESS DISTANCE

FIGURE 2

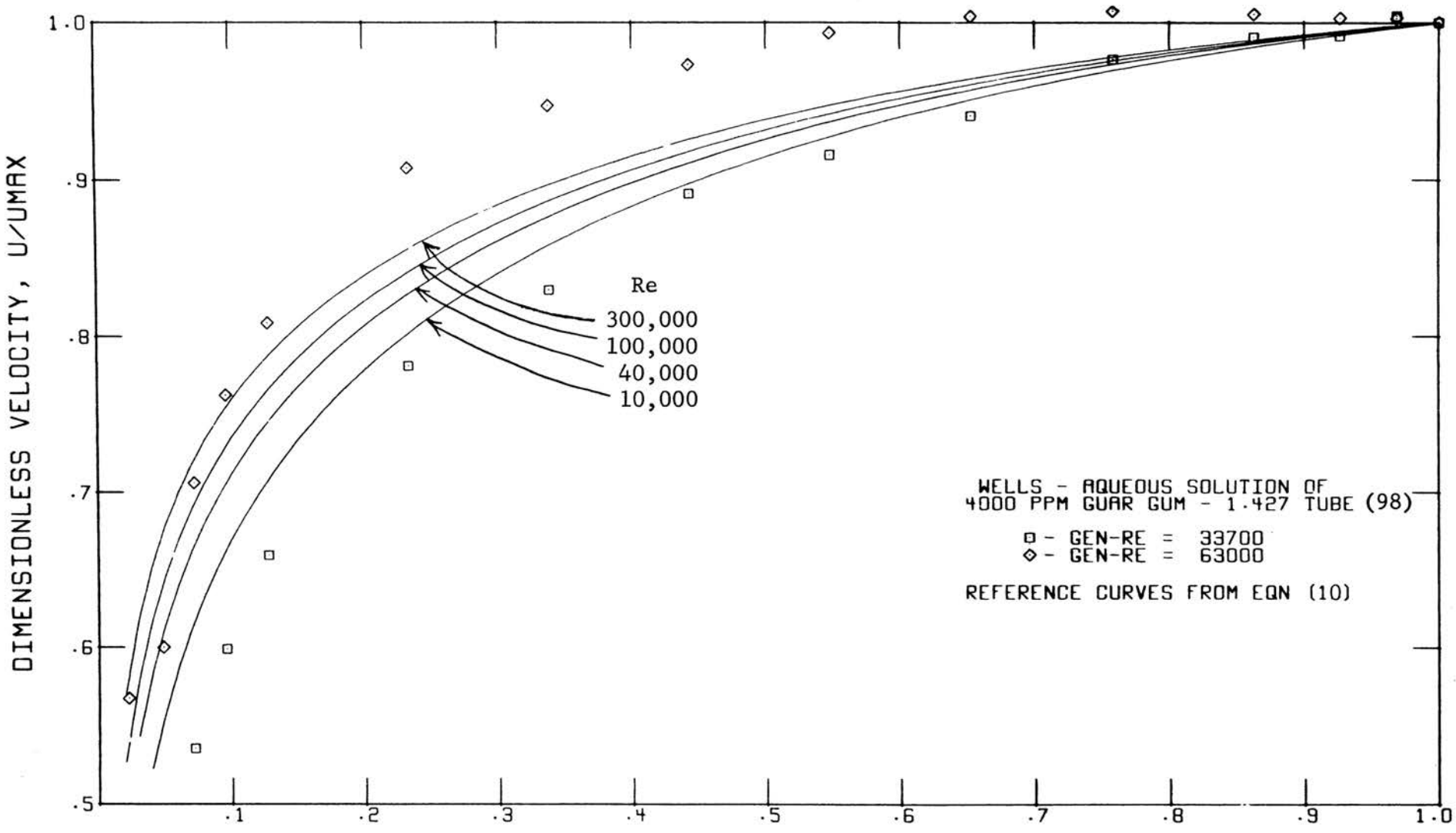


PLOT OF DIMENSIONLESS VELOCITY VERSUS DIMENSIONLESS DISTANCE

FIGURE 3

coefficient (which is actually $1/k_p$, the Prandtl mixing length constant) must be increased from 2.42 to some higher value. This means that $k_p$ is decreased, so $\ell = k_p y\sqrt{r/a}$, the mixing length, is decreased. Ernst's profiles are displaced upward in the $u^+$ direction only 20-30 per cent, whereas Wells' are displaced as much as 150 per cent giving rise to a much more significant slope change. Ernst used only 0.05 per cent CMC-7HSP[1] in his solutions, whereas Shaver's solutions were as high as 0.5 per cent CMC-70S[1] and Wells' solutions ranged from 0.05 per cent quar gum (J-2P)[2] to 0.4 per cent CMC-70[1], causing much larger effects on the velocity profiles.

It should be noted that Shaver's integrated velocity profiles average about six per cent below measured flow rates. Wells' were about 2.8 per cent below his flow rates. Ripken and Pilch (77) observed such poor agreement between integrated profiles and measured flow rates for CMC solutions, that they did not report their results pending further investigation. Savins (84) has suggested that impact tube measurements in turbulent flow might not indicate the correct velocity pressure head. This is because the wall pressure tap might indicate a pressure biased by the normal stress in the radial direction. All the present velocity profile data for drag reducing solutions show significant deviations from the average flow rates, but not in the same direction (Ernst's integrated velocity profiles were too high).[3] An intensive study of such profiles is needed to resolve this problem, as noted in the recommendations below.

---

1 Hercules Powder Co.

2 Westco Research Co.

3 Ernst's and Wells' data for water matched both the established friction factor data and velocity profile data (plotted as $u^+$ versus $\ln y^+$), so the profiles should integrate to yield the proper flow rates. Shaver's water profiles integrated to yield somewhat high flow rates (33).

## 1.6. Pressure drop in turbulent pipe flow

The pressure drop for turbulent flow in smooth round pipes is best correlated for Newtonian fluids as a dimensionless friction factor versus the Reynolds number. These two groups are predicted by dimensional analysis. The Fanning friction factor has the form:

$$f = \left(\frac{D\Delta P}{4L}\right) / \left(\frac{\rho U^2}{2g_c}\right) \tag{15}$$

For laminar flow in circular tubes, the friction factor may be obtained by a rearrangement of the Hagen-Poiseuille equation:

$$f = 16/Re \tag{16}$$

Von Karman (37) integrated the universal velocity profile equation to obtain an expression for the space mean velocity. He then substituted $U\sqrt{f/2}$ for $u^*$ and obtained the equation for turbulent flow friction factor:

$$1/\sqrt{f} = 4.06 \log (Re\sqrt{f}) - 0.60 \tag{17}$$

Nikuradse used the best data available to him for Reynolds numbers 4000 to 3,240,000 and obtained an empirical correlation of the form (65):

$$1/\sqrt{f} = 4.0 \log (Re\sqrt{f}) - 0.40 \tag{18}$$

These two equations are almost identical.

A much simpler correlation of friction factor with Reynolds number is that proposed by Blasius (40):

$$f = 0.079\ Re^{-1/4} \tag{19}$$

This equation represents the turbulent data from Reynolds number 3000 to 100,000 only.

Metzner and Reed (61) have proposed a generalized Reynolds number for non-Newtonian fluids based on the concepts of Rabinowitsch[1]:

---

[1] See Appendix for summary of non-Newtonian relationships.

$$Re' = \frac{D^{n'} U^{2-n'} \rho}{g_c K' 8^{n'-1}} \qquad (20)$$

where $K' = \tau_w/(8U/D)^{n'}$ and $n' = d(\log \tau_w)/d\ (\log(8U/D))$.

When $n'=1.0$ this generalized Reynolds number reduces to the conventional Reynolds number. Dodge (14) used the generalized Reynolds number to correlate the friction factors for the turbulent flow of non-Newtonian water solutions of Carbopol 934 (carboxypolymethylene) and Attasol (clay) suspensions in the form:

$$\sqrt{1/f} = 4.0 \log (Re' f^{(1-n')/2})/n'^{0.75} - 0.40/n'^{1.2} \qquad (21)$$

This equation correlated data from the systems mentioned above to within ±2.5 per cent of the measured friction factors. The friction factor correlation also reduces to the Newtonian relation when $n'=1$. The form of this generalized correlation can be derived by integrating the generalized universal velocity profile as used by Wells and making the same substitution as von Karman, namely $u^* = u\sqrt{f/2}$.

Clapp (9) measured friction factors in Carbopol 934 and correlated his data using an equation derived by integrating equation 13, assuming the power law. He obtained a correlation accurate to ±4 per cent using:

$$\sqrt{1/f} = 2.69/n - 2.95 + 4.53 \log (Re^{\circ} f^{(2-n)/2})/n + 0.69\ (5n-8)/n$$

$$\text{where} \qquad Re^{\circ} = 8D^n U^{2-n} \rho/K(6 + 2/n)^n \qquad (22)$$

$$\text{for} \qquad 0.698 < n < 0.813 \text{ and } 5480 < Re^{\circ} < 42,800.$$

Clapp stated that the consistency of this equation with the velocity profile equation for non-Newtonian fluids makes it more generally applicable than Dodge's empirical equation. As is shown in Appendix VII, the Metzner and Reed Reynolds number may be used in place of the power law Reynolds number with no change in the form of the equation.

## 1.7. Friction factors for "drag reducing" solutions

Several investigators have measured friction factors in both Newtonian and non-Newtonian fluids which are not correlated by the equations of Dodge and Clapp. Dodge attempted to correlate data for CMC-water solutions along with his Carbopol and Attasol data. The friction factors as shown in Figure 4 for the CMC were, however, far below the correlation at high Reynolds numbers, even though the laminar data were well correlated by the relation:

$$f = 16/Re' \tag{23}$$

Moreover, in the turbulent region ($Re' > 3000$) there is a pronounced diameter effect in his data, the smaller tubes causing the lower friction factors. There was no diameter effect in the laminar region. Dodge attributed this anomalous behavior to the viscoelasticity of CMC solutions (elastic as well as viscous response to shear).

At about the same time Shaver made extensive friction factor measurements using CMC-70, polyvinyl alcohol, ammonium alginate, and Carbopol 934 all in water, and polyisobutylene (Vistanex B-100) in cyclohexane. Shaver obtained a modified Blasius type correlation that fit his data with maximum deviations of +33 to -15 per cent. It is interesting to note that in addition to being a poor fit of the data his correlation is a strong function of n:

$$f = 0.079/(n^5(Re^{\circ})^{\gamma}) \tag{24}$$

where $\gamma = 2.63/10.5^n$

Most of the data below n=0.8 were obtained using CMC solutions, whereas the data above n=0.8 were obtained for primarily Carbopol and alginate solutions. Hershey (33) replotted Shaver's friction factor data

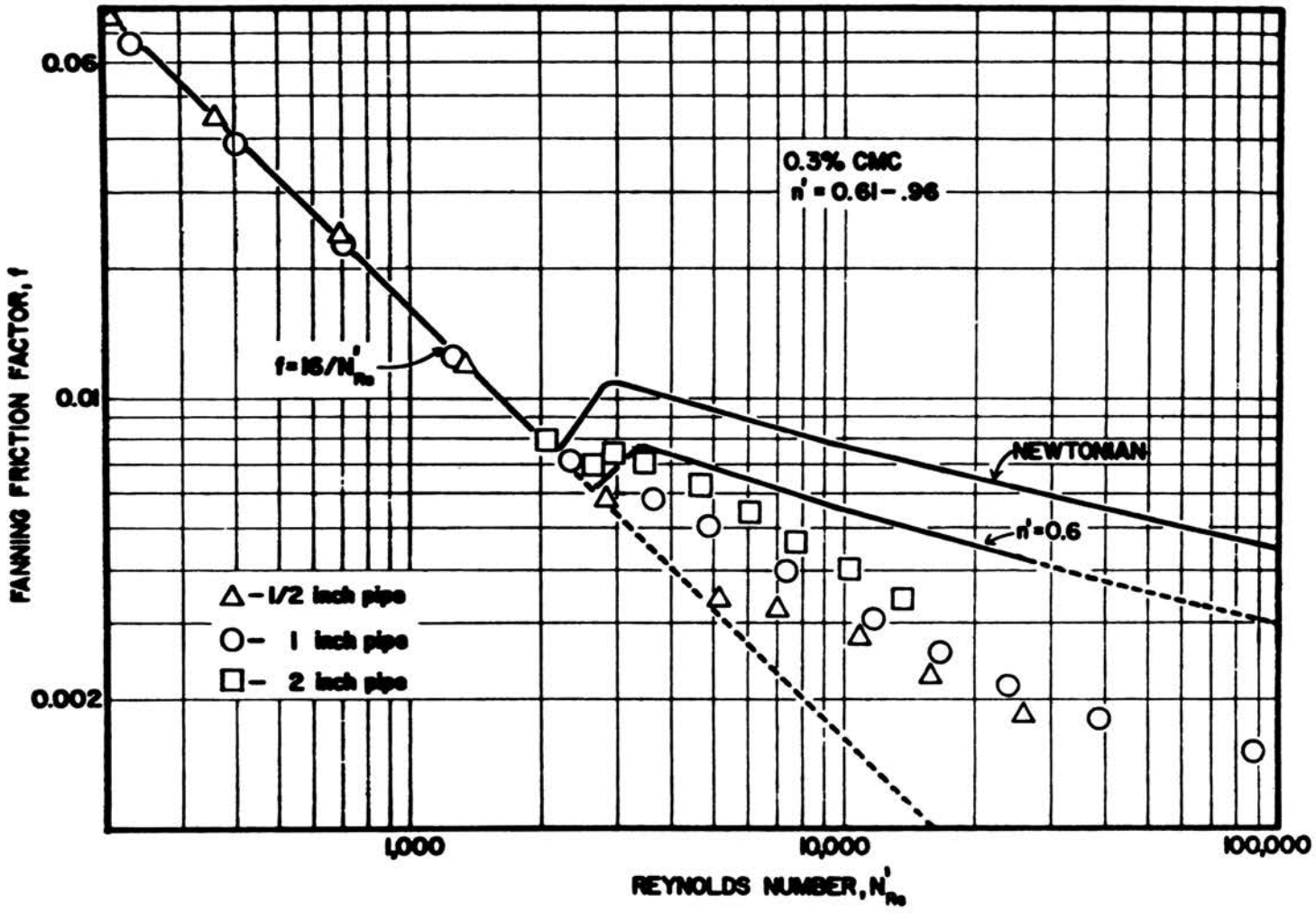


FIGURE 4. DODGE'S FRICTION FACTOR DATA FOR CMC SOLUTION (14)

using the solvent Reynolds number ($Re_s = D\bar{u}/\nu_s$, where $\nu_s$ is the solvent kinematic viscosity). These plots show that in the high Reynolds number turbulent region the ammonium alginate and Carbopol data are much like that of Dodge's Carbopol data with friction factors above the solvent friction factors and little diameter effect. Shavers turbulent CMC-water data and polyisobutylene (PIB)-cyclohexane data, however, fall below the solvent friction factors.

The transitions from laminar flow to turbulent flow are difficult to relate to the turbulent flow phenomena. Some data (Shaver's alcohol and ammonium alginate) actually dip below 16/2100 (the laminar friction factor for Newtonian fluids at Re=2100, the usual transition point). This effect has also been observed for Newtonian non-elastic fluids during carefully controlled vibration free experiments in round tubes for Reynolds numbers up to 26,000 (23). Since Shaver's data were all taken in the same set of tubes and he did not observe this effect on his purely viscous fluids, some turbulence damping seems evident. This effect seems to be more striking in the smaller tubes as shown by Figure 5. The CMC solutions of both Dodge and Shaver, however, do not seem to exhibit an abrupt transition at all, but the friction factor-Reynolds number slopes gradually decrease as the flow becomes turbulent. The solutions exhibiting low turbulent friction factors seem to delay the laminar-turbulent transition to higher Reynolds number, then suppress friction producing effects in the turbulent region.

Savins (82) reviewed the earlier non-Newtonian friction factor data, and Hershey (33) recently reviewed this and the later data as well. Savins replotted the data of Toms (95) for the flow of polymethyl methacrylate (PMMA)-mono-chlorobenzene solutions in small tubes. The data for 0.25 per

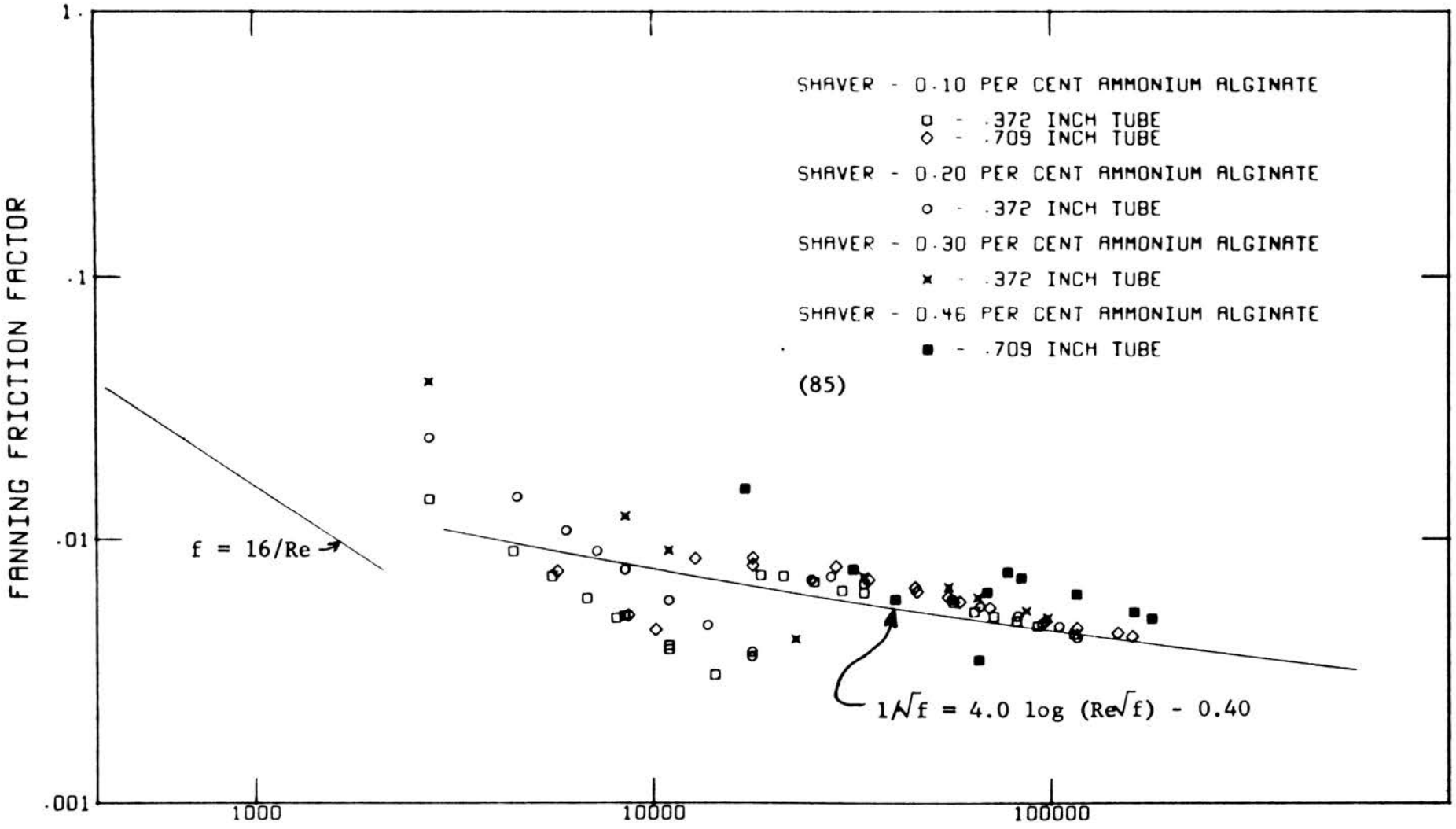


PLOT OF SOLVENT REYNOLDS NUMBER VERSUS FANNING FRICTION FACTOR

FIGURE 5

cent PMMA were shown as friction factor versus a Reynolds number calculated using the limiting high shear rate viscosity. The laminar points fell on the established laminar line, but a striking diameter effect existed for the turbulent region. The largest tube (0.202 cm) showed a normal transition to turbulent flow, then the friction factors dropped below the Newtonian line at high Reynolds numbers. The small tube (0.0645 cm) had no definite transition point, but changed slope slightly at the transition point.

Hershey also replotted Toms' data for several concentrations (0.156 g/l to 20 g/l) as friction factor versus solvent Reynolds number. Plotted in this way the effect of solution viscosity becomes evident. The concentration yielding the highest friction factor reduction below solvent friction factors depends on tube size. The 0.05-inch tube gave greatest reduction at about 0.5 g/l, but the 0.159-inch tube yielded greatest reduction at 2.5 g/l. It should also be noted that the drag reduction effect becomes evident only at higher Reynolds numbers for the larger tube, as is true for the data of Dodge and Shaver.

The effect observed by Dodge, Shaver, and Toms has been called drag reduction, turbulence suppression, and many other descriptive names. The following quantitative definitions will be used in the remainder of this discussion:

Drag reduction - the reduction in pressure drop at the same flow rate of a flowing fluid by the addition of a small amount of solute. This has been observed only in the turbulent region.

Drag ratio - the ratio of pressure drop for the solution to the pressure drop of the pure solvent at the same flow rate.

Friction factor reduction - the reduction of the friction factor of a flowing fluid below that predicted by the Dodge and Metzner correlation for purely viscous fluids.

Friction factor ratio - the ratio of measured friction factor to the friction factor predicted by the Dodge and Metzner correlation at the same Reynolds numbers. This definition is the same as Hershey's (33) "turbulence suppression".

It can be seen that the first definition has a practical basis - the comparison of pressure loss for the pumping of a treated fluid to the pressure loss for the untreated fluid. The definition of friction factor reduction, however, provides a better basis for the theoretical consideration of this phenomenon. This is because:

(1) The effect of viscosity increase with solute addition is eliminated, and

(2) the only effects then evident are those causing deviation from the behavior of a purely viscous liquid.

Several investigators have obtained additional friction factor data for systems which show drag reduction with about the same results as Toms, Dodge, and Shaver. Meter (59) measured friction factors for seven water solutions of Natrosol hydroxyethylcellulose and one 0.4 per cent Carbopol 934-water solution in 1/2 inch and 1-inch tubes. All of Meter's Natrosol solutions (types G and H) were quite viscous. Plotting his data as log friction factor versus log solvent Reynolds number shows a laminar region with a slope of minus one. The solutions of concentration 1.0 to 2.0 per cent Natrosol G and 0.3 to 0.5 per cent Natrosol H show laminar-turbulent transitions with drag reduction at higher Reynolds numbers. The 0.7 and 1.0 per cent solutions of Natrosol H did not

seem to exhibit transition points but extended to $f < 0.001$ on the laminar line. The data for these concentrations represent an extended laminar region even more striking than Shaver's ammonium alginate and PVA data.

Fabula (19) has measured the friction factors for dilute solutions of poly(ethylene oxide) in a single pass pipe flow system. Shaver (35) had reported considerable mechanical degradation of his CMC solutions (friction factors changed with pumping time), and his drag reducing PIB-cyclohexane solution degraded to a non-drag reducing solution after 24 hours of pumping. Fabula avoided this problem with his once through system and obtained drag reduction with concentrations as low as 1.1 parts per million poly(ethylene oxide) in a 0.4-inch pipe.

Hoyt and Fabula (36) in a later paper reported their work on drag reduction using rotating disks in the fluid. They compiled a list of nine major types of water soluble polymers (natural and synthetic) which caused a reduction in torque for a given disk speed. Of these, one type of poly(ethylene oxide) (Polyox coagulant) caused 35 per cent torque reduction at 40 revolutions per second at a concentration of only 12 parts per million. The disk used had a diameter of 45.7 cm. The other polymers giving torque reductions of at least 35 per cent at concentrations below 1000 parts per million were guar gum, locust bean gum, Irish moss, gum karaya, hydroxymethyl cellulose, CMC, polyacrylamide and Polyhall-27.

Park (70) measured drag reduction friction factors in water solutions of 0.3 per cent J-100[1] and 0.5 per cent CMC. He obtained a correlation

---

[1] Dow Chemical Co.

between the drag reduction of his J-100 solutions and their normal stress difference, $P_{zz} - P_{rr}$. This correlation will be discussed in the section on viscoelasticity. Ripken and Pilch (77) have also studied the turbulent flow of CMC solutions and, in addition, water solutions of Polyhall-27 and poly(methylene oxide). They studied solutions of CMC with values of flow index, n, from 0.433 to 0.835 and found, like Shaver, that for a given pipe size and given polymer, n is a good indication of the drag reducing characteristics. This is very misleading, however, because as has been shown earlier (data of Dodge (14)) drag reduction seems to have little general dependence on the value of flow index.

Hershey (33) in an effort to define those polymer properties which cause drag reduction, measured friction factors in several organic polymer solutions. He demonstrated drag reduction in a smooth 1/2-inch tube and several smaller tubes for cyclohexane solutions of polyisobutylene (PIB) L-80[1] at concentrations of 0.05 per cent to 1.0 per cent, the same polymer in benzene at concentrations of 0.25 per cent to 0.9 per cent, and in polymethyl methacrylate[1] in toluene at concentrations of 0.1 per cent to 1.0 per cent. His data show the same diameter effect as previous drag reduction data in water solutions. He did not obtain drag reduction using a medium molecular weight polystyrene (molecular weight about 240,000) in toluene and low molecular weight PIB LMMH (molecular weight about 45,000) in cyclohexane. This shows that molecular size in solution has an important effect on drag reduction. The drag reduction for PIB L-80 in benzene ( a poor solvent) was not as high as in cyclohexane (a good solvent). Since polymer molecules are more extended in good solvents (21),

---

1 See Appendix VI.

this also illustrates the effect of molecular size on drag reduction. The lack of drag reduction for the polystyrene solutions could be attributed to both the low molecular weight and to the rather inflexible polystyrene chain. Of particular interest, all the solutions studied by Hershey were Newtonian except the 1.0 per cent PIB L-80 in cyclohexane. The solutions obviously do not have to be non-Newtonian to be drag reducing.

The reduction in pressure drop below that predicted by the Dodge and Metzner equation causes the so called "friction velocity", $u^* = \sqrt{\tau_w/\rho}$, to be lower than for a purely viscous fluid since $\tau_w = \frac{D\Delta P}{4L}$ for a pipe. The velocity profile when plotted as $(\bar{u}_{max} - \bar{u})/u^*$ versus ln $y/r$, becomes steeper than the accepted Newtonian data, if the slope $d\bar{u}/d$ (ln y) remains the same. This effect was observed for Shaver's velocity profiles in the preceding section. Hershey's $(\bar{u}_{max} - \bar{u})/\bar{u}_{max}$ versus y/r plots of Wells' data show velocity profiles more blunt than purely viscous turbulent profiles. Since Wells' solutions exhibited great drag reduction at the flow rates studied, the slopes $d(\bar{u}/u^*)/d(\ln y)$ (from his $u^+ - y^+$ plots) were still steeper than for the purely viscous correlation of Nikuradse. Even though there is some doubt that the profiles of Shaver, Ernst, and Wells are accurate since they do not check the measured flow rates, the large increase in the slope $d(\bar{u}/u^*)/d(\ln y)$ over the viscous case for both Wells' and Shaver's data indicates a much lower rate of momentum exchange in the radial direction for a given velocity gradient. If all molecular effects[1]

---

[1] At a concentration of 0.005 per cent (50 ppm) of PIB with a molecular weight of $10^6$ in toluene, there are approximately $2 \times 10^{10}$ molecules per cubic millimeter. Since the microscale in 1-inch and 2-inch pipes is about 1 mm (experimental section), a solution of this concentration may be considered to be a continuum.

(even on the polymeric size scale) are negligible in the turbulent core, this means that the length scale of mixing must be diminished.

## 2. Statistical Theories of Turbulence

### 2.1. Turbulent energy dissipation in pipe flow

In an attempt to define the motion of a fluid in turbulent flow in a more detailed manner, it is necessary to consider the fluctuations of velocity which are superimposed upon the mean velocity of flow. This may be done by letting the velocity, u, be the sum of the average velocity and the fluctuating component, $\bar{u} + u'$. This can be done for each fluctuating quantity in the Navier-Stokes equations giving for constant viscosity (34):

$$(\rho + \rho')\frac{d(u_i + u'_i)}{dt} = -\frac{\partial(p + p')}{\partial x_i} + \mu\frac{\partial^2}{\partial x_j^2}(u_i + u'_i) + \frac{1}{3}\mu\frac{\partial}{\partial x_i}\frac{\partial(u_j + u'_j)}{\partial x_j} \tag{25}$$

where the summation convention for subscripts is used. Upon averaging this equation with respect to time, the following result is obtained:

$$\bar{\rho}\left(\frac{\partial \bar{u}_i}{\partial t} + \bar{u}_j\frac{\partial \bar{u}_i}{\partial x_j}\right) = -\frac{\partial \bar{p}}{\partial x_i} + \mu\frac{\partial^2 \bar{u}_i}{\partial x_i^2} + \frac{1}{3}\mu\frac{\partial}{\partial x_i}\frac{\partial \bar{u}_j}{\partial x_j} - \left\{\bar{\rho}\,\overline{u'_j\frac{\partial u'_i}{\partial x_j}} + \overline{\rho'\frac{\partial u'_i}{\partial t}} + \overline{\rho' u'_j}\frac{\partial \bar{u}_i}{\partial x_j} + \bar{u}_j\overline{\rho'\frac{\partial u'_i}{\partial x_j}} + \overline{\rho' u'_j\frac{\partial u'_i}{\partial x_j}}\right\} \tag{26}$$

The equation obtained for the time averaged turbulent motion is then the original Navier-Stokes equation plus the terms in the brackets which represent the effects of the turbulent motion. The equation of continuity states that $\rho\frac{\partial}{\partial x_i}u_i = 0$ for an incompressible fluid in stationary flow. The first term in brackets becomes, therefore, $\bar{\rho}\frac{\partial}{\partial x_j}\overline{u'_j u'_i} = \frac{\partial}{\partial x_j}\bar{\rho}\,\overline{u'_j u'_i}$, and the other four terms become insignificant for an incompressible fluid.

Equation 26 then becomes:

$$\rho\left(\frac{\partial \bar{u}_i}{\partial t} + \bar{u}_j \frac{\partial \bar{u}_i}{\partial x_j}\right) = -\frac{\partial \bar{p}}{\partial x_i} + \frac{\partial}{\partial x_j}\left(\mu \frac{\partial \bar{u}_i}{\partial x_j} - \rho \overline{u'_i u'_j}\right) \qquad (27)$$

(The term $\frac{1}{3}\mu \frac{\partial}{\partial x_i}\frac{\partial \bar{u}_j}{\partial x_j}$ is zero when incompressibility is assumed.)

The last term in equation 27 is called the Reynolds stress, because Reynolds first obtained this form of the equation. This term represents the additional average stress on the j plane in the i direction caused by the turbulent motion.

In cylindrical coordinates, which shall be used when considering turbulent flow in pipes, the Reynolds equations written for each direction become (where $u=u_z$, $v=u_r$, $w=u_\theta$):

$$\rho \frac{d\bar{u}}{dt} = -\frac{\partial \bar{p}}{\partial z} + \mu \nabla^2 \bar{u} - \rho \frac{\partial}{\partial z}\overline{(u')^2} - \frac{\rho}{r}\frac{\partial}{\partial r} r\,\overline{v'u'} - \frac{\rho}{r}\frac{\partial}{\partial \theta}\overline{w'u'}$$

$$\rho\left(\frac{\partial \bar{v}}{\partial t} - \frac{\bar{w}^2}{r}\right) = -\frac{\partial \bar{p}}{\partial r} + \mu\left(\nabla^2 \bar{v} - \frac{\bar{v}}{r^2} - 2\frac{\partial \bar{w}}{r^2 \partial \theta}\right) - \frac{\rho}{r}\frac{\partial}{\partial r} r\overline{(v')^2}$$

$$- \frac{\rho}{r}\frac{\partial}{\partial \theta}\overline{v'w'} - \rho \frac{\partial}{\partial z}\overline{v'u'} + \rho \frac{\overline{(w')^2}}{r} \qquad (28)$$

$$\rho\left(\frac{\partial \bar{w}}{\partial t} + \frac{\bar{v}\,\bar{w}}{r}\right) = -\frac{1}{r}\frac{\partial \bar{p}}{\partial \theta} + \mu\left(\nabla^2 \bar{w} - \frac{\bar{w}}{r^2} + \frac{2}{r^2}\frac{\partial \bar{v}}{\partial \theta}\right) - \frac{\rho}{r}\frac{\partial}{\partial \theta}\overline{(w')^2}$$

$$- \rho \frac{\partial}{\partial r}\overline{w'v'} - \rho \frac{\partial}{\partial z}\overline{w'u'} - 2\rho \frac{\overline{w'v'}}{r}$$

The development of these equations may be found in any text covering turbulence (10, 34, 40).

Laufer (47) and others have shown that for fully developed turbulent flow in a pipe these equations may be reduced considerably. The overall conditions are:

$$\bar{v} = \bar{w} = 0 \text{ for all } t$$

$$\frac{\partial \bar{u}}{\partial t} = 0$$

$$\frac{\partial \bar{A}}{\partial z} = 0 \text{ for A any variable except pressure}$$

$$\frac{\partial \bar{B}}{\partial \theta} = 0 \text{ for B any variable}$$

The Reynolds equations become:

$$\frac{\partial \bar{p}}{\partial z} = -\frac{\rho}{r}\frac{d}{dr}\left(r\,\overline{u'v'}\right) + \mu\left(\frac{d^2\bar{u}}{dr^2} + \frac{1}{r}\frac{d\bar{u}}{dr}\right)$$

$$\frac{d\bar{p}}{dr} = -\frac{\rho}{r}\frac{d}{dr}\,r\overline{(v')^2} + \frac{\overline{(w')^2}}{r} \tag{29}$$

$$0 = -\frac{d}{dr}\overline{v'w'} - 2\frac{\overline{v'w'}}{r}$$

The last equation may be integrated using the condition that $\overline{v'w'} = 0$ at r=a:

$$\overline{v'w'} = \frac{0}{r^2} = 0$$

Using the boundary conditions at r=0:

$$\overline{u'v'} = 0$$

$$\frac{d\bar{u}}{dr} = 0$$

and at r=a:

$$\overline{u'v'} = 0$$

$$\frac{\mu}{\rho}\frac{d\bar{u}}{dr} = -(u^*)^2$$

$$\overline{(v')^2} = 0$$

Laufer obtained:

$$\overline{u'v'} = \frac{\mu}{\rho}\frac{d\bar{u}}{dr} + \frac{r}{a}(u^*)^2 \tag{30}$$

$$-\overline{(v')^2} + \int_0^r \frac{\overline{(v')^2 - (w')^2}}{r}\,dr = \frac{\bar{p}}{\rho} + \frac{2(u^*)^2 z}{a} \tag{31}$$

where $\bar{p} = 0$ at $z = 0$.

These equations can be used as a convenient check on the Reynolds stresses, since the shear stress, $\rho\ \overline{u'v'}$, and velocity gradient $d\bar{u}/dr$, occur in one equation and the normal stresses, $\overline{(v')^2}$ and $\overline{(w')^2}$, occur with the pressure in the other equation.

Multiplying equation 30 by $d\bar{u}/dr$ puts it in the form of an energy balance:

$$u'v'\left(\frac{d\bar{u}}{dr}\right) - \frac{\mu}{\rho}\left(\frac{d\bar{u}}{dr}\right)^2 \quad \frac{r}{a}(u^x)^2\left(\frac{d\bar{u}}{dr}\right) \tag{32}$$

The right side represents the total energy loss per unit mass per unit time for the flow. The first term on the left side represents the turbulent energy production which is ultimately dissipated by the small scale turbulent eddies, and the second term represents the direct viscous dissipation by the average velocity gradient. This equation may be used to calculate the contributions of the turbulent fluctuations and the average velocity gradient to energy dissipation in the form of heat if the velocity gradient and pressure drop are known.

Laufer has calculated the gradient and turbulent energy dissipation profiles from his velocity profile data in air at two flow rates (Re=50,000 and 500,000). As shown in Figure 6 most of the gradient dissipation and turbulent energy production occurs very near the wall - below $y^+=30$. This is within the velocity profile transition region where measurements are very difficult in small pipes. The total energy for the two terms (both made dimensionless by multiplying by $(\mu/\rho u^{*4})$) may be obtained by integrating across the pipe cross section. It is found that the gradient dissipation accounts for about sixty per cent of the total energy dissipated for the turbulent flow of air in a 10-inch pipe.

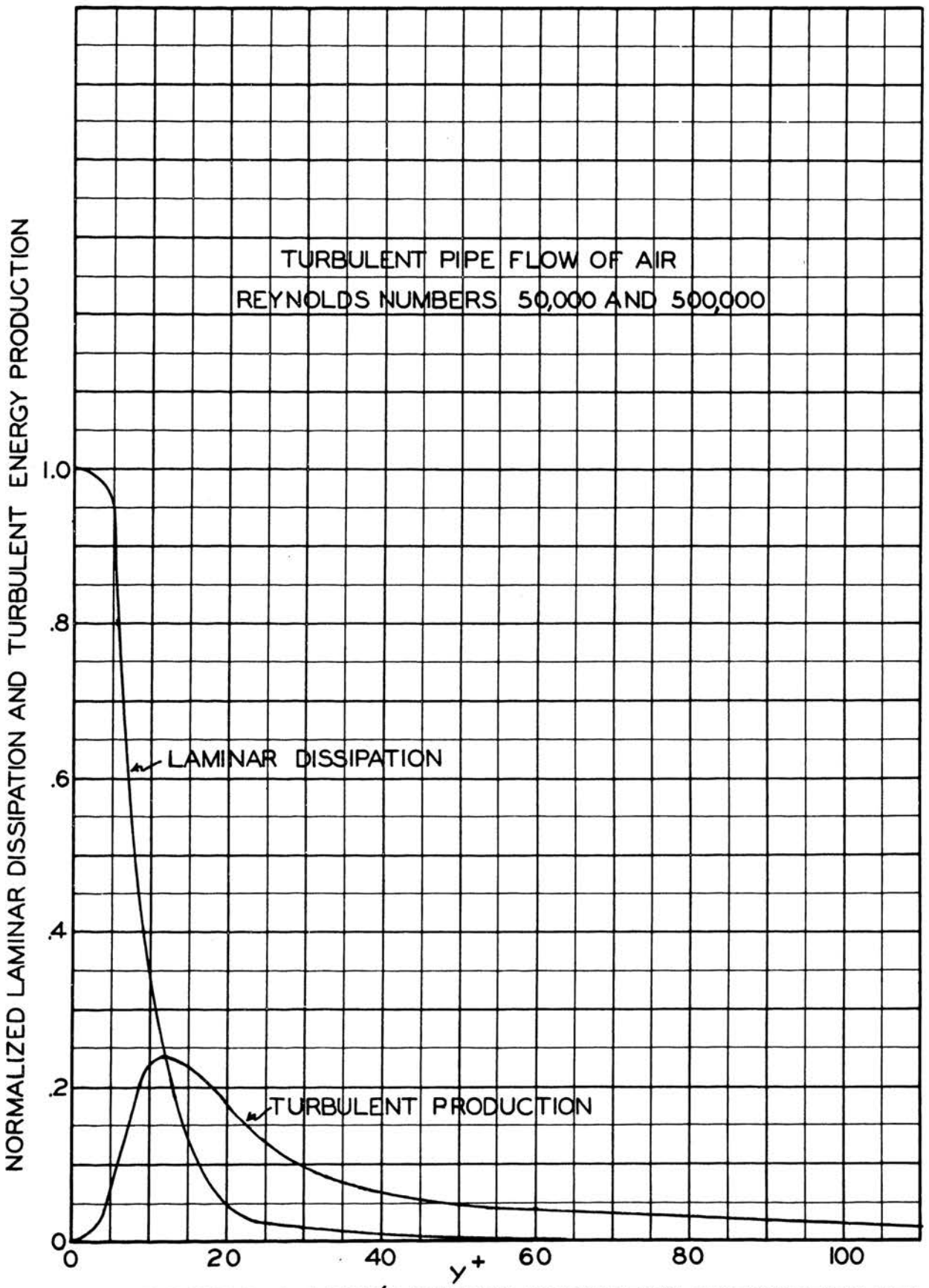


FIGURE 6. LAUFER'S ENERGY DISSIPATION DISTRIBUTION (47)

In order to study in detail the distribution of turbulent energy production and dissipation in pipe flow, it is necessary to consider the contributions of the various fluctuating terms to both the dissipation and diffusion of the energy. By adding the continuity equation, $\frac{\partial u_i}{\partial x_i} = 0$, multiplied by $u_j$, to the Navier-Stokes equation, the following result is obtained:

$$\frac{\partial u_i}{\partial t} + \frac{\partial}{\partial x_j}(u_i u_j) = -\frac{\partial \rho}{\partial x_i} + \mu \frac{\partial^2 u_i}{\partial x_j^2}, \tag{33}$$

for an incompressible fluid. When this equation is multiplied by $u_i$, the mechanical energy equation is obtained:

$$\frac{\partial u_i^2}{\partial t} + \frac{\partial}{\partial x_j}(u_i^2 u_j) = -2u_i \frac{\partial p}{\partial x_i} + \frac{\partial^2 u_i^2}{\partial x_j^2} - 2\mu\left(\frac{\partial u_i}{\partial x_j}\right)^2 \tag{34}$$

Laufer, assuming stationarity, wrote this equation in three components for cylindrical coordinates. He then followed the Reynolds averaging procedure with the sum of these three equations and obtained:

$$u'v'\frac{d\bar{u}}{dr} + \frac{1}{r}\frac{d}{dr}\, r\, \overline{v'\left(q + \frac{p}{\rho}\right)} = \frac{\mu}{\rho r}\frac{d}{dr}\left(r\frac{dq}{dr}\right)$$

$$+ \frac{\mu}{\rho r}\left(\frac{4}{r}\overline{w'\frac{dv'}{d\theta}} - \frac{\overline{(v')^2 + (w')^2}}{r}\right) - \frac{\mu}{\rho}\left(\overline{\frac{\partial u_i}{\partial x_j}}\right)\left(\overline{\frac{\partial u_i}{\partial x_j}}\right) \tag{35}$$

$$\text{where } q = \frac{1}{2}\left(\overline{(u')^2 + (v')^2 + (w')^2}\right)$$

The equation reads functionally as follows: the turbulent energy production + the radial diffusion of turbulent energy by radial velocity fluctuations = the radial diffusion of energy by the action of the velocity gradient + second order effect (usually neglected) + the viscous energy dissipation.

Laufer measured some of the terms in the turbulent energy balance equation for a pipe and assumed isotropy[1] to establish the others. He was

---

[1] Isotropic turbulence theory is reviewed later in this section.

able to measure $\overline{\left(\frac{\partial u'}{\partial z}\right)^2}$, $\overline{\left(\frac{\partial u'}{\partial r}\right)^2}$, $\overline{\left(\frac{\partial v'}{\partial z}\right)^2}$, $\overline{\left(\frac{\partial w'}{\partial z}\right)^2}$, $\overline{\left(\frac{\partial u'}{\partial \theta}\right)^2}$, q, $\overline{u'v'}$, $\frac{d\bar{u}}{dr}$, and $\overline{v'q}$. He assumed that:

$$\overline{\left(\frac{du'}{dr}\right)^2} = \overline{\left(\frac{\partial w'}{\partial r}\right)^2} = 2\,\overline{\left(\frac{\partial v'}{\partial r}\right)^2}$$
$$\overline{\left(\frac{\partial u'}{\partial \theta}\right)^2} = \overline{\left(\frac{\partial v'}{\partial \theta}\right)^2} = 2\,\overline{\left(\frac{\partial w'}{\partial \theta}\right)^2} \qquad (36)$$

By utilizing the above assumptions and disregarding the diffusion terms and integrating across the pipe cross section, Laufer obtained a check within 10 per cent of the dissipation calculated from pressure drop.

When the distributions of the nine turbulent energy dissipation terms are compared, it is found that the most important are $\overline{\left(\frac{\partial u'}{\partial r}\right)^2}$, $\overline{\left(\frac{\partial u'}{\partial \theta}\right)^2}$, and $\overline{\left(\frac{\partial u'}{\partial z}\right)^2}$. All the terms are at about the same level everywhere in the pipe except very near the wall ($r/a > 0.9$). Here the three important terms reach peak values which are about 35 times, 10 times, and 2.5 times the other terms, respectively. Thus, these three terms are responsible for most of the rise in turbulent energy dissipation near the wall.

The distribution of each of the terms of equation 35 for Laufer's data, show that the diffusion terms are small compared to the production and dissipation terms, which approximately balance at each point in the pipe.

It should be noted that by multiplying each of the energy terms by $(\mu/\rho u^{*4})$ and plotting the resulting dimensionless quantity versus $y^+$, Laufer's energy balance data near the wall for the two flow rates become a function of $y^+$ only.

The measurements made by Laufer in an effort to define the turbulent energy balance in pipe flow were done using hot-wire probes consisting of a fine resistance wire about 2 mm long which was electrically heated

above the ambient fluid temperature. The rate of heat transfer to the fluid was then a function of the fluid velocity across the wire, this function being directly measureable. The use and operation of the hot-wire anemometer and the hot-film modification are discussed in detail later.

The measurement most frequently made using the hot wire anemometer is the root mean square (rms) of the fluctuating velocity in a given direction. The intensity of turbulence is the root mean square fluctuating velocity divided by the average velocity at the point of measurement. Other ratios have been used, however, for pipe flow, these being the rms fluctuating velocity divided by friction velocity and the rms fluctuating velocity divided by the centerline velocity. These ratios are used in an effort to correlate the intensity data for different flow rates. Sanborn (81) found that the centerline longitudinal intensity of turbulence for air in 4-inch and 10-inch pipes and for a 5-inch channel are correlated to ± 10 per cent by the relation:

$$\frac{\langle u'_c \rangle}{\bar{u}_c} = 0.144\ Re^{-0.146} \tag{37}$$

A correlation of this form was made by Martin and Johanson (58) for the flow of water in a 6-inch pipe:

$$\frac{\langle u'_c \rangle}{\bar{u}_c} = 0.2415\ Re^{-0.189} \tag{38}$$

This correlation coincides with the Sanborn correlation at high Reynolds numbers ($Re > 60{,}000$), but is 16 per cent above it at a Reynolds number of 20,000. As will be shown later, the intensity data can be described as a function of position by correlating the rms fluctuating velocity divided by the friction velocity with a modified value of r/a.

The mean square of the fluctuating velocity is a normal Reynolds stress. The total Reynolds stress tensor can be written as:

$$\tau = \rho \begin{bmatrix} \langle u' \rangle^2 & \overline{u'v'} & \overline{u'w'} \\ \overline{v'u'} & \langle v' \rangle^2 & \overline{v'w'} \\ \overline{w'u'} & \overline{w'v'} & \langle w' \rangle^2 \end{bmatrix} \tag{39}$$

It has been shown above that the terms $\overline{w'u'}$, $\overline{v'w'}$, $\overline{w'u'}$, and $\overline{u'w'}$ do not appear in the equations for turbulent pipe flow. Also, it is easily shown that $\overline{u'v'} = \overline{v'u'}$. The terms $\rho\langle v' \rangle^2$ and $\rho\langle w' \rangle^2$ are the only normal stresses appearing in the equations. The data of Laufer (47) and Sanborn (81) show the dependence of $\langle u' \rangle$ (which does not appear in the equations of turbulent motion for pipe flow, equations 30 and 31), $\langle v' \rangle$, and $\langle w' \rangle$ on the radial position in the pipe. $\langle u' \rangle$ is much more dependent on radius than the other two normal stresses since it increases from about 0.03 $\bar{u}_c$ to about 0.1 $\bar{u}_c$ near the wall as shown in Figure 7. The terms $\langle v' \rangle$ and $\langle w' \rangle$ increase from about 0.03 $\bar{u}_c$ at the center to about 0.04 $\bar{u}_c$ near the wall. Though the normal stress $\rho\langle u' \rangle^2$ does not appear in the Reynolds equation for pipe flow, the importance of $\langle u' \rangle$ is in its contribution to the shear stress $\rho\ \overline{u'v'}$.

A point in a turbulent field having all three normal Reynolds stresses equal is said to exhibit isotropic turbulence. A turbulence field in which the three normal stresses do not change during translation is called homogeneous. A turbulent shear flow between flat plates or in a pipe is homogeneous in the direction of flow only, but is not truly isotropic anywhere. Flow in a pipe does approach isotropy near the center, however, as shown by Laufer's and Sanborn's data.

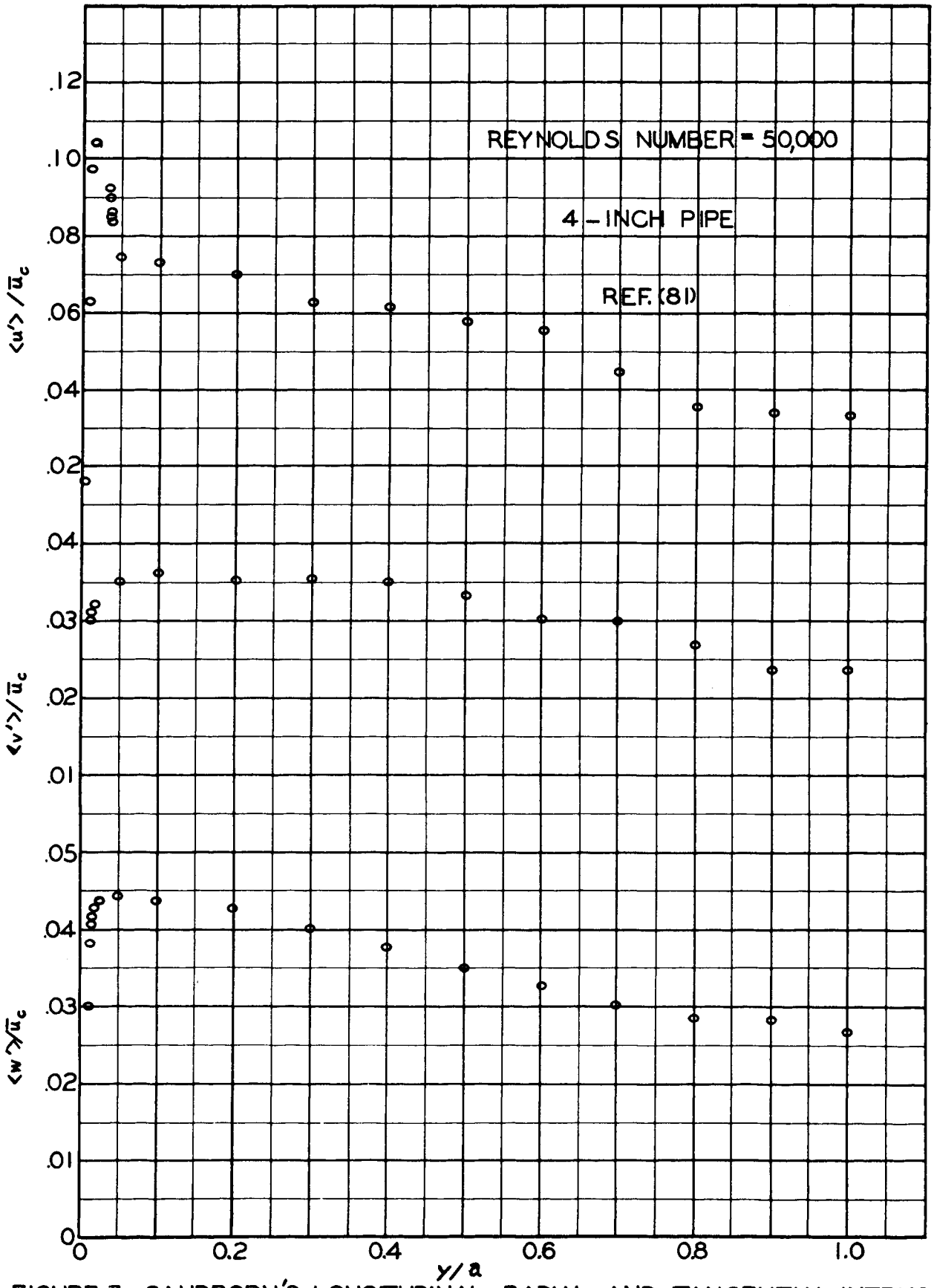


FIGURE 7. SANDBORN'S LONGITUDINAL, RADIAL, AND TANGENTIAL INTENSITIES

## 2.2. Time and space correlations

Much of the work in the theory of turbulence has been done utilizing the approximately isotropic field behind a uniform grid in a wind tunnel. Several diameters downstream of the grid the individual vortex trails of the bars merge to form an isotropic field homogeneous in the transverse direction. The decay of the turbulent eddies as they are carried downstream from the grid is representative of the decay with time when the turbulence producing agent is suddenly removed. By measuring various properties of this approximately isotropic turbulence, many of the mathematical consequences of isotropy have been experimentally demonstrated.

Taylor (92) introduced the Eulerian space correlation coefficient as a means of measuring the scale (average eddy size) of turbulence:

$$g(\delta) = \overline{u'(y)u'(y+\delta)}/\langle u'\rangle^2 \tag{40}$$

where $\delta$ is in the transverse direction. When $\delta=0$, $f(\delta)=1$. As $\delta$ increases $g(\delta)$ will drop toward zero, because the velocities at the two points will become more independent of one another. The scale of turbulence was defined by Taylor as:

$$Ly = \int_0^{\infty} g(\delta)\,d\delta \tag{41}$$

A correlation coefficient has also been defined for a spacing in the flow direction:

$$f(\delta) = \overline{u'(x)u'(x+\delta)}/\langle u'\rangle^2 \tag{42}$$

where $\delta$ is in the direction of flow.

The rate of viscous dissipation of turbulence energy per unit mass has been shown to be (34):

$$W = \frac{\mu}{\rho}\,\overline{\left(\frac{\partial u_i}{\partial x_j} + \frac{\partial u_j}{\partial x_i}\right)\left(\frac{\partial u_j}{\partial x_i}\right)} \tag{43}$$

Taylor showed that for isotropic turbulence:

$$W = 7.5 \frac{\mu}{\rho} \overline{\left(\frac{\partial u}{\partial y}\right)^2} \tag{44}$$

The transverse correlation coefficient may be expressed as a Taylor series (Brook Taylor):

$$g(\delta) = g(o) + \delta \left(\frac{\partial g}{\partial \delta}\right)_{\delta=0} + \frac{\delta^2}{2} \left(\frac{\partial^2 g}{\partial \delta^2}\right)_{\delta=0} + \ldots$$

For a homogeneous turbulence field it can be shown that the odd derivatives of $g(\delta)$ are zero (34), so:

$$g(\delta) = 1 + \frac{\delta^2}{2} \left(\frac{\partial^2 g}{\partial \delta^2}\right)_{\delta=0} + \frac{\delta^4}{4!} \left(\frac{\partial^4 g}{\partial \delta^4}\right)_{\delta=0} + \ldots$$

$$\left(\frac{\partial^2 g}{\partial \delta^2}\right)_{\delta=0} = - \frac{1}{\langle u' \rangle^2} \overline{\left(\frac{\partial u}{\partial y}\right)^2}_{\delta=0}$$

$$\left(\frac{\partial^4 g}{\partial \delta^2}\right)_{\delta=0} = + \frac{1}{\langle u' \rangle^2} \overline{\left(\frac{\partial^2 u}{\partial y^2}\right)^2}_{\delta=0}$$

The series thus becomes:

$$g(\delta) = 1 - \frac{\delta^2}{2\langle u' \rangle} \overline{\left(\frac{\partial u}{\partial y}\right)^2}_{\delta=0} + \frac{\delta^4}{4!\langle u' \rangle^2} \overline{\left(\frac{\partial^2 u}{\partial y^2}\right)^2} + \ldots \tag{45}$$

Taylor defined a microscale as follows:

$$\text{let } g(\delta)_{\delta \to 0} = 1 - \frac{\delta^2}{\lambda_g^2}$$

$$\text{then } \lambda_g^2 = \frac{2\langle u' \rangle^2}{\overline{\left(\frac{\partial u}{\partial y}\right)^2}_{\delta=0}} \tag{46}$$

This microscale is an indication of the average rate of change of u with distance. The microscale, $\lambda_f$, for the direction of flow may be defined in a similar manner.

The rate of isotropic energy dissipation may be expressed in terms of the microscale or the correlation function:

$$W = 15 \frac{\mu \langle u' \rangle^2}{\rho \lambda_g^2} = - 7.5 \langle u' \rangle^2 \frac{\mu}{\rho} \left( \frac{\partial^2 g}{\partial \delta^2} \right)_{\delta=0} \tag{47}$$

Karman and Howarth (38) extended Taylor's consideration of isotropic turbulence by defining a double correlation tensor:

$$R_{ij} = \frac{1}{\langle u' \rangle^2} \overline{u'_i u'_j(\delta)}, \text{ for } i,j = 1, 2, \text{ or } 3 \tag{48}$$

The equation of continuity was written in terms of $R_{ij}$, and the following relation obtained between $f(\delta)$ and $g(\delta)$:

$$f(\delta) - g(\delta) = - (r/2) \frac{\partial f(\delta)}{\partial \delta} \tag{49}$$

The applicability of this relation to grid induced turbulence has been demonstrated by Karman and Howarth by measuring both $f(\delta)$ and $g(\delta)$ and transforming $f(\delta)$ to $g(\delta)$, using equation 49.

Karman and Howarth also considered the triple correlations of velocity in isotropic turbulence. The various triple correlation coefficients are represented by:

$$T_{ijk} = \frac{1}{\langle u' \rangle^3} \overline{u'_i u'_j u'_k(\delta)} \tag{50}$$

where $u'_i$ and $u'_j$ are at the same point and $u'_k$ is separated by a distance $\delta$. Specific triple correlations relate to the direction of flow as shown below:

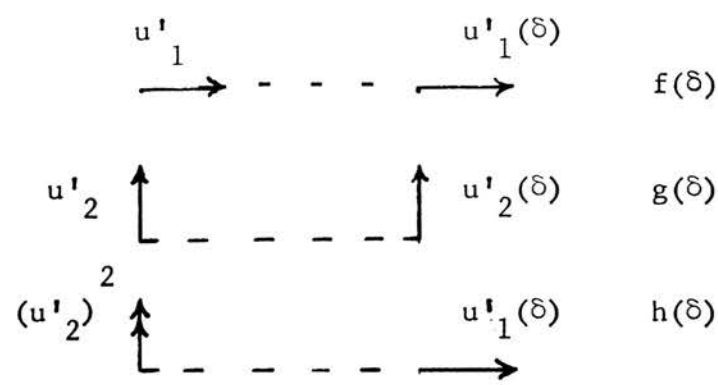

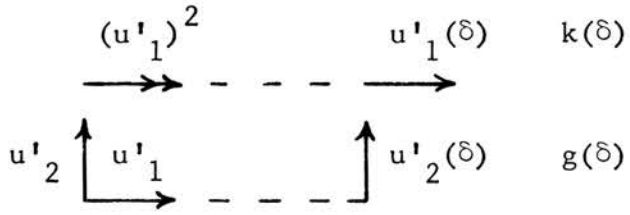


Double and Triple Correlations

Making use of the continuity equation, the relationship between k, h, and q is (38):

$$k = -2h$$

$$q = -h - (r/2)\frac{dh}{dr} \tag{51}$$

By forming triple correlations from the equation of motion, Karman and Howarth obtained a general relation for isotropic turbulence between the double and triple correlation tensors:

$$\frac{\partial}{\partial t}(\langle u'\rangle^2 R_{ik}) - \langle u'\rangle^3 \frac{\partial}{\partial x_j}(T_{ijk} + T_{kji}) = 2\frac{\mu}{\rho}\langle u'\rangle^2 \nabla^2 R_{ik} \tag{52}$$

From this equation, the relation between h and f was obtained by eliminating g, k, and q using the continuity equation:

$$\frac{\partial (f\langle u'\rangle^2)}{\partial t} + 2\langle u'\rangle^3 \left(\frac{\partial h}{\partial \delta} + \frac{4}{\delta} h\right) = 2\frac{\mu}{\rho}\langle u'\rangle^2 \left(\frac{\partial^2 f}{\partial \delta^2} + \frac{4}{\delta}\frac{\partial f}{\partial \delta}\right) \tag{53}$$

An equation for the dissipation of turbulent energy can be obtained from the Karman-Howarth equation for f and h (52). When $\delta=0$, $f=1$ and $\frac{dh}{d\delta} + \frac{4}{\delta} h=0$ because $q=h$. So:

$$\frac{\partial\langle u'\rangle^2}{\partial t} = 2\frac{\mu}{\rho}\langle u'\rangle^2 \left(\frac{\partial^2 f}{\partial \delta^2} + \frac{4}{\delta}\frac{\partial f}{\partial \delta}\right)_{\delta=0}$$

$$\text{using } f = 1 + 1/2\, f_o^{II}\, \delta^2 + \frac{1}{4!} f^{IV}\, \delta^4 + \ldots,$$

$$\frac{d\langle u'\rangle^2}{dt} = 10\frac{\mu}{\rho} f_o^{II} \langle u'\rangle^2$$

where $f_o^{II}$ and $f_o^{IV}$ are second and fourth distance derivatives at $\delta=0$,

respectively. Introducing Taylor's microscale:

$$\lambda_g^2 = -\frac{2}{g_o''} = -\frac{1}{f_o''}$$

$$\frac{d\langle u'\rangle^2}{dt} = -10\,\frac{\mu\langle u'\rangle^2}{\rho\,\lambda_g^2} \tag{54}$$

This is the rate of decay of the normal stress $\langle u'\rangle^2$ with time. The total turbulent energy is $q = 1/2\,(\langle u'\rangle^2 + \langle v'\rangle^2 + \langle w'\rangle^2)$,

so $W = -\frac{dq}{dt} = 15\,\frac{\mu\langle u'\rangle^2}{\rho\,\lambda^2_g}$ as above.

Other correlations may be formed for the fluctuating components of turbulent flow. In particular, the turbulent energy equation 35 for flow in a pipe involves the pressure-velocity correlation $\overline{v'p'}$. Laufer (47) did not measure this correlation because the technology for measuring high frequency pressure fluctuations has only recently been refined. Pressure-velocity correlations (6, 22, 101) and pressure spectra (15, 39, 100) have recently been made. Since these measurements are not pertinent to the research reported here, the reader is referred to the original literature for further discussion.

Taylor (94) postulated that if the turbulent velocity fluctuations are much smaller than the average velocity of flow the instantaneous velocity is the same function of $(\delta/\bar{u})$ as of time, that is:

$$u = \phi(t) = \phi(\delta/\bar{u})$$

This led Taylor to define the autocorrelation function:

$$R(\tau) = \frac{\overline{u\,(t)\;u\,(t+\tau)}}{\langle u'\rangle^2} \tag{55}$$

where $\tau = \delta/\bar{u}$. The equivalence of $R(\tau)$ to $f(\delta)$ has been demonstrated experimentally by Favre, Gaviglio, and Dumas (20). Their measurements were

made behind a grid in a wind tunnel, so the turbulence was probably nearly isotropic. Lin (53) has stated that the Taylor hypothesis is not generally valid in shear flows, because of the increased importance of the convective terms in the equation of motion. Care must be exercised, therefore, in the interpretation of autocorrelations in turbulent boundary layers.

More can be learned about the movement of large eddies by the mean flow through the use of time-space correlation. Favre, et al, and Baldwin and Walsh (2) have measured space correlations using variable time delays on one of the velocity signals. In this way the movement of an eddy (represented by the time correlation at each point) can be represented by a map of the lines of constant correlation on time-distance coordinates. If the Taylor hypothesis were strictly true for long times, the time-space map of the longitudinal correlation would be a single straight line. Since eddies are continually decaying and being replaced by others, the map of constant correlation coefficient consists of elongated ellipses, with the highest correlation at the center. Baldwin and Walsh have suggested that the locus of maxima for the time-space correlation curves is very close to the Lagrangian correlation coefficient. They show some similarity (even though the curve shapes are definitely different) by plotting these maxima versus time on the same graph with the Lagrangian correlation calculated from heat transfer measurements. A possible criticism of the comparison is that the Lagrangian correlation measured by heat transfer is for the radial direction, whereas their time-space measurement is a longitudinal correlation. One set of Favre's data is a transverse time-space correlation ($\delta$ is in radial direction). When the maxima

for these correlations are plotted, the curve shape is identical to the transverse (radial) Lagrangian correlation of Baldwin and Walsh.

The relationship between the Lagrangian correlation coefficient and the Eulerian correlation coefficient has not been defined mathematically. Experimental evidence showing the relationship suggests that the shapes of the correlation curves are very similar for the same flow conditions. Mickelsen (63) and Uberoi and Corrsin (96) have shown that the Eulerian and Lagrangian length scales have ratios of 0.5 to 0.8 in the range $10 < Re_L < 100$, where $Re_L$ is a Reynolds number using Eulerian length scale as the distance. Baldwin and Walsh (2) have found that comparisons of Eulerian autocorrelations to Lagrangian radial correlations gave almost constant ratios of Eulerian length to Lagrangian length at the same correlation coefficient for a given velocity. Their ratios of length scale are much higher than 0.8, however, probably because of the comparison of a longitudinal Eulerian scale to a radial Lagrangian scale.

## 2.3. Turbulent energy spectra

The most detailed description of the turbulence at a point is the energy spectrum, defined as $\frac{2}{3}\frac{dq}{dk}$ as a function of k, the wave number. Since $q = 1/2\ (\langle u' \rangle^2 + \langle v' \rangle^2 + \langle w' \rangle^2)$:

$$3E(k) = 2\frac{dq}{dk} = \frac{d\langle u' \rangle^2}{dk} + \frac{d\langle v' \rangle^2}{dk} + \frac{d\langle w' \rangle^2}{dk} \tag{56}$$

The spectrum measureable using a hot-wire anemometer is called the one-dimensional spectrum and is simply one component of E(k). For example:

$$E_x(k) = \frac{d\langle u' \rangle^2}{dk} \tag{57}$$

The normalized one-dimensional energy spectrum is $F_x(k) = E_x(k)/\langle u' \rangle^2$.

If the turbulence is isotropic, a three-dimensional[1] spectrum of turbulence may be defined which includes contributions from those velocity components in one direction only, that is, no partial contributions from other directions are included. The relation between the one-dimensional and three-dimensional spectrum is as follows (52):

$$E_x(k) = 3/2 \int_k^\infty (k'^2 - k^2)\, E(k')dk'/k'^3 \tag{58}$$

$$\text{or} \quad E(k) = 1/3\, (k^2 E_x^{II}(k) - k\, E_x^{I}(k)) \tag{59}$$

where E(k) is defined such that:

$$\int_o^\infty E(k)dk = \int_o^\infty E_x(k)dk = \langle u' \rangle^2$$

The concept of the three-dimensional spectrum is needed because the theories of energy transfer from wave number to wave number are formulated in its terms. The application of the theory to the results of the experimental work to be described, however, will be in terms of the measureable one-dimensional spectrum. Examination of equation 59 reveals that any linear regions in the log-log one-dimensional spectrum ($\log E_x^{II}$ ($\log k$) = 0) have the same slope as the corresponding linear log-log three-dimensional spectrum. This fact will be used in subsequent comparisons.

Taylor (94) first showed that the normalized one-dimensional spectrum is simply the Fourier cosine transform of the correlation function, f(δ), if the Taylor hypothesis is valid:

$$\begin{aligned} f(\delta) &= \int_o^\infty F_x(k)\cos k\delta\, dk \\ F_x(k) &= \frac{2}{\pi}\int_o^\infty f(\delta)\cos k\delta\, d\delta \end{aligned} \tag{60}$$

---

[1] The term "spherical" spectrum is clearer to the author, since spherical coordinates are used to determine the relation between this spectrum and the one-dimensional spectrum.

Expressed in terms of frequency and autocorrelation, these equations become:

$$R(\tau) = \int_o^\infty F_x(n) \cos 2\pi n\tau dn$$

$$F_x(n) = 4\int_o^\infty R(\tau) \cos 2\pi n\tau d\tau \tag{61}$$

If the expression, equation 60, for $f(\delta)$ is differentiated with respect to $\delta$ (where $F_x(k)$ is not a function of $\delta$):

$$\frac{\partial f(\delta)}{\partial \delta} = -\int_o^\infty F_x(k) k \sin k\delta \, dk$$

$$\frac{\partial^2 f(\delta)}{\partial \delta} = -\int_o^\infty F_x(k) k^2 \cos k\delta \, dk$$

Combining this result with equation 47 for the turbulent dissipation of energy in isotropic turbulence using the relation (34) that $\left(\frac{\partial^2 g}{\partial \delta^2}\right)_{\delta=0} = 2\left(\frac{\partial^2 f}{\partial \delta^2}\right)_{\delta=0}$:

$$W = -15 \frac{\mu}{\rho} \langle u' \rangle^2 \left(\frac{\partial^2 f}{\partial \delta^2}\right)_{\delta=0} = 15 \frac{\mu}{\rho} \int_o^\infty E_x(k) k^2 \, dk \tag{62}$$

The dissipation spectrum is, therefore, defined as:

$$D(k) = \frac{\rho}{15\mu} \frac{\partial W}{\partial k} = E_x(k) k^2 \tag{63}$$

This is also called the vorticity spectrum because $\langle \omega_x \rangle^2 = 5\langle u' \rangle^2 f_o^{II} = -5 \int_o^\infty E_x(k) k^2 \, dk$, where $\omega_x$ is the vorticity, $\left(\frac{\partial w'}{\partial y} - \frac{\partial v'}{\partial z}\right)$ (75a).

Since the microscale, $\lambda_f$, is related to $f_o^{II}$ (34), it may be found from a spectrum measurement:

$$\lambda_f = \frac{\sqrt{2} \langle u' \rangle}{\left[\int_o^\infty E_x(k) k^2 \, dk\right]^{1/2}} \tag{64}$$

All the above relations may be expressed in terms of frequency through

the relation $k = 2\pi n/\bar{u}$.

2.4. Turbulent energy transfer hypotheses

The primary objective of the study of turbulence spectra is the formulation of a general theory predicting the spectra using a minimum of parameters. The cosine transform of the Karman-Howarth equation results in the spectral energy balance (52):

$$\frac{\partial E(k)}{\partial t} - T(k) = - 2 \frac{\mu}{\rho} k^2 E(k) \tag{65}$$

The first term is the rate of change of the spectrum with time at wave number k, the second term is the transfer of energy to wave number k, and the right side is the rate of viscous dissipation at k. The transfer term is composed of terms involving the triple correlation $h(\delta)$, but since various hypotheses of a simpler nature are of primary concern the Karman-Howarth form will not be discussed here.

The simplest of the well known transfer hypotheses is the Kovasznay (45) "local transfer" theory:

$$T(k) = - 2K_k \frac{d}{dk} (k^{5/3} E(k)^{3/2}) \tag{66}$$

Obukhoff (66) proposed the "shear transfer" theory:

$$T(k) = - 2K_o \frac{d}{dk} \int_k^\infty E(k')dk' \left[ \int_o^k k'^2 E(k')dk' \right] \tag{67}$$

The most thoroughly tested energy transfer hypothesis is that of Heisenberg (32):

$$T(k) = -2K_h \int_k^\infty \sqrt{E(k')/k'^3}\, dk' \left[ \int_o^k k'^2 E(k')\, dk' \right] \tag{68}$$

For values of k such that $\int_o^k E(k')dk' \gg \int_k^\infty E(k')dk'$, $\frac{\partial}{\partial t} \int_o^k E(k')dk' \approx \frac{W}{3}$ (75a). The expression for the energy spectrum using the Heisenberg hypothesis is then:

$$3E(k) \approx \left(\frac{8W}{9K_h}\right)^{2/3} k^{-5/3} \left(1 + \frac{8\mu^3 k^4}{3K_h^2 \rho^3 W}\right)^{-\frac{4}{3}}$$

So for $(3K_h^2\rho^3W/8\mu^3)^{1/4} \gg k$, this reduces to:

$$3E(k) \approx \left(\frac{8W}{9K_h}\right)^{2/3} k^{-5/3} \tag{69}$$

If $k \gg (3K_h^2\rho^3W/8\mu^3)$, then

$$3E(k) \approx (K_h W \rho^2/2\mu^2)^2 k^{-7} \tag{70}$$

Kolmogoroff (43) arrived at the $k^{-5/3}$ law for energy transfer in the inertial range (where little dissipation takes place) by dimensional arguments. He also defined a length scale, $\lambda_k = (\mu^3/\rho^3 W)^{1/4}$, or a characteristic wave number, $k_k = 1/\lambda_k$, which is a parameter in his universal equilibrium spectrum for very high wave numbers (in the dissipative range):

$$E(k) = W^{2/3} k^{-5/3} A(k/k_k) \tag{71}$$

Kolmogoroff's analysis did not determine the form of the function A. A basic assumption of Kolmogoroff in the formulation of the spectrum function for the universal equilibrium range was that the velocity fluctuations at high wave number approach isotropy. This has been supported experimentally by Laufer (46). He measured the spectrum of both the normal stress $\rho\langle u'\rangle^2$ and the shear stress $\rho\,\overline{u'v'}$ in a channel. The spectrum for $\overline{u'v'}$ became nearly zero at frequencies far lower than for the normal stress. Since the shear stress for isotropic turbulence is zero, the high wave number spectrum must have been isotropic.

A number of investigators have confirmed the $k^{-5/3}$ law for several different types of turbulence. Gibson (24) obtained a $k^{-5/3}$ spectrum for a jet of air. He also obtained data supporting the universal spectrum. About the same time Gibson and Schwarz (25) published data yielding the $k^{-5/3}$ inertial energy transfer region for the flow of water behind a

grid (yielding nearly isotropic turbulence). Their data were combined with data of Stewart and Townsend (89) and the data of Grant, Stewart, and Moilliet (30) to show the existence of the universal spectrum at high wave numbers. The data were plotted as $E_x(k)k_k^3(\mu/\rho W)$ versus $k/k_k$ and became single valued at a wave number ratio of about $10^{-1}$ to $10^{o}$ with a log-log slope of -7. This is very strong support for the Heisenberg hypothesis (equation 70). The Stewart and Townsend data are for turbulent air behind a grid, and the Grant, Stewart, and Moilliet data are for the very high Reynolds number turbulence in tidal flow of sea water. The latter data were obtained using a probe mounted on a torpedo towed beneath a ship.

Betchov (3) obtained the $k^{-5/3}$ spectra for flow of air into a duct from a porcupine box[1]. After applying wire length correction factors to his data, however, the high wave number region exhibited a log-log slope of -6, instead of the -7 slope of the uncorrected data. Deviation from the Heisenberg hypothesis was also shown by the data of Tanenbaum (90). He showed a slightly better fit using the more complicated model of von Karman for energy transfer. This is to be expected because the von Karman model is a generalized version of the Heisenberg model and includes three adjustable parameters instead of one.

Pao (69) formulated a new energy transfer hypothesis for the high wave number region, based on a cascade model for energy transfer to higher wave numbers. The energy flux in wave number space is set equal to the product of the energy at k and the rate of increase of k. The rate of

---

[1] Many jets protruding into the box from all directions.

increase of k, $\frac{dk}{dt}$ , was given by dimensional reasoning as:

$$\frac{dk}{dt} = \alpha^{-1} W^{1/3} k^{5/3}$$

where $\alpha$ is a constant. This yields a transfer function:

$$T(k) = - \frac{d}{dk} (\alpha^{-1} W^{1/3} k^{5/3} E(k))$$

Pao then obtained the following expression for the universal equilibrium spectrum:

$$E(k) = \alpha W^{2/3} k^{-5/3} \exp(- 3/2\alpha W^{-\frac{1}{3}} k^{4/3} \mu/\rho) \qquad (72)$$

This expression fits all the above data for $k/k_k$ above $10^{-3}$. As k approaches zero, E(k) becomes proportional to $k^{-5/3}$. At high k the spectrum is approximately proportional to $k^{-7}$.

A large portion of the effort devoted to the study of energy spectra has been associated with attempts to formulate laws for turbulence decay behind a grid. In the case of steady flow in a conduit, however, the time derivative of the spectrum function in equation 65 becomes zero, and the energy balance is:

$$T(k) = 2 \frac{\mu}{\rho} k^2 E(k) \qquad (73)$$

Since $E(k) = 1/3(k^2 E_x^{II}(k) - k E_x^{I}(k))$, equation 73 may be expressed in terms of the one-dimensional spectrum in isotropic turbulence as follows:

$$T(k) = \frac{2}{3} \frac{\mu}{\rho} (k^4 E_x^{II}(k) - k^3 E_x^{I}(k)) \qquad (74)$$

The energy transfer function must then balance the dissipation spectrum. This relationship will be used in the treatment of the experimental spectra for the flow of drag reducing solutions described later.

3. The Measurement of Statistical Turbulence Phenomena

In order to obtain a mechanistic picture of turbulence in ordinary viscous fluids and in drag reducing fluids, it is necessary to obtain a

detailed experimental description of the occurrences the turbulent field. This means that techniques are needed to measure instantaneous velocity and instantaneous pressure as a function of time at any point. In general this is not possible, but may be approached.

Hot-wire or hot-film anemometers can be used to measure one component of velocity. Two components can be measured simultaneously using an X-wire anemometer probe. In addition to the limitation to measuring velocity components only, the frequency response of the anemometer system causes an attenuation of high frequency fluctuations. The successful use of hot-surface anemometry involves proper matching of anemometer frequency characteristics and turbulent field properties to obtain the desired information.

The measurement of rapid pressure fluctuations is not nearly as well developed as the measurement of fluctuating velocities. The best developed method involves the use of a piezoelectric crystal which generates a voltage signal as a function of pressure. It is difficult to make crystals small enough to have good space resolution with high sensitivity. The size of piezoelectric crystal required is usually much larger than the microscale of liquid turbulence in pipes. Eagleson and Perkins (16) have used a probe with a piezoelectric crystal inside a necked-down impact tube, but frequency response was limited by the restriction. Fluctuating pressure measurements will not be discussed in detail here, since none were made in this study.

### 3.1. Hot-surface anemometry

Hot-surface anemometry is based on the effect of fluid velocity on the heat transfer from a surface to a fluid. The most common surfaces are wires perpendicular to the flow, metal films plated on various shaped

probes, and metal films plated on surfaces mounted flush with the flow boundary. The wires or films are heated by an electrical current. Since the electrical resistance of the wire or film rises with temperature, resistance is used as an indication of surface temperature.

The rate of heat transfer from a cylinder perpendicular to the flow is adequately described for use in anemometry by the equation of King (29), which relates Nusselt number to Reynolds number:

$$Nu = A + B\ Re^{0.5} \tag{75}$$

This equation is also of the proper form for use with wedge type hot-film anemometer probes. For the calibration of hot-surface anemometers, it is necessary to relate the electrical power input to the probe to the instantaneous velocity of the fluid. This is usually expressed as (34):

$$i^2R/(R - R_0) = A' + B'\ u^{0.5} \tag{76}$$

where R is the probe operating resistance and $R_0$ the probe resistance at fluid temperature. The physical properties in the Nusselt and Reynolds numbers are absorbed into the calibration constants A' and B'. The value of R increases with temperature increase.

There are two common operating modes for hot-surface anemometry. The first, which was for many years the only practical mode, is constant current operation. This mode is applicable only to fine wires as shown below. The second mode of operation is the constant temperature or constant resistance mode in which the current is varied to maintain constant probe temperature.

In the constant current method the current, i, is held constant and the value of the wire resistance, R, is determined by the equilibrium wire temperature. If the wire is incorporated in a resistance bridge, this value of R may be measured. By measuring i with the bridge balanced for

several different velocities, A' and B' may be determined. The time average of equation 76 for turbulent flow is of the same form if the turbulence intensity is low. The time average velocity may be measured after A' and B' are known by measuring the i required to obtain a predetermined value of R. This method is usually more accurate than the simpler method of measuring bridge unbalance voltage for fixed i (29).

In order to measure the velocity fluctuations in turbulent flow, it is necessary to relate the resistance fluctuation of the wire to the velocity. If a large resistance is inserted in the supply current to the bridge containing the hot-wire, the current will remain constant despite small variations in wire resistance, which occur when velocity fluctuations cause wire temperature fluctuations. If $R = \bar{R} + R'$ and $u = \bar{u} + u'$ in equation 76, the following equation is obtained after some rearrangement (34):

$$\langle E' \rangle = i\langle R' \rangle = - (\bar{R} - R_o)^2 \, B' \langle u' \rangle / 2iR_o\sqrt{\bar{u}} \qquad (77)$$

where E' is the fluctuating voltage when the bridge is balanced for average wire resistance. By calibrating the wire to obtain the value of B', the root-mean-square (rms) velocity may be calculated from the measurement of the root-mean-square (rms) bridge voltage using equation 77.

The most serious performance problem inherent in the constant current technique is the attenuation of high frequency temperature fluctuations by the mass of the hot sensor. The necessity of using a low mass sensor limits the use of the constant current method to fine wires. The frequency response generally drops off with increasing frequency starting at about 100 cps (29). In order to extend the frequency response it is necessary to incorporate a compensation circuit in the bridge. In this manner the region of fairly flat frequency response can be extended to several thousand cycles per second.

Many difficulties are encountered in the use of wire probes for the measurement of velocity fluctuations in liquids (56). The small size and low strength of the wire probes limits their use in liquids to low velocities. (The author, however, used a 0.005 mm platinum plated tungsten wire 1 mm long in organic solvents at velocities up to 10 feet per second without breakage). A much more serious problem is the tendency of lint particles to wrap around the wire. Since large liquid pumping systems are very difficult to maintain completely free of lint, the wire quickly becomes covered, drastically affecting the calibration of the probe.

The wedge film probe developed by Ling (56, 57) is much more suitable for measurements in liquids because of the great strength of the probe and because the configuration allows lint to be swept away by the stream. The probe consists of a $30^{o}$ wedge of glass plated with platinum at the leading edge. The entire probe looks somewhat like a small screwdriver as shown in Figure 8. The electrical connections are usually gold or silver strips plated on the glass support from each end of the platinum plated wedge to the probe support leads. The dimensions of the platinum plated wedge are usually about 1 mm long (transverse to flow direction) and 0.2 mm wide (in flow direction).

The high frequency response of a film probe would be severely attenuated if it were used in the constant current mode, since the large mass of the glass support has a high heat capacity. For this reason film probes are used in the constant temperature mode of operation to extend their frequency response. This method requires the use of a feedback circuit which limits probe temperature variation to an insignificant amount. The anemometer makes use of the bridge balance technique in a slightly different manner than the constant current anemometer. In the

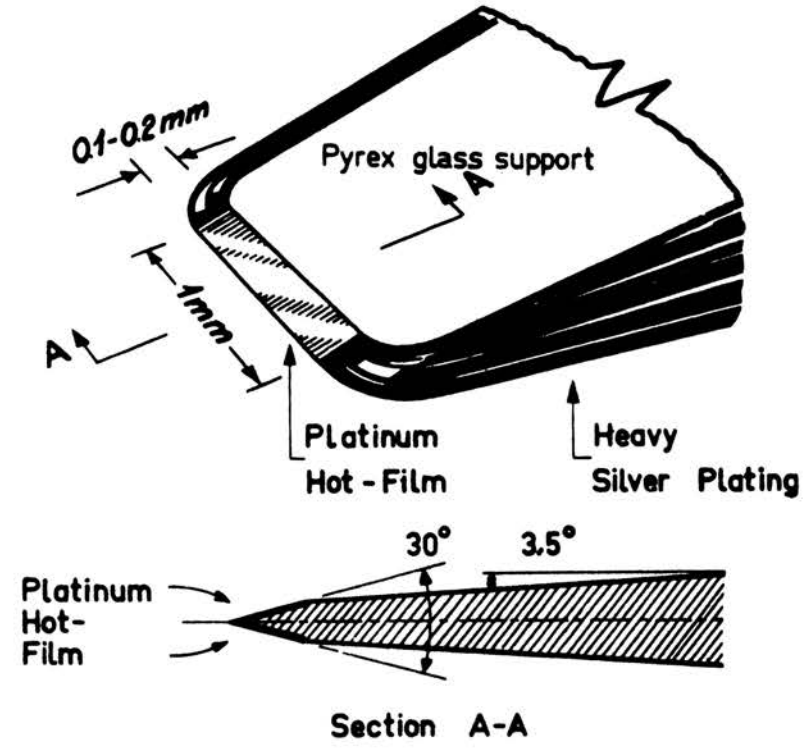


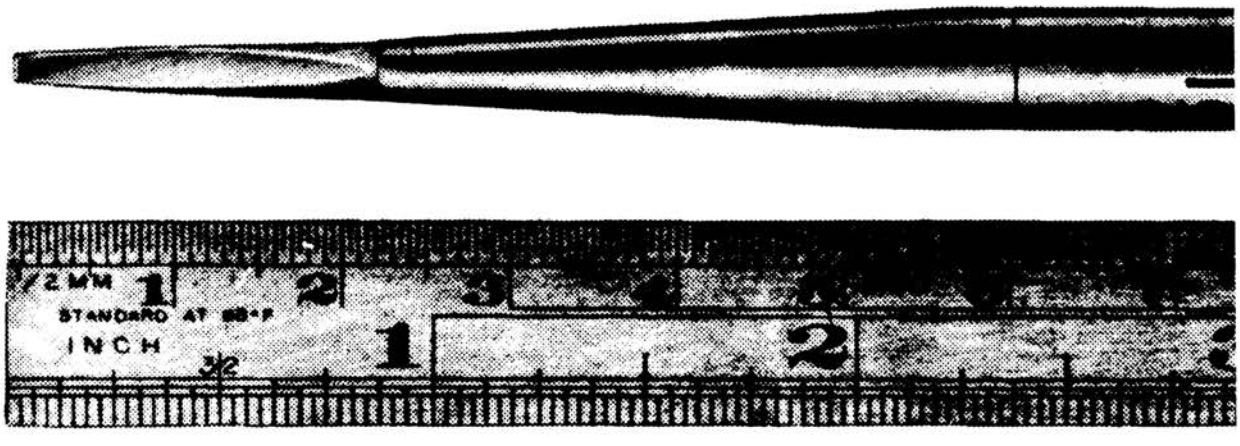


FIGURE 8. HOT-FILM PROBE

constant current anemometer the bridge is balanced for the measurement of time average velocity, but fluctuating components are indicated by the fluctuation of the probe voltage about the average. Although the bridge is in a time average balanced condition, it is not balanced during fluctuations from the average. The constant temperature anemometer utilizes a balanced bridge for the measurement of both fluctuating velocity and time average velocity. The bridge is maintained in balance by the feedback circuit which varies the bridge current to hold the probe temperature at the level required to give a preset resistance.

The balanced bridge mentioned above is not precisely balanced at all times. When the instantaneous velocity varies from the time average velocity, the bridge becomes slightly unbalanced. This unbalance is amplified by the feedback circuit, which then alters the bridge current in the direction required to restore balance. As with all amplifier feedback controllers, this system is prone to overcontrol and oscillate when improperly adjusted. Amplifier instability causing such oscillations hampered the development of the constant temperature anemometer until very recently (67). The development of successful circuits has been well covered in the literature (48, 49, 67, 99) and will not be discussed here.

Calibration of the constant temperature anemometer is straightforward. It can be conveniently done during the measurements of turbulence intensity in a stream where several known local velocities are used. This autocalibration procedure allows operation in dirty streams where occasional calibration changes occur because of particle impact. If three or more different velocities have been used since the last calibration change, a new calibration can be established. Equation 76 can be written:

$$E^2 = A + B\,u^c, \tag{78}$$

since $(R - R_o)$ is a constant value for a given overheat ratio, $R/R_o$. The overheat ratio is determined by the bridge resistance setting which must be matched by the probe resistance. The exponent, c, generally is not equal to 0.5 for liquids. It decreases in value for polymer solutions of increased viscosity, as will be seen. In this equation $\sqrt{A}$ is the voltage drop across the bridge for zero flow rate. The voltage drop across the bridge, E, is proportional to bridge current.

If the velocity fluctuations are small compared to the average velocity, the rms turbulent velocity fluctuation can be calculated from the rms bridge voltage fluctuation and the slope of the curve represented by equation 78 at the flow rate of interest:

$$u' \approx E'/(dE/d\bar{u})$$
$$\text{so } \langle u' \rangle \approx \langle E' \rangle/(dE/d\bar{u}) \tag{79}$$

This relation is usually accurate for turbulence intensities ($\langle u' \rangle/\bar{u}$) up to 10 per cent, and is only slightly in error for values as high as 20 per cent when using the flat part of the calibration curve. Care must be exercised, however, to make sure that the curvature of the calibration curve, E versus $\bar{u}$, is small at the point of interest. Linearizers which allow the measurement of a modified rms bridge voltage proportional to $\langle u \rangle$ without regard to curvature are coming into use.

Of utmost importance in hot-surface anemometry, particularly in the measurement of turbulence spectra, is the maintenance of a low noise to signal ratio. The tendency for feedback oscillation in the constant temperature anemometer has already been mentioned, but will not contribute to the noise if properly adjusted. Other noise sources within the circuit are more difficult to recognize and must be kept low through the use of sophisticated components.

The condition opposite to oscillation is undercontrol. The sensitivity of the bridge to inbalance must be run as high as possible without causing instability. The slight unbalance necessary to cause a feedback signal is not measured as a fluctuating voltage and represents a loss in measured turbulence intensity. This signal loss increases with frequency, since the response is a frequency dependent function. The typical response of a well adjusted DISA constant temperature anemometer with a hot-film in air flow is shown in Figure 9.

3.2. Turbulence measurements

The turbulence measurements made by Laufer and Sandborn for air flowing through large pipes have already been discussed. A number of measurements in air for other configurations have also been made, but will not be mentioned here because they have no direct bearing on this work.

Few turbulence measurements in liquids have been made, as the development of the hot-film anemometer was quite recent and interest in these measurements is just developing. All but one of the liquid turbulence investigations previous to the work described in this thesis were made in water, the earliest being those measurements made by Ling (56) during his development of the hot-film probe. His test measurements were made on a turbulent water jet.

Grant, Stewart, and Moilliet (30) made their measurements in a tidal channel (Discovery Channel, Canada) using a conical film probe. The platinum film was a tapered ring plated around the tip of the cone. In order to avoid probe current leakage and polarization in the sea water, it was necessary to use alternating current probe potential under 1.2 volts. The anemometer was the constant temperature type.

The probe signal was analyzed to determine the spectrum function during the tidal flow. The spectrum tended to support the existence of

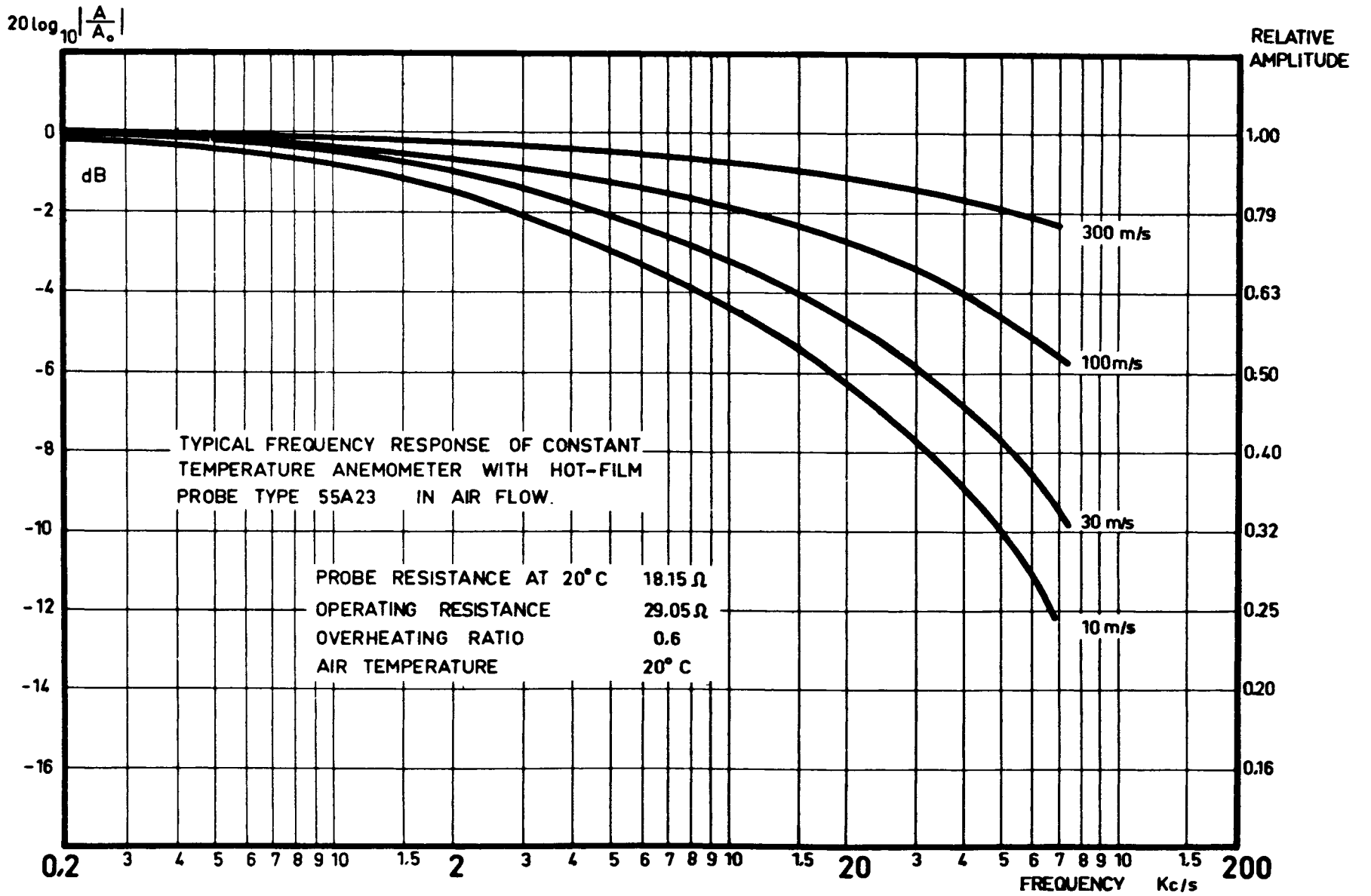


FIGURE 9. FREQUENCY RESPONSE OF HOT-FILM ANEMOMETER

the inertial subrange with a slope of $k^{-5/3}$ as proposed by Kolmogoroff. The high wave number region of the spectrum had a slope of $k^{-7}$, as expected from the Heisenberg transfer hypothesis.

A more comprehensive comparison of spectra with the concepts of Kolmogoroff was made by Gibson and Schwarz (25). Using their data for the flow of water behind a turbulence inducing grid, the data of Grant, Stewart, and Moilliet, and the data of Steward and Townsend for air, Gibson and Schwarz demonstrated excellent experimental support for both the inertial subrange and the universal equilibrium range. The data were normalized by plotting $E_x(k)k_k^3\nu/W$ versus $k/k_k$, where $k_k$ is the Kolmogoroff microscale. This normalization caused the spectra above $k/k_k$ of 1 to coincide with a slope of $k^{-7}$. The inertial subrange lay below $k/k_k$ of $10^{-1}$ with a slope of $k^{-5/3}$.

Gibson and Schwarz's measurements were made with a 1 mm X 0.2 mm wedge type film probe made by Lintronics. The purity of the water was high enough to avoid current leakage.

The work mentioned above was done with spectrum measurement as the primary objective. Measurements of the intensity of turbulence in water have been made by Rosler and Bankoff (79) for the flow of a jet into a large tank of water. These measurements were made using a Lintronics film probe and defined the intensity profiles at axial distances up to thirty diameters from the jet outlet. The data were very similar to air jet data taken previously by Corrsin and Uberoi (11). These data, however, are difficult to relate to pipe flow of liquids, which is of primary interest here.

Lee and Brodkey (50) measured the longitudinal intensity of turbulence in the pipe flow of water using a Lintronics film probe. The intensity,

energy spectrum, and microscale were measured in a 3.068-inch polyethylene pipe. The intensity data obtained are questionable because the investigators experienced calibration drift during their measurements causing a slight peak at the pipe center. This is commonly experienced in measurements in water with an uncoated probe. Lee and Brodkey obtained a microscale at the center of the pipe of 0.092 inches at a Reynolds number of 50,000. Their spectrum at the pipe center is compared with spectra determined in this investigation in Figure 52.

Corino and Brodkey (10a) have recently measured turbulence intensities in the turbulent flow of trichloroethylene in conjunction with visual studies of the turbulence in the boundary layer. Their data are not yet available to the author, however, so they cannot be discussed in detail.

The measurement of turbulence intensity in water by Martin and Johanson (58) has been mentioned above. They also measured the autocorrelation function at Reynolds numbers between 19,000 and 160,000 in a 6-inch pipe. They calculated macroscales from the autocorrelation functions and correlated the values with Reynolds number. The correlation is discussed in detail in section 6.4.

The most complete investigation of the longitudinal intensity of turbulence was done by Lindgren (54). His measurements were made with a film probe with a 2 mm long film in a 127 mm pipe. In order to obtain measurements of mean velocity and turbulence intensity near the wall, Lindgren cut a groove in the pipe wall deep enough to allow the probe tip to approach the wall very closely. Unfortunately his data were quite scattered even though they were in general agreement with Laufer's data for air flow in a 10-inch pipe. Lindgren measured intensity profiles for Reynolds numbers of 5500 to 51,000. Having strong Reynolds number effects, they did not correlate well when $\langle u \rangle / u^*$ was plotted versus r/a.

## 4. Viscoelastic Theories of Drag Reduction

A number of the fluids whose turbulent friction factors and velocity profiles were discussed above have been shown to exhibit elastic properties in laminar flow. This led Dodge (14) to postulate that the anomalous results he obtained in his friction factor measurements in CMC-water solutions were caused by elasticity. Savins (83) has reviewed the drag reduction literature and concluded that the elasticity of the polymer solutions studied caused the turbulent fluctuations to be damped. Savins did not propose quantitative expressions to describe the damping postulated. Some evidence of turbulence damping has been experimentally observed by Shaver (85) and Meter (59) in dye injection experiments. Meter recognized the need to correlate drag reduction with elasticity in a quantitative manner. Using a cone-and-plate rheogoniometer and a vibrating rod (0.1-400 cps Birnboim-Ferry apparatus), Meter measured elastic phenomena in Natrosol, CMC, and Carbopol solutions. He obtained higher elasticities for Carbopol (non-drag reducing in turbulent flow) than for CMC at infinitesimal rates. This anomaly was attributed to gel formation in the Carbopol solutions.

Meter devised an empirical correlation based on the ratio of wall shear stress to the shear stress $\tau_{1/2}$ at $\mu_o/2$ for his Natrosol solution friction factor data, where $\mu_o$ is the zero shear viscosity of the solution. This correlation was recognized by Meter to lack generality because $\tau_{1/2}$ does not exist for dilute solutions. It may also be criticized for a more basic defect. This correlation implies that elastic phenomena may be correlated as a function of solution viscosity. The elastic phenomena for a given polymer in solution may be a single-valued function of solution viscosity, if elasticity and viscosity are related to concentration in the same way. On this basis Fabula (19) was able to relate the drag reduction of a series of Polyox-water solutions to the intrinsic viscosity, which is a function of molecular size in solution.

Correlations of this type, however, have not been shown to be generally applicable to different polymer-solvent systems.

One of the properties of viscoelastic liquids which is frequently measured is the normal stress phenomenon in shear flow. Normal stresses in laminar flow through a capillary tube will be discussed here, since capillary tube flow can yield the high shear rates of interest in this study of turbulence. The equations of motion may be expressed as follows:

$$\frac{\partial p}{\partial z} = \frac{1}{r}\frac{\partial}{\partial r}(r\,\tau_{rz})$$

$$\frac{\partial p}{\partial r} = \frac{1}{r}\frac{\partial}{\partial r}(r\,\tau_{rr}) - \tau_{\theta\theta}/r \qquad (80)$$

$$= \frac{\partial\,\tau_{rr}}{\partial r} + \frac{1}{r}(\tau_{rr} - \tau_{\theta\theta})$$

The stress tensor may be divided into an isotropic and a deviatoric tensor for the capillary flow:

$$\begin{bmatrix} \tau_{zz} & \tau_{zr} & 0 \\ \tau_{rz} & \tau_{rr} & 0 \\ 0 & 0 & \tau_{\theta\theta} \end{bmatrix} = \begin{bmatrix} -p & 0 & 0 \\ 0 & -p & 0 \\ 0 & 0 & -p \end{bmatrix} + \begin{bmatrix} P_{zz} & \tau_{rz} & 0 \\ \tau_{rz} & P_{rr} & 0 \\ 0 & 0 & P_{\theta\theta} \end{bmatrix} \qquad (81)$$

The pressure is negative in this equation because the stress tensor is in terms of tension. The terms $P_{zz}$, $P_{rr}$, $P_{\theta\theta}$ are the normal stresses which arise in shear flow. The equation of motion for the r-direction may be expressed as a function of the deviatoric stresses:

$$\frac{\partial p}{\partial r} = \frac{\partial P_{rr}}{\partial r} + \frac{1}{r}(P_{rr} - P_{\theta\theta}) \qquad (82)$$

For Poiseuille flow it has been shown (as discussed by Metzner, et al (62)) that $P_{rr} \approx P_{\theta\theta}$. The second equation then gives upon integration:

$$p(r,z) = p(0,z) + P_{rr}(r) \qquad (83)$$

$P_{rr}$ is a deviatoric quantity. Therefore, if it exists, $P_{zz}$ must also exist and be of opposite sign. The difference, $P_{zz} - P_{rr}$, is usually measured.

Shertzer (87) measured this normal stress difference for J-100 and PIB solutions by measuring the thrust of a jet of the polymer solutions issuing from a capillary. Using this technique high shear rates are possible, allowing the range of shear rates encountered in turbulent flow to be covered. The method has a serious shortcoming, however, in that significant normal stress values cannot be measured for dilute polymer solutions (below 0.1 per cent) where a high degree of drag reduction has been observed by several investigators (Hershey (33), Fabula (19), Lindgren (55)). This is because the viscosities of dilute solutions are low giving high Reynolds numbers (in turbulent regime) at measureable thrusts. Shertzer reported unusual effects in measurements above a Reynolds number of 1000.

Park (70) has attempted to correlate his drag reduction data with normal stress as a parameter. Using dimensional analysis Park obtained the following groups for the correlation of the turbulent flow of a viscoelastic fluid:

$$\frac{f_{pv} - f}{f_{pv} - f_1}, \quad Re', \quad \frac{(P_{zz} - P_{rr})_w}{\tau_w}$$

where $f_{pv}$ is the friction factor for a purely viscous fluid, and $f_1$ is on the extension of the laminar line, $(16/Re')$. These groups were successfully used to correlate the friction factor data for a viscoelastic 0.3 per cent solution of J-100 in water. Park also measured friction factors for several solutions of CMC in water, but he was unable to use normal stress data for correlation because the normal stress-shear rate curves were

discontinuous for different capillary tubes. The thrust method of Shertzer was used to measure the normal stress difference, $P_{zz} - P_{rr}$.

The Park correlation promises to yield a practical means of representing turbulent friction factor data of drag reducing solutions, but it fails to lead to greater understanding of the mechanism of turbulence damping.

Astarita (1) has proposed a method of correlating turbulent drag reduction data based on the relaxation times of the polymer solution. He asserted that if the relaxation time (based on a Maxwell model) is longer than the reciprocal of the lowest dissipative frequency in the turbulent flow, drag reduction will result. Following the development of Levick (51), Astarita approximated the lowest dissipative frequency in pipe flow to be $(U/2a)Re^{1/2}$. The frequencies predicted are well above the frequencies of maximum dissipation for the liquids studied here. Astarita reasoned that drag reduction takes place because the dissipative frequency range of the energy spectrum becomes conservative as does a Maxwell model when stressed at frequencies higher than the reciprocal relaxation time. He further reasoned that as the total energy dissipation approaches laminar flow dissipation, the turbulent velocity profile must become steeper. There is no conclusive experimental evidence to support this contention nor is it a mathematical necessity.[1]

---

[1] As the drag reduction becomes greater, the shear rate at the wall must decrease, possibly causing a thicker laminar boundary layer (98). Depending upon the relationship between the Reynolds stress, $\rho\overline{uv}$, and the velocity gradient, the turbulent core may have a higher or lower velocity gradient. If the boundary layer thickness approaches the pipe radius, the laminar portion will approach the laminar flow profile, but the turbulent core may still have a velocity gradient much lower than the laminar case, depending on the reduction of turbulent momentum exchange during drag reduction.

Hershey (33) demonstrated the relationship between calculated relaxation times of the polymer solution and the experimentally determined onset of drag reduction in turbulent flow. Using the theory of Zimm (102), Hershey estimated the relaxation times (first five modes) for the polymer molecules in each of his solutions. The reciprocals of these relaxation times were then compared with the wall shear rates at incipient drag reduction in turbulent flow. It was found that better than "order of magnitude" agreement was obtained between these two reciprocal times, thus providing a basis for predicting the presence or absence of drag reduction based on the molecular weight, intrinsic viscosity, steady flow viscosity, and the temperature of the polymer solution in question. The time scale for turbulent flow used by Hershey, the wall shear rate, can be a rough estimate of the time scale of the dissipative eddies in the turbulent stream. Though the molecular relaxation times were calculated using a theory that has been little tested, the agreement was surprisingly good.

A more direct view of the mechanism of drag reduction can be obtained by considering the spectrum of the turbulent fluctuations. If the proper viscoelastic data are available, it should be possible to consider the elastic effects over the complete range of shear rates represented by the turbulence spectrum.

The simplest representation of a viscoelastic material is the Maxwell element, which is simply an elastic element in series with a viscous element. It is defined by:

$$s = s_g + s_\mu = \tau_{rz}/G + (1/\mu)\int_o^t \tau_{rz}\,dt \qquad (84)$$

where s is the amount of shear. This model can be used to represent the behavior of a viscoelastic material in an approximate manner, if the fluid

may be considered to be a continuum. The use of a complete relaxation spectrum function would allow an exact representation of the behavior of the material under stress, but this approach is too complex for the following considerations.

In order to determine the effect of viscoelasticity on the turbulence spectrum, it is necessary to know the shear rigidity, G, and the viscosity, $\mu$, as a function of shear rate. There is still some doubt as to the exact relationship between shear stress and normal stress. The relation accepted by Philippoff (71) and others (derived by starting with the strain energy function) is:

$$\begin{aligned} P_{zz} - P_{rr} &= G s_g^2 \\ \tau_{rz} &= G s_g \\ G &= \tau_{rz}^2/(P_{zz} - P_{rr}) \end{aligned} \tag{85}$$

The recoverable shear, $s_g$, is defined as the derivative $dz'/dr$, where $z'$ is the recoverable deformation in the shear direction. Philippoff has shown (71a) that the first equation above is valid even when G is not constant.

Considerations of the viscoelastic behavior are greatly simplified if the shear modulus of rigidity is constant (Hook's Law in shear). This has been found approximately true for only a few polymer solutions. Brodnyan, Gaskins, and Philippoff (5) have found, for instance, that low concentration PIB solutions follow Hook's Law in shear at shear rates up to $10^5$ seconds$^{-1}$. They used the flow birefringence technique to measure normal stresses. Other measurements of normal stresses in PIB solutions, however, do not indicate constant values of G. Shertzer's (86) measurements of $P_{zz} - P_{rr}$ for PIB in decalin and Green's (31) measurements for PIB in cyclohexane yield shear rigidity moduli which increase with shear

stress. These measurements were made using jet thrust apparatuses in different laboratories. Measurements using other methods and other solutions have shown the same trend of G with shear stress -- nitrocellulose in n-butyl acetate (72), methylcellulose in water (44), and J-100 in water (70, 87). This means that the shear stress must be known to determine the shear rigidity of the solution. A rigorous solution for the elastic effect in turbulence would require knowledge of the rigidity and viscosity as functions of shear rate. An approximation may be made to obtain a solution, which is shown below.

The term in the Maxwell model involving the viscosity represents the energy dissipative component of the model, and the term involving shear rigidity is the non-dissipative (conservative) term. For a given deformation history, the energy dissipation may then be calculated if the viscosity and rigidity are known. For a purely viscous material ($G \rightarrow \infty$) the entire deformation contributes to energy dissipation, but for a viscoelastic material the part of the deformation described by $\tau_{rz}/G$ is recoverable -- hence recoverable shear. For a steady shear flow (laminar) the elastic deformation is at equilibrium after reaching the value dictated by the shear stress. The viscous deformation increases until the shear stress is removed. Upon removal of the shear stress the conserved elastic deformation relaxes. It is this recovery of elastic deformation that lowers the amount of energy dissipation in a given volume of turbulent flow. Since the shear stress on each element of fluid is continually impressed and relaxed, the elastic potential energy is recovered at each relaxation. Even very low concentration polymer solutions may be considered a continuum at the microscale size of turbulent pipe flows[1].

---

[1] See footnote on page 23.

For application to turbulence fluctuations which can be resolved into a spectrum of periodic deformations, viscosity and shear rigidity data measured in a periodic oscillating device should be directly applicable. Such devices have been used consisting of vibrating reeds, longitudinally and torsionally vibrating rods, and torsionally vibrating piezoelectric transducers. For the high frequency data (10 kcps up) the piezoelectric transducers are preferable. A number of investigators have measured the spectrum of shear rigidity and viscosity using the latter method (1a, 72, 80a). Unfortunately the shear rates attainable with the piezoelectric crystals have been very low (less than 1 second$^{-1}$). This is much lower than the shear rates existing in turbulent flows (up to $10^5$ seconds$^{-1}$ in this investigation). For use in the study of viscoelastic turbulence, the instrument must be capable of shear rates in the range $10^3$ to $10^6$ seconds$^{-1}$. For this reason in this study normal stress data obtained at high shear rates in capillary tubes were used to calculate moduli of rigidity in the discussion of the mechanism of drag reduction.

# EXPERIMENTAL WORK

## 1. Objective

The experimental work was done to develop hot-film and hot-wire anemometry techniques suitable for studies of the flow of organic solvents and non-drag reducing and drag reducing polymer solutions, and to investigate the turbulence intensities, autocorrelations, and energy spectra of these fluids. Comparisons of the turbulence properties were to be made in order to determine the effects of polymer type and molecular weight, solution viscosity, polymer-solvent interaction, Reynolds number, and tube size. The effects of drag reducing polymers on turbulence were also to be investigated to help determine the mechanism of the energy dissipation reduction.

Anemometry measurements of turbulence intensities, autocorrelations, and spectra were made on solvents and non-drag reducing polymer solutions in a 2-inch smooth tube, using a wedge type hot-film probe. The solvents studied were toluene, cyclohexane, and benzene. The polymer solutions studied are listed in Appendix VI. All the solutions studied in the 2-inch tube (Runs 1-16) were the same as those used by Hershey (33) except the 0.95 percent V-100 PMMA[1] in toluene of Run 16. The solutions studied were of wide viscosity range, and so a large Reynolds number range was covered.

Progress was made on the development of a film probe for the determination of radial and tangential intensities of turbulence and the Reynolds stresses, $\overline{u'v'}$ and $\overline{u'w'}$. The probe is described in section 2.11. The results of the measurements are summarized in the discussion of results.

---

[1] See Appendix VI.

A few measurements were made with a hot-wire anemometer, but they did not yield good results because of the poor lint shedding characteristics of the wire. The calibration of the wire changed too rapidly for reliable intensity measurements.

In order to obtain measurements in a solution having substantial drag reduction characteristics, it was necessary to use a higher molecular weight polyisobutylene[1] than that used in Runs 8, 9, 11, and 12[2] and to make the measurements in a 1-inch smooth tube instead of the 2-inch tube used previously. Hershey has discussed the relative drag reduction in tube sizes from 2-inch down to 0.033 inch diameter for all the solutions studied here except the V-100 PMMA in toluene and the toluene and cyclohexane solutions of PIB L-200. No significant drag reduction was found in the solutions studied by Hershey in a tube larger than 0.5-inch diameter. Because of the high molecular weight of the PIB L-200, toluene and cyclohexane solutions of this polymer were significantly drag reducing in a 1-inch tube. Several energy spectra were measured for three concentrations of this polymer in toluene, but only two intensity of turbulence measurements were made. This is because of the rapid degradation of the polymer by shear which caused much of the drag reduction to be lost in a very short time. Intensity measurements were made in one concentration of PIB L-200 in cyclohexane, which was drag reducing in the 1-inch tube. Thus, only exploratory data were obtained for solutions under drag reducing flow conditions.

---

1 Vistanex L-200
2 Vistanex L-80

## 2. Equipment

### 2.1. Pipe flow system

The recirculating pipe flow system consisted of a reservoir tank, with a ± 0.05°C temperature control system, two Viking gear pumps in parallel yielding flow rates of one gpm to 100 gpm, pressure surge damping cylinders on each pump and in the test section feed header, three smooth wall tubes (2-inch I.D., 1-inch I.D., and 0.51 inch I.D.) making up the test section, a calibrating tank on a platform scale, and two turbine meters for flow rate measurements. The pipe flow unit has been described in great detail by Hershey (33), so only those points of special interest will be covered here. A schematic of the unit is shown in Figure 10.

The pressure surge damping cylinders on each pump discharge consisted of vertical pipes of 0.1 cu ft capacity. Closed at the top, the air in these cylinders served to damp the low frequency surges created by the gear pumps. Another surge damping cylinder of 0.3 cu ft volume was located on the inlet manifold to the smooth wall tubes. This surge volume further reduced any remaining disturbances. Spectrum data indicated that the surge volumes were adequate since no peaks were found near the expected surge frequencies of the gear pumps.

The smooth wall tubes were of carbon steel. The 0.510-inch and 1.00-inch tubes were welded and drawn tubing of exceptional smoothness procured from Tube Sales, St. Louis, Missouri. The 2-inch tube was a seamless cylinder tube procured from Babcock and Wilcox Company, St. Louis, Missouri. The tube inside diameter tolerences were ± 0.0025 inch for the 0.51-inch and 1-inch tubes, and ± 0.005 inch for the 2-inch tube. The tube lengths were as follows: 0.510-inch tube, 17.5 feet;

1.00-inch tube, 24.0 feet; 2.00-inch tube, 27.0 feet. The lengths of the tubes were, therefore, more than sufficient for good velocity profile development. Friction factor data for Newtonian solvents were obtained using test sections 100 or more diameters in length after entrance sections of 50 or more diameters in these tubes. These friction factors showed average deviations from equation 18 of only ± 2.0 per cent (33). The turbulence measurements with a hot-film anemometer were, therefore, made on fully developed turbulent pipe flow with smooth walls.

The hot-film anemometer and the impact tube were installed in the tubes using the same probe mount. The installation in the 2-inch tube was at a point 2 feet upstream of the end of the tube. This point was 150 diameters downstream of the tube entrance.

As shown in Figure 11, nylon bushings were used to mount the probe and the micrometer positioner. This was necessary to insulate the probe support surface, which was a conductor, from grounding on the tube. Swagelok fittings with Teflon ferrules were used as packing glands for the sliding probe support rod. Since the probe was insulated from the tube, it was possible to use an electrical resistance method of probe positioning. When the probe contacted the wall, the resistance between the probe support rod and the tube fell to zero. This established the reference position for use in locating the probe by the micrometer to within ± 0.0005 inch. Since the probe could not be allowed to contact the wall during measurements, the reference position could only be approached.

Velocity profiles and turbulence measurements in the 1-inch tube required the construction of a different type of probe mount. The same

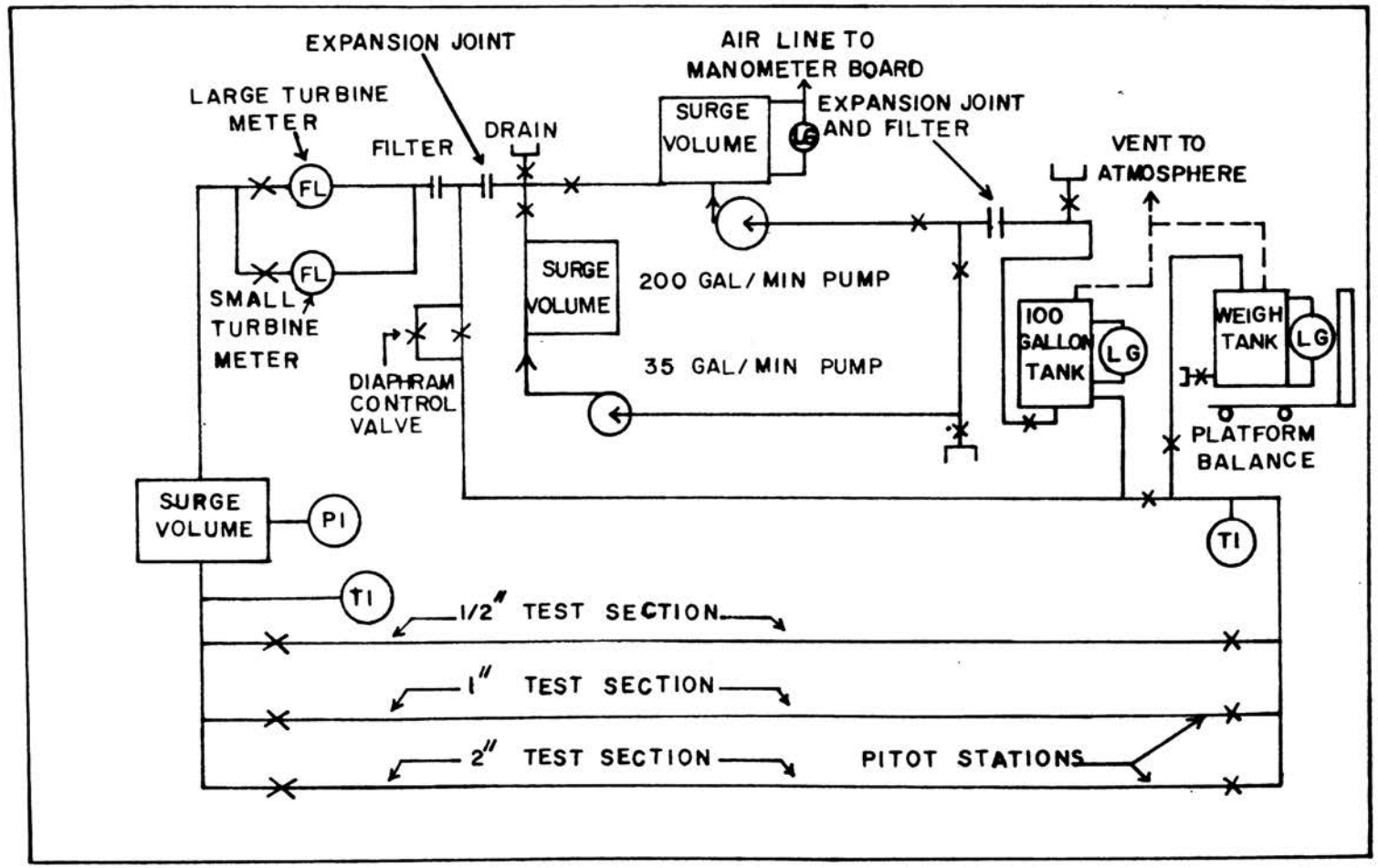


FIGURE 10. SCHEMATIC DIAGRAM OF PIPE FLOW APPARATUS

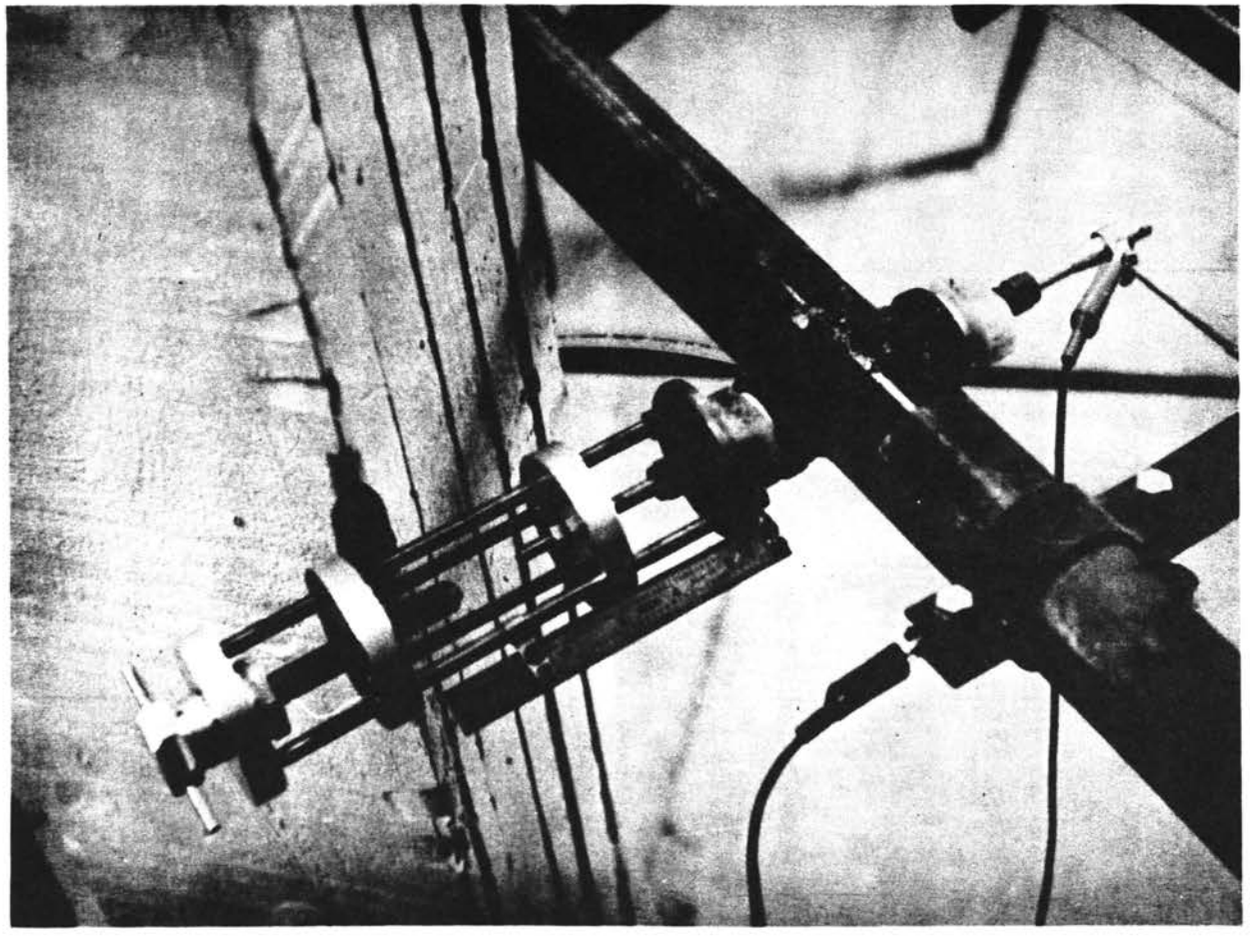

FIGURE 11. MICROMETER POSITIONER AND PROBE MOUNT FOR 2 – INCH TUBE

nylon bushings were used, but instead of installing the probe through the tube wall (as in the 2-inch tube) it was installed in a modified 1-inch pipe cross. As shown in Figure 12, the pipe cross was fitted with a sleeve of 1-inch inside diameter to provide a relatively smooth wall behind the probe tip. This sleeve minimized flow disturbances propagated upstream toward the probe tip from the pipe cross. Since electrical contact with the sleeve wall was not an accurate reference position for the probe in the 1-inch tube, an inside caliper and micrometer were used to establish the reference distance from the tube wall each time the probe was installed.

The temperature of the fluid during hot-film measurements must be held within $\pm$ 0.05°C inorder to maintain a constant probe calibration. A sensitive temperature control system was used, the diagram of which is shown in Figure 13. The temperature sensor was a Jumo thermoregulator with a precision of $\pm$ 0.01°C. The sensor was installed in the side of the surge tank with a Swagelok connector. The glass thermometer bulb was protected by a perforated steel sleeve inside the tank and by a slotted sleeve (to expose the scale) outside the tank. The thermoregulator operated an electonic relay which in turn operated a 30 watt relay in the electric heater circuit. The relay operated a 1500 watt heater installed in the inlet line to the water coils in the surge tank. Another heater (2000 watts) was controlled manually. The heated water flowed through two 30-foot stainless steel coils in the tank and then to the drain. The water flow rate was controlled by a 3/8-inch globe valve on the coil exit. Provision for water preheating with steam was provided for use during the winter by a concentric tube heat exchanger. The test fluid temperature was measured at the smooth tube inlets and

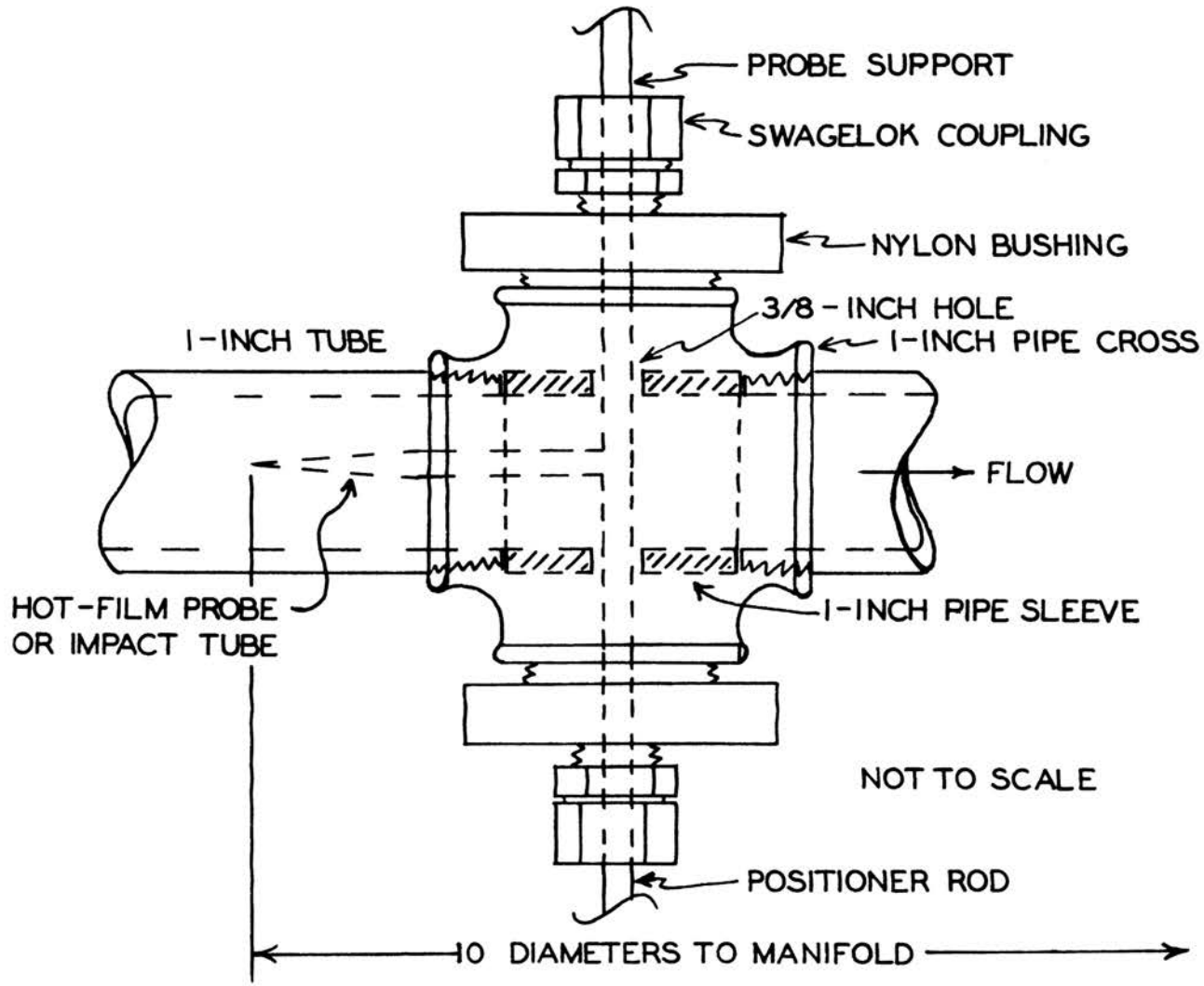


FIGURE 12. PROBE MOUNT FOR 1-INCH TUBE

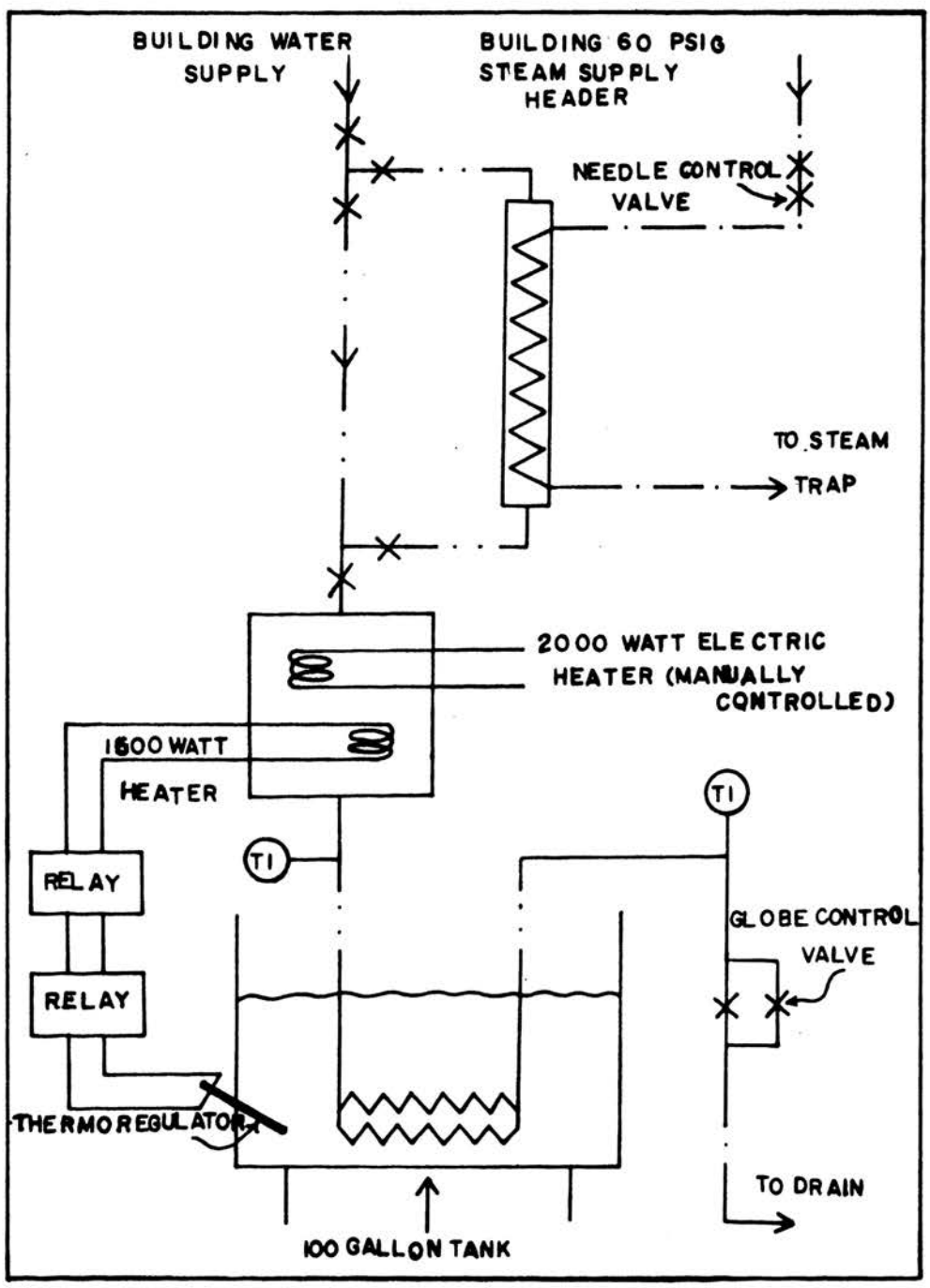


FIGURE 13. TEMPERATURE CONTROL SYSTEM

outlets by thermometers graduated in 0.1°C intervals. They were found to be accurate to better than 0.05°C by Hershey (33).

The filter used to remove small lint and dirt particles and yet allow high flow rates was a 200 mesh Tyler sieve of about 3 square inches area. As noted above, it was not able to remove all lint particles in the flow.

## 2.2 Manometers

The tube pressure drops and velocity profiles were measured by three manometers described in detail by Hershey (33). They were as follows:

(1) a mercury U-tube manometer 9 feet high,

(2) an inverted U-tube manometer with process fluid as the indicator 9 feet high,

(3) an inverted slant U-tube manometer with process fluid as the indicator. The range was 0 to 4.75 inches of fluid using 6-foot gauge tubes inclined at an angle of 3.78° from the horizontal.

## 2.3 Flow meters

The flow rate in the pipe flow system was measured by either of two turbine meters-a 1½-inch Brooks Hydropoise Model HP-24N for flows between 10 and 40 gpm, and a 3/4-inch Brooks Hydropoise Model HP-12N for flows between 1.5 and 15 gpm. These meters produce a fluctuating voltage whose frequency is proportional to flow rate with a linearity of ± 0.5 per cent. The frequency was measured by a Heath Audio Frequency Meter. This meter had a tendency to drift, so it was calibrated at each use by a Heath Audio Signal Generator which was very stable and accurate at all frequencies to better than one percent. The primary use of the flow meters was to show any deviations from a constant flow rate, because weight calibrations were made for every measurement.

2.4. Impact tubes

Velocity profile measurements, made by Hershey in the 2-inch tube using an impact tube, were used for calibration of the hot film anemometer. They are described in detail in his thesis. Additional measurements were made in the 1-inch tube for use in calibrating the anemometer for the intensity measurements made in that tube.

Because of the limited clearance in the 1-inch tube, a special impact probe was designed which was not inserted through the side of the tube as it was in the 2-inch tube. The design of this special probe allowed the impact tube to be removed from the support tube so that it could be easily inserted through the sleeve in the mount. The impact tube was then replaced on the support tube by means of threads which were sealed with teflon pipe dope. A diagram of the probe is shown in Figure 14. Both the original and the special impact tubes had outside diameters of 0.036 inches at their tips.

2.5. Viscometers

The capillary viscometer used to measure the laminar flow behavior of the fluids studied and also to measure some of the turbulent friction factors was described by Green (31) and Hershey (33). The characterizations used by Hershey are used here for the solutions which are in common for both investigations. The viscometry measurements for the solutions used only in this investigation are reported by Rodriguez (78).

Intrinsic and low shear rate viscosities were measured using an Ubbelohde suspended level viscometer. The fluid densities were measured with a Lipkin pycnometer. These measurements were described by Chang (8).

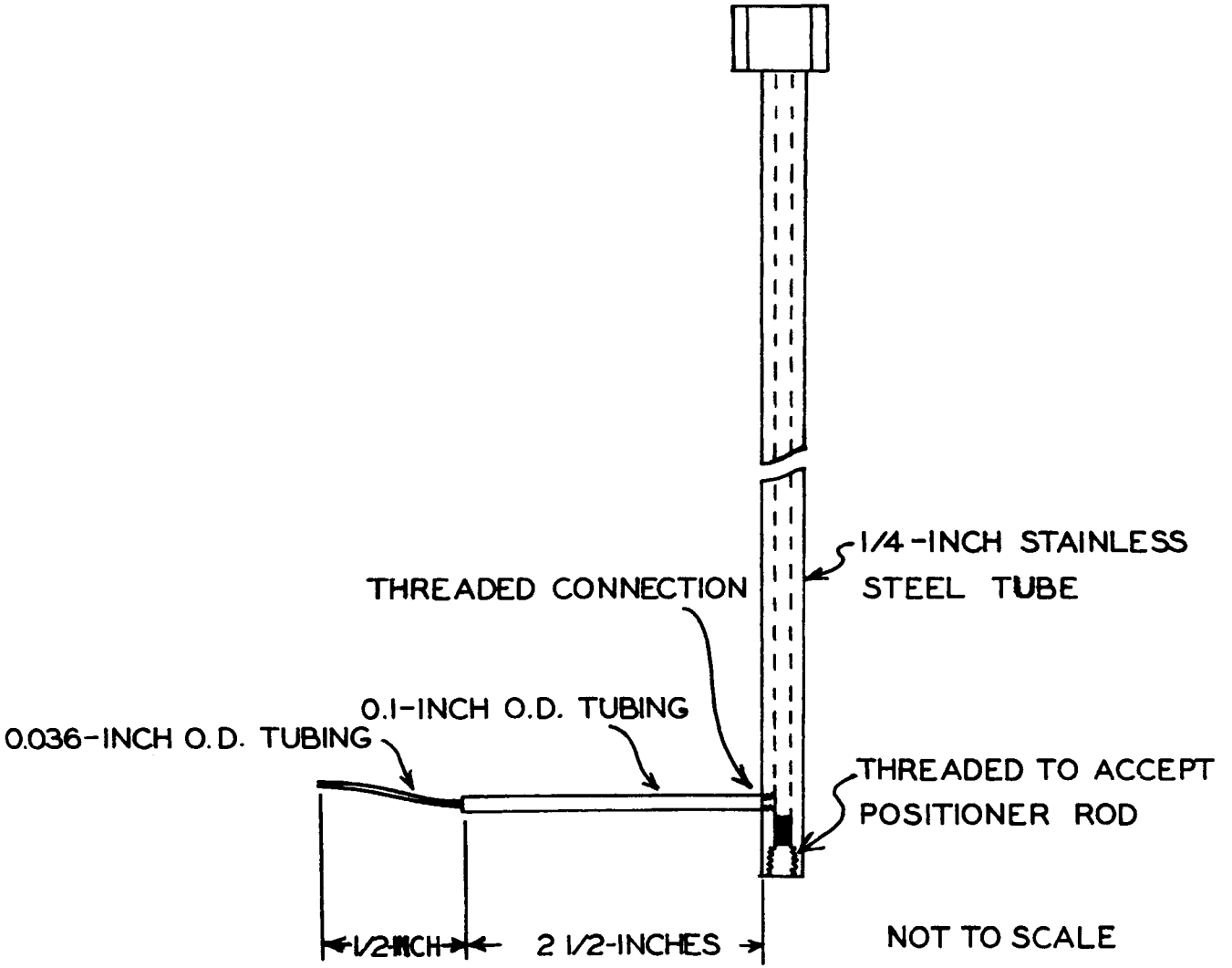


FIGURE 14. IMPACT TUBE FOR 1-INCH TUBE

## 2.6. Normal stress apparatus

An improved version of the analytical balance thrustometer described by Green (31) was used to measure the normal stress difference, $P_{zz}-P_{rr}$, of the 0.42 per cent PIB L-200 in toluene solution. These measurements, described below, were made using a 24-inch loop of ¼-inch nylon tubing in place of the 6-inch length of tygon tubing used by Green to connect the constant temperature bath coil to the capillary mounted on the balance. The nylon tube did not expand under pressure as did the tygon tube. As a result, the zero thrust reading of the balance was preserved. The sensitivity of the balance was about 100 mg/division, allowing measurements to the nearest 12 mg of thrust. A thermometer telescope was used to observe deflections of the indicating needle.

## 2.7. Constant temperature anemometers

The constant temperature anemometers used in this study were model 55A01 manufactured by DISA Elektronic, Herlev, Denmark. The anemometers were designed to operate with hot-wire or hot-film probes with resistances between 1 and 50 ohms. The maximum probe current available was 250 milliamperes, thus setting maximum power at about 1.25 watts for a 20 ohm probe. The anemometers were equipped with a three decade balance resistor system for measuring cold resistance to the nearest 0.01 ohm and for setting probe operating resistance. Each anemometer had a damped d.c. voltmeter which was equipped with four ranges and four zero shift bias voltages for the measurement of time average bridge voltages up to 30 volts. The rms fluctuating bridge voltages were measured by a thermocouple meter in the anemometers with ranges from 5 millivolts to 1000 millivolts. The anemometers were each

equipped with both a high pass and a low pass filter to eliminate any undesired high or low frequencies. The frequency response of the anemometer-probe combination was determined using the 2.5 kcps square-wave generator, which is part of each anemometer. Detailed specifications of the instruments including drift, transductances, and noise levels are given in Appendix I.

2.8. Correlator

The DISA Elecktronic 55A06 correlator was used to measure auto-correlation coefficients, microscale, and the sums and differences required when using an X-wire probe or V-film probe. The instrument consisted of an rms voltmeter (thermocouple type) with ranges of 0.01 volts to 100 volts on 9 scales with variable gain and a calibrating voltage source, a ratio meter for measuring the rms value of the ratio of two signals, and circuits to supply the signals to the meters. The voltmeter could be used on either of two channels or could measure the sum or difference of the two channels. The ratio meter could be used to measure the ratio of the two channels, the ratio of the sum to the difference of two channels, or the microscale. The microscale was measured as the ratio of the signal to the time derivative of the signal. The frequency response of the amplifiers in the instrument was 3 cps to 200,000 cps with less than 3 db drop in signal. More detailed specifications are given in Appendix I and in the DISA catalog.

2.9. Tape recorder

The autocorrelation and spectrum measurements were done on recorded signals. The recorder used was an Ampex 601-2 two channel model using ¼-inch standard tape at a speed of 7.5 inches per second. The frequency response of the recorder was adjusted by the author to give the best

range for this study. This is described in detail in Table 8, Appendix IV. Three response calibrations were used during the work. These values were used as correction factors for the spectrum measurements. Detailed manufacturer's specifications are given in Appendix I.

The recorder was modified for the autocorrelations. The photograph in Figure 15 shows the installation of a movable playback head and a stationary recording head on the side of the recorder. The auxiliary recording head recorded one channel and the standard recording head recorded the other. On playback the movable playback head could be moved by the micrometer to cause the auxiliary channel to be delayed compared to the standard channel. The calibration of delay time with micrometer movement was linear and is shown in Figure 16 for a recorded 100 cps signal. Each complete cycle of autocorrelation value is equivalent to 0.01 seconds. The average calibration value was 8.88 inches of movement per second of delay. The calibration was obtained by playing both the standard and delayed channels into the correlator and varying the delay time (see Appendix II).

2.10. Spectrum analyzer

The spectra were measured using a 34 band active band-pass filter designed and built by T. B. Watson (97). The bands each covered 1/3-octave and covered the range of 10 cps to 20,000 cps. The broader bands at high frequency allowed more accurate measurement of the low energy occurring at high frequency. The frequency response of each band was shown in detail by Watson, but a typical band is shown in Figure 17. The filter instrument was designed to operate with constant response for signals up to 200 millivolts for a given band or 400 millivolts total input signal. The noise level was 0.2 millivolts for

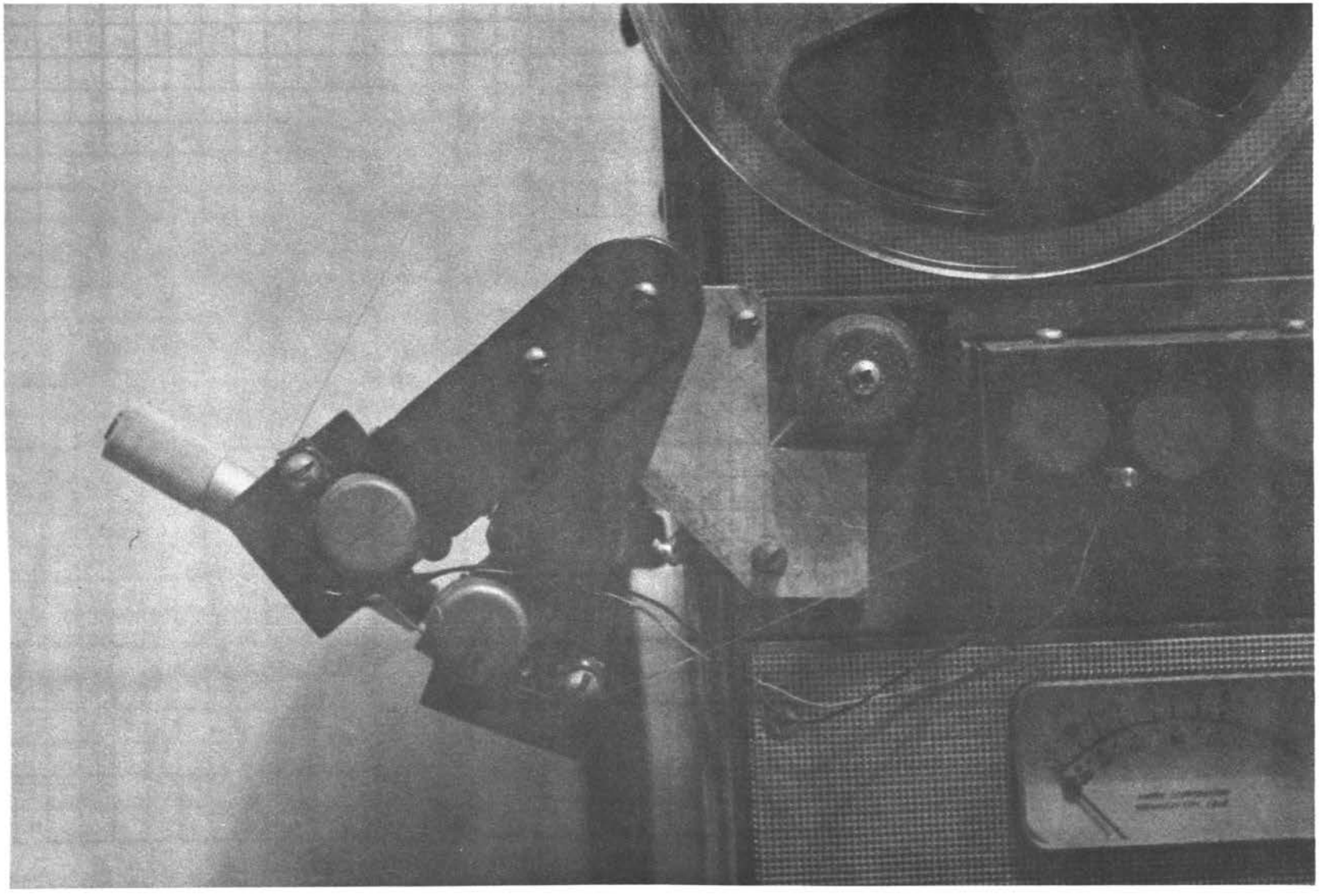

FIGURE 15. MOVABLE PLAYBACK HEAD ON RECORDER

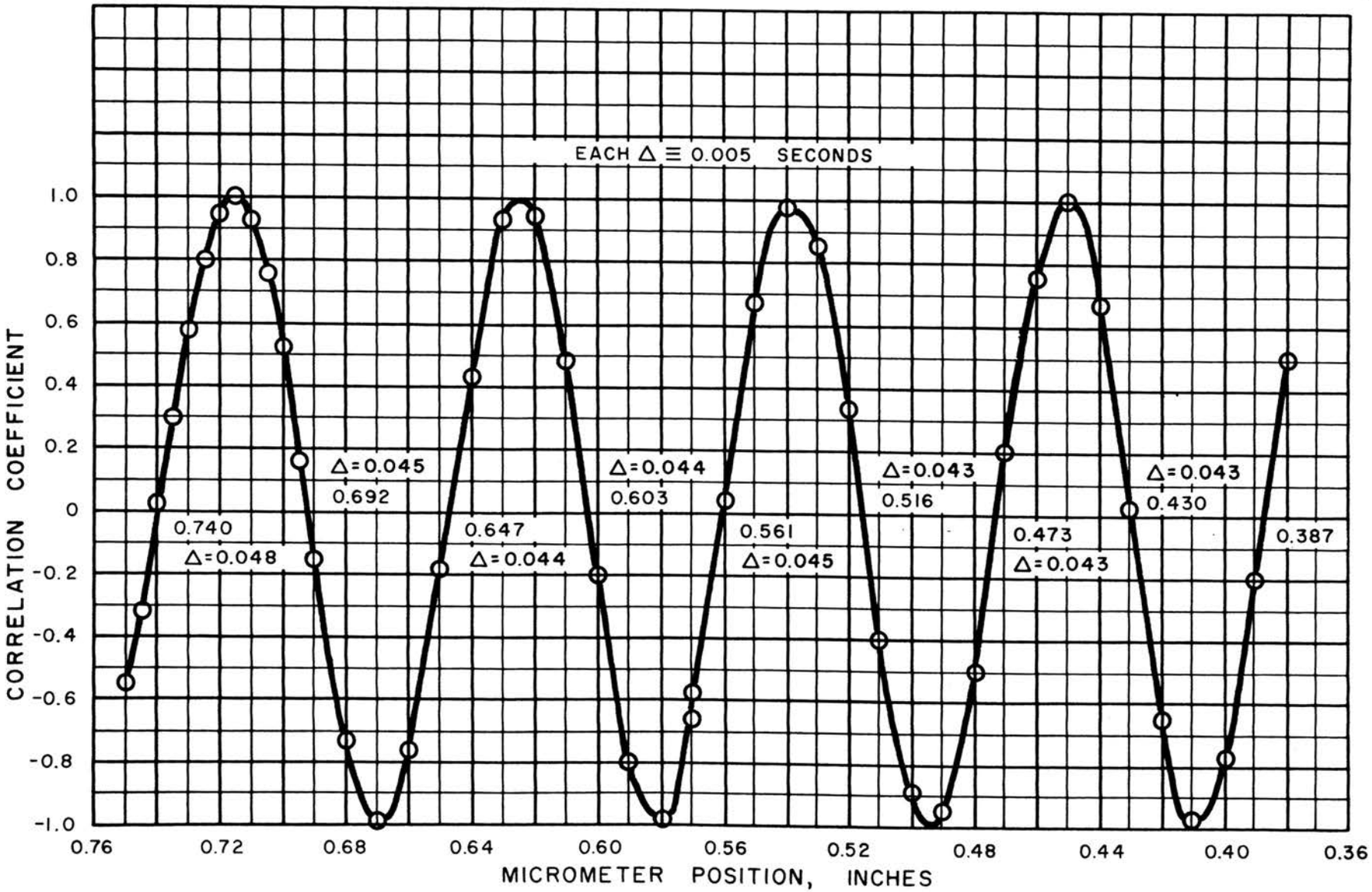


FIGURE 16. TIME DELAY CALIBRATION

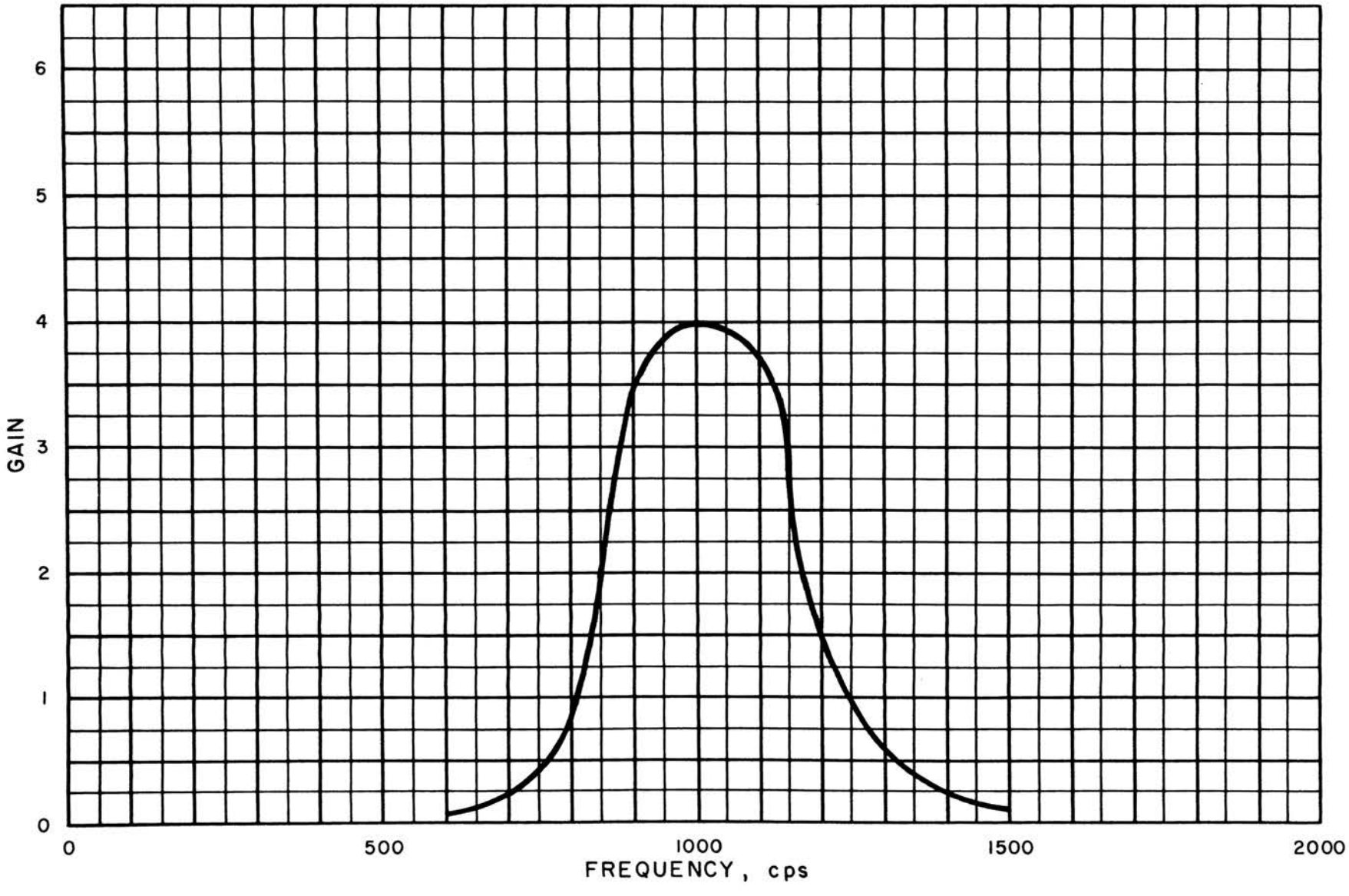


FIGURE 17. TYPICAL BAND RESPONSE FOR BAND PASS FILTER

all bands except those centered at 100 cps and 126 cps, which had noise outputs of 1.2 mv and 2.2 mv, respectively. This increased noise was caused by the second harmonic of the 60 cps cathode heater supply. The band gain factors are shown in Table 9, Appendix IV.

2.11. Hot-film probes

The hot-film probe made by DISA is shown in Figure 8. The dimensions of the film and the general shape show that the probe is very similar to the one used by Ling (56, 57). Detailed specifications are given in Appendix I.

The V-film probe used for the Reynolds stress and transverse fluctuating velocity measurements is shown in Figure 18. This probe was too large for the small microscale in 1-inch and 2-inch pipes. The characteristics and interpretation of the data would be the same as for an X-wire probe if the films were centered at the same point as are crossed wires. Unfortunately this is not true and the film separation had to be accounted for in the data interpretation. This is discussed in section 6.1.

2.12. Experimental procedures

The procedures for using the equipment described above to make the desired measurements are discussed in detail in Appendix II. The measurements of friction factor, velocity profile, and viscometry were discussed by Hershey (33) and are not repeated here. The procedure used for normal stress measurements was covered by Green (31).

3. Materials

The specifications of solvents and polymers used in this study are given in Appendix VI. Table 11 shows the solution concentrations used. The solution of the polymers in the solvents was accomplished by using

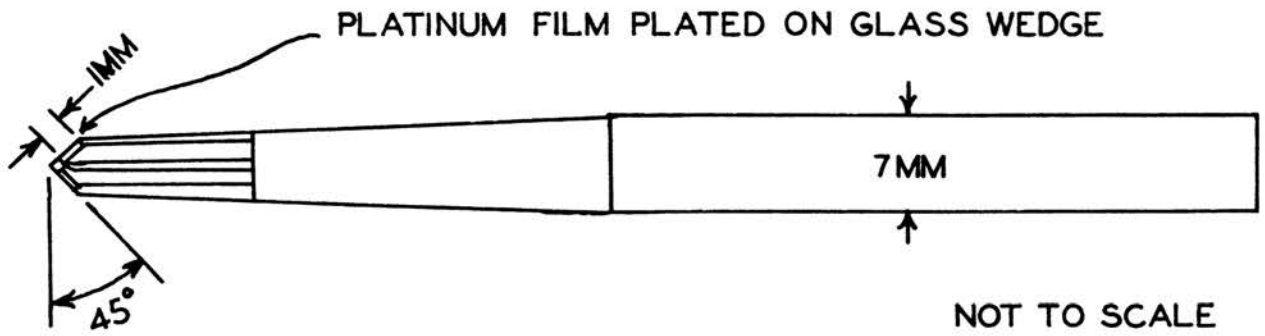


FIGURE 18. V - FILM PROBE

a slow stirrer in 12-inch diameter by 18-inch high Pyrex vessels. These stock solutions were then added in the proper amounts to produce the desired concentrations in the pipe flow unit. A short period of pumping was used to disperse the stock solution uniformly in the fluid already present in the pipe flow system.

4. Calculations

The calculations necessary for conversion of raw data to turbulence intensities, correlation coefficients, and energy spectra are discussed in Appendix V. All these calculations were done using an IBM 1620 Model II computer with disk files and would have been extremely laborious by hand or desk calculator. The large number of spectra converted to autocorrelations and vice versa by Fourier transforms would not have been possible without the computer.

5. Results

The results of the longitudinal turbulence intensity measurements are shown in Figures 19-38. Each figure indicates polymer concentration, solvent, location in the pipe, flow rate, and Reynolds number. Runs 1-16 were in the 2-inch tube, and Runs 17-23 were in the 1-inch tube.

The results of the radial and tangential turbulence and Reynolds stress measurements for toluene in the 2-inch and 1-inch tubes are shown in Figures 39-43. These data represent initial efforts toward development of a film probe suitable for measurement of radial and tangential turbulence intensities in liquid flow in small tubes.

The velocity profiles measured for Run 16 in the 2-inch tube and Runs 19 and 20 in the 1-inch tube are shown in Figures 44-46. The velocity profiles for all runs before Run 16 were reported by Hershey (33).

Velocity profiles were not measured for all runs because all the Newtonian solvents and polymer solutions measured had velocity profiles little different from accepted data, except for the drag reducing solution of Run 19 which was more parabolic in shape, but which integrated to give a flow rate 13 per cent below the measured value. For hot-film anemometer calibration, therefore, calculated profiles based on established non-drag reducing data were more accurate than measured profiles for the drag reducing solutions.

Figures 47-58 show the energy spectra measured. The figures indicate fluid composition, probe location, fluid time average velocity, microscale (calculated from the integral of the dissipation spectrum), and the macroscale (calculated from the integral of the autocorrelation transformed from the spectrum function)[1]. Run numbers correspond to intensity run numbers.

The autocorrelation data were not all plotted since they served primarily as a check on the spectrum measurements and their transformations. Figure 59 shows a comparison of a spectrum measured by the band pass filter and a spectrum calculated from autocorrelation data for Run 8. These comparisons and the limitations of the Fourier transformation methods will be discussed later.

Figure 65 shows the results of the microscale measurements plotted against radius. These data were obtained from measured spectra.

The viscometry and drag reduction data obtained since Hershey's thesis are reported in detail by Rodriguez (78). The normal stress data ($P_{zz}$-$P_{rr}$ vs shear rate) for the solution used in Run 19 (0.42 per cent PIB L-200 in toluene) is shown in Figure 67.

---

[1] See Appendix V.

Computer printouts of the numerical results for turbulence intensities, energy spectra, and autocorrelations are listed in Appendix III, Tables 5, 6, and 7.

The calculations involved in conversion of data to results and in making the Fourier transforms are described in Appendix V.

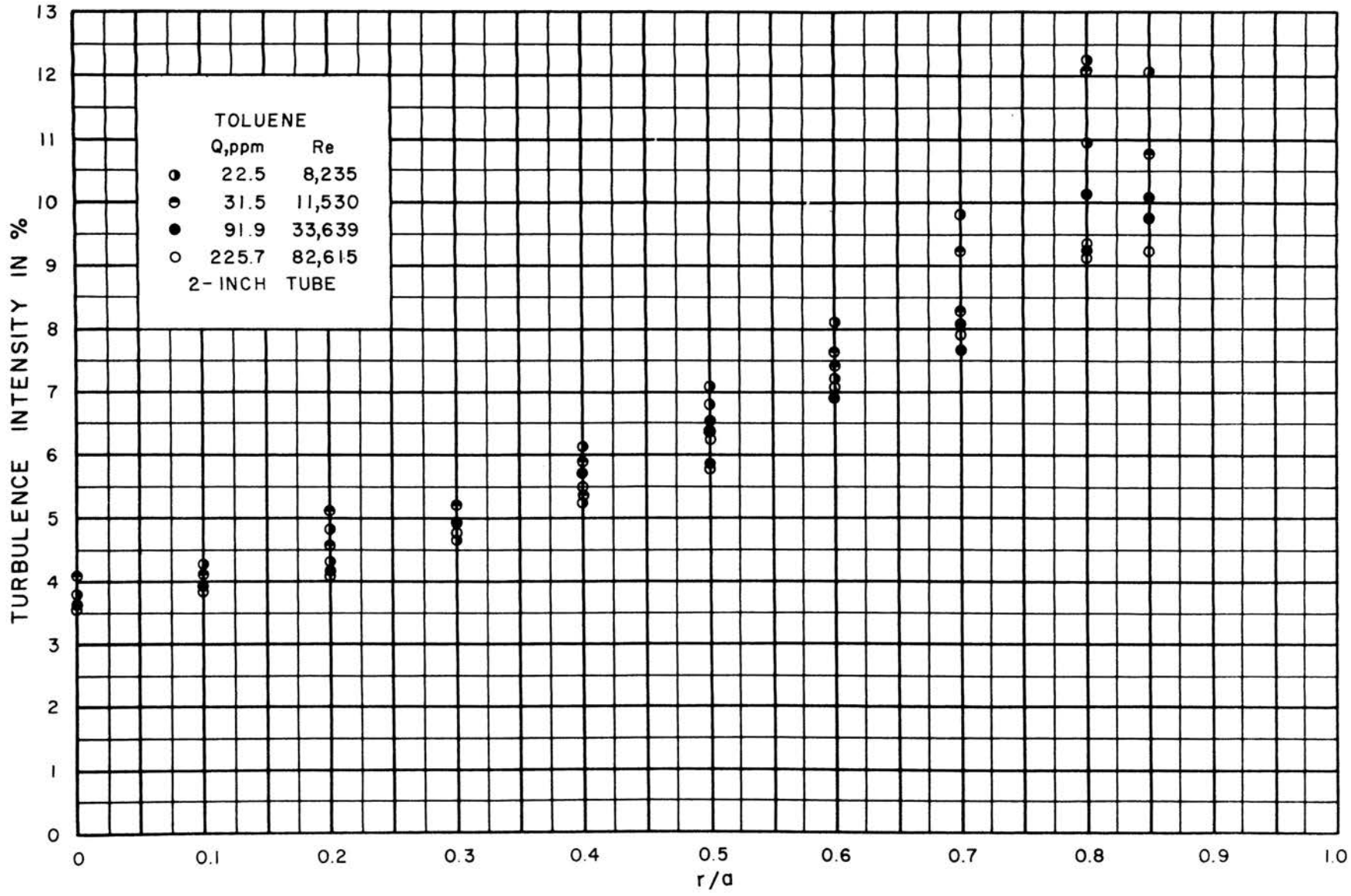


FIGURE 19. TURBULENCE INTENSITY PROFILE FOR RUN 2

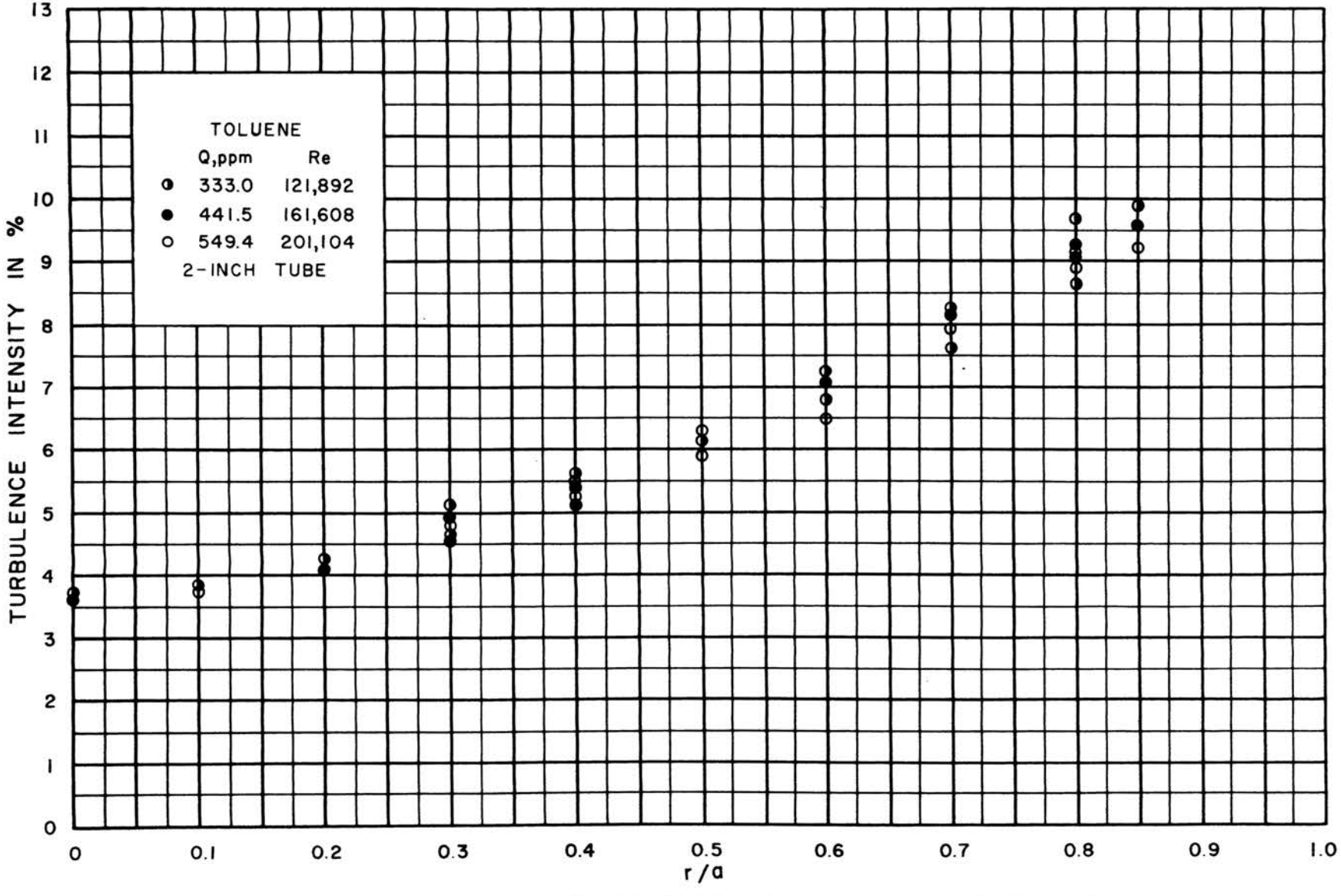


FIGURE 20. TURBULENCE INTENSITY PROFILE FOR RUN 2

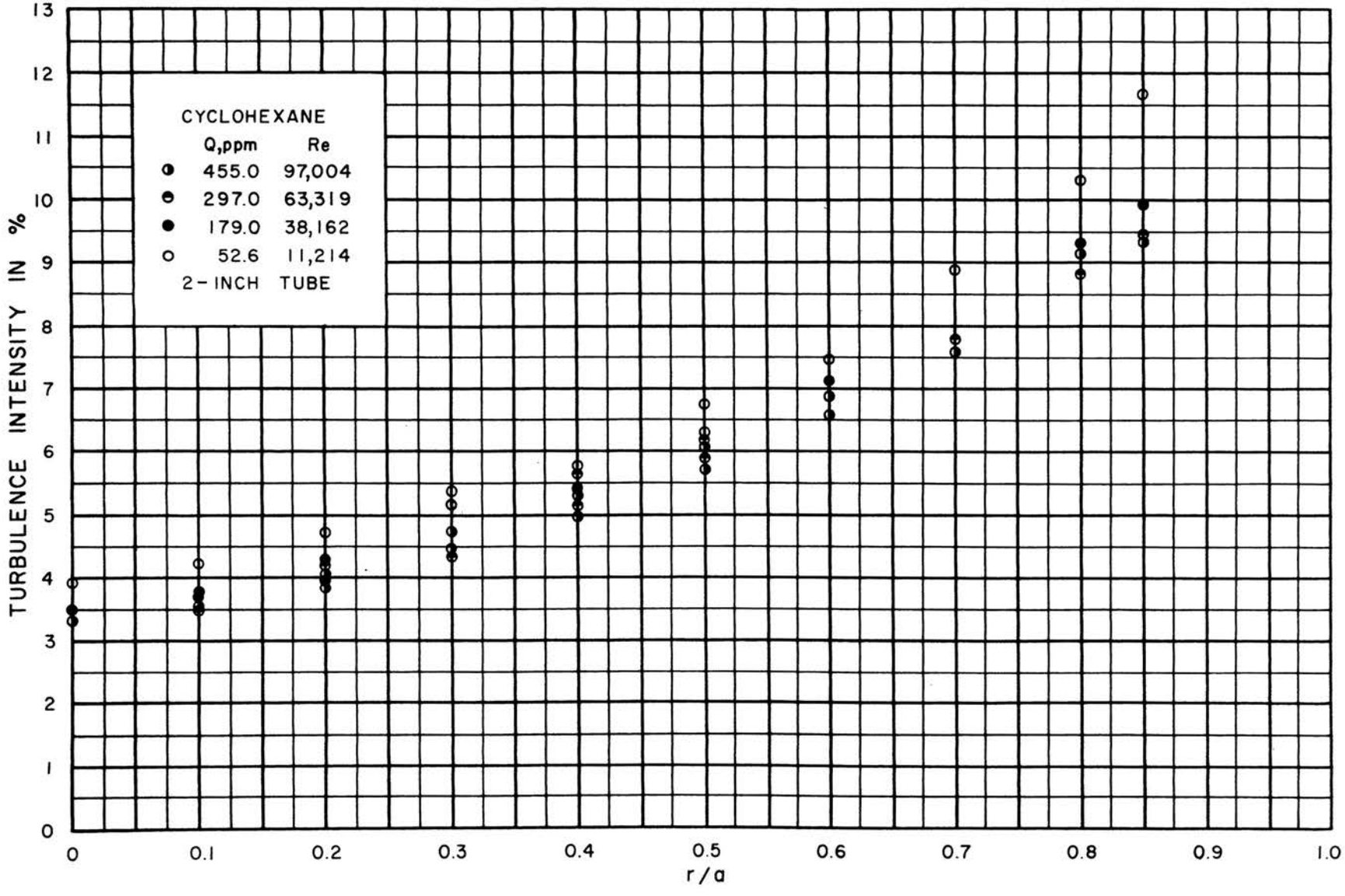


FIGURE 21. TURBULENCE INTENSITY PROFILE FOR RUN 3

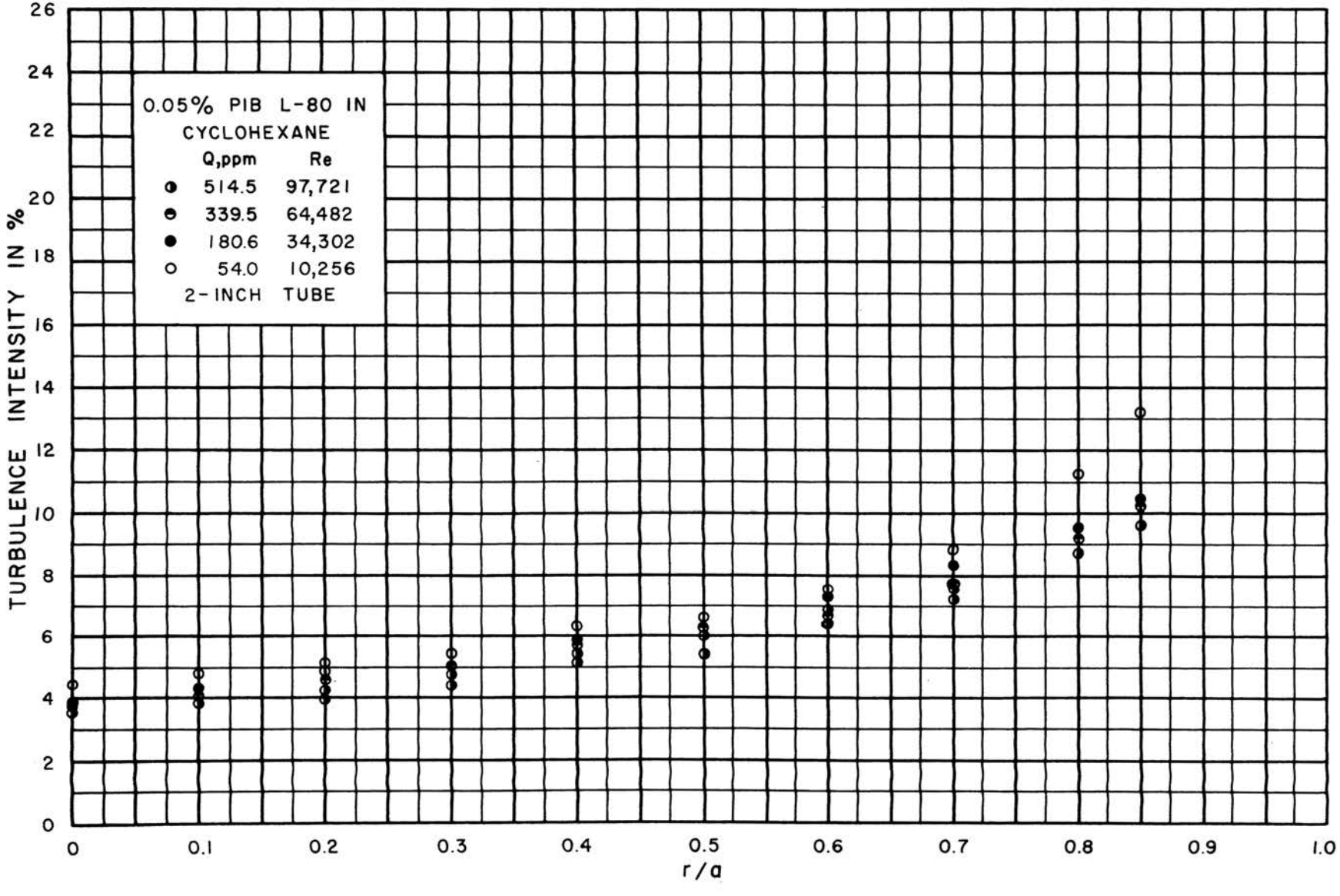


FIGURE 22. TURBULENCE INTENSITY PROFILE FOR RUN 4

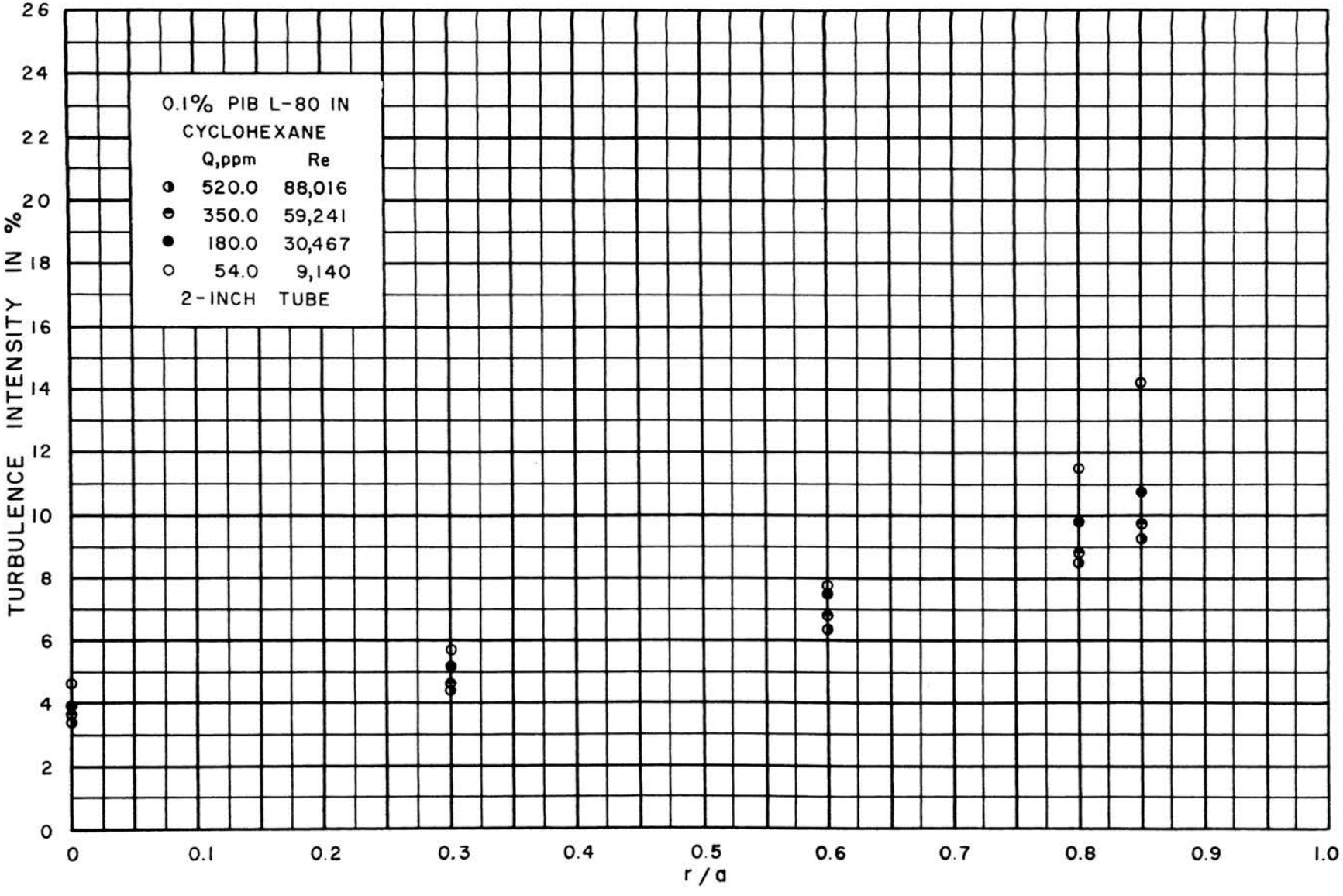


FIGURE 23. TURBULENCE INTENSITY PROFILE FOR RUN 6

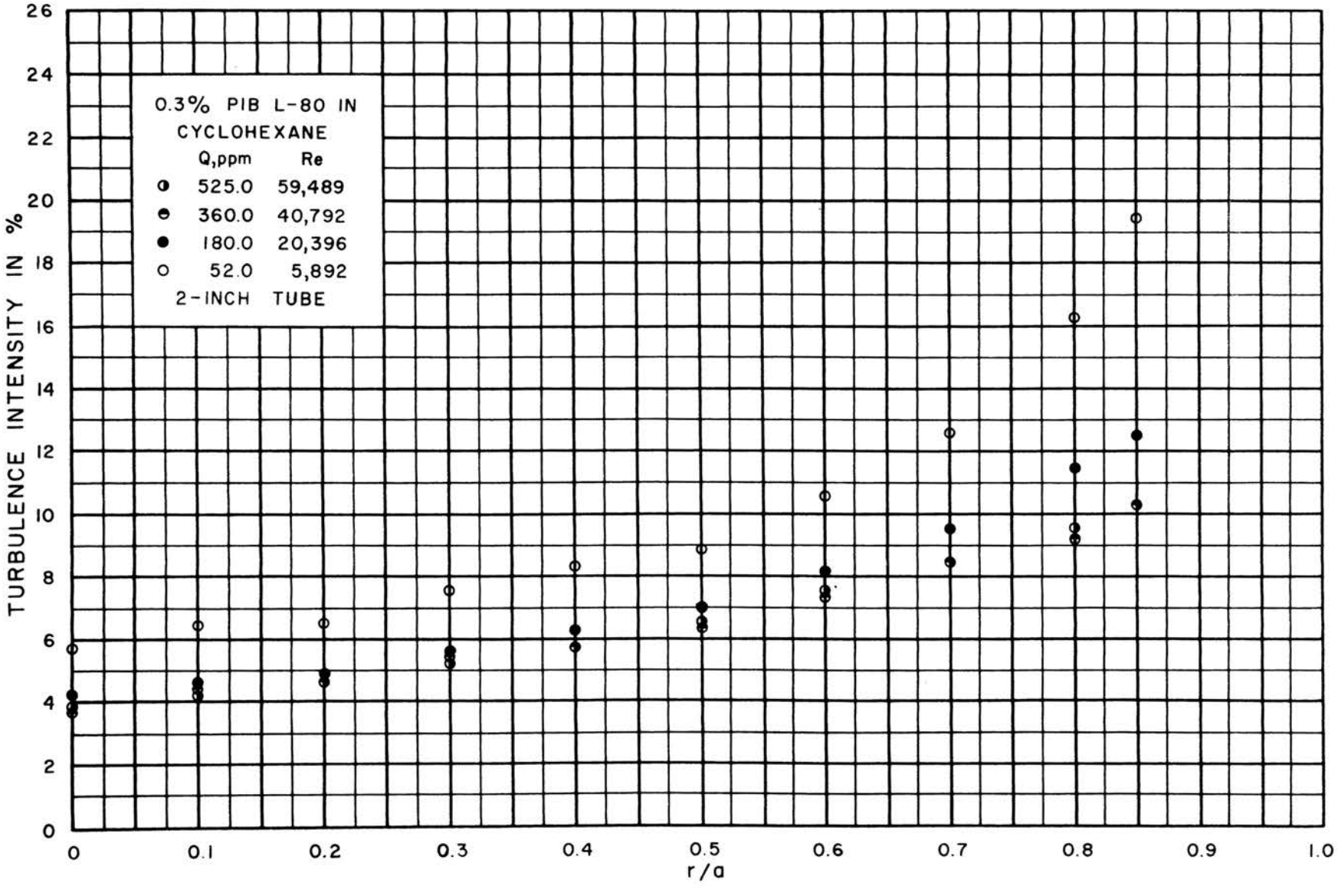


FIGURE 24. TURBULENCE INTENSITY PROFILE FOR RUN 7

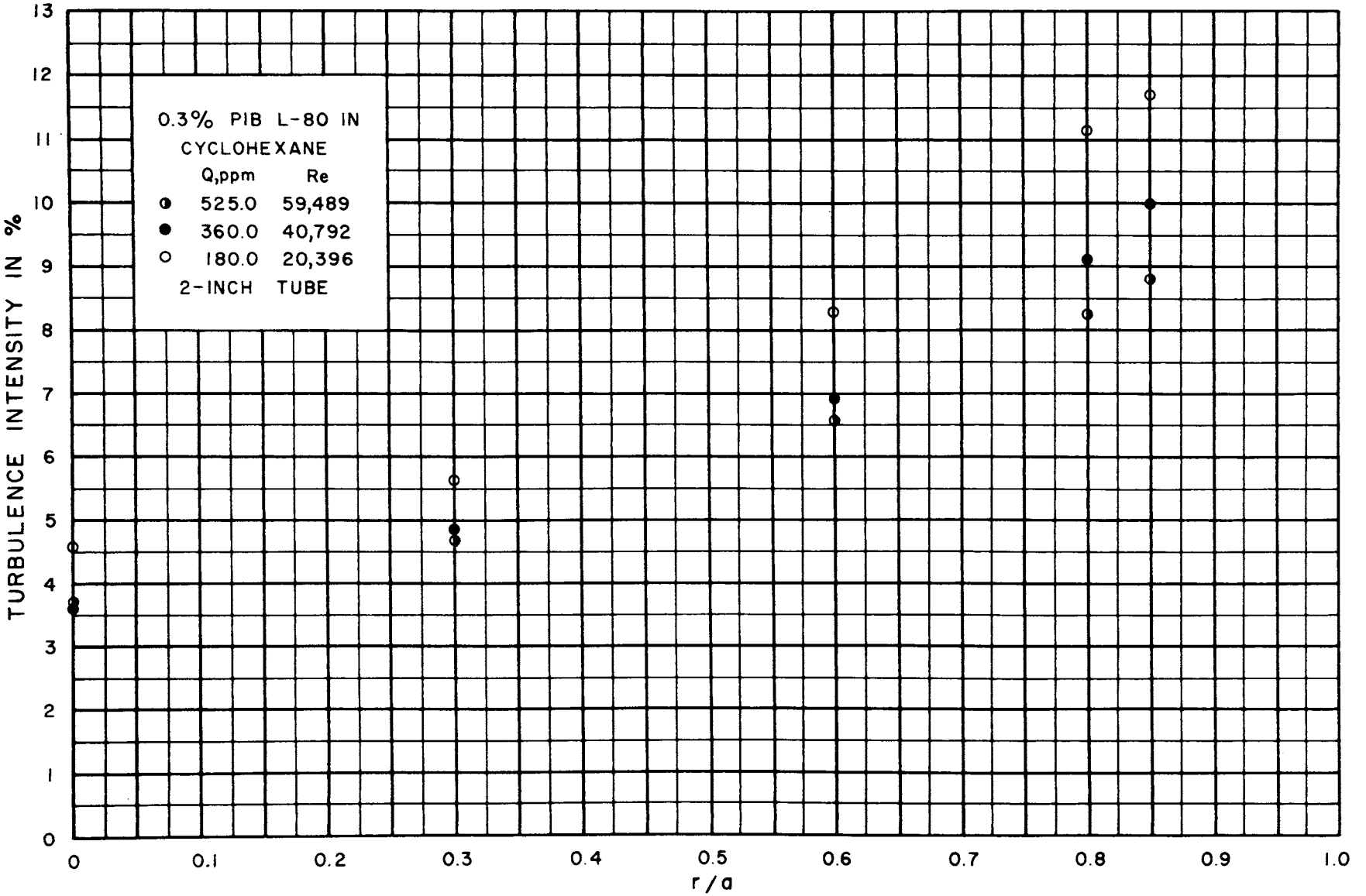


FIGURE 25. TURBULENCE INTENSITY PROFILE FOR RUN 8

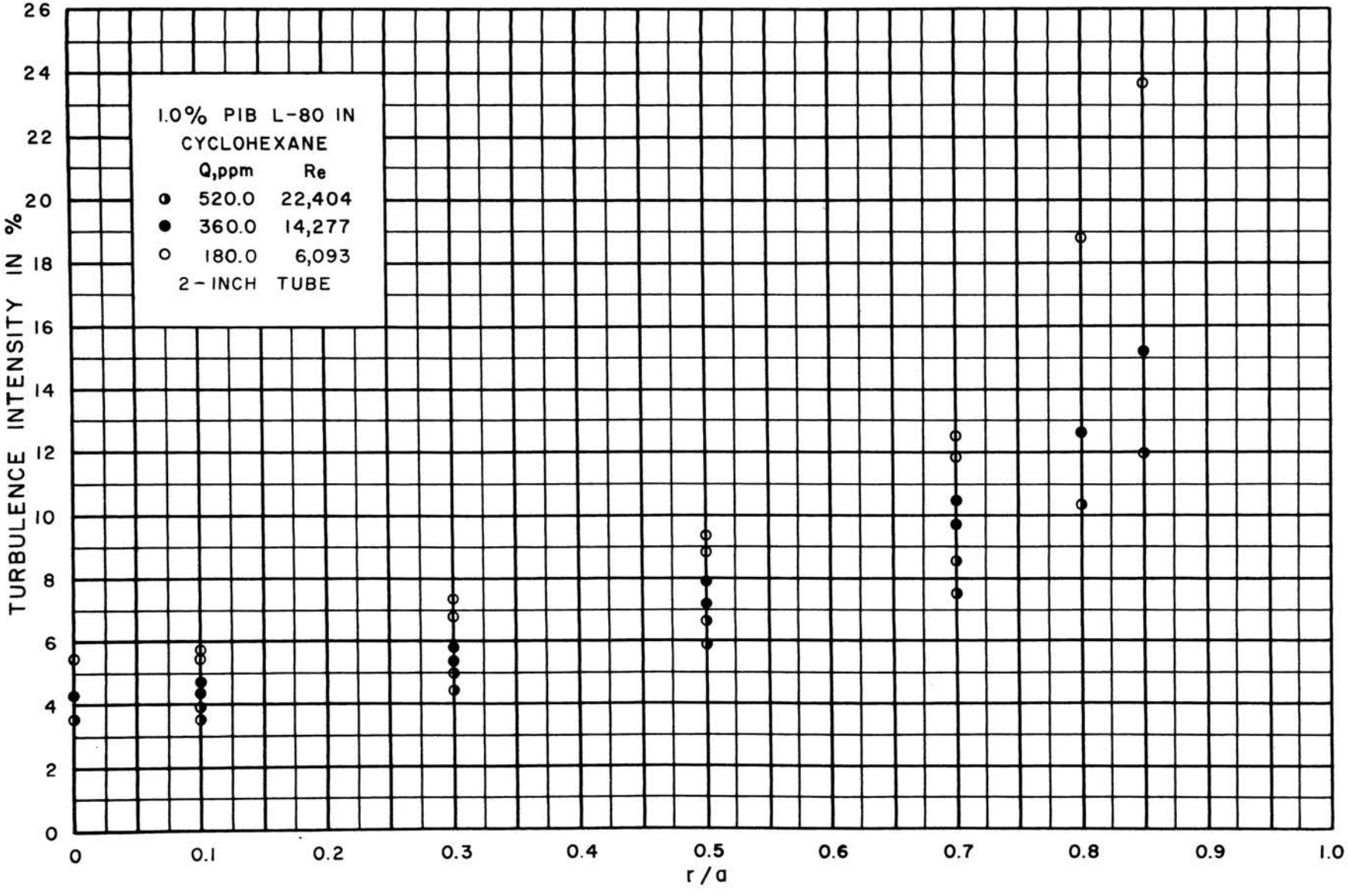


FIGURE 26. TURBULENCE INTENSITY PROFILE FOR RUN 9

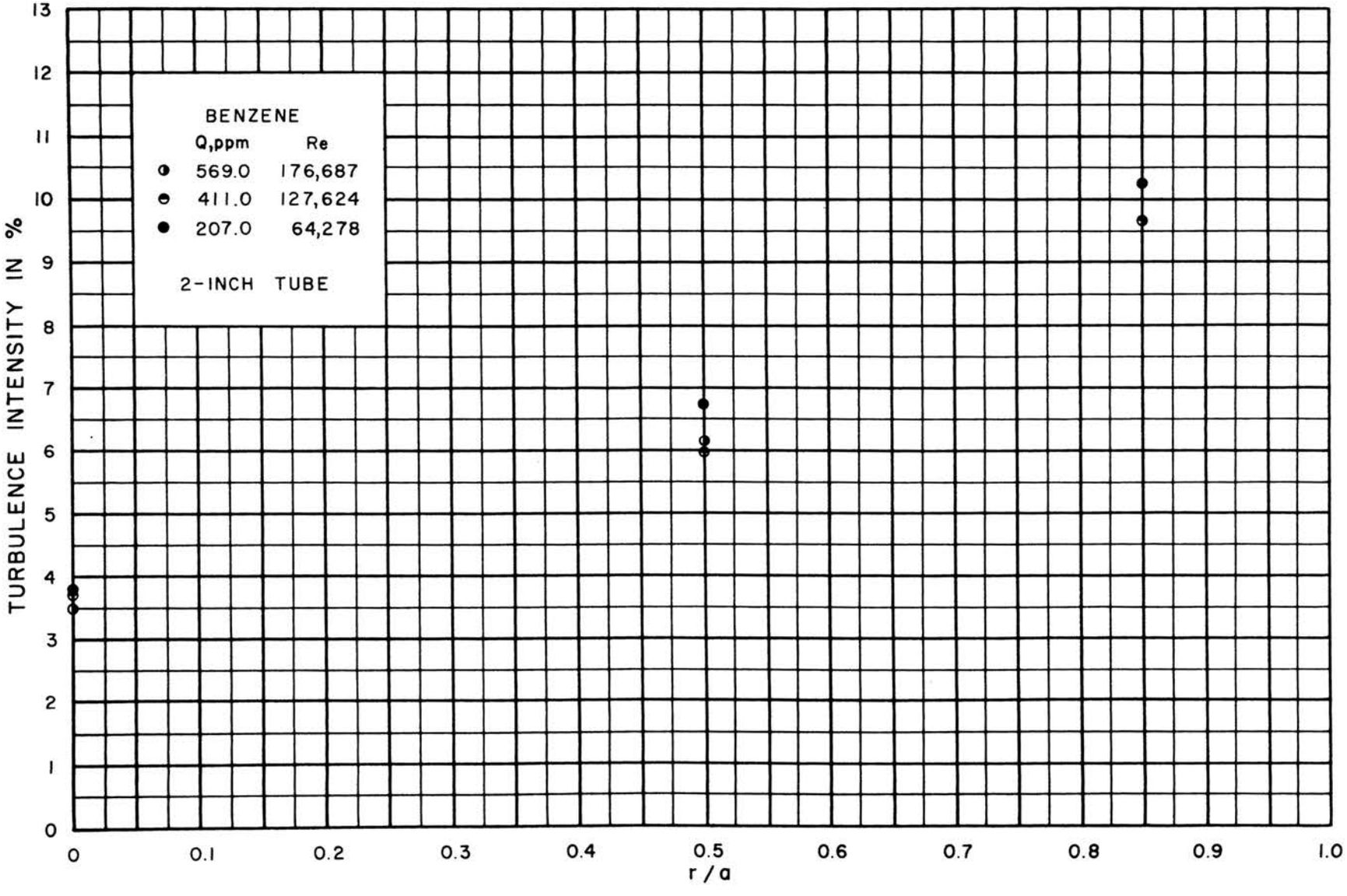


FIGURE 27. TURBULENCE INTENSITY PROFILE FOR RUN 10

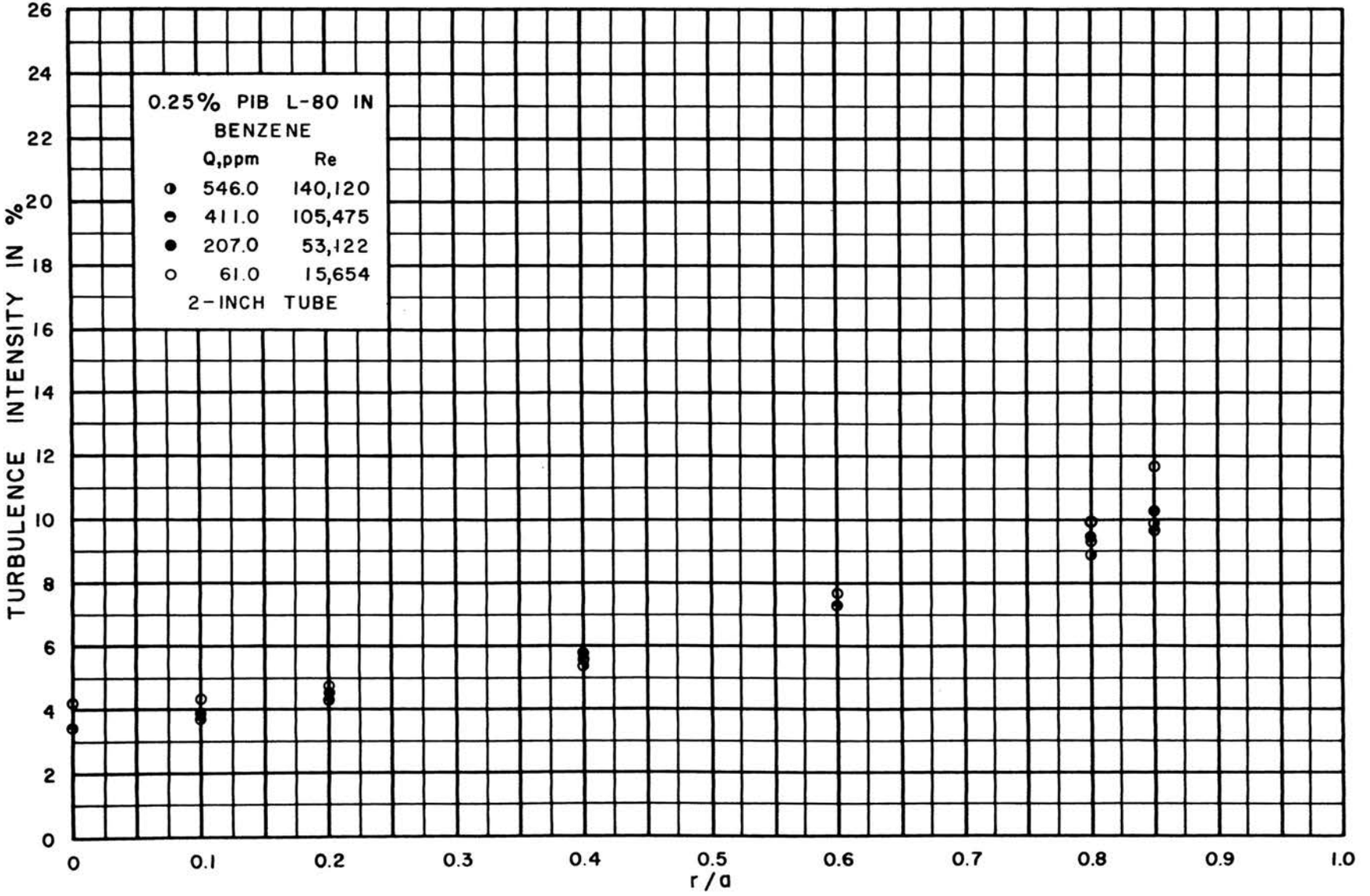


FIGURE 28. TURBULENCE INTENSITY PROFILE FOR RUN II

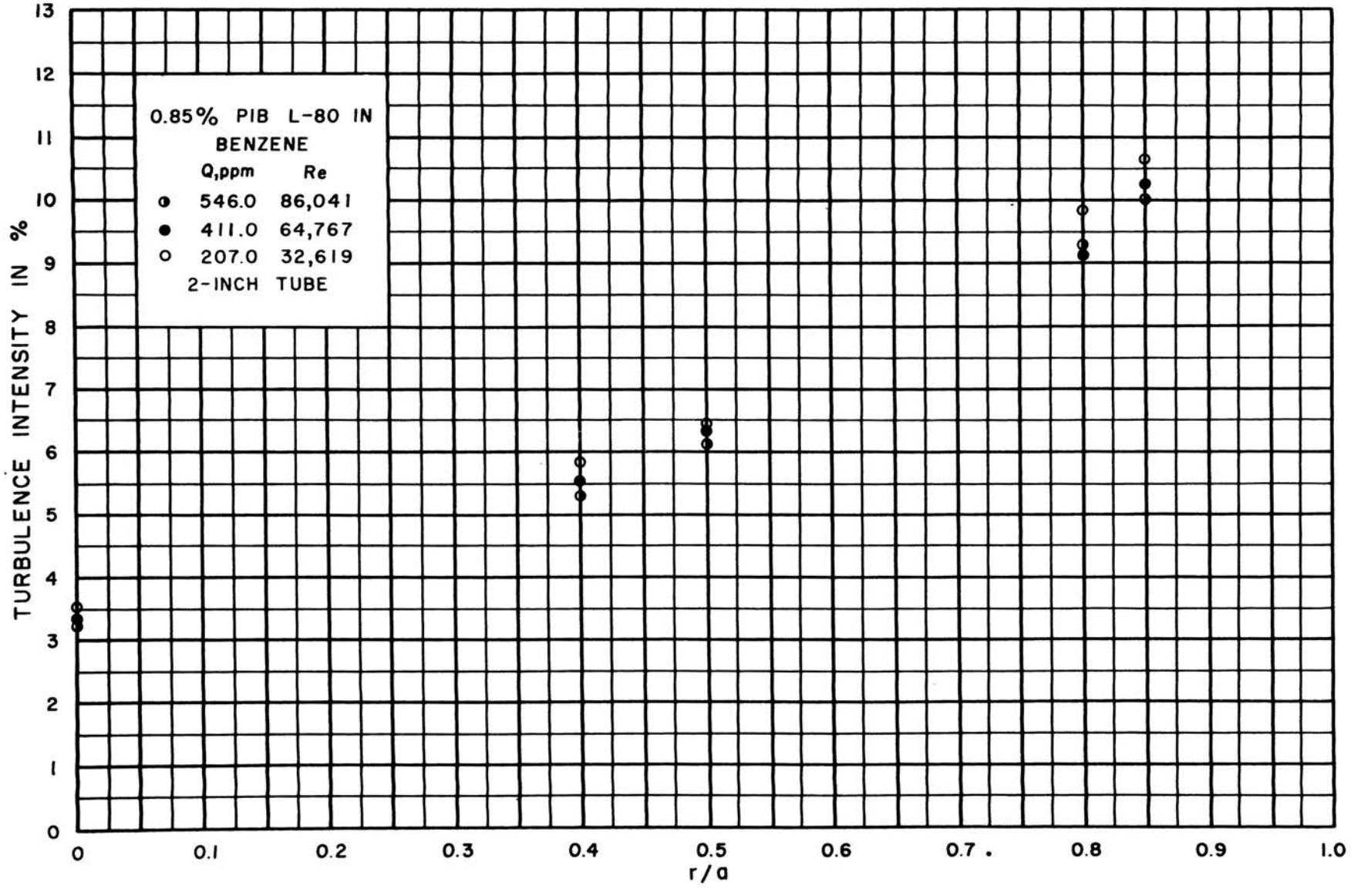


FIGURE 29. TURBULENCE INTENSITY PROFILE FOR RUN 12

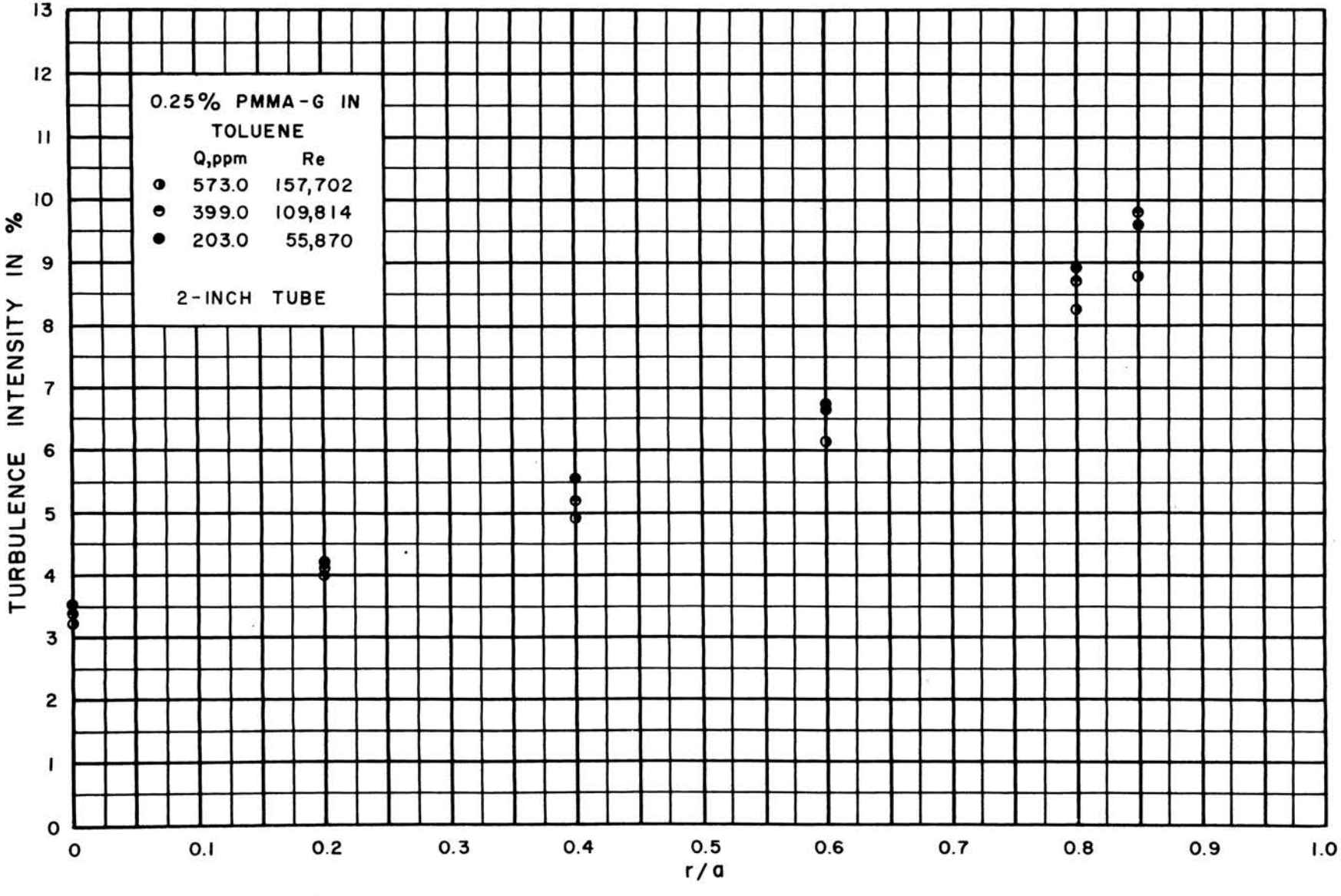


FIGURE 30. TURBULENCE INTENSITY PROFILE FOR RUN 13

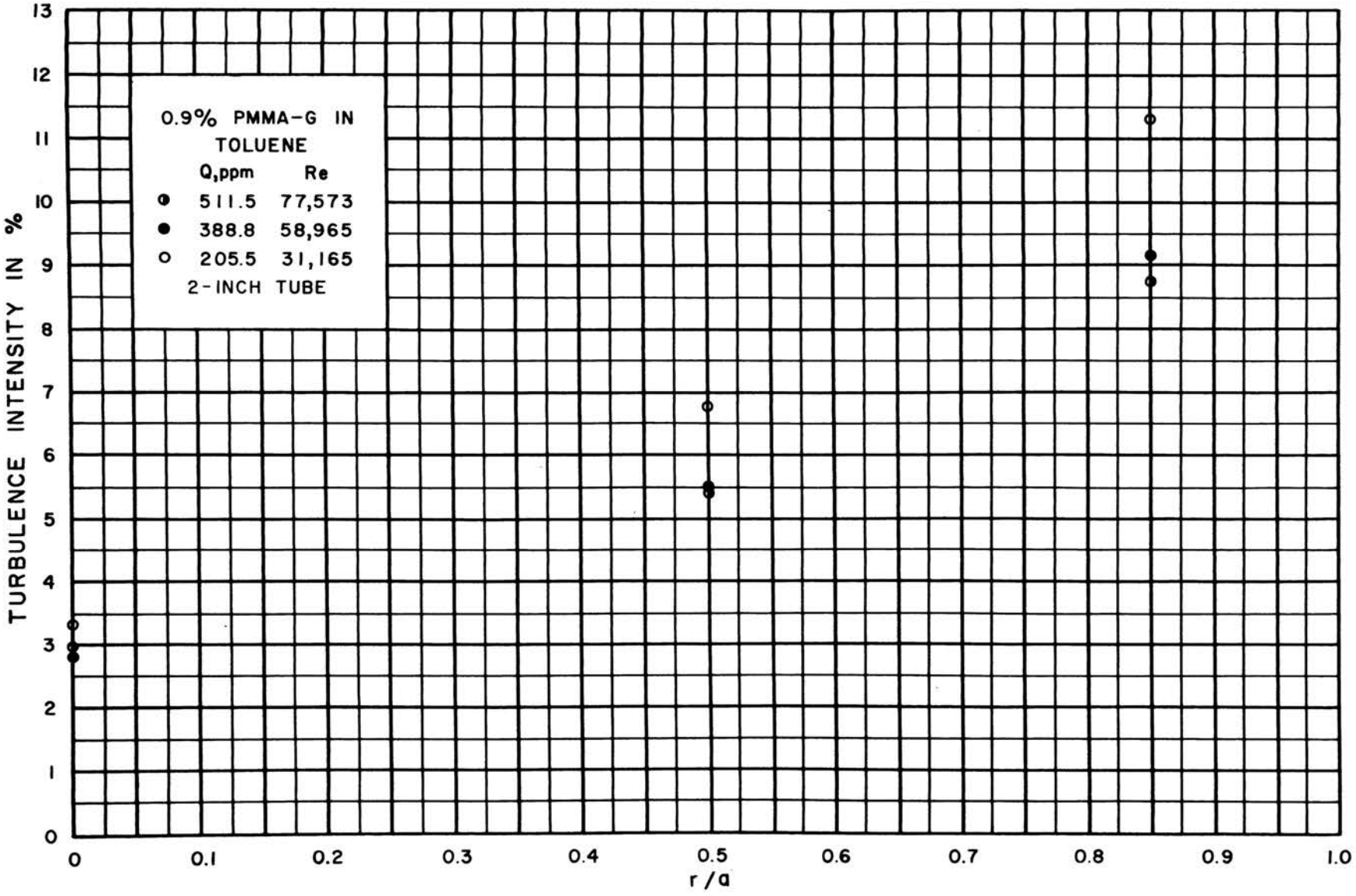


FIGURE 31. TURBULENCE INTENSITY PROFILE FOR RUN 14

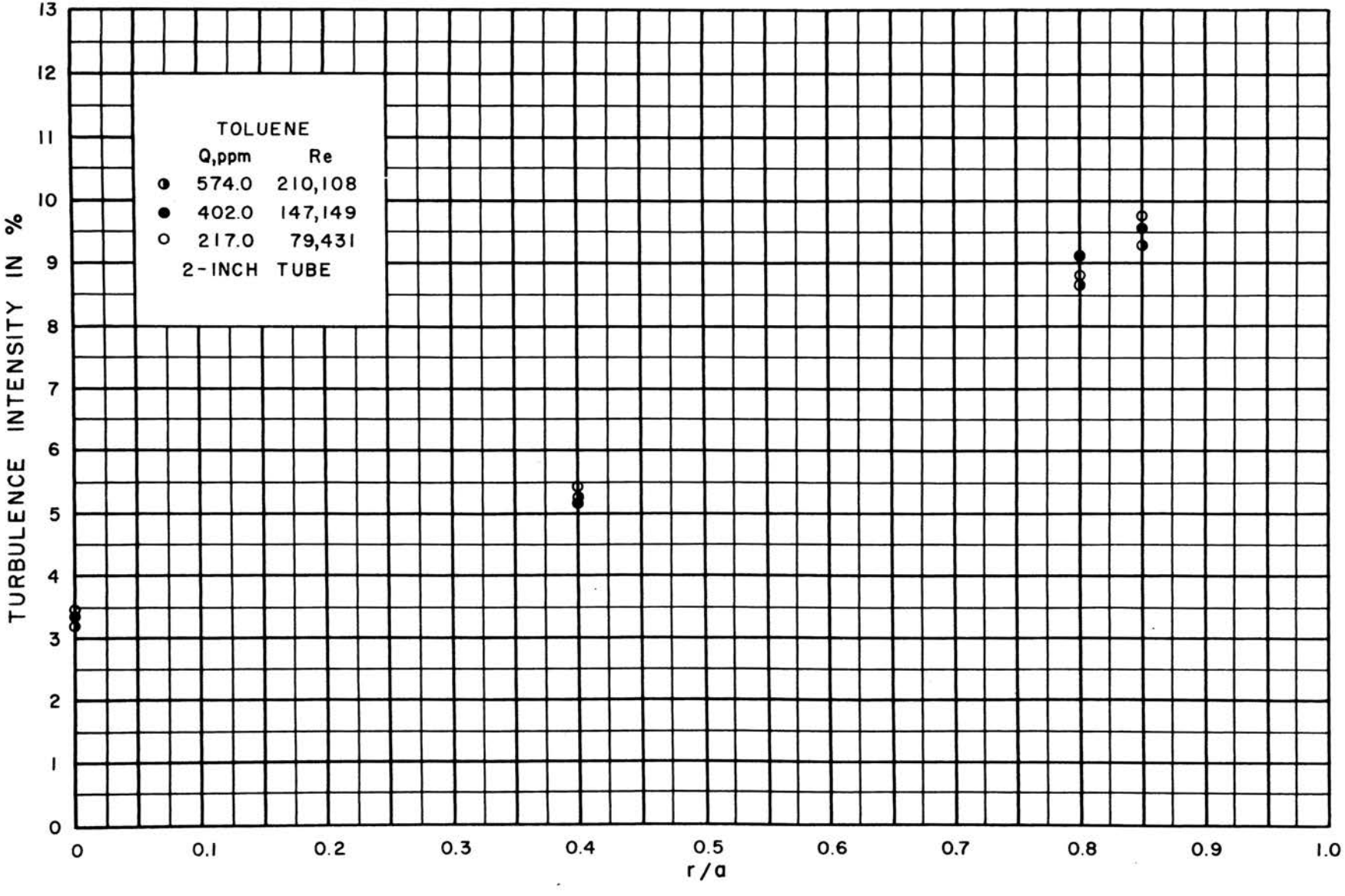


FIGURE 32. TURBULENCE INTENSITY PROFILE FOR RUN 15

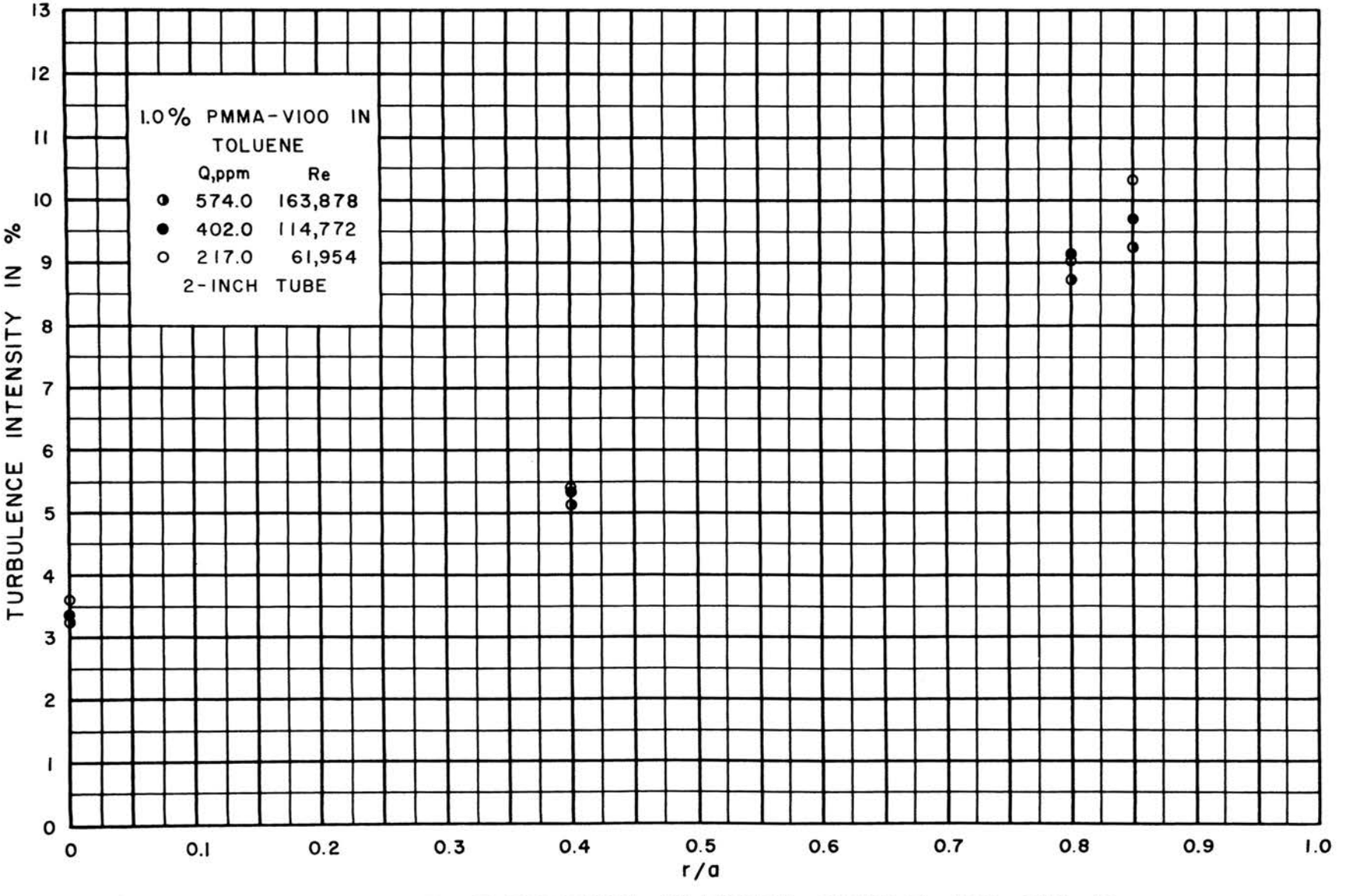


FIGURE 33. TURBULENCE INTENSITY PROFILE FOR RUN 16

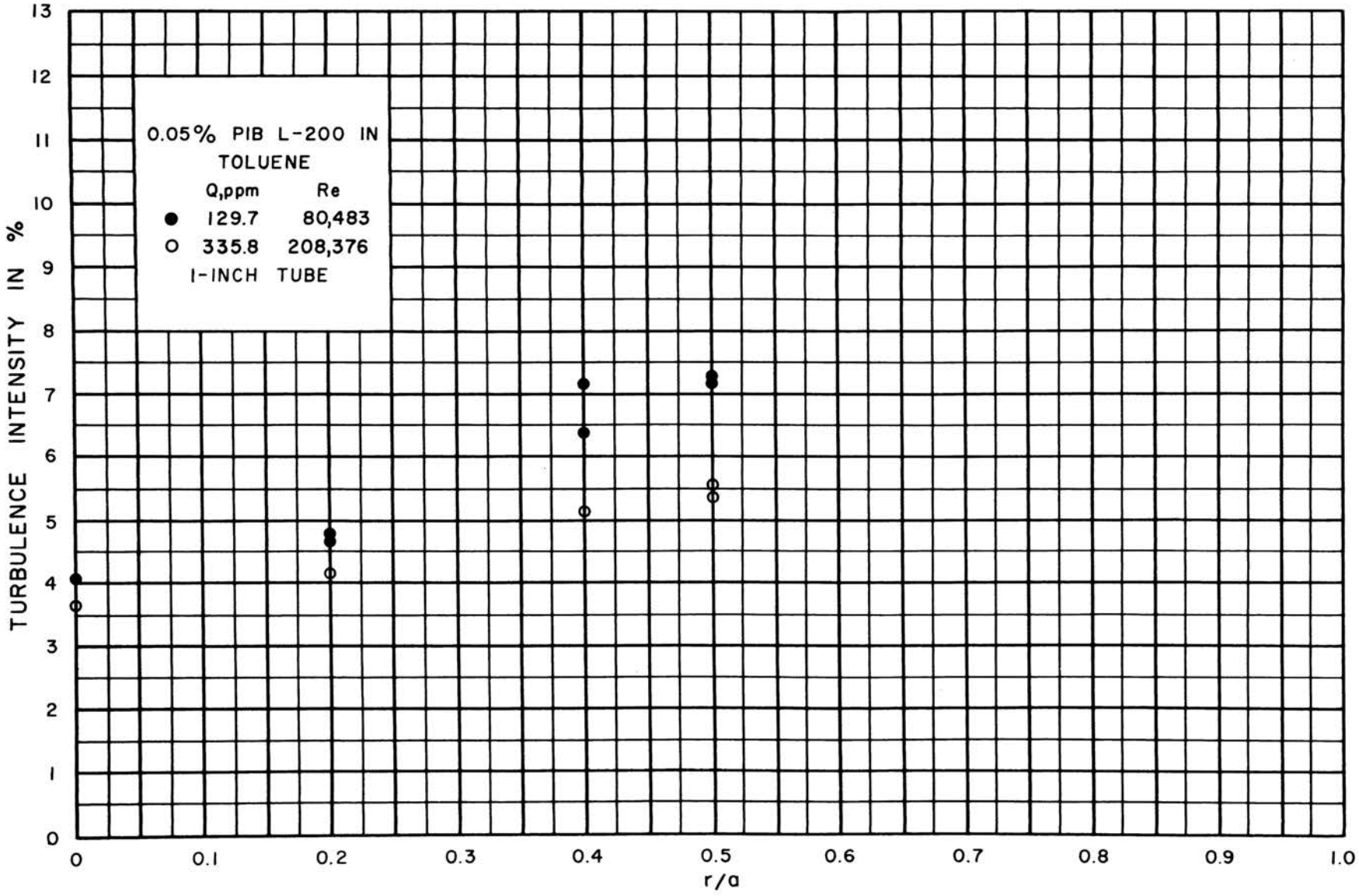


FIGURE 34. TURBULENCE INTENSITY PROFILE FOR RUN 17

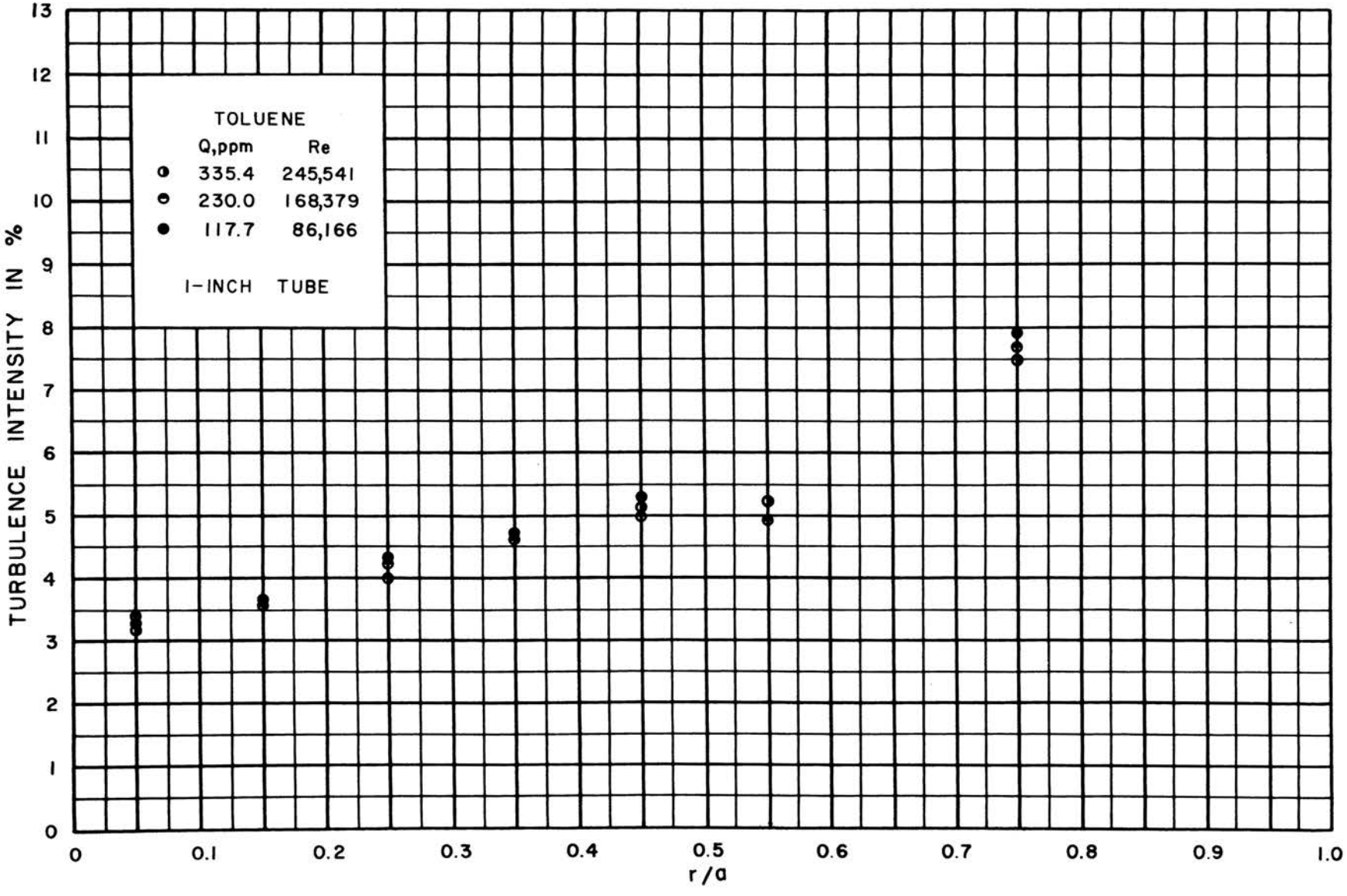


FIGURE 35. TURBULENCE INTENSITY PROFILE FOR RUN 20

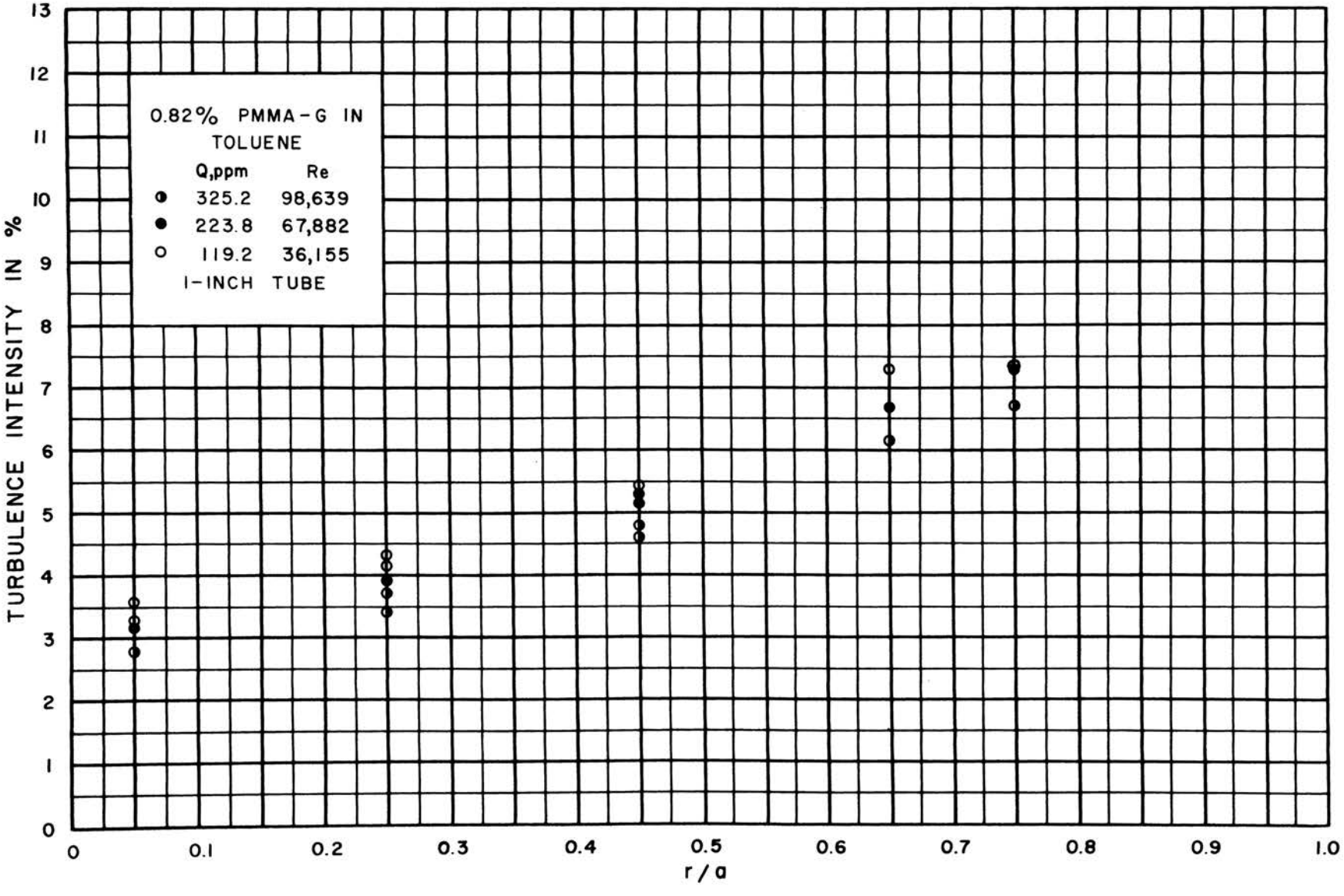


FIGURE 36. TURBULENCE INTENSITY PROFILE FOR RUN 21

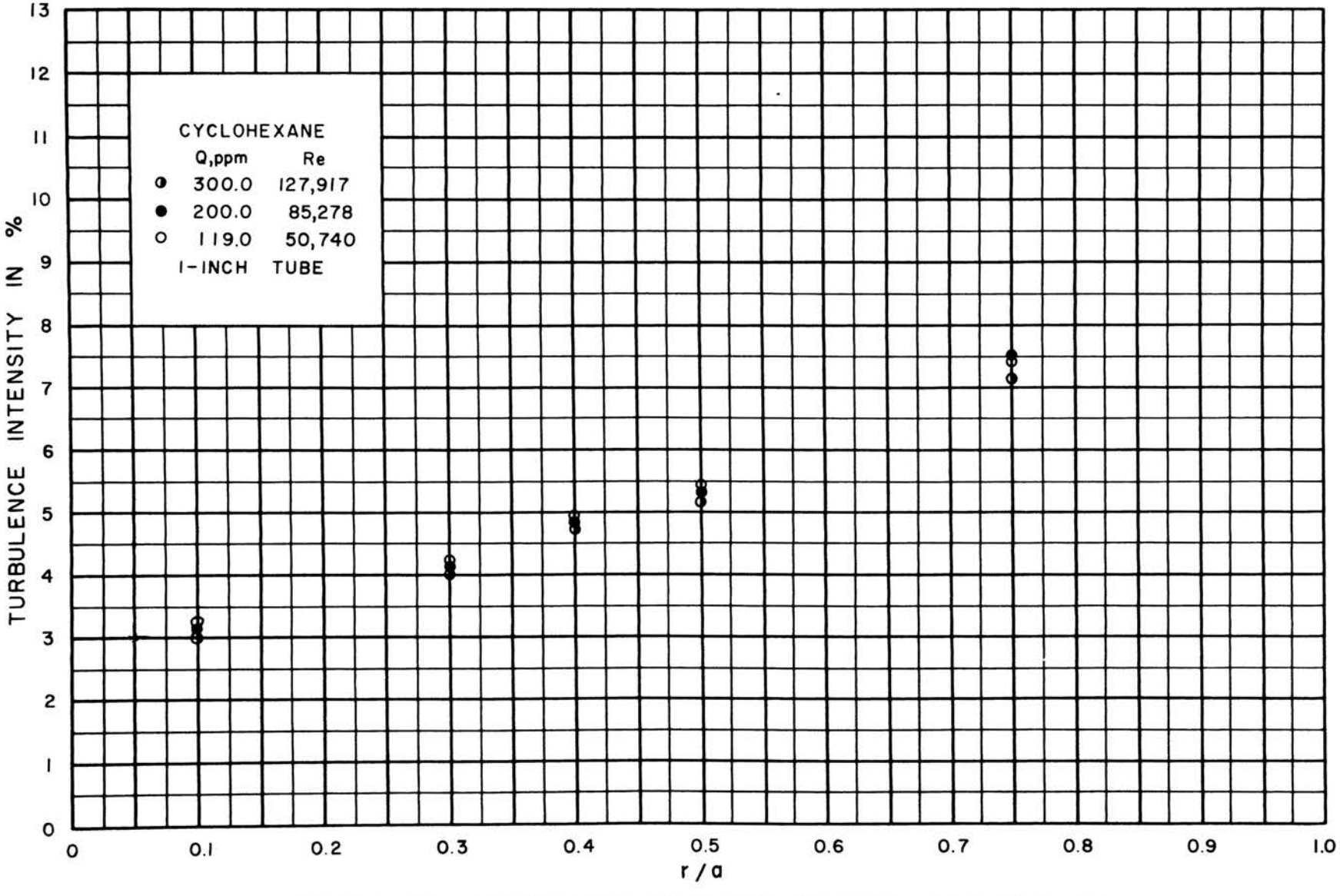


FIGURE 37. TURBULENCE INTENSITY PROFILE FOR RUN 22

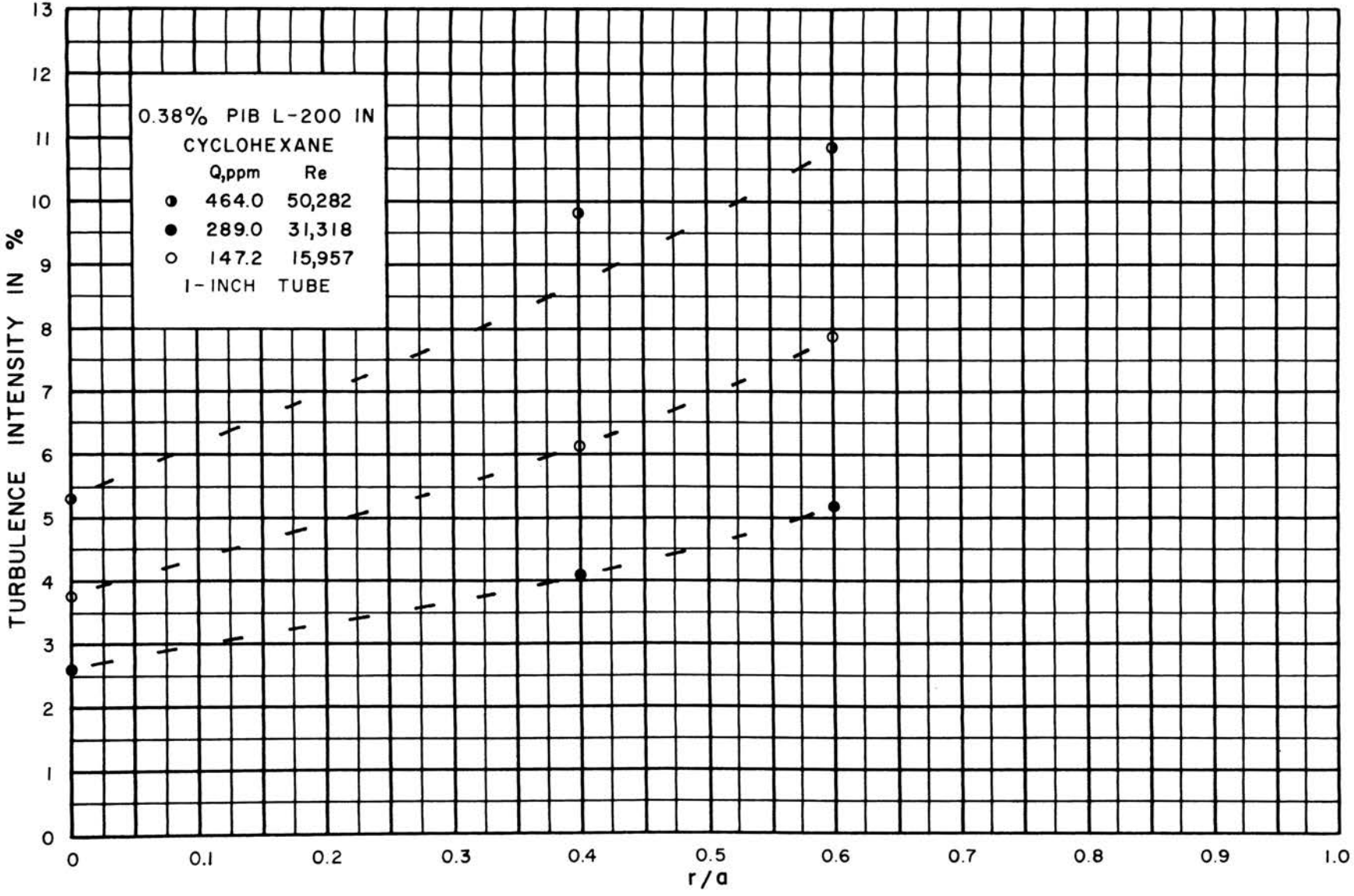


FIGURE 38. TURBULENCE INTENSITY PROFILE FOR RUN 23

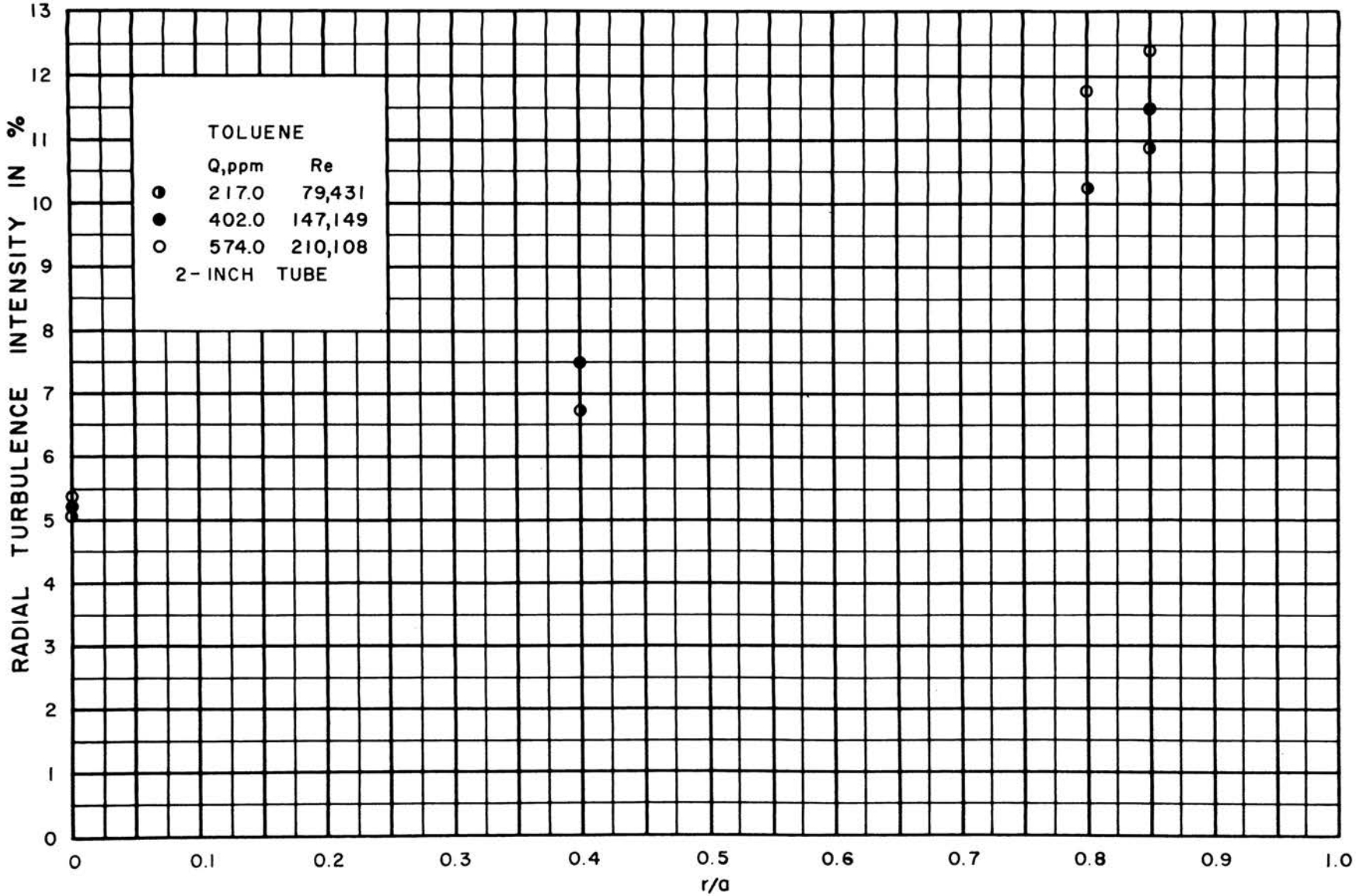


FIGURE 39. RADIAL TURBULENCE INTENSITIES FOR RUN 15

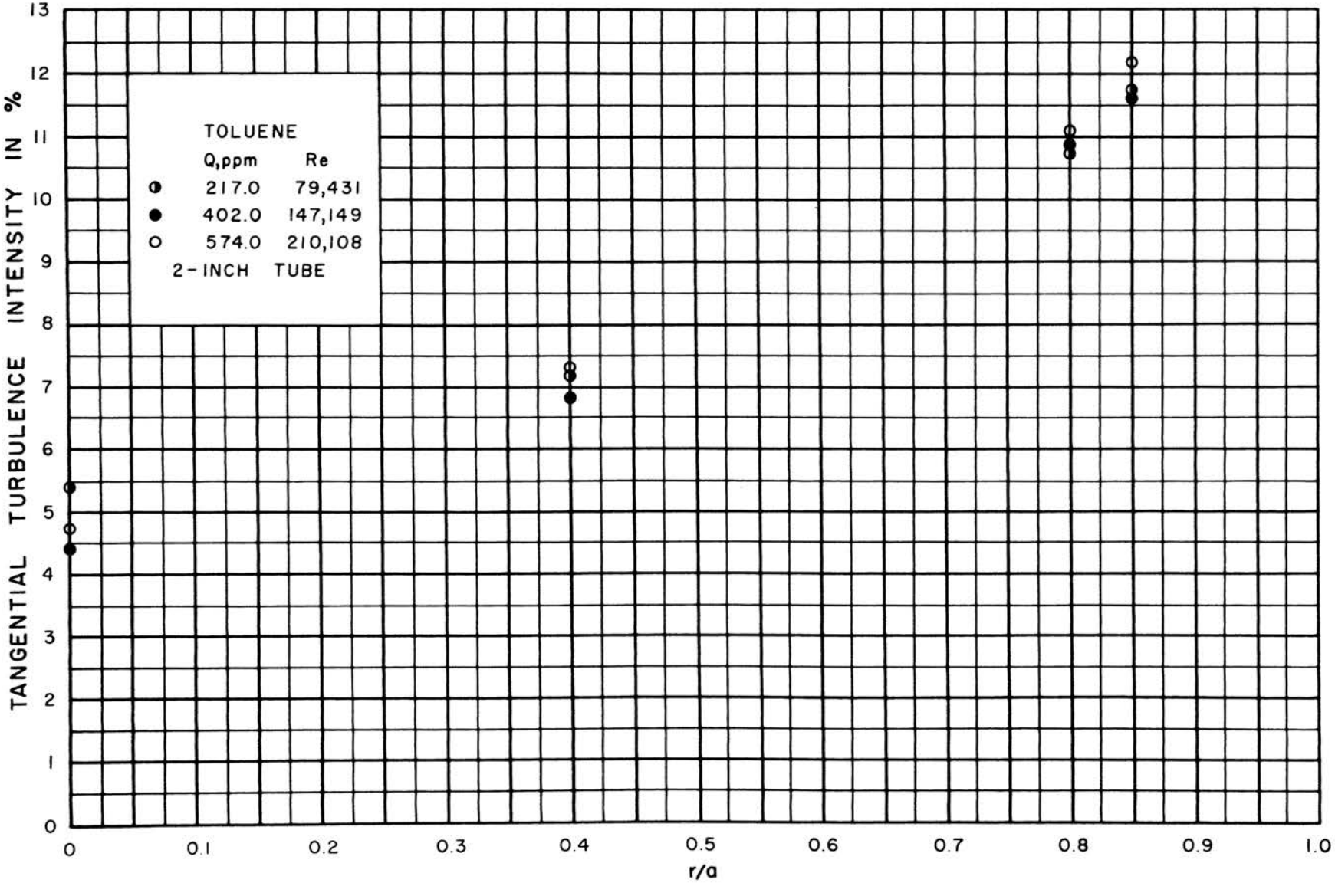


FIGURE 40. TANGENTIAL TURBULENCE INTENSITIES FOR RUN 15

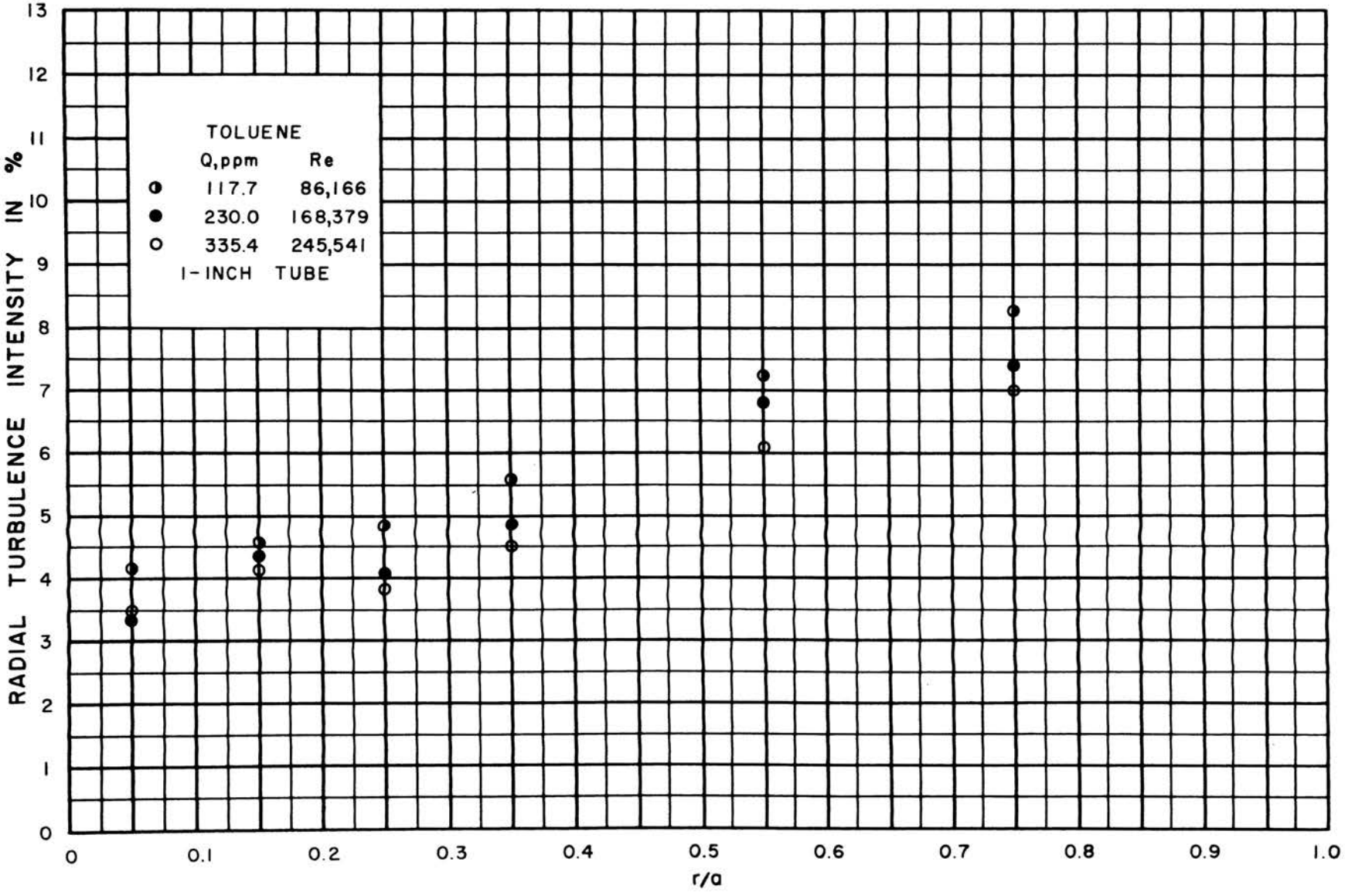


FIGURE 41. RADIAL TURBULENCE INTENSITIES FOR RUN 20

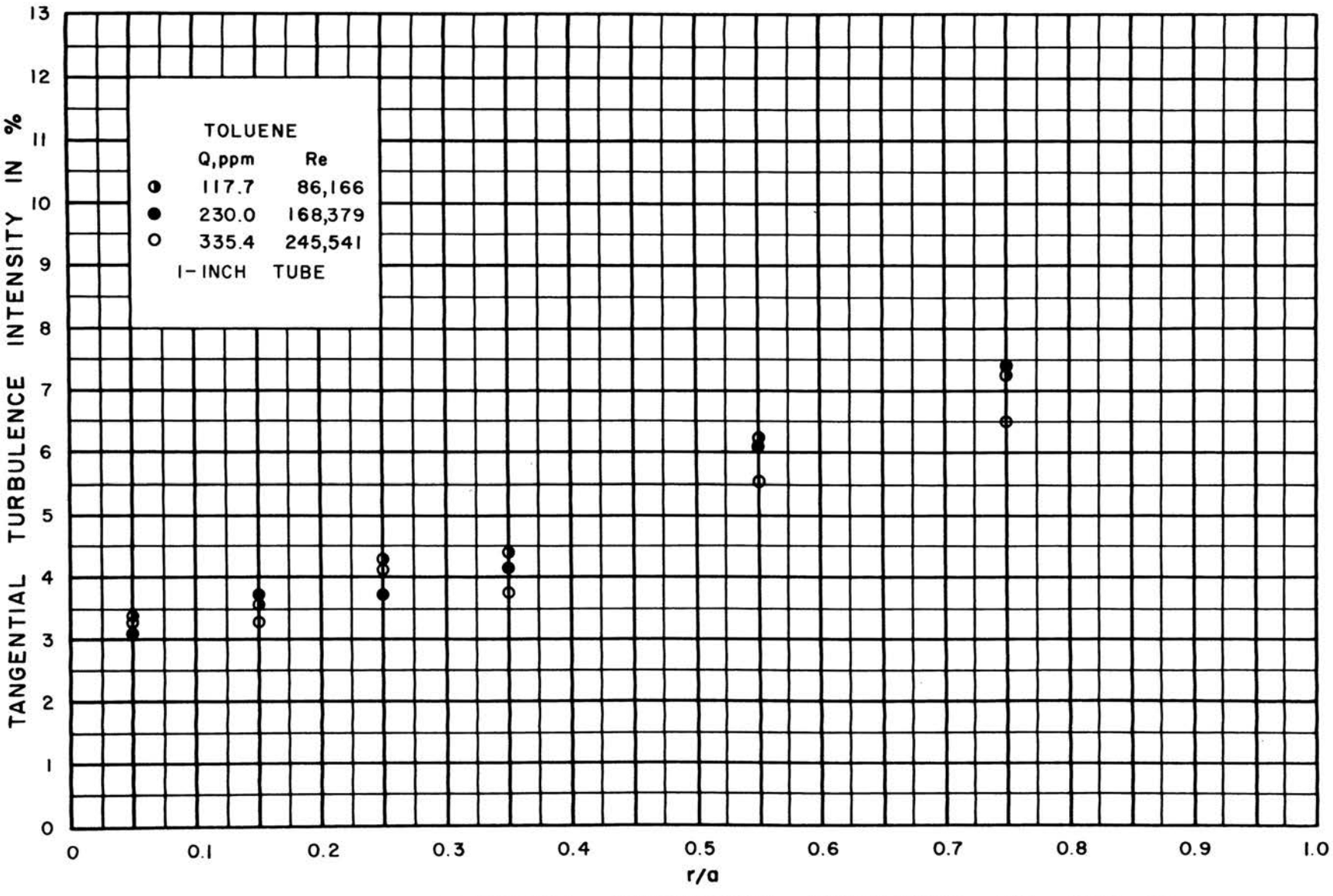


FIGURE 42. TANGENTIAL TURBULENCE INTENSITIES FOR RUN 20

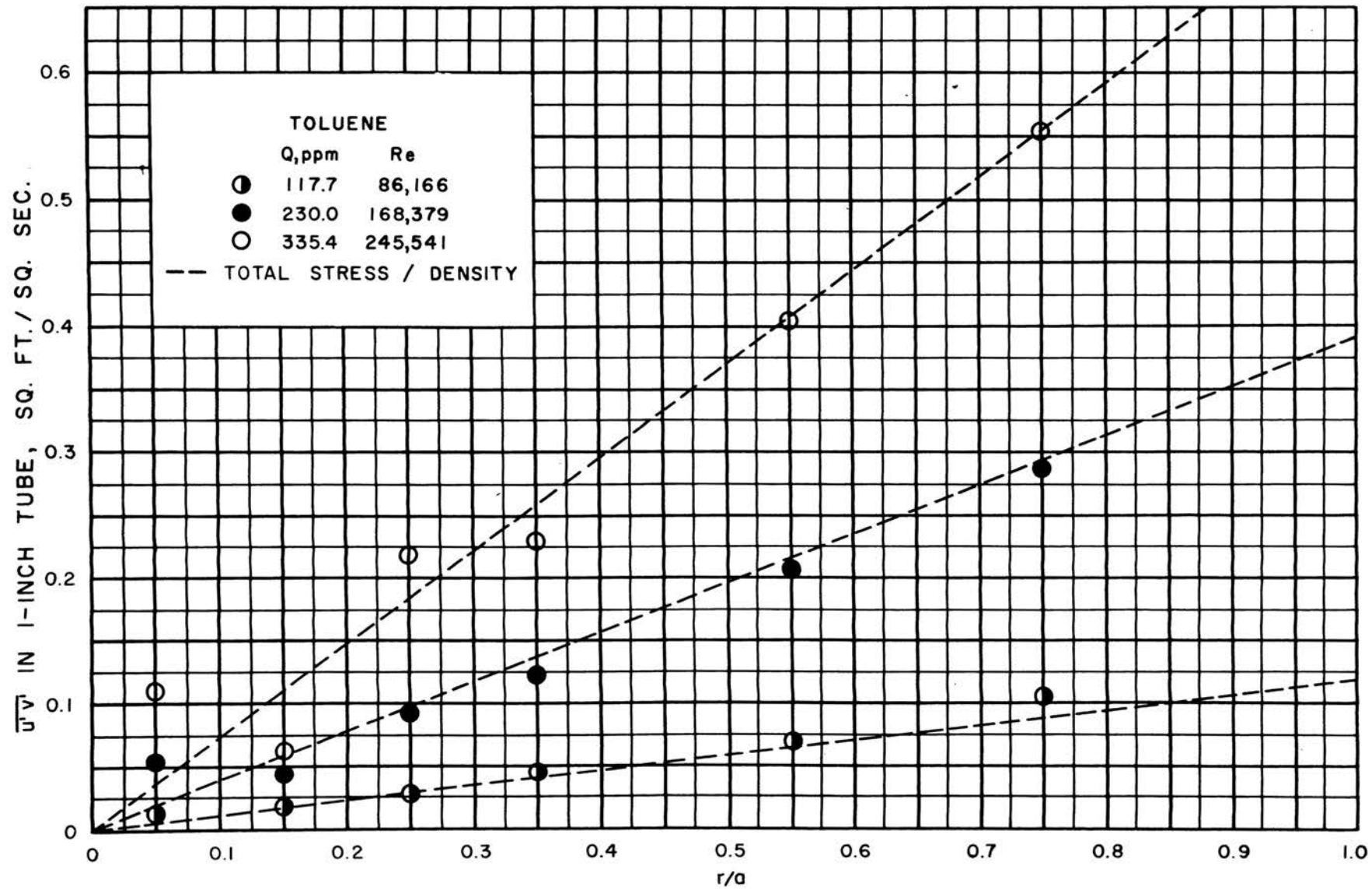


FIGURE 43. REYNOLDS STRESSES FOR RUN 20

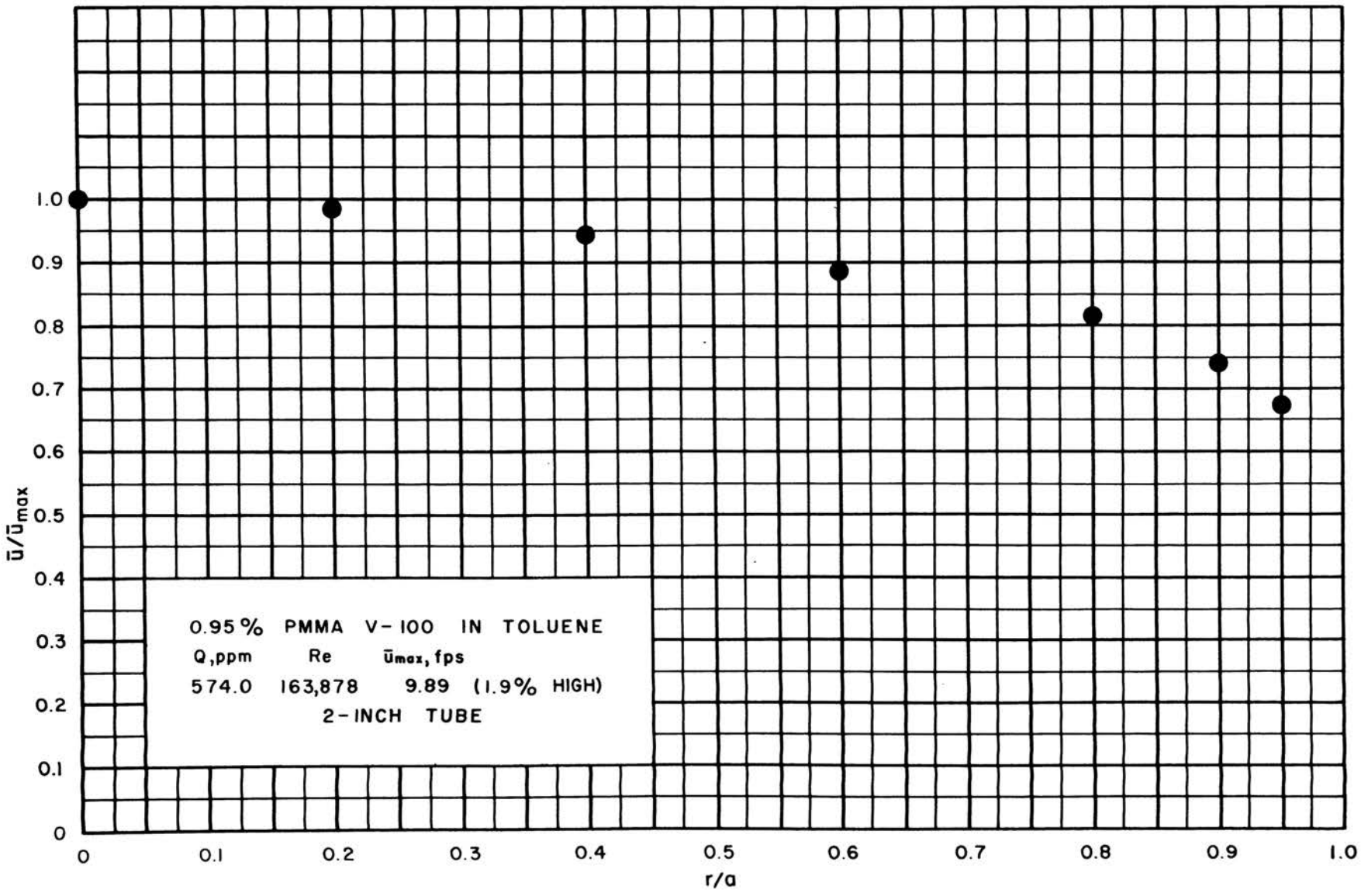


FIGURE 44. VELOCITY PROFILE FOR RUN 16

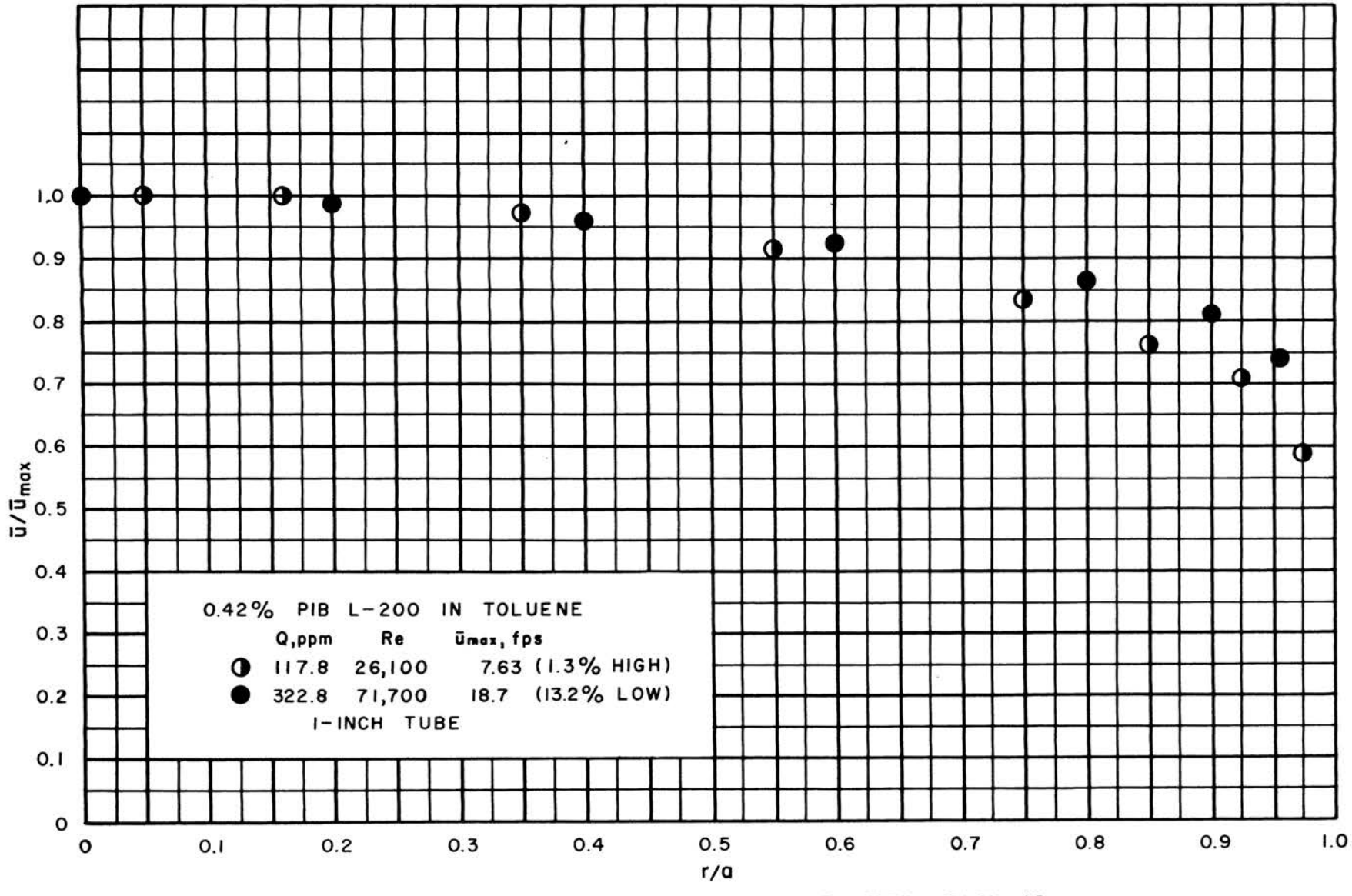


FIGURE 45. VELOCITY PROFILE FOR RUN 19

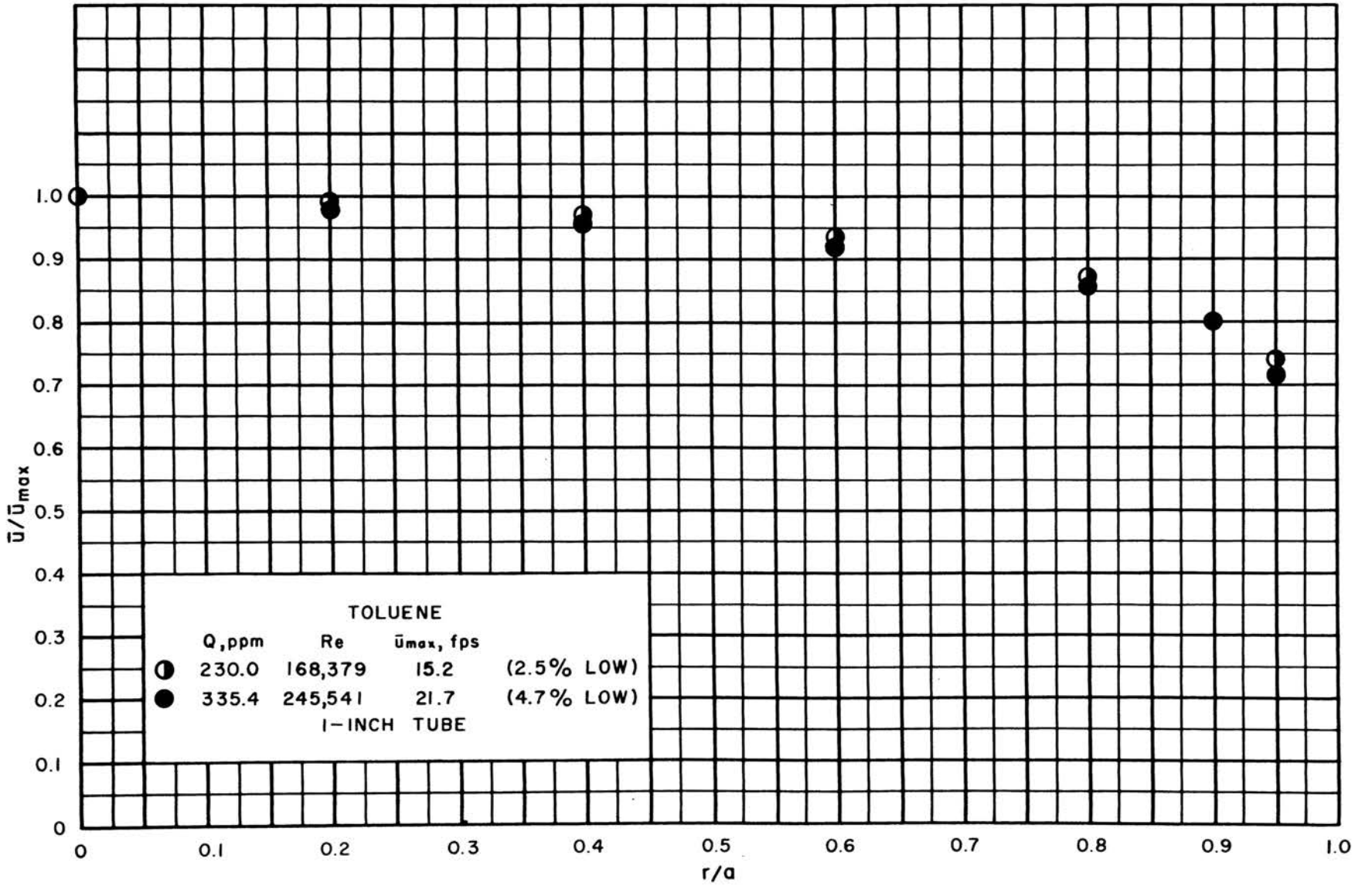


FIGURE 46. VELOCITY PROFILE FOR RUN 20

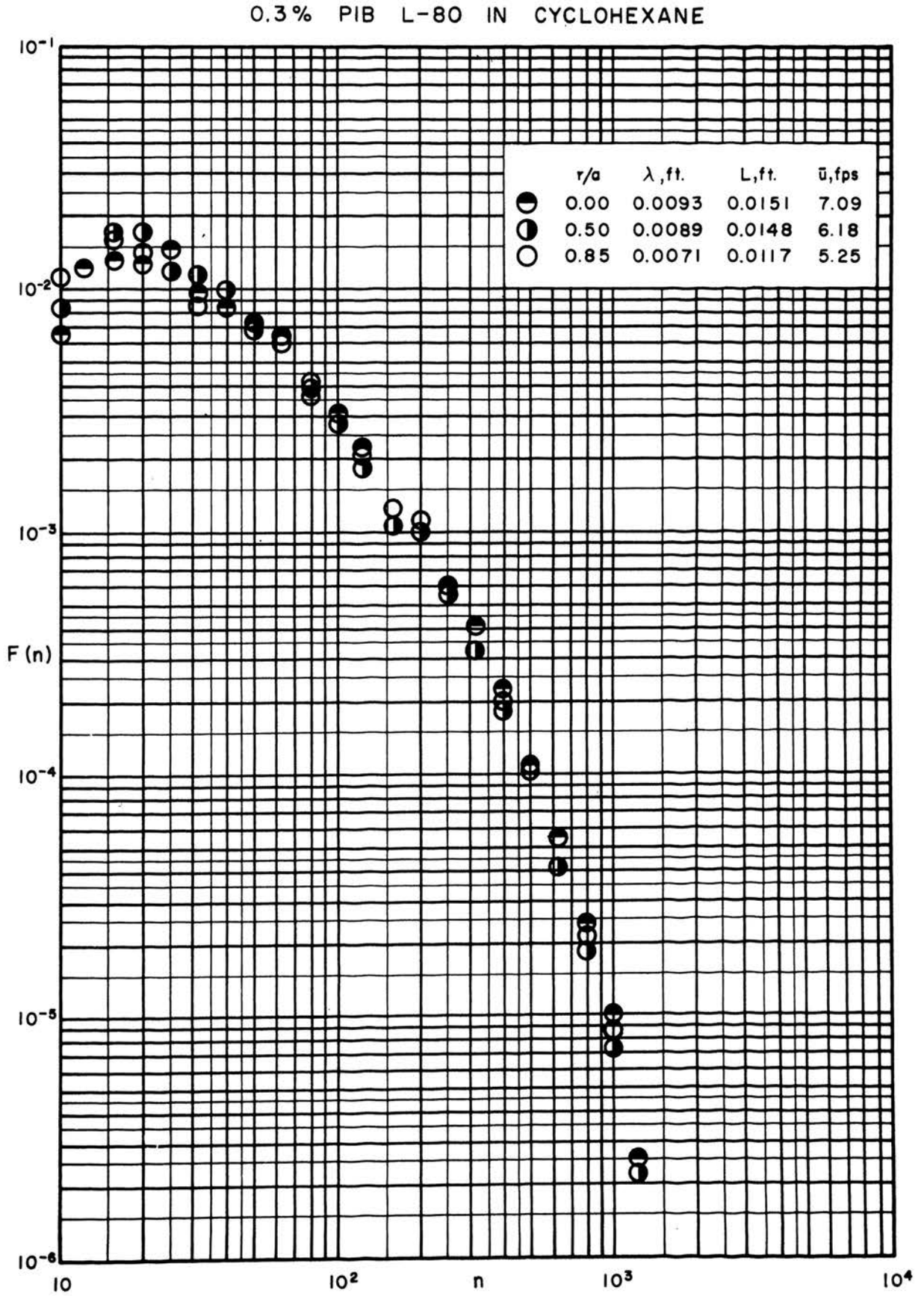


FIGURE 47. ENERGY SPECTRA FOR RUN 8

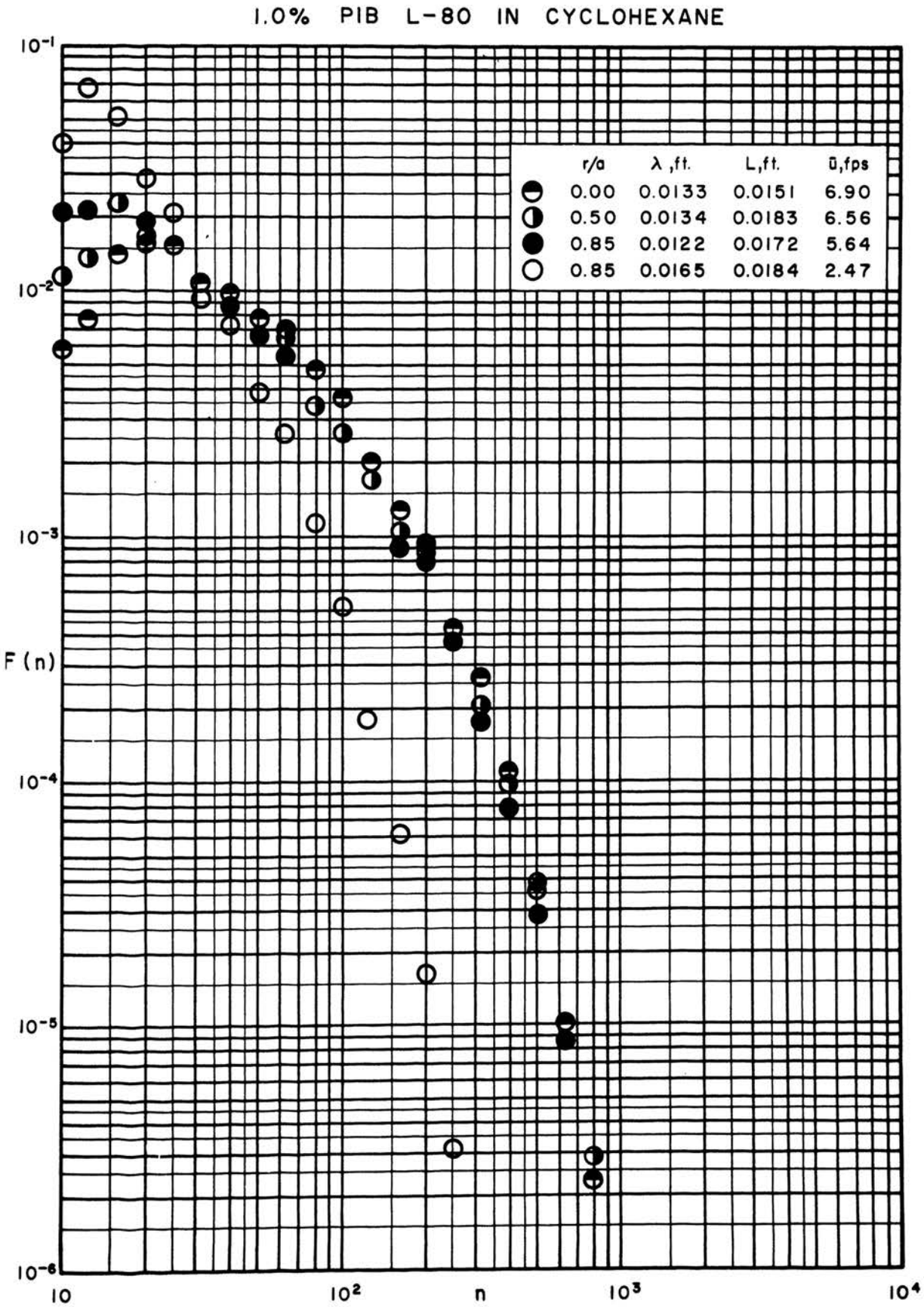


FIGURE 48. ENERGY SPECTRA FOR RUN 9

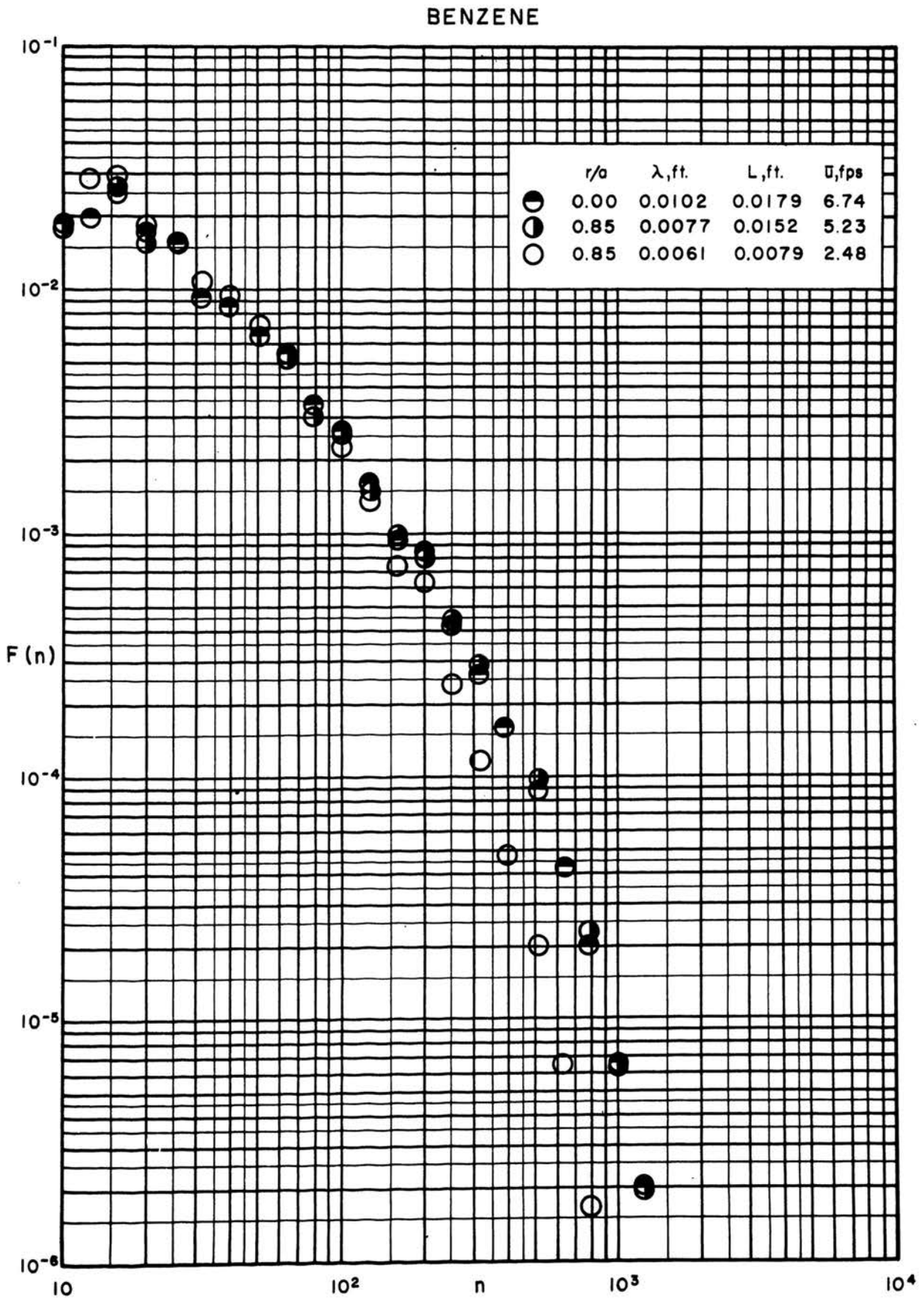


FIGURE 49. ENERGY SPECTRA FOR RUN 10

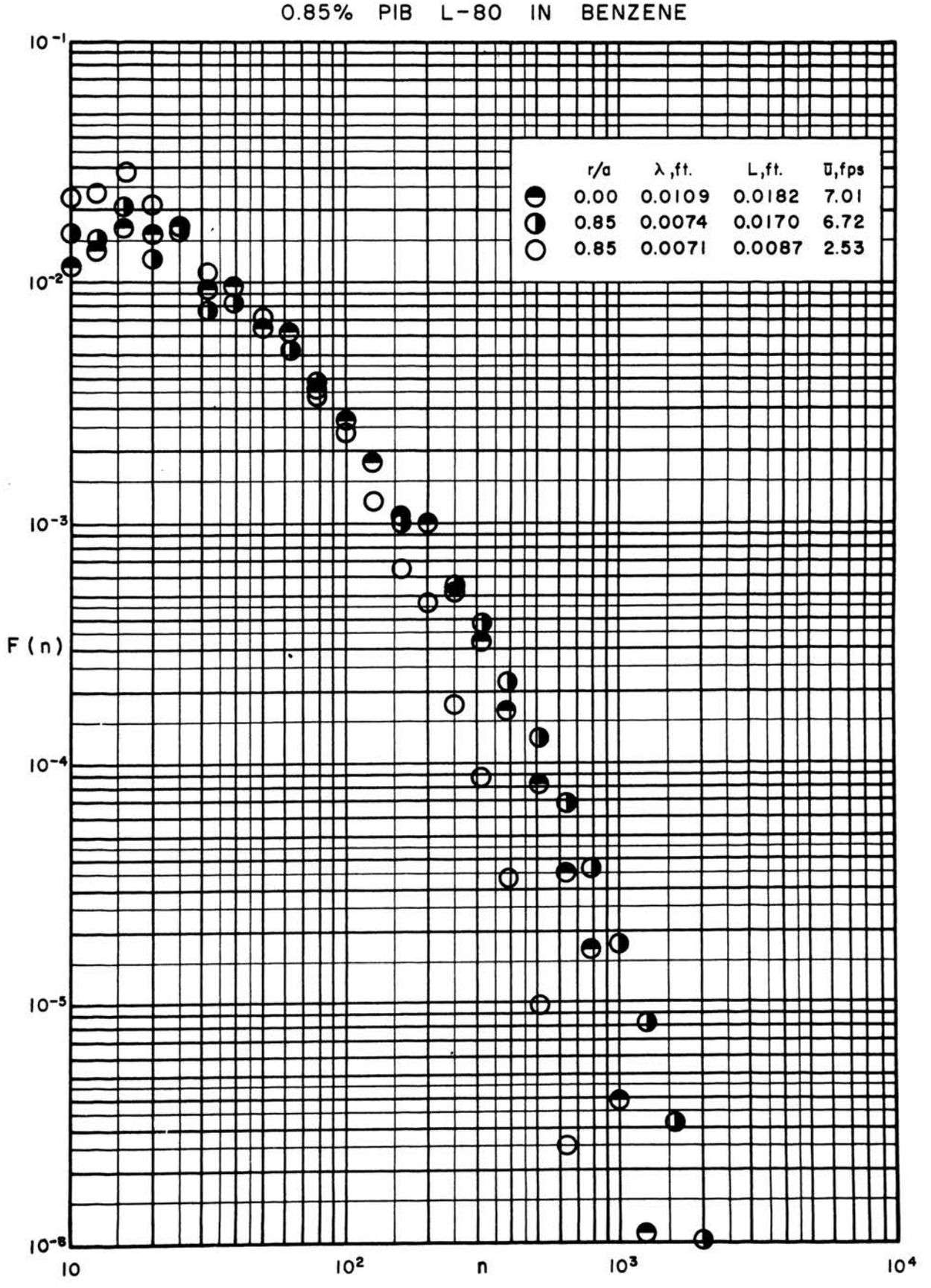


FIGURE 50. ENERGY SPECTRA FOR RUN 12

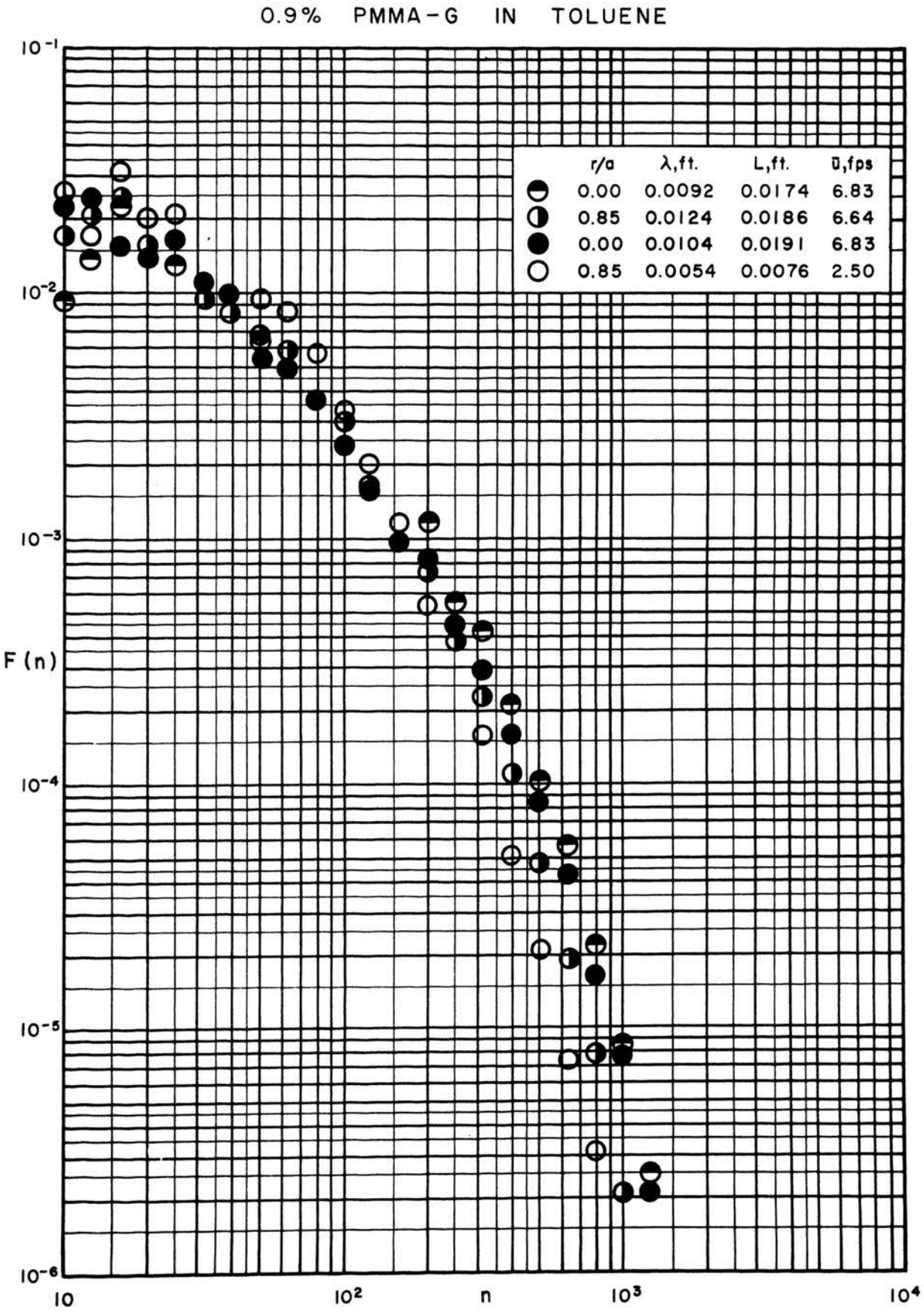


FIGURE 51. ENERGY SPECTRA FOR RUN 14

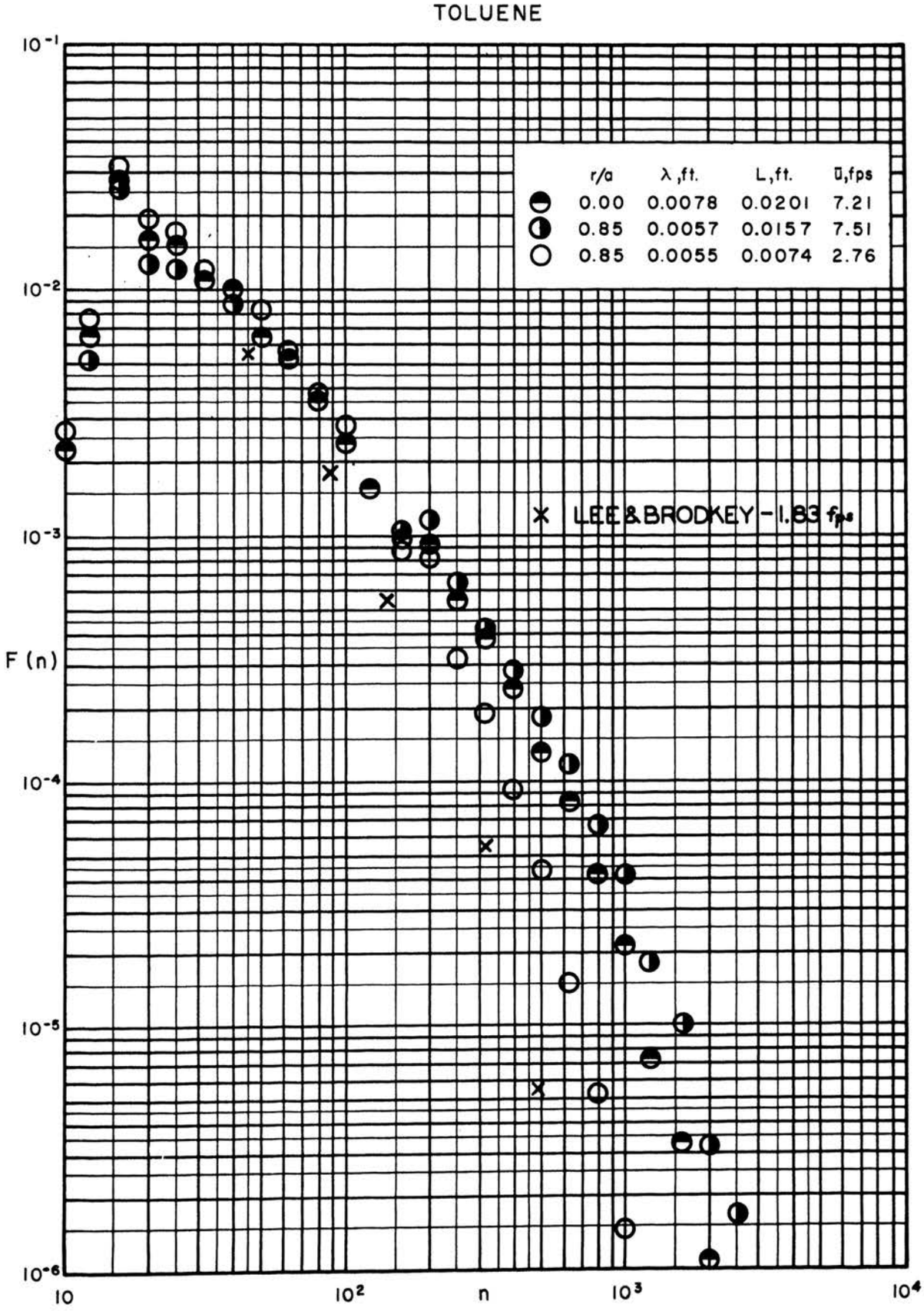


FIGURE 52. ENERGY SPECTRA FOR RUN 15

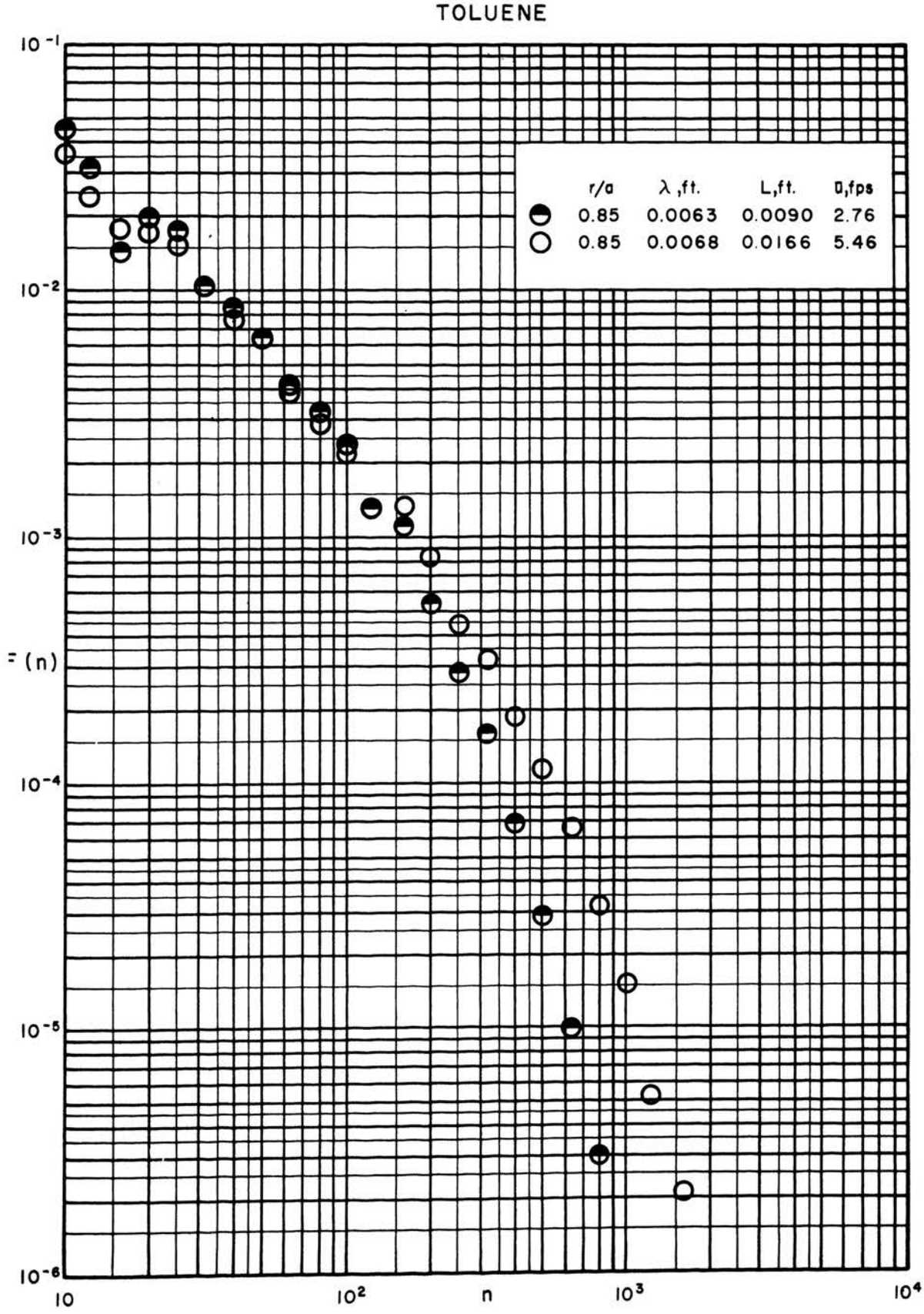


FIGURE 53. ENERGY SPECTRA FOR RUN 15 (PDM)

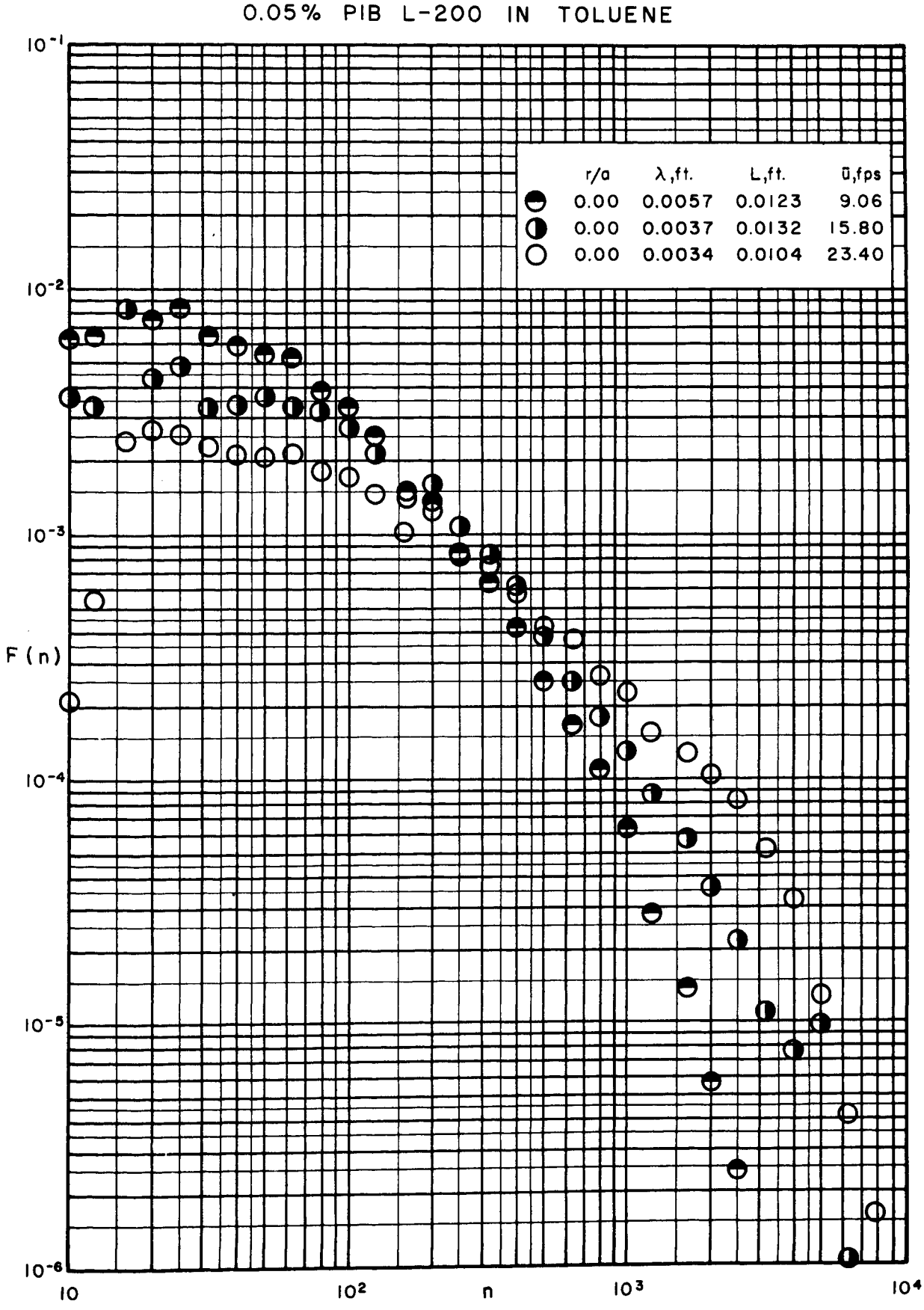


FIGURE 54. ENERGY SPECTRA FOR RUN 17

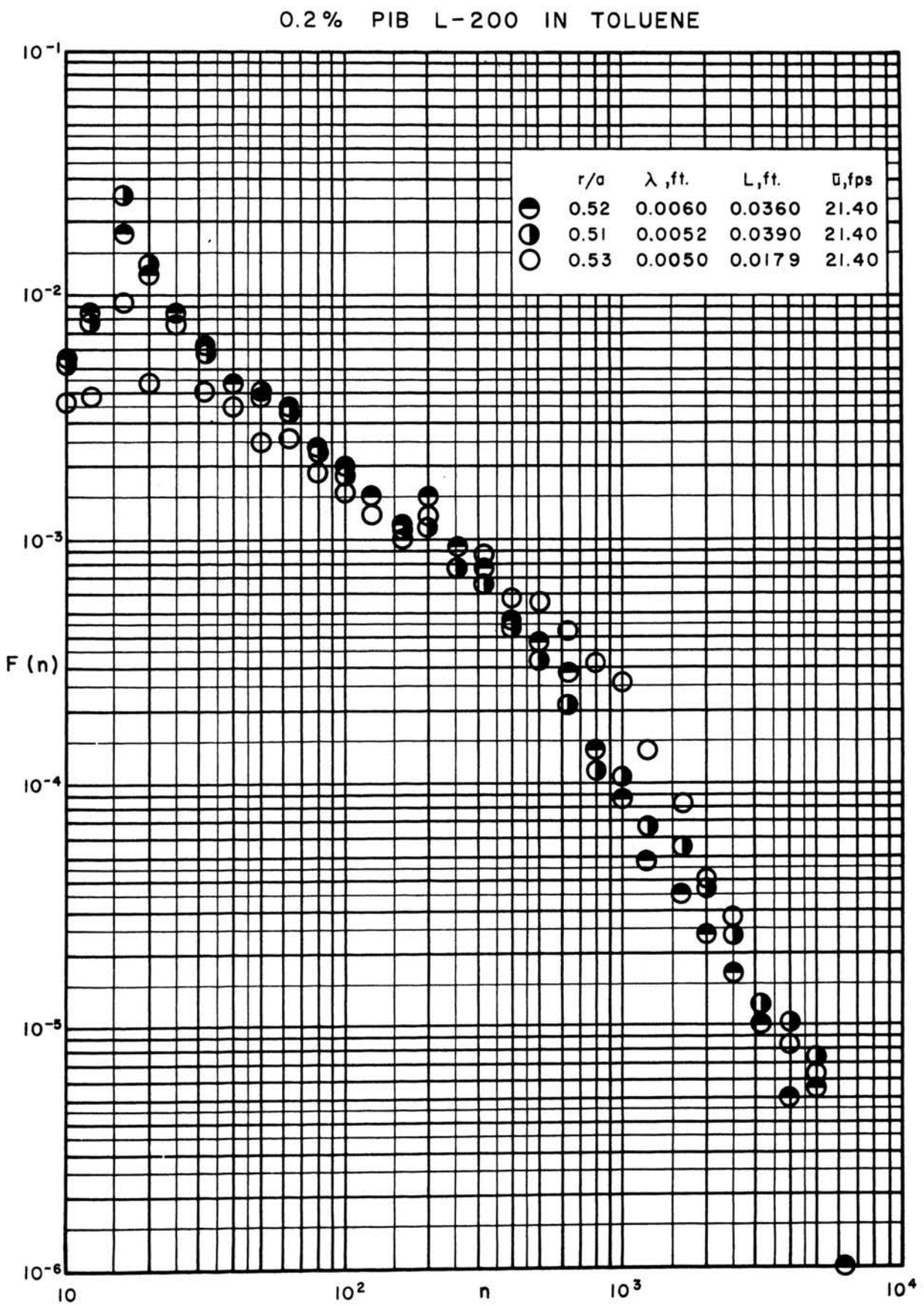


FIGURE 55. ENERGY SPECTRA FOR RUN 18

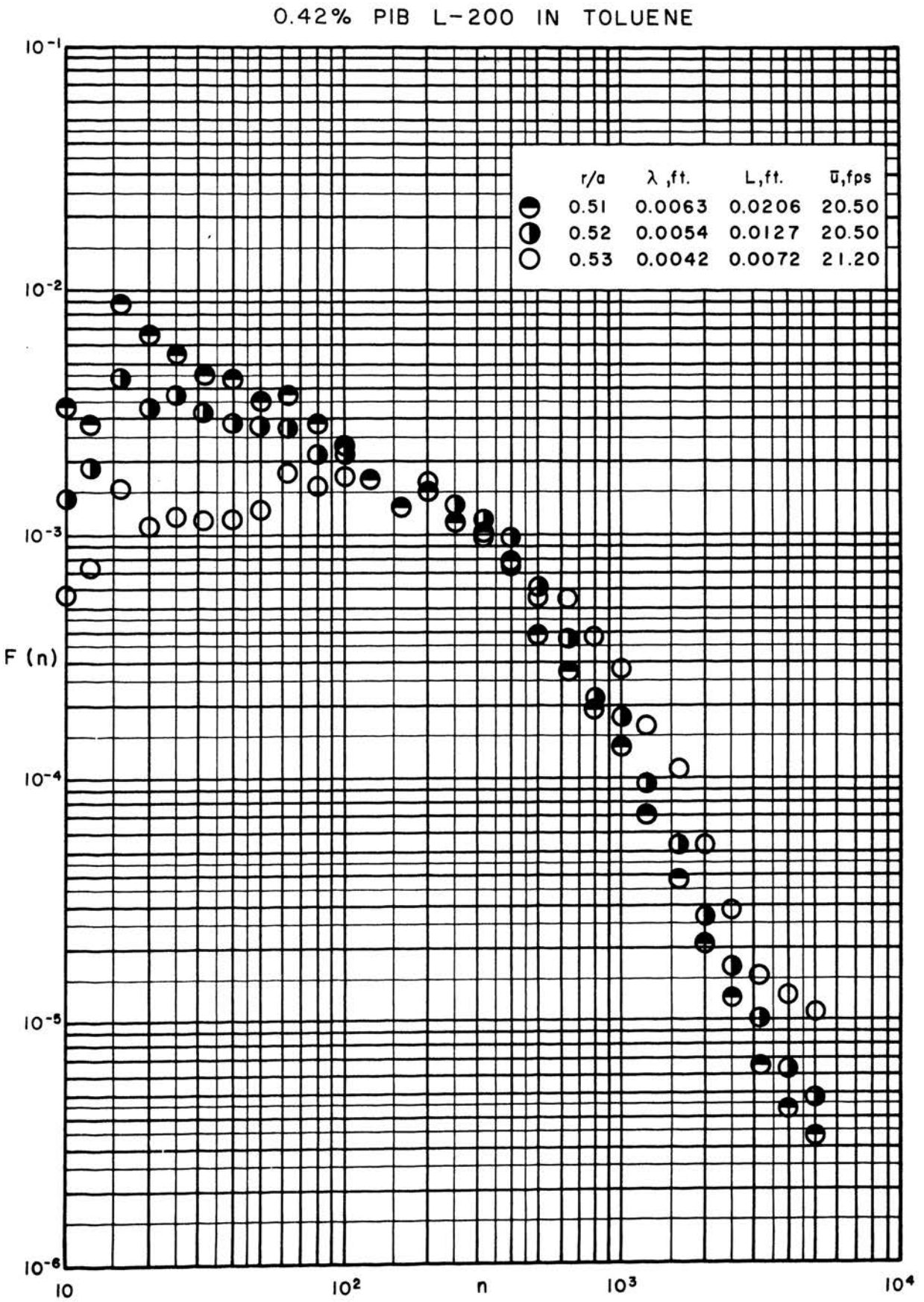


FIGURE 56. ENERGY SPECTRA FOR RUN 19

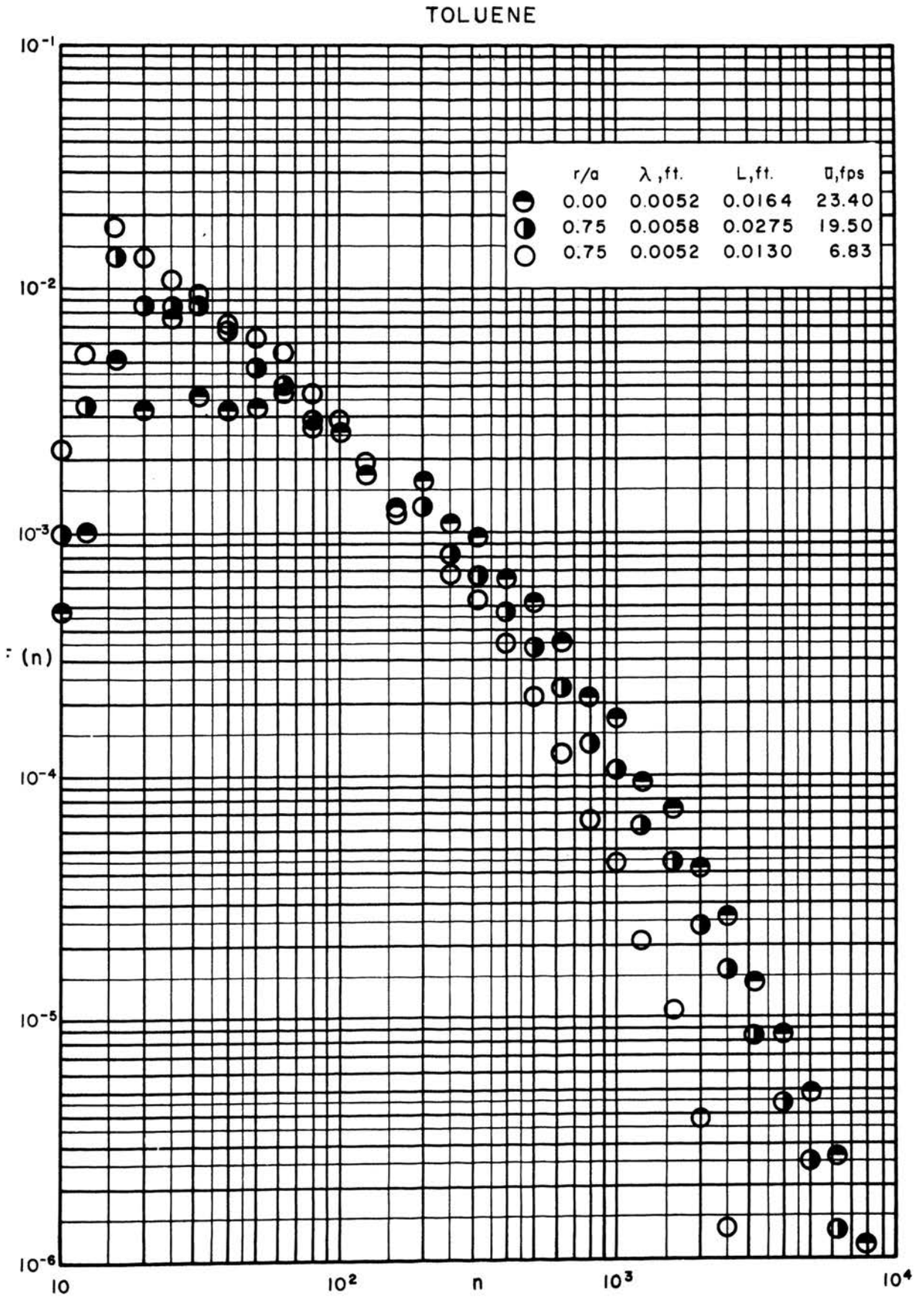


FIGURE 57. ENERGY SPECTRA FOR RUN 20

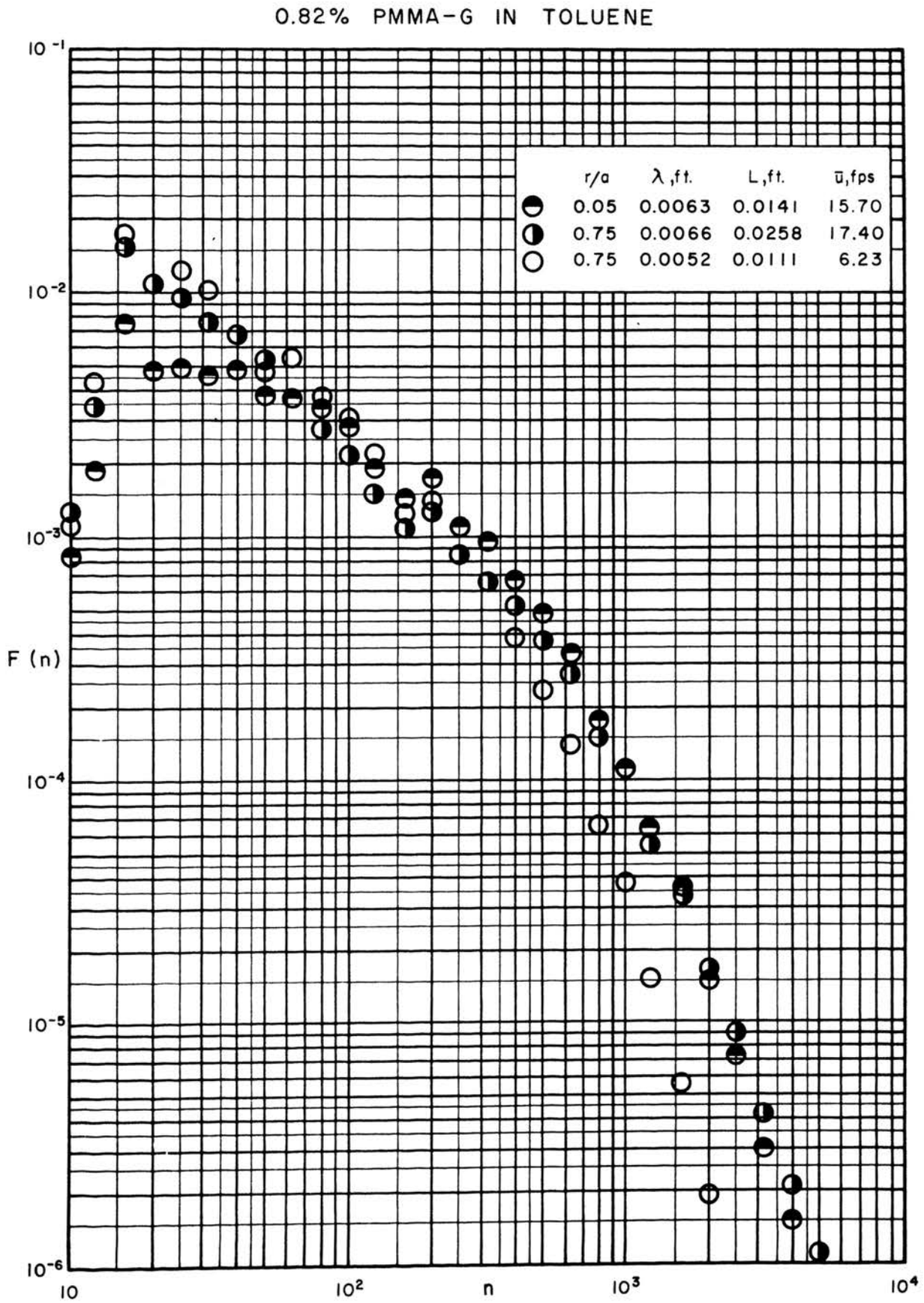


FIGURE 58. ENERGY SPECTRA FOR RUN 21

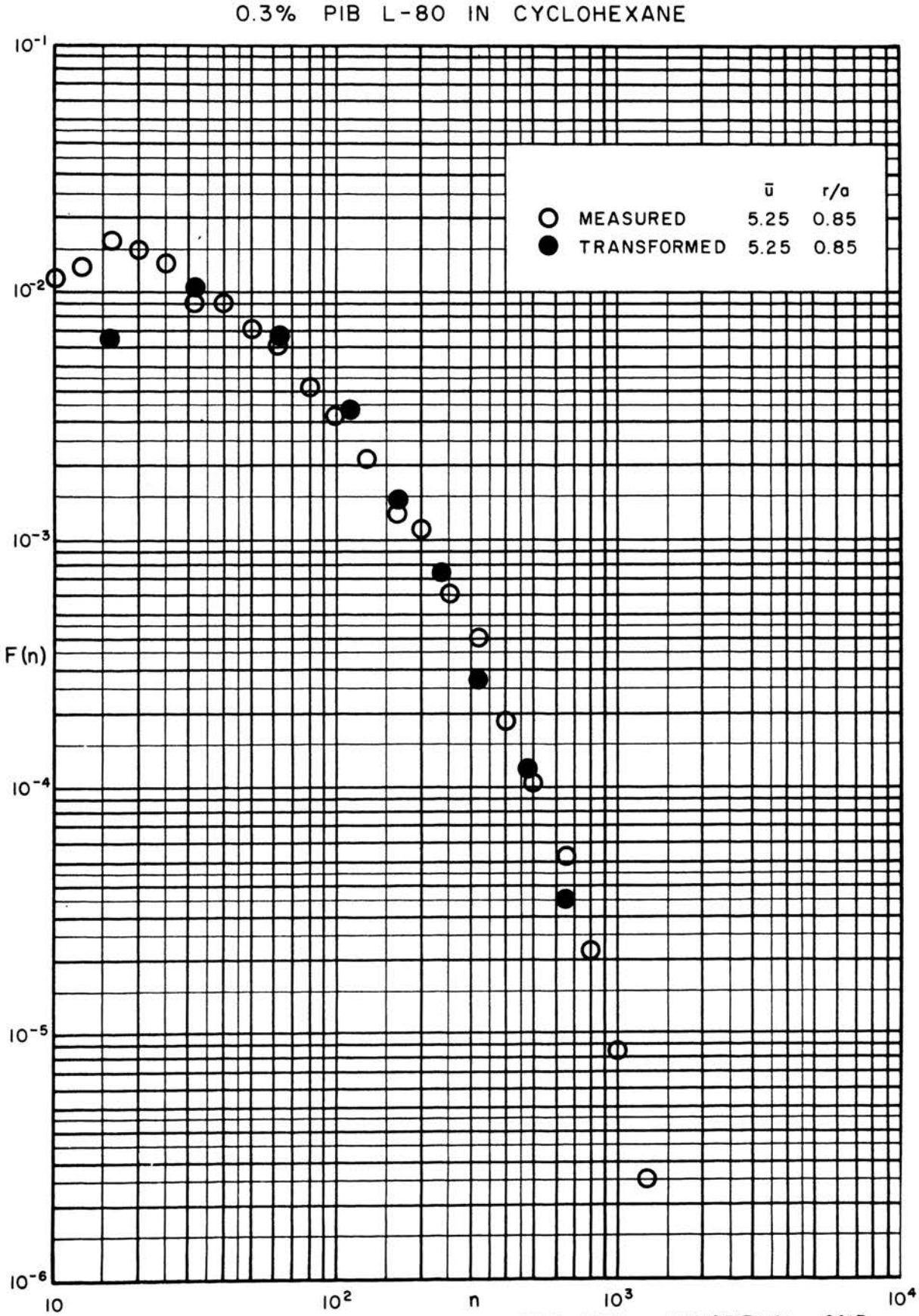


FIGURE 59. COMPARISON OF MEASURED SPECTRUM AND TRANSFORMED AUTOCORRELATION FOR RUN 8

## 6. Discussion of Results

Since the two main phases of this investigation were a study of turbulence intensities and energy spectra in the pipe flow of polymer solutions without drag reduction and the measurement of the same quantities for drag reducing flow, the discussion of results will contain separate sections for non-drag reducing turbulent flow (Runs 2-16 and 20-22) and for drag reducing turbulent flow (Runs 17-19 and 23).

### 6.1. Turbulence intensity in non-drag reducing flow

Longitudinal turbulence intensity data were obtained for Runs 2-16 and 20-22. The intensities are plotted in Figures 19-38 as a function of reduced distance from the tube center, r/a, with Reynolds number as a parameter. The turbulence intensities ($\langle u' \rangle / \bar{u}$) for these runs showed increases from about 3-6 per cent at the tube center to about 9-23 per cent at r/a=0.85. The trends for these results in liquids are similar to those for air reported by Laufer (47) and Sandborn (81). There are differences in absolute intensity levels, however, which will be discussed below.

The turbulence intensities for the flow of all solutions without drag reduction studied are plotted versus Reynolds number for r/a=0.0, 0.8, and 0.85 in Figures 60, 61, and 62, respectively. A small diameter effect may be seen in Figures 60 and 61 with the 1-inch tube data giving lower intensities. This is similar to the diameter effect shown for Laufer's 10-inch pipe data for air and Sandborn's 4-inch pipe data for air.

The turbulence intensity data for organic solvents and polymer solutions increase with decreasing Reynolds number in a manner similar to the Laufer and Sandborn data for air and the Martin-Johanson (58) data for water shown in Figures 60, 61, and 62. The Laufer air data

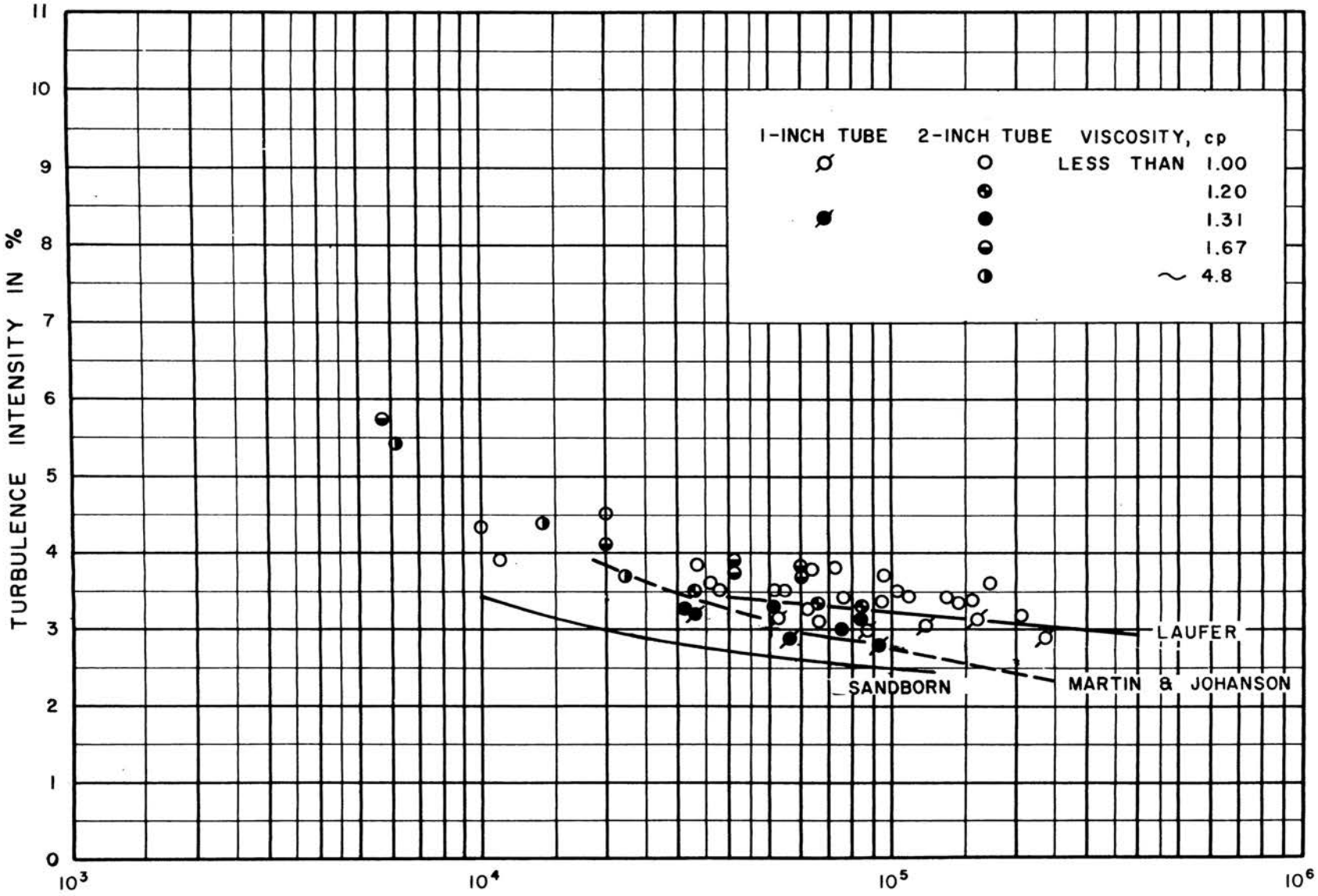


FIGURE 60. INTENSITIES AT TUBE CENTER

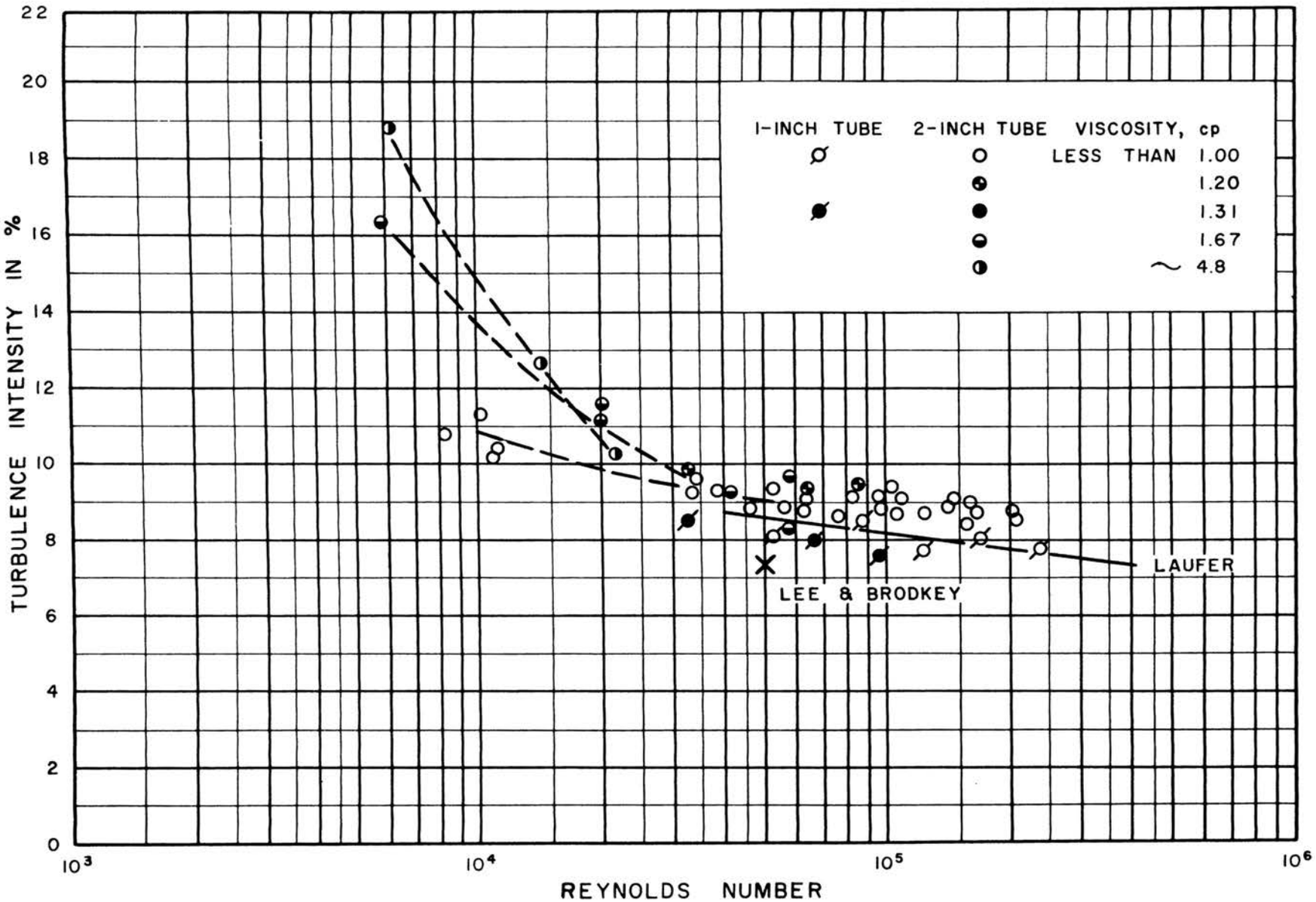


FIGURE 61. TURBULENCE INTENSITY AT r/a = 0.80

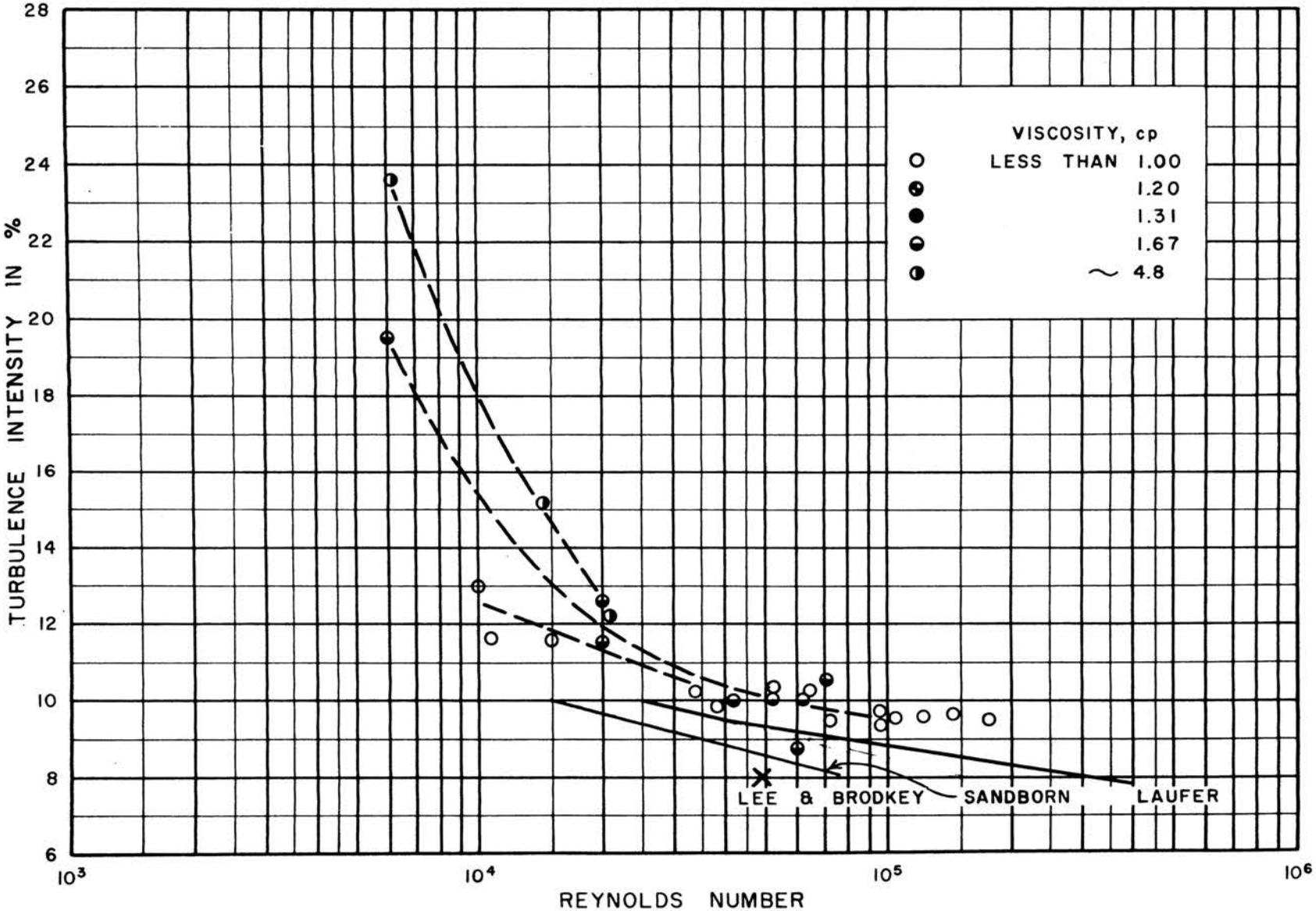


FIGURE 62. TURBULENCE INTENSITY AT r/a = 0.85

are in closest agreement with the data of this investigation, lying in the lower portion of the 2-inch tube data at the tube center. Laufer's data do not rise as high at r/a=0.85 (Figure 62), probably because of the large size of his pipe compared to the boundary layer thickness giving higher $y^+$ values at r/a=0.85. The air data of Sandborn are lower than Laufer's data both at the pipe center and near the wall. Baldwin and Walsh (2) measured air turbulence intensities at the same laboratory as Sandborn and obtained a value of 3.5 per cent at the center of an 8-inch pipe at Reynolds numbers of 290,000-640,000, compared to Sandborn's value of 2.5 per cent. Although Baldwin and Walsh ascribed the difference to calibration procedures, there may also be some diameter effect as observed in this investigation.

The effect of Reynolds numbers above 30,000 on turbulence intensity in this investigation is closest to that observed by Laufer, although the Sandborn data show a very similar slope in Figures 60 and 62. This is not the case, however, for the data taken in a 6-inch pipe for the turbulent flow of water by Martin and Johanson. Their data are in approximate agreement with Sandborn's, but show a stronger dependence on Reynolds number effect (Figure 60). Their absolute intensity levels were lower at high Reynolds numbers than the levels obtained in this investigation. The intensity profile of Lee and Brodkey (50) at a Reynolds number of 50,000 in a 3.068-inch pipe is also lower than the data reported here except for a rise in intensity level at the pipe center. They attribute this to anemometer drift. The data of Lindgren (54) are quite scattered and since he did not discuss them in detail in his report, they will not be compared with the data of this investigation.

Below a Reynold's number of 30,000 there seems to be an effect of solution properties which becomes very evident near the tube wall (Figures 61 and 62), causing much higher turbulence intensities. The effect could have been caused by the viscosity or the elasticity of the higher viscosity fluids. The two solutions showing the strongest effects were 0.3 per cent and 1.0 per cent PIB L-80 in cyclohexane with viscosities of 1.67 cp and about 4.8 cp, respectively. The 1.0 per cent solution showed significant normal stress effects in jet thrust measurements by Green (31). Although these solutions were not even friction factor reducing[1] in the 2-inch tube where the intensity measurements were made, they were drag reducing in tube sizes of 0.5-inch down for the flow rates obtainable (33). From dimensional considerations, it seems unlikely that the high intensities could be caused by high viscosity. In order to demonstrate that the effect is caused by elasticity, turbulence intensities must be measured on high viscosity, non-elastic fluids.

The hot-film probe used in this investigation did not permit measurements to be made closer than 0.15 inches from the 2-inch tube wall or 0.12 inches from the 1-inch tube wall. This corresponds to a minimum $y^+$ value of 30 in the 2-inch tube for the 1.0 per cent PIB L-80 solution at a Reynolds number of 6100. The high intensity effect could not be determined for the location of maximum intensity at $y^+=12$ (47). Intensity profiles through this point would show whether the intensity peak is located at this point but with a much higher peak for viscoelastic or viscous fluids or whether the peak is simply displaced further from the pipe wall.

---

[1] See definition page 20.

If the normal stress, $\rho\langle u'\rangle^2$, were closely related to the Reynolds stress, $\rho\overline{u'v'}$, equation 32 suggests that $\langle u'\rangle$ might be proportional to u* where du/dr is small. This is the same as saying that $\langle u'\rangle$ is proportional to $\sqrt{\tau_w/\rho}$, which seems reasonable. $\langle u'\rangle/u^*$ was plotted versus r/a for the data of this investigation to determine the validity of this assumption for data of widely varying viscosity. The graph of typical data points is shown in Figure 63. The points are plotted to distinguish Reynolds number ranges of 0-10,000; 10,000-20,000; 20,000-50,000; 50,000-100,000; and 100,000-up. The lowest values of $\langle u'\rangle/u^*$ are generally in the intermediate Reynolds number range, 20,000-50,000. These results show the difference of dependence on Reynolds number of $\langle u'\rangle$ and u*. The solution property effect discussed above causes the low Reynolds number points (lower than 10,000) to be much higher than the grouped data near the tube wall. In the correlation r/a was modified slightly to make "a" the distance from $y^+=12$, the point of maximum intensity, to the pipe center. Since most of the data are for $y^+>100$ the modification made little difference in the correlation, but it spread the data points somewhat to make them easier to plot.

The solid and broken lines in Figure 63 are Laufer's data for air at Reynolds numbers of 400,000 and 40,000, respectively. The Laufer data are in general agreement with the data of this investigation for the low viscosity solutions. Comparisons with this correlation will be made for the drag reducing fluids discussed in Section 6.7 to show the relative changes of turbulence intensity with wall shear stress during drag reduction.

The precision of the data obtained here is indicated in two ways. For many of the intensity profiles, data were obtained on both sides of

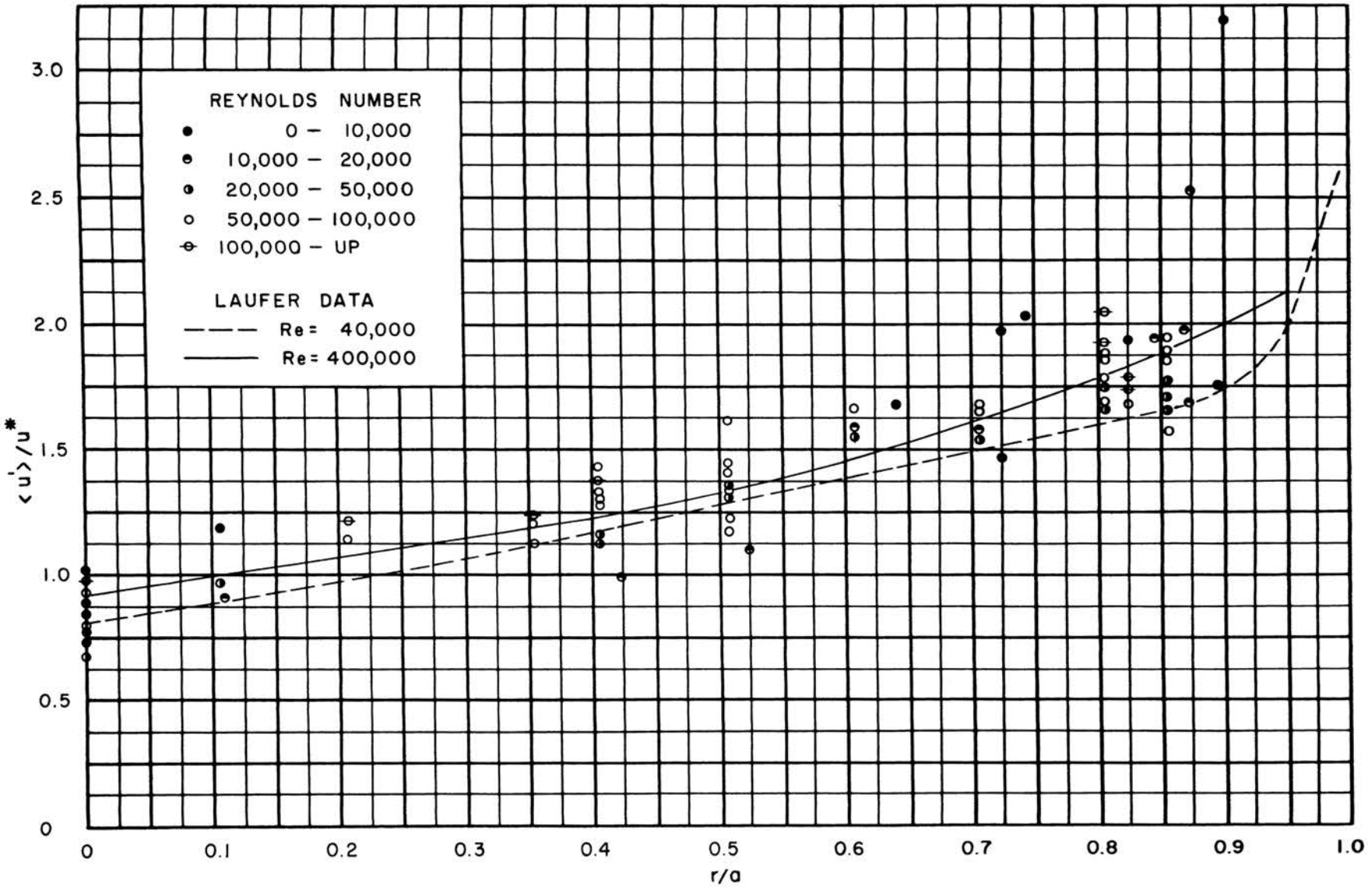


FIGURE 63. INTENSITY CORRELATION

the tube center to check axisymmetry of the flowing stream. Indications of the symmetry may be seen in the plots for Runs 2,3,4,9,17,20,21,22. The worst checks are for Run 2, Reynolds numbers 8240 and 11,500, where differences of about 2 per cent in intensity values were observed for regions near opposite walls, where the intensities were about 10 per cent. These two profiles were measured at very low velocities in a low viscosity solvent (toluene) where the flow rates were difficult to maintain constant. All the rest of the data exhibited good axisymmetry checks, that is, differences of less than 10 per cent of the average of the two points with most being less than 5 per cent different. Hershey (33) discussed the axisymmetry of the velocity profiles, which showed good checks.

If it is assumed that there is no significant viscosity effect above a Reynolds number of 30,000, the mean deviation of the intensity measurements from the average may be calculated from these data. Using the data for the tube center, this deviation for all non-drag reducing solutions was ± 0.2 per cent intensity or about ± 6 per cent of the average value (about 3.5 per cent). If more were known about the effects of viscosity, elasticity, and diameter, the average <u>random</u> deviation would not be this large. Martin and Johanson, using a hot-film probe for measurements in water in one pipe size, obtained an average deviation of about ± 8 per cent for the data plotted in their article (58). Sandborn using a hot-wire probe in air, obtained an average deviation of about ± 1 per cent.

## 6.2. <u>Radial and tangential turbulence intensities</u>

The preliminary results of the measurements of radial and tangential turbulence intensities using the V-probe are shown in Figures 39-42. Measurements were made in both the 1-inch and 2-inch tubes. Comparisons

of the results for the two pipes indicates that the 1-inch tube data are apparently more reliable than the 2-inch tube data. The 2-inch pipe data show a reverse trend with Reynolds number (lower intensities at lower Reynolds numbers). Also, the Reynolds stresses $\rho\overline{u'v'}$ for the 2-inch tube were about 15 per cent higher than the total shear stresses, and the Reynolds stresses $\rho\overline{u'w'}$ for the 2-inch tube were not near zero. The radial and tangential intensities in the 1-inch tube showed the same trend of decreasing intensity with increasing Reynolds number as the Laufer and Sandborn data.

The $\overline{u'v'}$ values shown in Figure 43 were very close to the total stress curves, and the $\overline{u'w'}$ values were about 10 per cent of the magnitude of the $\overline{u'v'}$ values. The Reynolds stress calculations involve the subtraction of two large numbers (see Appendix V) and are, therefore, very sensitive to small calibration errors. This might have caused the poorer results in the 2-inch tube.

The results show a marked deviation from the data of Laufer and Sandborn for radial and tangential turbulence intensities. The Laufer and Sandborn data for air showed only small increases of $\langle v' \rangle/\bar{u}$ and $\langle w' \rangle/\bar{u}$ close to the wall. The tangential and radial turbulence intensities measured in this investigation increased toward the tube wall in almost the same manner as our longitudinal turbulence intensities. The tangential intensities in the 1-inch tube are slightly higher than the longitudinal intensities at the tube center and are slightly lower than the longitudinal intensities at r/a=0.75. The radial intensities are slightly higher than the tangential intensities at all locations. The data for the 2-inch tube are all much higher than the longitudinal turbulence intensities and are probably in error since the Reynolds stresses did not check the total stresses.

These data are for an incompressible liquid of much higher density and viscosity than air, and so the deviations from air measurements may be significant. Since the data were for trial runs of a somewhat unsatisfactory (too large) prototype V-probe, however, further work will be necessary to verify the results.

6.3. Velocity profiles

The velocity profiles used for anemometer probe calibrations for Runs 2-15 were reported by Hershey (33) and will not be discussed here. Additional profiles were measured using the impact tubes described above for Runs 16, 19, and 20 (see Figures 44-46). For non-drag reducing flow conditions (Runs 16 and 20) these velocity profiles were similar to the Newtonian profiles obtained by Hershey. Since all measured profiles for non-drag reducing fluids were quite similar, profiles were calculated from the Run 16 and 20 measurements assuming Reynolds number similarity for Runs 21 and 22.

In Run 19 the low flow rate velocity profile was similar to the profiles measured in Runs 16 and 20, but the high flow rate profile, where the drag ratio was 0.85, was more blunt than the others (as shown in Figure 45). In addition the blunt profile yielded an integrated flow rate 13.2 per cent lower than the flow rate measured in a weigh tank. This is the same sort of behavior observed by Shaver (85) and Wells (98), again indicating the need for a detailed study of the effects of viscoelasticity on turbulent velocity profiles using either corrected impact tube measurements or another type of instrument. Because of the poor check between integrated flow rates and measured flow rates, velocity profiles calculated from established Newtonian data were used in Runs 17, 18, 19, and 23 where drag reduction was observed.

## 6.4. Energy spectra for non-drag reducing flow

The energy spectra in Figures 47-58 show that there are no large differences in the spectra for different solvents and polymer solutions at similar flow conditions in the same size tube. The slopes of all the spectra measured in the 2-inch tube approach the -7 value (on log-log plots) expected from Heisenberg's transfer theory (32) at the high frequency end (above 1000 cps). Many of these spectra exhibit the -5/3 log-log slope in the energy transfer region, although this region is short and the curve is sometimes rounded because of the low micro-scale Reynolds numbers ($Re_\lambda = \lambda\bar{u}/\nu$) obtained in the 2-inch pipe.

The spectra measured in the 1-inch tube for non-drag reducing fluids at high velocities in Runs 20 and 21 (Figures 57 and 58) do not exhibit a slope of -7 at the high frequency end (about 5000 cps). This slope is not reached in the frequency range studied because of broader energy transfer regions (slopes of -5/3) in these spectra.

The data for Runs 8, 9, 10, 14, 15, 20, and 21 show that spectra at different radial locations up to r/a=0.85 are nearly identical. The differences that do occur show slightly higher frequencies at the tube center than near the wall. Laufer (47) found that for the flow of air in a 10-inch pipe, differences in the spectra occur only within 0.1a of the wall. These differences are small when the spectra are plotted as a function of frequency. When wave number is used ($k = 2\pi n/\bar{u}$), the lower mean velocity near the wall causes the spectra to be shifted to higher wave numbers than spectra measured at the pipe center. This is shown in Laufer's plots of $F_x(k)$ versus k. It should also be noted that since Laufer made his measurements at high velocities giving high micro-scale Reynolds numbers, his spectra exhibit a long energy transfer region with -5/3 log-log slope.

The effect of flow rate on the spectrum curves is much more evident. As may be seen in Runs 9, 12, 14, 15, 20, and 21, the spectra have a smaller portion of their energy in the high frequency range at low flow rate than at high flow rate. These differences are magnified when comparing the dissipation spectra, as shown in Figure 64 for Run 15, because of the strong effect of the $n^2$ term at high frequencies. The normal rise in turbulence intensity at low Reynolds numbers might be explained by the lowered dissipation caused by the spectrum changes discussed above. Higher intensity might be necessary to obtain a balance between turbulence production and dissipation.

At the same velocities in the 2-inch tube all the spectra for different solutions seem about the same except for Run 9. This solution had an apparent wall viscosity of 4.8 cp at a time average velocity of 6.5 fps at the tube center (Appendix VI). As mentioned before, it also showed a strong normal stress effect in a jet thrust apparatus. The effect of the viscosity and/or elasticity of this solution on energy spectra may be seen by comparing the spectra of Runs 8 and 9 (Figures 47 and 48). There is some evidence that, unlike the turbulence intensity effect mentioned above, the spectrum effect is caused by viscosity instead of elasticity. Comparison of spectra for Runs 19 and 20 (Figures 56 and 57) shows that there is little difference in these spectra, even though the 0.42 per cent PIB L-200 in toluene was more elastic (longer relaxation time) than the 1.0 per cent PIB L-80 in cyclohexane of Run 9.

The energies at high frequencies for Run 9 are much lower (by about 50%) than at the same frequencies and comparable flow rate for

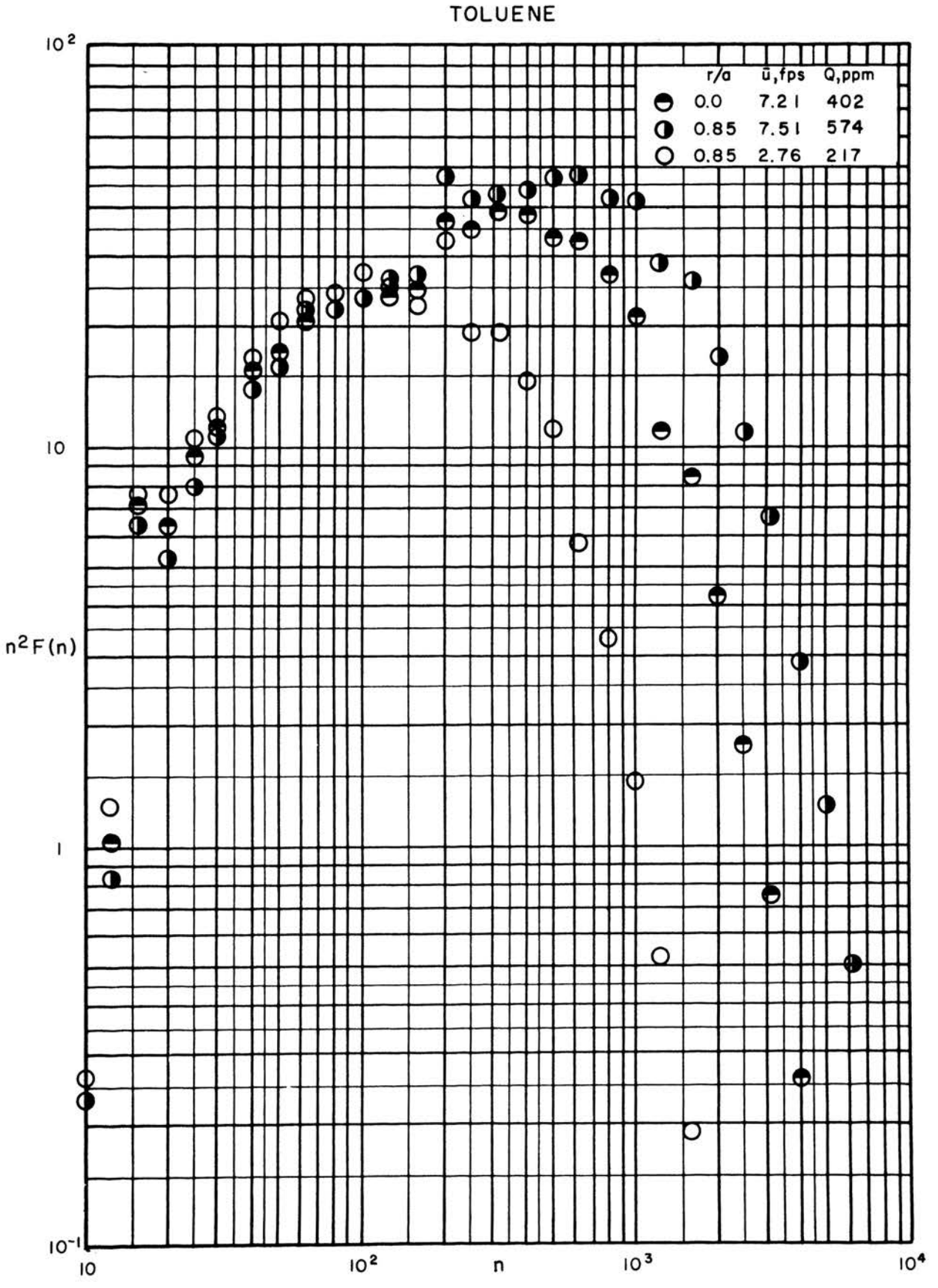


FIGURE 64. DISSIPATION SPECTRA FOR RUN 15

Run 8. This will not cause drag reduction, however, because the viscosity increase as well as the turbulence intensity increase at the lower Reynolds number compensate for the lowered dissipation spectrum.

Small differences in spectra are caused by pipe size as shown by comparing Runs 20 and 21 (Figures 57 and 58) for the 1-inch tube with Runs 15 and 14 (Figures 52 and 51) for the 2-inch tube. At comparable velocities (about 6-7 fps) the high frequency data from the 1-inch tube are slightly higher in energy level than the 2-inch pipe data. The slopes at high frequencies are about the same (approaching -7). As mentioned above, however, the slopes of the higher velocity runs in the 1-inch pipe (about 20 fps) did not approach -7 in the frequency range covered.

Most of the measured energy spectra were obtained using a recording of the anemometer bridge voltage made on an Ampex 601-2 audio recorder. In order to determine any errors introduced by the recorder, some comparisons were made with measurements of spectra obtained directly from the output of the anemometer. For Run 14 (Figure 51), comparison of the direct spectrum with the recorded spectrum shows that the recorded spectrum was almost identical to the directly measured spectrum.

Another comparison in Run 15 shows the correspondence of spectra measured from recordings on the Ampex audio tape recorder and Lyrec pulse-duration-modulation (pdm) tape recorder loaned by Zitzewitz Engineering Associates [1]. Comparison of the spectra at $r/a=0.85$ and $\bar{u}=2.76$ fps for the audio and pdm recordings in Figures 52 and 53, respectively, shows that they are almost identical except at frequencies of 10 cps and 12.6 cps. The response characteristics of the audio recorder are very poor below 15 cps, and even with calibration corrections

---

[1] Wyckoff, N.J.

some scatter is expected at these low frequencies. This scatter is the reason that an fm or pdm recorder is desireable to study the low frequency spectrum. Fortunately, these low frequency results are unimportant when considering the dissipation spectrum, $n^2 F(n)$.

6.5. Autocorrelation functions

The autocorrelation function is useful for the calculation of microscale and macroscale values and for transformation to the energy spectrum. The autocorrelations measured in this investigation were used primarily to establish the validity of the energy spectra measured with the band pass filter.

Figure 59 shows a comparison of a spectrum measured using the band pass filter and the transformed autocorrelation for Run 8, $\bar{u}$=5.24, r/a=0.85. The fair agreement between the two completely different methods of measurement supports the validity of the spectrum measurements. The low values at low frequencies (below 30 cps) for the transformed autocorrelation were caused by the lack of correction for the poor low frequency response of the recorder. Response corrections were used in the band pass spectrum measurements (see Appendix V). The transformed spectra did not extend to frequencies above about 600 cps because the autocorrelation measurements were not precise enough at very low delay times to give good high frequency transforms. Autocorrelation measurements were made for Runs 8-12, but are not plotted because their use was primarily to demonstrate the validity of the spectrum measurements.

Details of the Fourier transformation are discussed in Appendix V. The experimental methods used to record and measure spectra and autocorrelation functions of the anemometer output are discussed in Appendix II.

## 6.6. Macroscale and microscale for non-drag reducing flow

The macroscale (integral scale) and the microscale may be calculated from the autocorrelation function, upon which their definition is based (93). These quantities were calculated from the autocorrelation functions measured in Runs 8-12 (see Table 7). Macroscale and microscale obtained from the energy spectrum measurements were more reliable than the autocorrelation values because of the improved high and low frequency results. The high frequency region of the spectrum was more reliable than the corresponding very low delay time portion of the autocorrelation. The low frequency region of the spectrum was corrected for recorder response down to 10 cps, giving a more reliable representation of the low frequency occurrences than the uncorrected autocorrelation function.

Microscale values were measured using the anemometer differentiator circuit for Runs 14-17 and 19-23. The values shown in Table 5 for Runs 2-14 are in error because very high frequency anemometer noise was not filtered out. Table 1 lists the microscale and macroscale values for Runs 8-23.

The macroscale was calculated from each energy spectrum by first transforming it to an autocorrelation function, then integrating to find the area under the curve of $R(\tau)$ versus delay time (see Appendix V). As may be seen by comparing the directly measured spectrum with the audio recorder spectrum of Run 14 (Figure 57) and by comparing the audio recorder spectrum with the pdm spectrum of Run 15 (Figures 52, 53), the macroscales measured using audio recordings are 10 to 15 percent low. This is because the low frequency occurrences (below

Table 1

Microscale and Macroscale

| Run No. | r/a | $\bar{u}$, fps | Microscale, ft | | Macroscale, ft |
|---|---|---|---|---|---|
| | | | spectrum | differentiator | |
| 8 | 0.0 | 7.09 | 0.0093 | | 0.0151 |
| | 0.5 | 6.51 | 0.0089 | | 0.0148 |
| | 0.85 | 5.25 | 0.0071 | | 0.0117 |
| 9 | 0.0 | 6.90 | 0.0133 | | 0.0157 |
| | 0.5 | 6.56 | 0.0134 | | 0.0183 |
| | 0.85 | 5.64 | 0.0122 | | 0.0172 |
| | 0.85 | 2.47 | 0.0165 | | 0.0184 |
| 10 | 0.0 | 6.74 | 0.0102 | | 0.0179 |
| | 0.85 | 5.23 | 0.0077 | | 0.0152 |
| | 0.85 | 2.48 | 0.0061 | | 0.0079 |
| 12 | 0.0 | 7.03 | 0.0104 | | 0.0191 |
| | 0.85 | 6.71 | 0.0074 | | 0.0170 |
| | 0.85 | 2.53 | 0.0071 | | 0.0087 |
| 14 | 0.0 | 6.83 | 0.0092 | 0.0049 | 0.0174 |
| | 0.0 | 6.83 | 0.0104 (direct) | | 0.0191 |
| | 0.85 | 6.64 | 0.0124 | 0.0079 | 0.0186 |
| | 0.85 | 2.50 | 0.0054 | 0.0073 | 0.0076 |
| 15 | 0.0 | 7.21 | 0.0078 | 0.0065 | 0.0201 |
| | 0.85 | 7.51 | 0.0057 | 0.0082 | 0.0157 |
| | 0.85 | 2.76 | 0.0055 | 0.0078 | 0.0074 |
| | 0.85 | 2.76 | 0.0063 (pdm) | | 0.0090 |
| 16 | 0.0 | 7.16 | | 0.0086 | |
| | 0.4 | 6.71 | | 0.0095 | |
| | 0.85 | 5.38 | | 0.0084 | |
| | 0.85 | 2.72 | | 0.0077 | |
| 17 | 0.0 | 23.2 | 0.0034 | 0.0033 | 0.0104 |
| | 0.0 | 16.0 | 0.0037 | | 0.0132 |
| | 0.0 | 9.06 | 0.0057 | 0.0055 | 0.0123 |
| 18 | 0.5-1 | 20.7 | 0.0052 | | 0.0390 |
| | 0.5-2 | 20.7 | 0.0060 | | 0.0360 |
| | 0.5-3 | 20.7 | 0.0050 | | 0.0172 |
| 19 | 0.5-1 | 20.5 | 0.0063 | 0.0075 | 0.0206 |
| | 0.5-2 | 20.7 | 0.0054 | | 0.0127 |
| | 0.5-3 | 21.2 | 0.0042 | 0.0058 | 0.0072 |

Table I (continued)

| Run No. | r/a | $\bar{u}$, fps | Microscale, ft | | Macroscale, ft |
|---|---|---|---|---|---|
| | | | spectrum | differentiator | |
| 20 | 0.05 | 23.4 | 0.0052 | 0.0064 | 0.0164 |
| | 0.75 | 19.5 | 0.0058 | 0.0071 | 0.0275 |
| | 0.75 | 6.8 | 0.0052 | 0.0071 | 0.0130 |
| 21 | 0.05 | 15.7 | 0.0063 | 0.0058 | 0.0141 |
| | 0.75 | 17.5 | 0.0066 | 0.0063 | 0.0258 |
| | 0.75 | 6.2 | 0.0052 | 0.0049 | 0.0111 |
| 22 | 0.1 | 16.0 | | 0.0056 | |
| | 0.75 | 19.8 | | 0.0064 | |
| | 0.75 | 7.5 | | 0.0065 | |
| 23 | 0.6 | 31.0 | | 0.0066 | |
| | 0.6 | 20.3 | | 0.0079 | |
| | 0.6 | 9.6 | | 0.0078 | |

10 cps) have an important effect on the macroscale value, and these are lost in an audio recording.

Martin and Johanson (58) integrated their autocorrelation curves to obtain macroscales for the flow of water in the center of a 6-inch pipe. Their data were fit by the equation:

$$L_x = 1.692 \times 10^{-2}\, a(Re \times 10^{-3})^{0.509}$$

where $L_x$ is in feet. A comparison of values calculated using this correlation with values measured in this investigation shows that the correlation probably does not account for pipe diameter correctly. The macroscale calculated using the above equation for toluene flowing in the 2-inch pipe with a centerline velocity of 7.21 fps is 0.0178 feet, whereas the value measured in Run 15 was 0.0201 feet. The calculated value deviated even more from the measured value in the 1-inch pipe. Run 20 for toluene in the 1-inch pipe yielded a measured macroscale of 0.0164 feet and a calculated value of 0.0110 feet for toluene flowing at 23.4 fps.

The macroscale measurements in more viscous solutions show that viscosity does not have as strong effect on macroscale as calculated using the Martin-Johanson correlation. The measured macroscale in Run 8 ($\mu$=1.67 cp) was 0.0151 feet at a velocity of 7.08 fps, but the calculated value was only 0.0093 feet. Run 9 ($\mu$=4.8 cp) yielded a measured macroscale of 0.0157 feet at a velocity of 6.90 fps and a calculated value of 0.0056 feet. These comparisons indicate that the effect of viscosity is far weaker than given in the equation. In fact, comparison of all the solutions used shows that the viscosity effect is insignificant.

Examination of the macroscale data reveals that the dependence of macroscale on radial position is different for the 2-inch and 1-inch tubes.

There is no consistent change of macroscale with r/a in the 2-inch tube. In some cases microscale values increase with r/a (Runs 9 and 14) and in others it decreases (Runs 8, 10, and 15). Most of the changes are small. In the 1-inch tube, however, macroscales at r/a=0.75 are nearly double the values at r/a=0.05 for Runs 20 and 21. There is no obvious explanation for this behavior at this time.

Values of microscale were calculated by integrating the dissipation spectra and making use of equation 64, as described in Appendix V. The microscales for space average velocities of about 7 fps in the 2-inch tube and 18 fps in the 1-inch tube are plotted versus r/a in Figure 65. The general trend of the data shows that, unlike macroscale, microscale increased with viscosity when flow rate was constant (viscosity values are shown beside each curve in Figure 65). This is to be expected since microscale is closely related to the high frequency region of the energy spectrum, which also showed a dependence on viscosity.

Data listed in Table 1 show that there is no clear trend of microscale with velocity. Laufer's (46) investigation in a 5-inch channel for the flow of air showed very slight increases in microscale with decreasing velocity. Thus, the variation in microscale among the various solutions cannot be explained in terms of Reynolds number, because no consistent velocity effect was observed.

The effect of pipe size on microscale is more evident at the center than near the wall. Near the wall, microscale values for all the fluids studied (except the very high viscosity solution used in Run 9) seem to approach the same value. Closer to the wall than r/a=0.85, the Run 9 microscales might also approach the others. At equal velocities and viscosities the microscales at the center of the 1-inch tube are smaller than those at the center of the 2-inch tube, but the microscales are

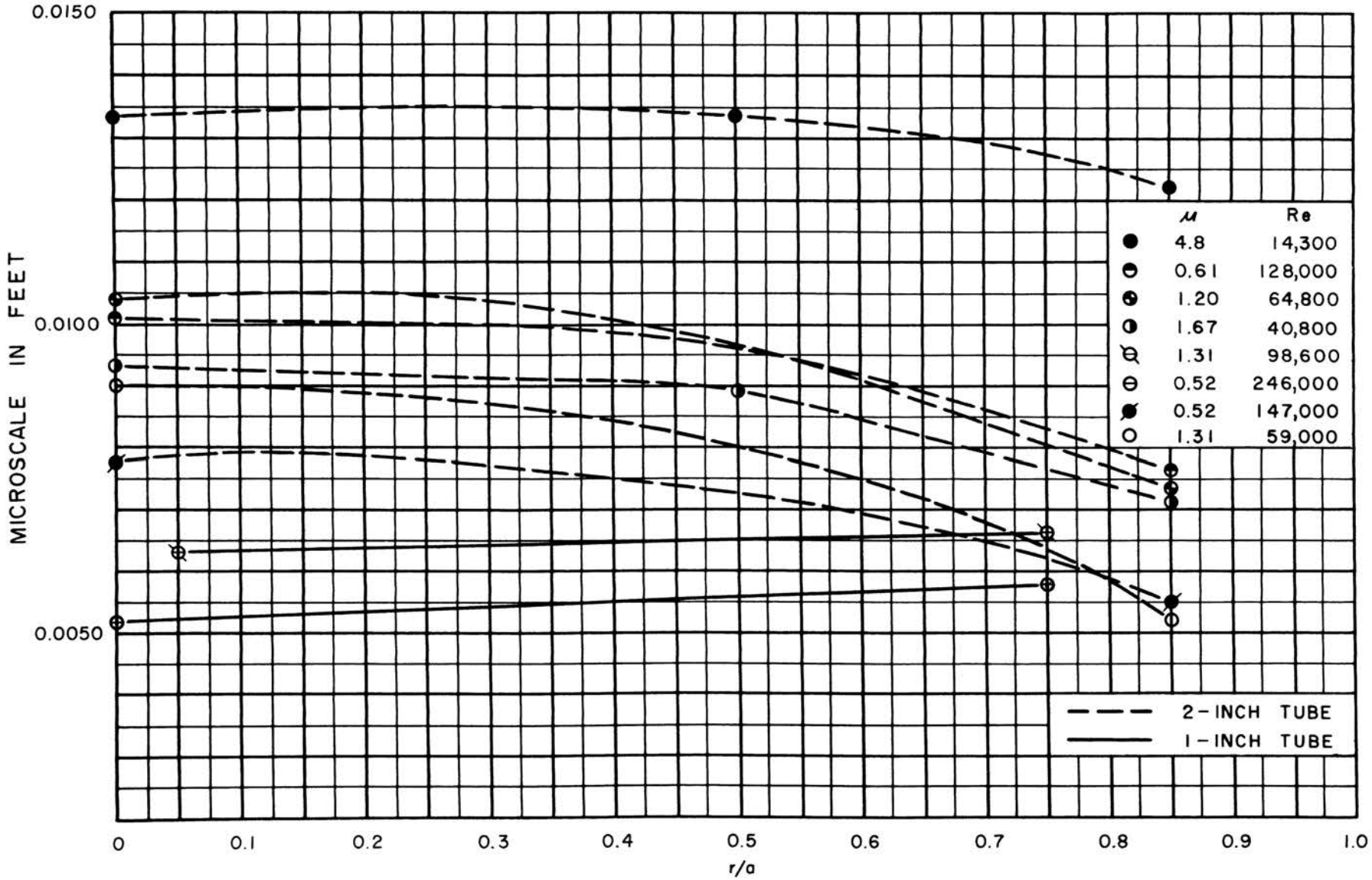


FIGURE 65. MICROSCALE vs. r/a

not proportional to pipe size. Data for a greater range of tube size are needed to determine the dependence of microscale on diameter.

Table 1 shows values of microscale measured by the DISA differentiator circuit in comparison with the spectrum values. The average difference between corresponding values is about 20 per cent. For the 2-inch tube the differentiator values at the pipe center are smaller than the spectrum values, and the opposite condition prevails near the wall. The checks in the 1-inch tube are better with Run 21 giving nearly identical values for the two methods. The very poor check in Run 14 is probably because the spectrum microscale value at $r/a=0.85$, $\overline{u}=6.64$ is a bad point, caused by some gross error. These comparisons show that the accuracy of the microscale determinations is no better than about $\pm$ 20%. Since most of the runs show internally consistent results, for either the spectrum or differentiator values, the errors are probably systematic in nature, but the causes are not yet known.

6.7. Normalized energy spectra

The energy spectra measured in Runs 9, 10, 19, and 20 were normalized in the manner of Gibson and Schwarz (25) in order to determine how these data correspond to the air and water data correlated by them. The plot of $E_x(k)k_k^3 \nu/w$ versus $k/k_k$ in Figure 66 shows that there is general correspondence between the Gibson and Schwarz (G-S) correlation and selected data for Runs 9, 10, 19, and 20.

The greatest deviation is in the high wave number region where the slopes of the spectra increase to about -7. The data of this investigation have slightly greater negative slopes and are lower than the G-S correlation starting at about $k/k_k=0.25$. All the data plotted for Runs 9, 10, 19, and 20, which are for solutions of widely different viscosities (0.518 - 4.8 cp) and two pipe sizes (1-inch and 2-inch

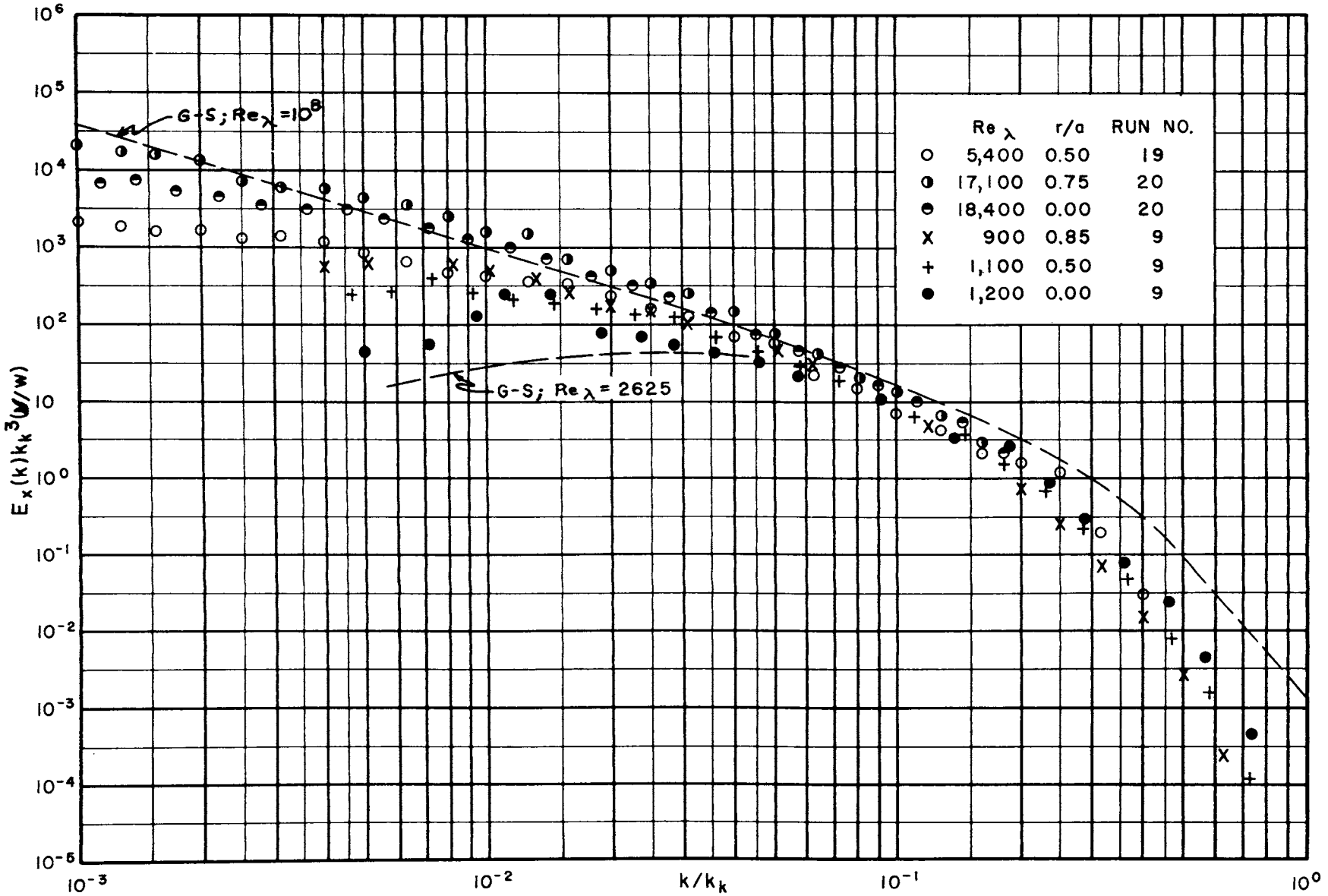


FIGURE 66. NORMALIZED ENERGY SPECTRA

diameters), coincide with some scatter in the high wave number region. The slope between a normalized wave number of 0.3 and 1.0 seems to be slightly greater than -7 on the log-log plot. The main reason for deviation from the G-S correlation, however, is that the -7 slope is reached at a lower normalized wave number.

The low normalized spectrum values at high wave numbers are accompanied by high normalized values at low wave numbers for corresponding microscale Reynolds numbers ($Re_\lambda = \lambda\bar{u}/\nu$). The energy levels where the spectra of this investigation level out are in general about 10 times the levels for the G-S correlation.

Reference to Figure 66 shows that normalized energy spectra of comparable Reynolds number are lower in the low wave number region for the tube center than near the wall. All the data used by Gibson and Schwarz in their correlation were probably isotropic, because all but one set of data (the tidal turbulence data of Grant, Stewart, and Moilliet (30)) were for grid induced turbulence. The plotted spectrum data of this study for a $Re_\lambda \approx 1000$ at r/a=0.0, 0.5, and 0.85 are above the G-S curve for $R_\lambda = 2625$ in the low wave number region. However, the tube center data approach the G-S curve, where the turbulence is more isotropic.

The highest normalized energy spectrum values in the high wave number region correspond to the lowest spectrum values in the low wave number region for the three spectra with $Re_\lambda \approx 1000$. If true isotropy existed, the tube data would probably correspond to the grid turbulence data. These data show that the tube center energy spectra approach the isotropic spectrum.

## 6.8. Turbulence measurements in drag reducing flow

Since none of the fluids studied jointly by Hershey (9) and the author (Runs 1-15) nor the PMMA V-100[1] solution of Run 16 were highly drag reducing in the 1-inch or 2-inch tubes, high molecular weight polyisobulylene solutions, Vistanex L-200, dissolved in toluene and cyclohexane, were used to establish drag reduction in the 1-inch tube. No appreciable drag reduction has yet been found in the 2-inch tube for any organic polymer solution. Details of the friction factor data for Runs 17, 18, 19, and 23 are presented by Rodriguez (78), but only the results will be used in this discussion.

The turbulence data obtained with the hot-film anemometer in these drag reducing solutions are limited because of the high rate of degradation of the high molecular weight polyisobutylene in toluene during pumping. One solution (0.2 per cent L-200 in toluene, Run 18) degraded at such a rate that the intrinsic viscosity decreased from 4.21 to 3.91 dl/g in one hour. The 0.42 per cent PIB L-200 in toluene solution used in Run 19 degraded from an intrinsic viscosity of 4.81 to 4.22 dl/g in the same length of time. In both cases the drag ratio rose from about 0.70 to about 0.85. The initial intrinsic viscosities of the two solutions were different because the solution concentrations were increased by adding fresh polymer to the unit at each change, so the ratio of degraded to fresh polymer was not constant. The PIB L-200 in cyclohexane did not degrade as rapidly and should be more suitable for future turbulence measurements. A 0.38 per cent solution still had a drag ratio of 0.69 in the 1-inch tube after 6 hours of pumping.

---

[1] See Appendix VI.

The turbulence intensities at different velocities and radial positions for Runs 17, 19, and 23 are shown in Table 2 along with measured <u'>/u* values, <u'>/u* values from Figure 63, drag reduction values, intrinsic viscosities, and low shear rate viscosities (Ubbelohde viscometer). Data for Run 18 are not shown in the table as no intensities were measured for that run.

These data show an unusual dependence of turbulence intensity on velocity. The most complete set of data is that for Run 23, 0.38 per cent PIB L-200 in cyclohexane. This solution showed extremely high drag reduction in the 1-inch tube (drag ratio of 0.5 at an average velocity of 35 fps before degradation (78)). After 4 hours of degradation the lowest velocity produced no drag reduction (drag ratio of 1.17) and the turbulence intensities are about normal for this velocity and viscosity. At the intermediate flow rate, where the drag ratio was 0.89, the <u'>/u* values were slightly lower than for non-drag reducing solutions as shown in Table 2. At the highest flow rate, however, where the drag ratio was 0.69, the <u'>/u* values were very high. Thus, as drag ratio dropped from 1.17 to 0.69, the turbulence intensity first dropped slightly below normal, then increased to a level much higher than normal.

The toluene solutions of PIB L-200 were not as highly drag reducing after equivalent degradation as the cyclohexane solution. Toluene is not as good a solvent for polyisobutylene as cyclohexane, and Hershey (33) found that better solvents produced higher drag reduction for a given polymer and concentration. The 0.05 per cent PIB L-200 in toluene (Run 17) was not highly drag reducing, the drag ratios being above 0.9 as shown in Table 2. The <u'>/u* values were very close to the

Table 2

Turbulence Intensities During Drag Reduction

1-Inch Tube

| Run No. | r/a | $\bar{u}$, fps | $\langle u' \rangle / \bar{u}$ | $\langle u' \rangle / u^*$ measured | $\langle u' \rangle / u^*$ Fig. 63 | Drag Ratio | $[\eta]$ dl/g | $\mu_o$ cp |
|---|---|---|---|---|---|---|---|---|
| 17 | 0.0 | 23.2 | 0.0364# | 1.05 | 1.05 | 0.92 | 3.72 | 0.579 |
| | 0.0 | 9.06 | 0.0406# | 0.97 | 0.95 | 0.96 | | |
| | 0.5 | 21.4 | 0.0541# | 1.40 | 1.45 | 0.92 | | |
| | 0.5 | 7.73 | 0.0725# | 1.61 | 1.40 | 0.96 | | |
| 19 | 0.5 | 20.5 | 0.0387# | 1.19 | 1.40 | 0.70 | 4.81 | 2.17 |
| | 0.5 | 14.2 | 0.0493# | -- | 1.20 | -- | | |
| | 0.5 | 7.63 | 0.0429# | -- | 1.30 | -- | | |
| | 0.5 | 21.2 | 0.0737* | 2.12 | 1.40 | 0.85 | 4.22 | 1.85 |
| | 0.5 | 13.9 | 0.0741* | -- | 1.20 | -- | | |
| | 0.5 | 7.26 | 0.0476* | -- | 1.30 | -- | | |
| 23 | 0.0 | 37.0 | 0.0543+ | 1.76 | 0.80 | 0.69 | | |
| | 0.0 | 23.4 | 0.0268+ | 0.71 | 0.75 | 0.89 | | |
| | 0.0 | 11.4 | 0.0376+ | 0.83 | 0.85 | 1.17 | | |
| | 0.6 | 31.0 | 0.1084+ | 2.95 | 1.35 | 0.69 | | |
| | 0.6 | 20.3 | 0.0519+ | 1.18 | 1.30 | 0.89 | | |
| | 0.6 | 9.57 | 0.0788+ | 1.45 | 1.45 | 1.17 | | |

# Fresh solutions.
* After pumping for one hour.
+ After pumping for four hours.

values from Figure 63 for non-drag reducing solutions. These results fit the pattern of the results of Run 23.

The turbulence intensity measurements in Run 19 produced anomalous results. The <u'>/u* value for fresh solution at the highest flow rate and drag ratio 0.70 was slightly lower than the non-drag reducing values in Figure 63. After one hour of pumping, however, the drag ratio increased to 0.85 at the same flow rate, and the turbulence intensity increased to a level much higher than normal. The low velocity intensities measured at both times fell on the <u'>/u* correlation. Although pressure drops were not measured at the lowest velocity, it is believed that there was no drag reduction.

This behavior indicates different behavior patterns for fresh and degraded polymer solutions in drag reducing turbulent flow. The degraded toluene solution in Run 19 behaved similarly to the degraded cyclohexane solution in Run 23. The fresh solution in Run 19 showed a slightly reduced turbulence intensity. This means that the polymer molecular weight distribution probably has a very strong effect on the drag reduction mechanism.

The behavior for the degraded solutions indicates that the turbulence intensity is reduced slightly in the region of low friction factor reduction (drag ratios slightly below one up to the drag ratio of the purely viscous solution). At higher friction factor reductions, however, the turbulence intensity relative to u* increases. In no case can the large <u'>/u* values be completely accounted for by the decrease in u* caused by the drag reduction. For polymers of increased drag reduction power, the drag ratio or friction factor ratio where the intensity starts to increase seems to be lower than for poorly drag reducing polymers, based on the comparison of the fresh and degraded solutions of Run 19.

The energy spectra measured during drag reduction in Runs 17, 18, and 19 (Figures 54-56) did not show large deviations from non-drag reducing spectra (Runs 20 and 21, Figures 57 and 58). The small effects observed are best seen in Runs 18 and 19 where three spectra measured during the degradation of the polymer are plotted on each figure. The first two spectra (labeled r/a=0.5-1 and 0.5-2 to indicate run order at r/a=0.5) in each case were measured during the first 15 minute period of the run. The last spectrum for each run (labeled r/a=0.5-3) was measured during the last ten minutes of the one hour period. As the polymer degradation and drag reduction was lost, the spectra shifted to slightly higher relative energy levels in the high frequency region, lowering the relative low frequency energies. The effect is most pronounced in Run 19 where the concentration of PIB L-200 was highest (0.42 per cent).

For stationary turbulence, equation 74 expresses the equality of the spectral energy transfer function and the energy dissipation function. The energy spectrum changes for the drag reducing polymer solution in Run 19 are the result of changes in the transfer function. From the data of this investigation, it is impossible to determine whether the spectrum changes are a result of the viscosity change during degradation, the changes in solution elasticity, or both. In any case it is evident that a successful transfer function theory for liquids must include the effects of liquid properties in order to account for the changes caused by viscosity in the non-drag reducing spectra and the changes in the drag reducing spectra in Runs 18 and 19.

The shift to higher frequencies caused the microscale values to become lower, as may be seen in Table 5, Runs 18 and 19. In Run 19 the microscale changed from 0.0063 feet to 0.0042 feet as drag ratio changed from 0.70 to 0.85. This means that the isotropic energy dissipation

calculated using equation 47 at a drag ratio of 0.70 is about 45 per cent of the value at a drag ratio of 0.85 for the same turbulence intensity. The turbulence intensity change brings the dissipation at 0.70 drag ratio to about 12 per cent of the dissipation at a drag ratio of 0.85. Most of this decrease is brought about by the high turbulence intensity when the drag ratio is 0.85.

Unless the energy spectra change drastically near the wall where dissipation is greatest, the changes in dissipation spectrum, or micro-scale, cannot explain drag reduction. The dissipation calculated using equation 47 is 230 per cent higher at a drag ratio of 0.85 in Run 19 than in Run 20 at $\overline{u}$ =18.5 and r/a=0.75 for toluene. If the dissipation at r/a=0.5 were estimated for Run 20, the difference would be even greater because the turbulence intensity would be lower than at r/a=0.75.

# MECHANISM FOR VISCOELASTIC DRAG REDUCTION

## 1. Development of the Mechanism

The viscoelastic mechanisms for drag reduction proposed by Savins (83), Park (70), and Astarita (1) were not developed quantitatively. Hershey's (33) comparisons of polymer solution relaxation times calculated using Zimm's theory with wall shear rates at incipient drag reduction offered a means of determining flow conditions necessary for drag reduction with a polymer solution. Park's dimensionless correlation offered a means of relating drag reduction to measured solution properties. Both of these correlations demonstrated the dependence of drag reduction on solution elasticity, but did not offer quantitative insight into the mechanism.

In this section a quantitative expression for the reduction of turbulent energy dissipation during drag reduction will be developed and tested using normal stress data measured with the jet thrust apparatus. The relation of turbulent energy dissipation reduction to laminar boundary layer dissipation will be discussed with reference to the observed anomalies in velocity profiles and turbulence intensities for drag reduction.

A Maxwell model was assumed to approximate the viscoelastic response of the polymer solution under shear. If the shear stress is a cosine function of time, $\tau = A \cos \omega t$, substitution into equation (84) gives:

$$s = s_g + s_\mu = (A/G) \cos \omega t + (A/\mu\omega) \sin \omega t \qquad (86)$$

The energy dissipation equals $\int \tau ds_\mu$. Differentiation of equation 86 with respect to time and substitution into the integral yields the equation for viscous dissipation for the Maxwell model:

$$W = A^2 \omega/2\mu$$

For a purely viscous fluid, the energy dissipation would be:

$$W_s = B^2 \omega/2\mu_s$$

$$\text{if} \quad s = (B/\mu_s\omega) \sin \omega t$$

For equal rms displacement amplitudes, the viscoelastic model and purely viscous model may be related:

$$(B/\mu_s\omega)^2 \sin^2\omega t = (A/G)^2 \cos^2\omega t + (A/\mu\omega)^2 \sin^2\omega t + (A^2/\mu G\omega) \sin \omega t \cos \omega t$$

After time averaging, this relation yields:

$$A^2 = B^2 G^2 \mu^2/\mu_s^2 (G^2 + \mu^2 \omega^2)$$

So the ratio of viscoelastic to viscous dissipations at equal rms displacement is:

$$W/W_s = \mu/\mu_s (1 + \mu^2 \omega^2/G^2) \tag{87}$$

For application of this relationship to turbulent flow, the spectrum of shear fluctuation frequencies on a fluid element must be known. This would be a Lagrangian spectrum and, therefore, impossible to measure with known techniques. Using the approximate relationship between the Lagrangian and Eulerian autocorrelation coefficients, the Lagrangian energy spectrum can be calculated. This spectrum expresses the distribution of frequencies of velocity fluctuation of a particle of fluid.

It is easily shown that if the Eulerian and Lagrangian correlation functions are of the same form, that is:

$$R(\tau) = R(\beta\langle u'\rangle \tau_L/\bar{u}) \tag{88}$$

where $\tau$ and $\tau_L$ are Eulerian and Lagrangian time delays, and $\beta$ is the ratio of Eulerian to Lagrangian length scales. Then the relation between Eulerian and Lagrangian energy spectra is:

$$E(n) = E(\bar{u}n_L/(\beta\langle u'\rangle))$$

$$\text{or} \qquad n_L = n\beta\langle u'\rangle/\bar{u} \tag{89}$$

This relation will generally produce Lagrangian frequencies much lower than Eulerian frequencies, since the intensity of turbulence, $\langle u'\rangle/\bar{u}$, is usually a small fraction.

Equation 89 provides the needed relation between Eulerian and Lagrangian velocity fluctuation frequencies to determine the latter from measurements of the former. If the shear stress fluctuations occur at frequencies equal to the Lagrangian velocity fluctuations, then the viscoelastic energy dissipation is the viscous dissipation function times the ratio of viscoelastic to purely viscous dissipation, calculated from equation 87.

From equation 62, the isotropic viscoelastic energy dissipation is:

$$W = 60\mu(\pi\langle u'\rangle/\bar{u})^2 \int_o^\infty n^2 F(n)\,(1/(1 + \omega^2\mu^2/G^2))\ dn \tag{90}$$

The radial frequency $\omega$ must be the Lagrangian radial frequency:

$$\omega = 2\pi\ n_L = 2\pi\ n\beta\langle u'\rangle/\bar{u}$$

Thus, the ratio of viscoelastic dissipation to purely viscous dissipation is:

$$\frac{W}{W_s} = \frac{\mu \int_o^\infty n^2 F(n)\,(1/(1 + 4\pi^2 n^2 \beta^2 \langle u'\rangle^2 \mu^2/\bar{u}^2 G^2))\ dn}{\mu_s \int_o^\infty n^2 F(n)\ dn} \tag{91}$$

This relationship describes a turbulent energy dissipation reduction mechanism which involves the following assumptions:

1. The Lagrangian and Eulerian spectra have the relationship described by equation 89.

2. $\beta$, if not a true constant, shows less than order of magnitude variation, with tube size, radial location, flow rate, and fluid properties.
3. The shear stress fluctuation frequencies are approximately equal to the Lagrangian velocity fluctuation frequencies.
4. The polymer solution viscoelasticity may be adequately described by a Maxwell model.
5. The ratio of non-isotropic purely viscous dissipation to non-isotropic viscoelastic dissipation in turbulent tube flow is nearly equal to the ratio for isotropic turbulence.

In order to test the validity of the proposed mechanism for turbulence energy dissipation reduction, it was necessary to postulate an approximate relation between turbulence energy dissipation reduction and wall shear stress reduction. This was possible because the retardation of turbulent momentum flux (turbulent shear stress) near the tube wall in elastic fluids is apparently caused by the recovery of elastic fluid shear displacement. This is a phenomenon directly related to recovery of elastic shear energy described in equation 87.

The relation between turbulent energy dissipation and wall shear stress in the tube flow of purely viscous fluids will be used to establish the relation between reductions of both.

The wall shear stress in the turbulent flow of non-drag reducing fluids is approximately proportional to Reynolds number to the 1.8 power. In laminar flow $\tau_w \propto Re$. The ratio of turbulent wall shear stress to laminar wall shear stress is then proportional to $Re^{0.8}$.

It was observed that for the energy spectra measured in this investigation the high frequencies were proportional to velocity to a power of approximately 0.8 at a given normalized energy level. Combining this with the above relation, the ratio of turbulent to laminar wall shear stresses is proportional to $n/\mu^{0.8}$.

Equation 62 shows that the isotropic energy dissipation rate, W, is approximately proportional to $\mu n^3$. This means that the ratio of turbulent to laminar wall shear stress is approximately proportional to the cube root of the rate of turbulent energy dissipation divided by viscosity to the 1.1 power:

$$(\tau_w^t/\tau_w^l) \propto (W/\mu)^{1/3}/\mu^{0.8} = W^{1/3}/\mu^{1.1} \tag{92}$$

The ratio of the above ratio for the polymer solution and the solvent yields:

$$\frac{(\tau_\omega^t/\tau_\omega^l)}{(\tau_\omega^t/\tau_\omega^l)_s} = \left(\frac{W}{W_s}\right)^{1/3} \left(\frac{\mu_s}{\mu}\right)^{1.1} \tag{93}$$

Since for the same flow rates:

$$\tau_w^l/\tau_{w_s}^1 = \mu/\mu_s \ ,$$

$$\text{then } \tau_w^t/\tau_{w_s}^t = (W/W_s)^{1/3}(\mu_s/\mu)^{0.1} \tag{94}$$

2. Application of the Mechanism

The turbulent energy dissipation ratio of equation 90 has been computed for several radial positions in both the 1-inch and 2-inch tubes for two polymer solutions (1.0 per cent PIB L-80 in cyclohexane and 0.42 per cent PIB L-200 in toluene). Normal stress data were obtained on the first solution by Green (31), and normal stress differences were measured by the author on fresh and degraded samples of the second solution. Figure 67 shows a comparison of the L-80 and L-200 normal stress ($P_{zz} - P_{rr}$) data.

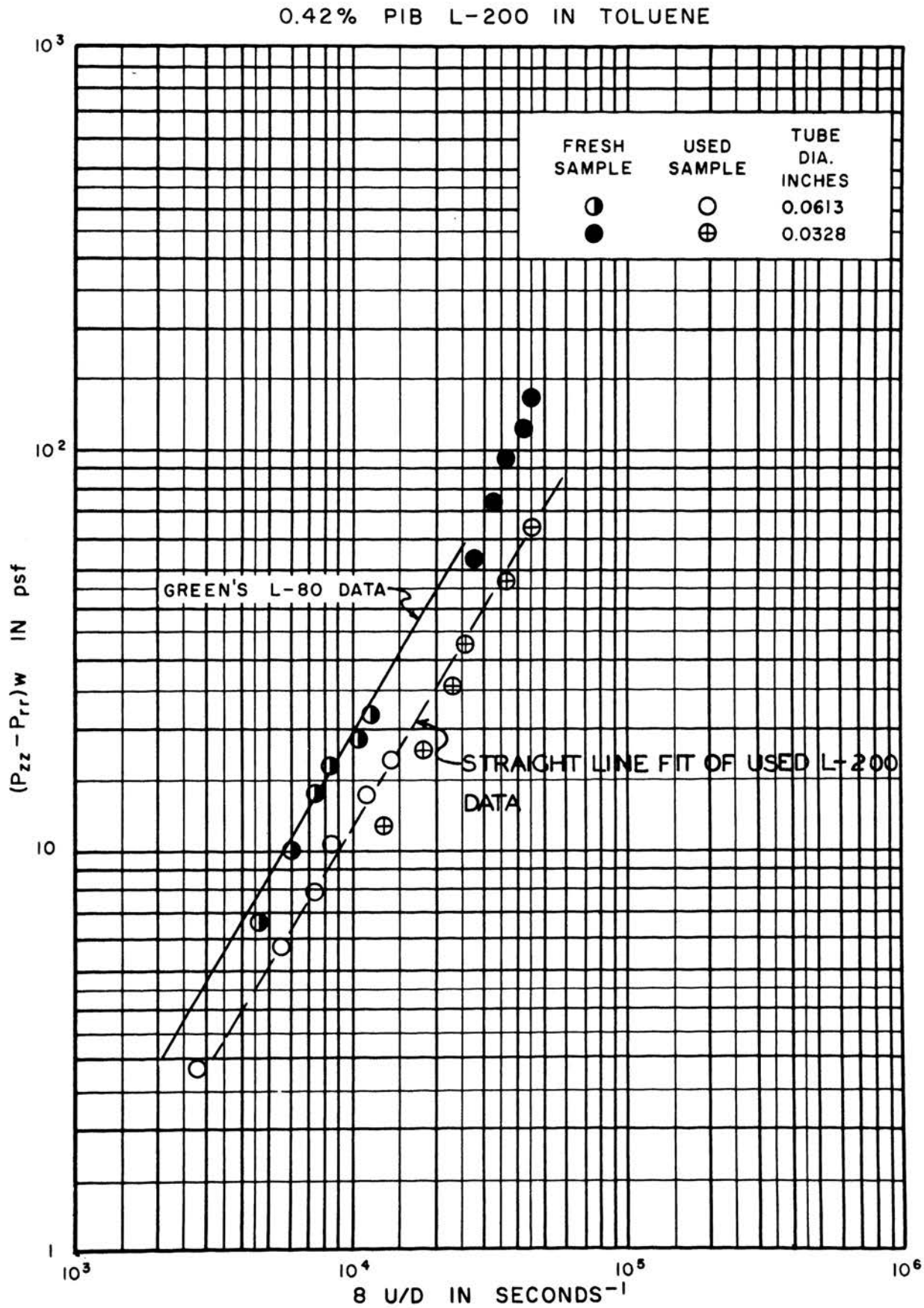


FIGURE 67. NORMAL STRESS DIFFERENCE

Turbulence intensities for the locations close to the wall were estimated from Laufer's data for air (47). Since turbulence intensity measurements were not possible very near the wall in this investigation, the effect of drag reduction on intensity near the wall was not known. No attempt was made, therefore, to account for this effect. Calculations were made for turbulent core locations and locations as close to the wall as $y^+ = 12$, the point of maximum energy dissipation according to Laufer's data. Use of measured intensity results using a close wall probe in drag reducing solutions will improve the accuracy of the calculations. The turbulence intensities and average velocities used in each pipe are shown in Table 3.

The shear rates used to calculate viscosities and normal stresses were calculated using the following equation for isotropic turbulence (see equations 44, 47, and 64):

$$\langle du'/dr \rangle = \left[30\pi^2 \langle u' \rangle^2 \int_o^\infty n^2 F(n)\, dn\right]^{1/2} / \bar{u} \qquad (95)$$

The rms turbulent shear rates obtained from this equation are only an approximation of the true shear rates experienced by the polymer solution. The instantaneous shear rate calculated for non-isotropic turbulence would yield a more rigorous result. This was impossible with present knowledge of turbulence. Nevertheless, as shown below the final results are still close to measured drag ratios.

The comparison of the calculated results using the proposed mechanism of turbulent energy dissipation reduction and its approximate relation to wall shear stress with experimental results is shown in Table 4. Calculated drag ratios were obtained by using the $W/W_s$ value at $y^+ = 12$. Since energy dissipation at this location is dominant, integration over the entire tube cross section caused only small changes in drag ratio from

Table 3

Velocities and Turbulence Intensities Used in Drag Reduction Mechanism Calculations

| Tube Size Inches | Space Average Velocity, fps | $y^+$ | $\langle u' \rangle / \overline{u}$ | $\overline{u}$, fps |
|---|---|---|---|---|
| 1.0 | 18 | 12* | 0.28 | 9.0 |
| | | 24* | 0.20 | 11.5 |
| | | 48* | 0.15 | 13.7 |
| | | 100 | 0.13 | 16.0 |
| | | 300 | 0.10 | 18.2 |
| | | 1000 | 0.04 | 20.5 |
| | | 2000 | 0.03 | 22.8 |
| 1.0 | 6.6 | 12* | 0.30 | 3.14 |
| | | 24* | 0.22 | 4.29 |
| | | 48* | 0.17 | 5.11 |
| | | 100 | 0.15 | 5.76 |
| | | 300 | 0.12 | 6.60 |
| | | 1000 | 0.05 | 7.42 |
| | | 2000 | 0.03 | 8.25 |
| 2.0 | 5.5 | 12* | 0.35 | 2.62 |
| | | 24* | 0.25 | 3.59 |
| | | 48* | 0.20 | 4.28 |
| | | 200 | 0.12 | 5.51 |
| | | 667 | 0.05 | 6.22 |
| | | 1334 | 0.03 | 6.90 |
| 2.0 | 2.8 | 12* | 0.40 | 1.32 |
| | | 24* | 0.30 | 1.81 |
| | | 48* | 0.25 | 2.16 |
| | | 200 | 0.15 | 2.78 |
| | | 667 | 0.06 | 3.14 |
| | | 1334 | 0.04 | 3.48 |

* Laufer (46)

Table 4

Turbulent Energy Dissipation Ratios and Drag Ratios
Calculated Using Viscoelastic Mechanism

(all values for $y^+ = 12$, $\beta = 0.1$)

| Tube Size, Inches | Space Average Velocity, fps | Polymer in Solution | $W/W_s$ | Calculated Drag Ratio | Measured Drag Ratio |
|---|---|---|---|---|---|
| 1.0 | 18 | L-80 | 2.08 | 1.04 | 1.21 |
| 1.0 | 6.6 | L-80 | 3.56 | 1.21 | 1.55 |
| 1.0 | 18 | used L-200 | 0.84 | 0.84 | 0.85 |
| 1.0 | 6.6 | used L-200 | 1.21 | 0.95 | ~1.0 * |
| 1.0 | 18 | fresh L-200 | 0.48 | 0.69 | 0.70 |
| 1.0 | 6.6 | fresh L-200 | 0.69 | 0.77 | ~0.9 * |
| 2.0 | 5.5 | L-80 | 4.59 | 1.40 | 1.50 |
| 2.0 | 2.8 | L-80 | 7.12 | 1.60 | 1.59 |
| 2.0 | 5.5 | used L-200 | 1.51 | 1.02 | + |
| 2.0 | 2.8 | used L-200 | 2.28 | 1.17 | + |
| 2.0 | 5.5 | fresh L-200 | 0.93 | 0.85 | + |
| 2.0 | 2.8 | fresh L-200 | 1.57 | 1.01 | + |

* extrapolated from data for a lower concentration.
\+ not measured, but estimated to be 1.0 or slightly higher.

values calculated for $y^+ = 12$. $W/W_s$ values were obtained using a value of $\beta = 0.1$, this adjustment from measured values of 0.4 - 0.8 for air turbulence being necessary to obtain correct absolute drag ratio levels. The necessity of using such a low value for $\beta$ indicates that the dissipation ratio overestimates the elastic effect or that the ratio of Eulerian to Lagrangian scales is lower in viscoelastic turbulence.

Since two flow rates were used in each of two tube sizes for three polymer systems, the good checks with measured values indicate that the assumptions and approximations involved did not seriously affect the calculated results. Calculated drag ratios were generally slightly lower than measured values, but the trends with velocity, pipe size, and solution properties were all very close to measured trends. This mechanism shows quantitatively the relative importance of solution properties (viscosity and shear rigidity modulus) and flow conditions (velocity, turbulence intensity, and pipe size). A relatively viscous solution may be very friction factor reducing (friction factor ratio may be calculated by using the solution viscosity in place of solvent viscosity in equations 91 and 94), if it has a long relaxation time, yet not be drag reducing at a given flow rate because of the high ratio of its viscosity to that of the solvent.

The diameter effect observed for drag reduction (greater reduction in smaller tubes at the same Reynolds number) occurs because of the small effect of pipe size on spectrum frequencies at the same space average fluid velocity.

The effect of pipe size on macroscale (a reflection of the proportion of low frequency energy) does not affect the drag reduction mechanism greatly, because of the insensitivity of energy dissipation to low frequency fluctuations.

The retardation of turbulent momentum transfer near the wall has not been explained quantitatively. The elasticity of the solution probably has little effect on momentum transfer far from the wall where low frequencies predominate. Near the wall, however, high frequency momentum transfer must gain in importance because of the restriction of the wall to low amplitude fluctuations. It is visualized that the elastic portion of the velocity fluctuations does not contribute to momentum transfer, because the elastic displacements are always recovered. This leaves momentum transfer to the viscous portion of the velocity fluctuations, whose displacements are not recovered.

The mechanism described above probably accounts for the success of the empirical relation between turbulent energy dissipation reduction and wall shear stress reduction. If the momentum transfer rate near the wall were not modified as described above, there would probably be no drag reduction, because the turbulence intensities in the turbulent core were actually seen to increase with drag reduction. These increases would tend to cause the turbulent momentum flux far from the wall to increase. This suggests that flatter velocity profiles should be obtained in the turbulent core during drag reduction to account for the reduction in the total shear stress.

# CONCLUSIONS

Turbulence intensities measured for the tube flow of low viscosity organic solvents and non-drag reducing polymer solutions showed good agreement with data for the pipe flow of air. A diameter effect was found which causes turbulence intensities to be slightly lower for smaller tubes.

A strong viscous and/or elastic effect exists for high viscosity polymer solutions, causing turbulence intensities near the wall to be much higher than for low viscosity solvents and solutions.

A $\langle u' \rangle / u^*$ versus r/a correlation for the two tube sizes used in this investigation shows that $\langle u' \rangle / u^*$ is a weak function of Reynolds number. The $\langle u' \rangle / u^*$ values reach a minimum for a given r/a in the range of Reynolds numbers from 20,000 to 50,000. The Laufer data for air flow in a 10 inch pipe agree very well with the low viscosity $\langle u' \rangle / u^*$ values for liquids.

Transverse turbulence intensity measurements using a prototype hot-film V-probe yielded good Reynolds stress results. Smaller models of this probe design promise to be applicable to transverse intensity measurements in small tubes for the study of drag reduction.

Energy spectra for the solvents and non-drag reducing solutions show only small diameter effects at the same flow rates, but a strong viscous and/or elastic effect exists, the more viscous solutions having lower frequency spectra and higher microscale values (this shift cannot, however, account for drag reduction). Tube flow turbulence energy spectra differ from isotropic grid induced turbulence energy spectra as demonstrated by comparison of Gibson-Schwarz normalized data.

Velocity profiles measured during drag reduction using an impact tube are generally unreliable. Data obtained in this investigation confirmed the low velocities obtained by previous investigators.

Turbulence intensities in drag reducing tube flow depend on flow rate in a manner different from non-drag reduction intensities. At low drag ratios (high drag reduction) the $\langle u' \rangle / u^*$ values were higher than for non-drag reduction results, causing the turbulence intensities to increase with flow rate. The degree of polymer degradation has an effect on the amount of turbulence intensity increase during drag reduction. This effect has not yet been well characterized.

The energy spectra during drag reduction are little different from non-drag reduction results. Changes occur during polymer degradation, but no explanation is offered because of the lack of an energy transfer function involving solution properties. Irregularities in the drag reduction spectra may be indications of characteristic solution frequencies, because these irregularities were not observed for any other spectra.

A quantitative viscoelastic mechanism for turbulent energy dissipation reduction and an approximate relation between turbulent energy dissipation and wall shear stress successfully predict drag reduction levels. The mechanism makes possible the estimation of drag ratios for the turbulent flow of polymer solutions using measurements of the solution viscosity and normal stress difference ($P_{zz} - P_{rr}$) and a knowledge of the energy spectrum. In practice the energy spectrum may be estimated from available data for limited viscosity, velocity, and pipe size ranges, since the spectra do not vary greatly. Since measured energy spectra have been Gibson-Schwarz normalized and are well correlated for pipe flow in the dissipation frequency range, a microscale estimate could be used to calculate a spectrum for use in the mechanism.

The mechanism demonstrates the relative importance of elasticity and viscosity in drag reduction. The predicted reduction in turbulent energy dissipation probably allows the observed increases in turbulence intensities during high drag reduction.

# RECOMMENDATIONS FOR FUTURE INVESTIGATIONS

Further investigation of the turbulence intensity increase during drag reduction would lead to a better understanding of the drag reduction mechanism and would provide data for better drag ratio predictions. Measurements closer to the wall than obtained here are necessary.

The relation between Eulerian and Lagrangian energy spectra must be studied in detail to improve the usefulness of the drag reduction mechanism proposed and to improve our knowledge of the mechanisms of turbulence production and dissipation.

Complete energy balance profiles in the pipe flow of liquids, both non-elastic and elastic, would provide more detailed comparisons between the turbulence structures in the two types of fluids. These profiles must approach the pipe wall very closely, since most of the turbulence production and dissipation occur at about $y^+ = 12$.

A study of the effect of viscosity using non-elastic fluids would help separate elastic and viscous effects in polymer solutions.

Velocity profiles should be measured during drag reduction with an instrument not affected by the normal stress phenomenon. With a probe designed for close wall measurements and a long time averaging circuit on the dc bridge voltmeter, the hot film anemometer should be such an instrument.

Further work should be done to relate the normal stress effect to the shear relaxation spectrum of polymer solutions. A more rigorous viscoelastic energy dissipation mechanism should include such a relaxation spectrum rather than the Maxwell model approximation.

A shear rate distribution function for turbulent pipe flow should be used in the viscoelastic mechanism for energy dissipation reduction,

instead of using the root-mean-square shear rate based on an isotropic turbulence relationship. Efforts to measure the shear rate spectrum as a function of radial position should, therefore, be made.

# APPENDIX I

## EQUIPMENT SPECIFICATIONS

1. Anemometer

The detailed specifications for the DISA 55A01 constant temperature anemometer as stated in the DISA Instruction Manual are as follows:

Frequency Response - 0 - 50 kcps. The upper level is dependent on the fluid conditions and probe used. With a hot-film in a flow of air at about 600 fps the response is at the -3db level for 50 kcps (Figure 9). For the work described here the 3db response drop occurred at about 8000 cps for all velocities using the hot-film probe.

Probe Resistance Range - 1 - 50 ohm probes may be used.

Maximum Probe Resistance Range - 250 ma, continuous or peak. This value sets the maximum power output of a given probe.

Amplifier Transductance, ac - approximately 8 ma/mv at 125 ma current output.

Amplifier Transductance, dc - approximately 300 ma/mv at 125 ma current output.

Equivalent Input dc Drift - ± 25 microvolts at 125 ma current output.

Cold Resistance Measurement Accuracy - 0.5 per cent.

Direct Current Voltmeter - 1 per cent of full scale accuracy using scales of 0-2, 0-5, 0-10, and 0-20 volts with zero shift voltages of 1, 2, 5, and 10 volts.

RMS Voltmeter - 2 per cent of full scale accuracy using scales of 0-5, 0-10, 0-20, 0-50, 0-100, 0-200, 0-500, and 0-1000 mv.

Low Pass Filter - RC filter with seven calibrated positions of 100, 50, 20, 10, 5, 2, and 1 kcps.

High Pass Filter - RC filter with seven calibrated positions of 5, 20, 50, 100, 500, and 1000 cps.

Square Wave Generator - 2.5 kcps for frequency response checking.

Output Impedance - 1000 ohms

Noise Level - With either a hot-film probe or a hot-wire probe, the noise level at the RMS voltmeter is less than 3.7 mv without filtering. (Since nearly all the rms voltages measured in this investigation were about 100 mv and most were above 200 mv, this noise level represents less than 3.7 per cent error. Also, since most of this noise is above 20,000 cps, it was possible to filter it out of the measured signal, lowering the error.)

2. Correlator

The detailed specifications for the DISA 55A06 random signal indicator and correlator are tentatively stated in the instruction manual as follows:

Root-Mean-Square Voltmeter:

Frequency Response - 3 cps - 200,000 cps above -3db.

Accuracy - 2 per cent of full scale for ranges 0-10, 0-31.5, 0-100, 0-315, and 0-1000 mv; 0-3.15, 0-10, 0-31.5 and 0-100 volts.

Input Impedance - 1 megohm in parallel with 50 picofarads for each of two inputs.

Noise and Hum Level - less than 50 microvolts rms.

Output Impedance - 100,000 ohms in parallel with 200 picofarads for the five outputs which are two amplified inputs, sum, difference, and differentiator. The voltmeter measures the value of each of these outputs.

Differentiator - differentiates one input signal using a time constant of 0.05, 0.1, 0.2, 0.5, 1.0, or 2.0 milliseconds.

Reference Voltage - 50 cps for calibration, varies less than 0.2 per cent when line voltage varies 10 per cent.

Ratiometer (measures the ratio of two input signals):

Indicates - ratio of voltmeter inputs, ratio of sum to difference of voltmeter inputs, ratio of voltmeter input to differentiator output.

Scale - ratios 0-$\infty$; calibrated for correlation coefficient -1 to +1.

Correlator Accuracy - 0.03 at 50 cps - 10 kcps

0.06 at 15 cps - 50 kcps

3. Hot-Film Probe

The specifications for the DISA 55A23 hot-film probe are:

Metal Film - platinum

Film Dimensions - 1 mm x 0.2 mm

Resistance at 20°C - 15 ± 3 ohms

Temperature Coefficient of Resistance at 20°C - approximately 0.0031 ohms/°C

Maximum Film Operating Temperature - 500°C

Maximum Ambient Temperature - 150°C

Maximum Fluid Velocity - 500 mps air

10 mps water

Frequency Response - typical frequency response is shown in Figure 9 for air flow.

4. Two Channel Recorder

The detailed specifications for the Ampex 601-2 two channel audio tape recorder as stated in the instruction manual are as follows:

Tape Width - 1/4 inch

Reel Size - 7 inch maximum

Tape Speed - 7 1/2 inches per second

Reproduce Time Accuracy - 0.2 per cent

Flutter and Wow - below 0.17 per cent rms.

Frequency Response - 40 to 15,000 cps; ± 2db, 50 to 10,000 cps
(As shown in Table 8 the response varies according to adjustment.)

Inputs - high impedance microphone and line inputs for each channel.

Outputs - 600 ohm load required.

Head Assembly - separate two track record and reproduce heads, and a full-track erase head.

Signal-to-Noise Ratio-below 0.0032, or noise more than 50 db below peak record level.

Monitor - v-u meter for each channel.

# APPENDIX II

## EXPERIMENTAL PROCEDURES

### 1. Instrument Calibrations

#### 1.1. Hot-film probe calibration and turbulence intensity measurements

In order to measure the intensity of turbulence using a hot-film probe the relation between fluid velocity and probe voltage must be established. With a constant temperature (constant resistance) anemometer the calibration may be done at the same time as the intensity measurements. The procedures for making the calibration and intensity measurements are combined.

The probe resistance at the fluid temperature was measured after installing the probe. Using this resistance and the temperature coefficient of resistance for the film probe, the operating resistance at a temperature well below the fluid boiling point was calculated. In this work the operating temperatures were 70°C for toluene solutions and 60°C for cyclohexane and benzene. These temperatures gave good sensitivity without any evidence of gas bubble formation. (The normal solvent boiling points are: toluene - 110.6°C, cyclohexane - 81.4°C, and benzene - 80.1°C.)

After setting the probe operating resistance, the frequency response of the anemometer was measured using the internal square wave generator. With the fluid flowing at the desired velocity, the square wave voltage was impressed on the probe. The rate of recovery of the anemometer from this disturbance was measured by observing the anemometer output signal on an oscilloscope. This procedure is described in detail in the DISA Instruction Manual.

After determining the frequency response, a low pass filter above the maximum desired frequency was switched in to remove high frequency anemometer noise from the output signal. This was particularly important when using the correlator differentiator circuit to measure microscale because high frequency noise has a very strong effect on the rms value of the signal time derivative.

After this preparative procedure, dc bridge voltage and rms bridge voltage were measured for three or more fluid velocities plus the zero velocity values. In practice these values were measured at several radial locations in the pipe, at flow rates for which velocity profiles had been measured. (Some flow rates were used for which velocity profiles were calculated by interpolation of velocity profiles at higher and lower flow rates.)

The calibration of the hot-film probe was done by determining the best least squares fit to the equation:

$$E^2 = A + B\,(\bar{u})^c$$

The calibration constants A, B, and c are given in Table 10 in Appendix IV. The root-mean-square of the standard deviations of $E^2$ for all the calibrations made in this study is approximately one per cent of $E^2$. This is equivalent to a two per cent rms deviation for $\bar{u}$. Since the average deviation of the integrated velocity profiles from measured flow rates was 1.5 per cent (33), the precision of the calibrations was about as good as possible.

The rms bridge voltages were used to calculate turbulence intensity after the calibration constants were determined. The calculation of turbulence intensities is discussed in Appendix V.

The radial location of the probe during measurements was measured by the micrometer positioner shown in Figure 11. The point of contact between the probe and the wall was found by connecting an ohmmeter from the positioner to the pipe, since the positioner was insulated from the pipe. This contact point established a reference position which was used to calculate the radial position of the probe.

1.2. Tape recorder frequency response calibration

The frequency response of the Ampex tape recorder was measured by recording an input of known voltage produced by a Heath Signal Generator using frequencies from 10 cps to 10,000 cps. The recorded signals were played back into the rms voltmeter on the DISA correlator to determine the relative response value for each frequency. The measured responses are shown in Table 6.

1.3. Band pass filter frequency response calibration

The characteristic response of each band was measured by using an input of known voltage from the Heath Signal Generator and by measuring the relative output values on the rms voltmeter. This was done for several frequencies covering each band's response range. A typical characteristic response curve for the band centered at 1000 cps is shown in Figure 17. Characteristic curve shapes were similar enough that peak values could be used to obtain the relative gain of the bands. The peak value gain factors are shown in Table 9.

1.4. Flow meter calibration

The flow meter system was calibrated during each run because the Heath frequency meter used as an indicator exhibited tendencies to drift from day to day. The procedure involved diverting the total flow into a weigh tank downstream of the test sections for a known time, usually 30-120 seconds. Since the pressure drop in the test

section was much greater than the change in pressure drop in the return line caused by the flow diversion, the flow rate measured was unchanged from the undiverted condition.

## 2. Energy Spectrum and Autocorrelation Measurements

### 2.1. Recording

The anemometer output signal was recorded by connecting the output terminal to the recorder using coaxial cables to reduce stray noise pickup. Before the recording was made, the flow conditions were identified by recording the date, flow rate, radial position of probe, and run number using the microphone. At the beginning of the recording an attempt was made to record about the same signal strength on each channel. After initial adjustments the same signal strength was maintained throughout the recording (about ten minutes), so that spectrum measurements would not be biased. A recording ten minutes long was necessary for making energy spectrum and autocorrelation measurements, since continuous loop operation was impossible on the Ampex 601-2 recorder.

### 2.2. Energy spectrum measurements

The spectra were measured by playing the recorded signal into the input of the band pass filter and measuring the rms output voltage for each band. The Ampex recorder is designed to playback to a load of 600 ohms, so a 600 ohm resistor was connected across the output of each channel. Very close checks were made during the measurements to insure constant total rms voltage of the playback signal. The corrections for the tape recorder response and band gain levels and the calculations of the spectra are discussed in Appendix V.

## 2.3. Autocorrelation measurements

Autocorrelations were measured using the time delay device constructed by the author shown in Figure 15. The movable playback head allowed the playback of one channel to be delayed as much as 100 milliseconds in reference to the other channel. The delay time calibration was made by playing a recording of a 100 cps signal and measuring the autocorrelation coefficients using the DISA correlator. Enough micrometer positions were used to cover several cycles. The points of zero correlation coefficients were 0.005 seconds apart, giving a time base to determine the delay time for a given micrometer movement. Since autocorrelation functions are symmetrical for stationary signals, the zero delay position was found by determining the peak of the autocorrelation function (theoretically a value of one). The peak values were usually about 0.98 - 0.99 for this instrument.

The reduction of the data to autocorrelation coefficient versus time delay is discussed in Appendix V.

# APPENDIX III

## TABULATED DATA AND RESULTS

1. Turbulence Intensity Data and Results

The computer printouts showing data and results for Runs 1-23 constitute Table 5.

2. Energy Spectrum Results and Transformations to Autocorrelations

Table 6 shows the numerical results for each energy spectrum measured in Runs 8, 9, 10, 12, 14, 15, 17, 18, 19, 20, and 21. In each run spectra were measured for two or three positions at one or two flow rates for each position. With each spectrum printout is the corresponding autocorrelation obtained by calculating the Fourier transform of the spectrum function.

3. Autocorrelation Results and Transformations to Energy Spectra

Table 7 contains the computer printouts for each autocorrelation function and the corresponding energy spectra obtained by transforming the autocorrelations.

Table 5

Turbulence Intensity Data and Results

The table contains information identified by the following symbols for each turbulence intensity run:

R/A - corresponds to r/a in the text, radial position divided by pipe radius.

E - hot-film anemometer dc bridge voltage in volts.

U - corresponds to $\bar{u}$ in the text, time average velocity in feet per second.

VRMS - hot-film anemometer rms fluctuating bridge voltage in millivolts.

TURB - longitudinal turbulence intensity, $\langle u' \rangle / \bar{u}$.

MICRO - microscale in feet determined using DISA differentiator circuit.

Q - flow rate in pounds per minute.

RE - Reynolds number using solution viscosity.

(Note: The microscale values listed for Runs 2-14 are not valid because of insufficient high frequency noise filtering.)

RUN NO. 2

| R/A | E | U | VRMS | TURB | MICRO | Q | RE |
|---|---|---|---|---|---|---|---|
| -.80 | 11.4 | .232 | 200.0 | .1226 | .00002 | 22.5 | 8235. |
| -.80 | 12.2 | .366 | 230.0 | .1204 | .00005 | 31.5 | 11530. |
| -.80 | 14.9 | 1.167 | 280.0 | .1002 | .00020 | 91.9 | 33639. |
| -.80 | 18.0 | 3.036 | 350.0 | .0938 | .00060 | 225.7 | 82615. |
| -.80 | 19.4 | 4.336 | 400.0 | .0967 | .00088 | 333.0 | 121892. |
| -.80 | 20.7 | 5.860 | 420.0 | .0932 | .00128 | 441.5 | 161608. |
| -.80 | 21.8 | 7.422 | 440.0 | .0914 | .00157 | 549.4 | 201104. |
| -.70 | 11.4 | .232 | 160.0 | .0981 | .00001 | 22.5 | 8235. |
| -.70 | 12.3 | .385 | 180.0 | .0925 | .00003 | 31.5 | 11530. |
| -.70 | 15.1 | 1.252 | 230.0 | .0805 | .00018 | 91.9 | 33639. |
| -.70 | 18.2 | 3.202 | 300.0 | .0792 | .00052 | 225.7 | 82615. |
| -.70 | 19.7 | 4.659 | 350.0 | .0829 | .00085 | 333.0 | 121892. |
| -.70 | 21.1 | 6.398 | 380.0 | .0823 | .00116 | 441.5 | 161608. |
| -.70 | 22.1 | 7.895 | 390.0 | .0796 | .00150 | 549.4 | 201104. |
| -.60 | 11.7 | .278 | 140.0 | .0806 | .00002 | 22.5 | 8235. |
| -.60 | 12.5 | .426 | 150.0 | .0745 | .00003 | 31.5 | 11530. |
| -.60 | 15.4 | 1.389 | 210.0 | .0712 | .00016 | 91.9 | 33639. |
| -.60 | 18.5 | 3.463 | 275.0 | .0709 | .00051 | 225.7 | 82615. |
| -.60 | 19.9 | 4.884 | 310.0 | .0724 | .00079 | 333.0 | 121892. |
| -.60 | 21.3 | 6.679 | 330.0 | .0706 | .00106 | 441.5 | 161608. |
| -.60 | 22.3 | 8.223 | 340.0 | .0686 | .00141 | 549.4 | 201104. |

RUN NO. 2

| R/A | E | U | VRMS | TURB | MICRO | Q | RE |
|---|---|---|---|---|---|---|---|
| -.50 | 11.8 | .294 | 125.0 | .0705 | .00001 | 22.5 | 8235. |
| -.50 | 12.7 | .470 | 135.0 | .0649 | .00003 | 31.5 | 11530. |
| -.50 | 15.7 | 1.535 | 195.0 | .0641 | .00016 | 91.9 | 33639. |
| -.50 | 18.7 | 3.645 | 250.0 | .0635 | .00050 | 225.7 | 82615. |
| -.50 | 20.3 | 5.356 | 270.0 | .0615 | .00077 | 333.0 | 121892. |
| -.50 | 21.6 | 7.118 | 290.0 | .0609 | .00104 | 441.5 | 161608. |
| -.50 | 22.6 | 8.732 | 320.0 | .0635 | .00129 | 549.4 | 201104. |
| -.40 | 11.9 | .311 | 110.0 | .0608 | .00001 | 22.5 | 8235. |
| -.40 | 12.8 | .493 | 125.0 | .0591 | .00003 | 31.5 | 11530. |
| -.40 | 15.8 | 1.586 | 175.0 | .0570 | .00014 | 91.9 | 33639. |
| -.40 | 18.8 | 3.738 | 230.0 | .0580 | .00046 | 225.7 | 82615. |
| -.40 | 20.4 | 5.479 | 250.0 | .0565 | .00071 | 333.0 | 121892. |
| -.40 | 21.7 | 7.269 | 260.0 | .0543 | .00094 | 441.5 | 161608. |
| -.40 | 22.8 | 9.084 | 280.0 | .0550 | .00131 | 549.4 | 201104. |
| -.30 | 12.2 | .366 | 90.0 | .0471 | .00001 | 22.5 | 8235. |
| -.30 | 12.8 | .493 | 110.0 | .0520 | .00003 | 31.5 | 11530. |
| -.30 | 15.9 | 1.639 | 150.0 | .0483 | .00013 | 91.9 | 33639. |
| -.30 | 19.0 | 3.931 | 200.0 | .0497 | .00039 | 225.7 | 82615. |
| -.30 | 20.6 | 5.731 | 230.0 | .0513 | .00062 | 333.0 | 121892. |
| -.30 | 21.9 | 7.578 | 240.0 | .0495 | .00085 | 441.5 | 161608. |
| -.30 | 22.9 | 9.264 | 250.0 | .0488 | .00112 | 549.4 | 201104. |

RUN NO. 2

| R/A | E | U | VRMS | TURB | MICRO | Q | RE |
|---|---|---|---|---|---|---|---|
| -.20 | 12.3 | .374 | 95.0 | .0481 | .00001 | 22.5 | 8235. |
| -.20 | 13.0 | .523 | 100.0 | .0453 | .00002 | 31.5 | 11530. |
| -.20 | 16.0 | 1.620 | 130.0 | .0412 | .00011 | 91.9 | 33639. |
| -.20 | 19.1 | 3.839 | 175.0 | .0430 | .00033 | 225.7 | 82615. |
| -.20 | 20.6 | 5.453 | 195.0 | .0434 | .00047 | 333.0 | 121892. |
| -.20 | 22.0 | 7.352 | 200.0 | .0409 | .00066 | 441.5 | 161608. |
| -.20 | 23.0 | 8.973 | 210.0 | .0406 | .00085 | 549.4 | 201104. |
| -.10 | 12.2 | .355 | 85.0 | .0438 | .00001 | 22.5 | 8235. |
| -.10 | 13.0 | .523 | 95.0 | .0430 | .00002 | 31.5 | 11530. |
| -.10 | 16.1 | 1.672 | 125.0 | .0392 | .00011 | 91.9 | 33639. |
| -.10 | 19.2 | 3.934 | 155.0 | .0378 | .00031 | 225.7 | 82615. |
| -.10 | 20.8 | 5.700 | 180.0 | .0395 | .00047 | 333.0 | 121892. |
| -.10 | 22.2 | 7.658 | 195.0 | .0394 | .00065 | 441.5 | 161608. |
| -.10 | 23.2 | 9.326 | 195.0 | .0373 | .00079 | 549.4 | 201104. |
| 0.00 | 12.3 | .374 | 75.0 | .0380 | .00001 | 22.5 | 8235. |
| 0.00 | 13.1 | .548 | 90.0 | .0401 | .00002 | 31.5 | 11530. |
| 0.00 | 16.1 | 1.672 | 117.0 | .0367 | .00011 | 91.9 | 33639. |
| 0.00 | 19.3 | 4.031 | 150.0 | .0363 | .00030 | 225.7 | 82615. |
| 0.00 | 20.9 | 5.826 | 172.0 | .0375 | .00046 | 333.0 | 121892. |
| 0.00 | 22.3 | 7.814 | 180.0 | .0362 | .00063 | 441.5 | 161608. |
| 0.00 | 23.3 | 9.506 | 195.0 | .0371 | .00077 | 549.4 | 201104. |

RUN NO. 2

| R/A | E | U | VRMS | TURB | MICRO | Q | RE |
|---|---|---|---|---|---|---|---|
| .10 | 12.3 | .374 | 85.0 | .0431 | .00001 | 22.5 | 8235. |
| .10 | 13.0 | .523 | 90.0 | .0407 | .00002 | 31.5 | 11530. |
| .10 | 16.0 | 1.620 | 125.0 | .0396 | .00011 | 91.9 | 33639. |
| .10 | 19.1 | 3.839 | 155.0 | .0381 | .00030 | 225.7 | 82615. |
| .10 | 20.7 | 5.575 | 175.0 | .0387 | .00046 | 333.0 | 121892. |
| .10 | 22.1 | 7.504 | 190.0 | .0386 | .00062 | 441.5 | 161608. |
| .10 | 23.3 | 9.506 | 200.0 | .0381 | .00082 | 549.4 | 201104. |
| .20 | 12.2 | .355 | 85.0 | .0438 | .00001 | 22.5 | 8235. |
| .20 | 12.9 | .500 | 110.0 | .0506 | .00002 | 31.5 | 11530. |
| .20 | 16.0 | 1.620 | 130.0 | .0412 | .00011 | 91.9 | 33639. |
| .20 | 19.2 | 3.934 | 170.0 | .0415 | .00033 | 225.7 | 82615. |
| .20 | 20.8 | 5.700 | 195.0 | .0428 | .00051 | 333.0 | 121892. |
| .20 | 22.1 | 7.504 | 200.0 | .0407 | .00068 | 441.5 | 161608. |
| .20 | 23.2 | 9.326 | 210.0 | .0402 | .00085 | 549.4 | 201104. |
| .30 | 12.2 | .355 | 90.0 | .0464 | .00001 | 22.5 | 8235. |
| .30 | 12.8 | .477 | 110.0 | .0514 | .00002 | 31.5 | 11530. |
| .30 | 15.9 | 1.569 | 155.0 | .0496 | .00012 | 91.9 | 33639. |
| .30 | 19.0 | 3.745 | 190.0 | .0470 | .00034 | 225.7 | 82615. |
| .30 | 20.6 | 5.453 | 210.0 | .0467 | .00054 | 333.0 | 121892. |
| .30 | 21.9 | 7.203 | 220.0 | .0453 | .00072 | 441.5 | 161608. |
| .30 | 23.0 | 8.973 | 240.0 | .0465 | .00092 | 549.4 | 201104. |

RUN NO. 2

| R/A | E | U | VRMS | TURB | MICRO | Q | RE |
|---|---|---|---|---|---|---|---|
| .40 | 12.1 | .337 | 100.0 | .0525 | .00001 | 22.5 | 8235. |
| .40 | 12.8 | .477 | 115.0 | .0537 | .00002 | 31.5 | 11530. |
| .40 | 15.8 | 1.519 | 165.0 | .0533 | .00013 | 91.9 | 33639. |
| .40 | 18.9 | 3.653 | 220.0 | .0549 | .00044 | 225.7 | 82615. |
| .40 | 20.5 | 5.333 | 250.0 | .0560 | .00065 | 333.0 | 121892. |
| .40 | 21.9 | 7.203 | 250.0 | .0514 | .00091 | 441.5 | 161608. |
| .40 | 22.9 | 8.800 | 270.0 | .0526 | .00118 | 549.4 | 201104. |
| .50 | 12.1 | .337 | 130.0 | .0683 | .00001 | 22.5 | 8235. |
| .50 | 12.8 | .477 | 140.0 | .0654 | .00003 | 31.5 | 11530. |
| .50 | 15.7 | 1.470 | 180.0 | .0588 | .00015 | 91.9 | 33639. |
| .50 | 18.7 | 3.474 | 230.0 | .0582 | .00046 | 225.7 | 82615. |
| .50 | 20.4 | 5.214 | 270.0 | .0608 | .00072 | 333.0 | 121892. |
| .50 | 21.7 | 6.911 | 290.0 | .0604 | .00096 | 441.5 | 161608. |
| .50 | 22.8 | 8.630 | 300.0 | .0587 | .00125 | 549.4 | 201104. |
| .60 | 11.8 | .287 | 130.0 | .0722 | .00002 | 22.5 | 8235. |
| .60 | 12.7 | .455 | 160.0 | .0759 | .00003 | 31.5 | 11530. |
| .60 | 15.6 | 1.423 | 210.0 | .0693 | .00015 | 91.9 | 33639. |
| .60 | 18.7 | 3.474 | 280.0 | .0709 | .00051 | 225.7 | 82615. |
| .60 | 20.3 | 5.097 | 300.0 | .0680 | .00077 | 333.0 | 121892. |
| .60 | 21.7 | 6.911 | 325.0 | .0677 | .00111 | 441.5 | 161608. |
| .60 | 22.7 | 8.462 | 330.0 | .0649 | .00131 | 549.4 | 201104. |

RUN NO. 2

| R/A | E | U | VRMS | TURB | MICRO | Q | RE |
|---|---|---|---|---|---|---|---|
| .70 | 11.8 | .287 | 145.0 | .0805 | .00002 | 22.5 | 8235. |
| .70 | 12.4 | .393 | 165.0 | .0822 | .00003 | 31.5 | 11530. |
| .70 | 15.5 | 1.377 | 230.0 | .0766 | .00019 | 91.9 | 33639. |
| .70 | 18.6 | 3.387 | 310.0 | .0790 | .00054 | 225.7 | 82615. |
| .70 | 20.1 | 4.870 | 330.0 | .0758 | .00086 | 333.0 | 121892. |
| .70 | 21.5 | 6.627 | 360.0 | .0758 | .00119 | 441.5 | 161608. |
| .70 | 22.4 | 7.973 | 380.0 | .0760 | .00140 | 549.4 | 201104. |
| .80 | 11.6 | .256 | 190.0 | .1098 | .00002 | 22.5 | 8235. |
| .80 | 12.3 | .374 | 200.0 | .1014 | .00004 | 31.5 | 11530. |
| .80 | 15.2 | 1.244 | 270.0 | .0928 | .00019 | 91.9 | 33639. |
| .80 | 18.3 | 3.135 | 350.0 | .0913 | .00056 | 225.7 | 82615. |
| .80 | 19.8 | 4.542 | 370.0 | .0867 | .00086 | 333.0 | 121892. |
| .80 | 21.2 | 6.217 | 420.0 | .0901 | .00121 | 441.5 | 161608. |
| .80 | 22.2 | 7.658 | 440.0 | .0890 | .00151 | 549.4 | 201104. |
| .85 | 11.4 | .228 | 200.0 | .1205 | .00002 | 22.5 | 8235. |
| .85 | 12.2 | .355 | 210.0 | .1083 | .00004 | 31.5 | 11530. |
| .85 | 15.1 | 1.201 | 280.0 | .0973 | .00020 | 91.9 | 33639. |
| .85 | 18.1 | 2.974 | 350.0 | .0927 | .00058 | 225.7 | 82615. |
| .85 | 19.7 | 4.436 | 420.0 | .0991 | .00090 | 333.0 | 121892. |
| .85 | 21.0 | 5.954 | 440.0 | .0955 | .00122 | 441.5 | 161608. |
| .85 | 22.0 | 7.352 | 450.0 | .0921 | .00153 | 549.4 | 201104. |

RUN NO. 3

| R/A | E | U | VRMS | TURB | MICRO | Q | RE |
|---|---|---|---|---|---|---|---|
| -.60 | 19.6 | 7.686 | 285.0 | .0657 | .00265 | 455.0 | 97004. |
| -.60 | 18.0 | 5.206 | 265.0 | .0682 | .00169 | 297.0 | 63319. |
| -.60 | 16.1 | 3.074 | 220.0 | .0659 | .00089 | 179.0 | 38162. |
| -.60 | 12.6 | .872 | 170.0 | .0748 | .00015 | 52.6 | 11214. |
| -.50 | 19.7 | 7.865 | 250.0 | .0572 | .00238 | 455.0 | 97004. |
| -.50 | 18.0 | 5.206 | 230.0 | .0591 | .00147 | 297.0 | 63319. |
| -.50 | 16.1 | 3.074 | 200.0 | .0599 | .00065 | 179.0 | 38162. |
| -.50 | 12.7 | .911 | 145.0 | .0629 | .00013 | 52.6 | 11214. |
| -.40 | 19.9 | 8.231 | 220.0 | .0497 | .00180 | 455.0 | 97004. |
| -.40 | 18.2 | 5.479 | 205.0 | .0520 | .00112 | 297.0 | 63319. |
| -.40 | 16.2 | 3.167 | 175.0 | .0519 | .00060 | 179.0 | 38162. |
| -.40 | 12.7 | .911 | 125.0 | .0542 | .00011 | 52.6 | 11214. |
| -.30 | 20.0 | 8.419 | 200.0 | .0449 | .00163 | 455.0 | 97004. |
| -.30 | 18.2 | 5.479 | 175.0 | .0443 | .00097 | 297.0 | 63319. |
| -.30 | 16.3 | 3.262 | 155.0 | .0456 | .00054 | 179.0 | 38162. |
| -.30 | 12.7 | .911 | 120.0 | .0520 | .00010 | 52.6 | 11214. |
| -.20 | 20.0 | 8.419 | 170.0 | .0382 | .00142 | 455.0 | 97004. |
| -.20 | 18.3 | 5.619 | 160.0 | .0402 | .00090 | 297.0 | 63319. |
| -.20 | 16.3 | 3.262 | 135.0 | .0397 | .00047 | 179.0 | 38162. |
| -.20 | 12.7 | .911 | 110.0 | .0477 | .00010 | 52.6 | 11214. |
| -.10 | 20.2 | 8.804 | 155.0 | .0344 | .00135 | 455.0 | 97004. |
| -.10 | 18.4 | 5.762 | 140.0 | .0350 | .00083 | 297.0 | 63319. |
| -.10 | 16.4 | 3.359 | 128.0 | .0373 | .00045 | 179.0 | 38162. |
| -.10 | 12.8 | .951 | 100.0 | .0428 | .00010 | 52.6 | 11214. |

RUN NO. 3

| R/A | E | U | VRMS | TURB | MICRO | Q | RE |
|---|---|---|---|---|---|---|---|
| 0.00 | 20.2 | 8.804 | 150.0 | .0333 | .00134 | 455.0 | 97004. |
| 0.00 | 18.4 | 5.762 | 133.0 | .0332 | .00083 | 297.0 | 63319. |
| 0.00 | 16.4 | 3.359 | 120.0 | .0350 | .00042 | 179.0 | 38162. |
| 0.00 | 13.0 | 1.035 | 95.0 | .0395 | .00009 | 52.6 | 11214. |
| .10 | 20.2 | 8.804 | 160.0 | .0355 | .00136 | 455.0 | 97004. |
| .10 | 18.4 | 5.762 | 140.0 | .0350 | .00085 | 297.0 | 63319. |
| .10 | 16.5 | 3.458 | 125.0 | .0361 | .00047 | 179.0 | 38162. |
| .10 | 12.9 | .992 | 100.0 | .0422 | .00010 | 52.6 | 11214. |
| .20 | 20.0 | 8.419 | 180.0 | .0404 | .00151 | 455.0 | 97004. |
| .20 | 18.4 | 5.762 | 165.0 | .0412 | .00097 | 297.0 | 63319. |
| .20 | 16.4 | 3.359 | 145.0 | .0423 | .00049 | 179.0 | 38162. |
| .20 | 12.7 | .911 | 110.0 | .0477 | .00010 | 52.6 | 11214. |
| .30 | 19.9 | 8.231 | 210.0 | .0475 | .00168 | 455.0 | 97004. |
| .30 | 18.3 | 5.619 | 185.0 | .0465 | .00109 | 297.0 | 63319. |
| .30 | 16.2 | 3.167 | 160.0 | .0475 | .00053 | 179.0 | 38162. |
| .30 | 12.7 | .911 | 125.0 | .0542 | .00011 | 52.6 | 11214. |
| .40 | 19.9 | 8.231 | 235.0 | .0531 | .00249 | 455.0 | 97004. |
| .40 | 18.1 | 5.341 | 220.0 | .0562 | .00151 | 297.0 | 63319. |
| .40 | 16.2 | 3.167 | 180.0 | .0534 | .00060 | 179.0 | 38162. |
| .40 | 12.6 | .872 | 130.0 | .0572 | .00012 | 52.6 | 11214. |
| .50 | 19.7 | 7.865 | 265.0 | .0607 | .00255 | 455.0 | 97004. |
| .50 | 18.1 | 5.341 | 240.0 | .0613 | .00166 | 297.0 | 63319. |
| .50 | 16.1 | 3.074 | 205.0 | .0614 | .00089 | 179.0 | 38162. |
| .50 | 12.7 | .911 | 155.0 | .0672 | .00014 | 52.6 | 11214. |

RUN NO. 3

| R/A | E | U | VRMS | TURB | MICRO | Q | RE |
|---|---|---|---|---|---|---|---|
| .60 | 19.6 | 7.686 | 300.0 | .0691 | .00278 | 455.0 | 97004. |
| .60 | 18.0 | 5.206 | 270.0 | .0694 | .00184 | 297.0 | 63319. |
| .60 | 16.0 | 2.983 | 235.0 | .0710 | .00092 | 179.0 | 38162. |
| .60 | 12.6 | .872 | 170.0 | .0748 | .00020 | 52.6 | 11214. |
| .70 | 19.4 | 7.337 | 325.0 | .0759 | .00311 | 455.0 | 97004. |
| .70 | 17.8 | 4.943 | 300.0 | .0783 | .00184 | 297.0 | 63319. |
| .70 | 16.0 | 2.983 | 260.0 | .0785 | .00099 | 179.0 | 38162. |
| .70 | 12.5 | .834 | 200.0 | .0892 | .00022 | 52.6 | 11214. |
| .80 | 19.2 | 7.000 | 385.0 | .0911 | .00312 | 455.0 | 97004. |
| .80 | 17.6 | 4.690 | 335.0 | .0888 | .00196 | 297.0 | 63319. |
| .80 | 15.7 | 2.721 | 300.0 | .0931 | .00103 | 179.0 | 38162. |
| .80 | 12.3 | .762 | 225.0 | .1034 | .00023 | 52.6 | 11214. |
| .85 | 19.0 | 6.674 | 390.0 | .0935 | .00302 | 455.0 | 97004. |
| .85 | 17.3 | 4.327 | 350.0 | .0949 | .00189 | 297.0 | 63319. |
| .85 | 15.5 | 2.555 | 315.0 | .0996 | .00108 | 179.0 | 38162. |
| .85 | 12.2 | .727 | 250.0 | .1166 | .00023 | 52.6 | 11214. |

RUN NO. 4

| R/A | E | U | VRMS | TURB | MICRO | Q | RE |
|---|---|---|---|---|---|---|---|
| -.70 | 19.5 | 8.612 | 315.0 | .0726 | .00299 | 514.5 | 97721. |
| -.70 | 17.8 | 5.685 | 300.0 | .0777 | .00189 | 339.5 | 64482. |
| -.70 | 15.6 | 3.050 | 250.0 | .0775 | .00092 | 180.6 | 34302. |
| -.70 | 12.2 | .858 | 190.0 | .0868 | .00020 | 54.0 | 10256. |
| -.60 | 19.6 | 8.813 | 285.0 | .0653 | .00276 | 514.5 | 97721. |
| -.60 | 18.0 | 5.985 | 265.0 | .0676 | .00181 | 339.5 | 64482. |
| -.60 | 15.8 | 3.244 | 230.0 | .0700 | .00087 | 180.6 | 34302. |
| -.60 | 12.3 | .897 | 160.0 | .0721 | .00019 | 54.0 | 10256. |
| -.50 | 19.8 | 9.224 | 245.0 | .0554 | .00260 | 514.5 | 97721. |
| -.50 | 18.2 | 6.297 | 240.0 | .0604 | .00172 | 339.5 | 64482. |
| -.50 | 15.8 | 3.244 | 210.0 | .0639 | .00078 | 180.6 | 34302. |
| -.50 | 12.4 | .938 | 140.0 | .0621 | .00017 | 54.0 | 10256. |
| -.40 | 20.0 | 9.648 | 230.0 | .0514 | .00245 | 514.5 | 97721. |
| -.40 | 18.3 | 6.457 | 215.0 | .0537 | .00160 | 339.5 | 64482. |
| -.40 | 15.9 | 3.344 | 180.0 | .0543 | .00077 | 180.6 | 34302. |
| -.40 | 12.5 | .981 | 130.0 | .0569 | .00016 | 54.0 | 10256. |
| -.30 | 20.1 | 9.865 | 205.0 | .0455 | .00231 | 514.5 | 97721. |
| -.30 | 18.3 | 6.457 | 180.0 | .0450 | .00142 | 339.5 | 64482. |
| -.30 | 15.9 | 3.344 | 160.0 | .0482 | .00068 | 180.6 | 34302. |
| -.30 | 12.4 | .938 | 120.0 | .0533 | .00010 | 54.0 | 10256. |
| -.20 | 20.1 | 9.865 | 180.0 | .0399 | .00163 | 514.5 | 97721. |
| -.20 | 18.2 | 6.297 | 160.0 | .0402 | .00096 | 339.5 | 64482. |
| -.20 | 16.0 | 3.446 | 145.0 | .0433 | .00050 | 180.6 | 34302. |
| -.20 | 12.4 | .938 | 112.0 | .0497 | .00009 | 54.0 | 10256. |

RUN NO. 4

| R/A | E | U | VRMS | TURB | MICRO | Q | RE |
|---|---|---|---|---|---|---|---|
| 0.00 | 20.0 | 9.648 | 165.0 | .0368 | .00152 | 514.5 | 97721. |
| 0.00 | 18.3 | 6.457 | 150.0 | .0375 | .00098 | 339.5 | 64482. |
| 0.00 | 16.0 | 3.446 | 130.0 | .0388 | .00047 | 180.6 | 34302. |
| 0.00 | 12.4 | .938 | 100.0 | .0444 | .00009 | 54.0 | 10256. |
| .10 | 20.0 | 9.648 | 175.0 | .0391 | .00155 | 514.5 | 97721. |
| .10 | 18.3 | 6.457 | 160.0 | .0400 | .00102 | 339.5 | 64482. |
| .10 | 15.9 | 3.344 | 140.0 | .0422 | .00048 | 180.6 | 34302. |
| .10 | 12.4 | .938 | 110.0 | .0488 | .00009 | 54.0 | 10256. |
| .20 | 19.9 | 9.434 | 190.0 | .0427 | .00166 | 514.5 | 97721. |
| .20 | 18.2 | 6.297 | 180.0 | .0453 | .00108 | 339.5 | 64482. |
| .20 | 15.8 | 3.244 | 150.0 | .0456 | .00049 | 180.6 | 34302. |
| .20 | 12.4 | .938 | 115.0 | .0510 | .00010 | 54.0 | 10256. |
| .30 | 19.8 | 9.224 | 215.0 | .0486 | .00237 | 514.5 | 97721. |
| .30 | 18.2 | 6.297 | 200.0 | .0503 | .00154 | 339.5 | 64482. |
| .30 | 15.9 | 3.344 | 165.0 | .0498 | .00070 | 180.6 | 34302. |
| .30 | 12.5 | .981 | 125.0 | .0547 | .00011 | 54.0 | 10256. |
| .40 | 19.7 | 9.017 | 240.0 | .0546 | .00242 | 514.5 | 97721. |
| .40 | 18.0 | 5.985 | 225.0 | .0574 | .00155 | 339.5 | 64482. |
| .40 | 15.7 | 3.146 | 190.0 | .0583 | .00074 | 180.6 | 34302. |
| .40 | 12.3 | .897 | 140.0 | .0630 | .00015 | 54.0 | 10256. |
| .50 | 19.7 | 9.017 | 265.0 | .0603 | .00270 | 514.5 | 97721. |
| .50 | 18.0 | 5.985 | 245.0 | .0625 | .00169 | 339.5 | 64482. |
| .50 | 15.8 | 3.244 | 210.0 | .0639 | .00079 | 180.6 | 34302. |
| .50 | 12.3 | .897 | 145.0 | .0653 | .00017 | 54.0 | 10256. |

RUN NO. 4

| R/A | E | U | VRMS | TURB | MICRO | Q | RE |
|---|---|---|---|---|---|---|---|
| .60 | 19.5 | 8.612 | 300.0 | .0692 | .00280 | 514.5 | 97721. |
| .60 | 17.9 | 5.834 | 265.0 | .0681 | .00183 | 339.5 | 64482. |
| .60 | 15.7 | 3.146 | 235.0 | .0722 | .00088 | 180.6 | 34302. |
| .60 | 12.2 | .858 | 165.0 | .0754 | .00018 | 54.0 | 10256. |
| .70 | 19.4 | 8.415 | 330.0 | .0766 | .00309 | 514.5 | 97721. |
| .70 | 17.7 | 5.539 | 295.0 | .0770 | .00191 | 339.5 | 64482. |
| .70 | 15.6 | 3.050 | 270.0 | .0837 | .00100 | 180.6 | 34302. |
| .70 | 12.2 | .858 | 195.0 | .0891 | .00023 | 54.0 | 10256. |
| .80 | 19.2 | 8.031 | 375.0 | .0882 | .00516 | 514.5 | 97721. |
| .80 | 17.5 | 5.255 | 345.0 | .0914 | .00364 | 339.5 | 64482. |
| .80 | 15.3 | 2.776 | 300.0 | .0956 | .00180 | 180.6 | 34302. |
| .80 | 12.0 | .781 | 240.0 | .1130 | .00038 | 54.0 | 10256. |
| .85 | 18.9 | 7.479 | 405.0 | .0971 | .00507 | 514.5 | 97721. |
| .85 | 17.3 | 4.982 | 380.0 | .1022 | .00359 | 339.5 | 64482. |
| .85 | 15.1 | 2.603 | 320.0 | .1039 | .00174 | 180.6 | 34302. |
| .85 | 11.8 | .710 | 270.0 | .1312 | .00040 | 54.0 | 10256. |

RUN NO. 6

| R/A | E | U | VRMS | TURB | MICRO | Q | RE |
|---|---|---|---|---|---|---|---|
| 0.00 | 19.8 | 9.836 | 150.0 | .0343 | .00139 | 520.0 | 88016. |
| 0.00 | 18.2 | 6.684 | 140.0 | .0357 | .00089 | 350.0 | 59241. |
| 0.00 | 16.1 | 3.736 | 130.0 | .0392 | .00051 | 180.0 | 30467. |
| 0.00 | 12.8 | 1.142 | 106.0 | .0459 | .00012 | 54.0 | 9140. |
| .30 | 19.6 | 9.393 | 190.0 | .0440 | .00172 | 520.0 | 88016. |
| .30 | 18.2 | 6.684 | 180.0 | .0459 | .00121 | 350.0 | 59241. |
| .30 | 16.0 | 3.624 | 170.0 | .0517 | .00061 | 180.0 | 30467. |
| .30 | 12.7 | 1.094 | 130.0 | .0571 | .00014 | 54.0 | 9140. |
| .60 | 19.2 | 8.551 | 270.0 | .0642 | .00283 | 520.0 | 88016. |
| .60 | 17.8 | 6.027 | 260.0 | .0683 | .00192 | 350.0 | 59241. |
| .60 | 15.5 | 3.102 | 235.0 | .0749 | .00103 | 180.0 | 30467. |
| .60 | 12.4 | .956 | 170.0 | .0781 | .00022 | 54.0 | 9140. |
| .80 | 18.9 | 7.956 | 350.0 | .0849 | .00495 | 520.0 | 88016. |
| .80 | 17.3 | 5.271 | 325.0 | .0887 | .00357 | 350.0 | 59241. |
| .80 | 15.2 | 2.815 | 300.0 | .0984 | .00183 | 180.0 | 30467. |
| .80 | 12.2 | .870 | 245.0 | .1160 | .00046 | 54.0 | 9140. |
| .85 | 18.7 | 7.577 | 375.0 | .0923 | .00487 | 520.0 | 88016. |
| .85 | 17.2 | 5.129 | 355.0 | .0976 | .00366 | 350.0 | 59241. |
| .85 | 14.9 | 2.547 | 320.0 | .1082 | .00180 | 180.0 | 30467. |
| .85 | 12.0 | .790 | 290.0 | .1417 | .00049 | 54.0 | 9140. |

RUN NO. 7

| R/A | E | U | VRMS | TURB | MICRO | Q | RE |
|---|---|---|---|---|---|---|---|
| 0.00 | 18.2 | 9.576 | 125.0 | .0392 | .00117 | 525.0 | 59489. |
| 0.00 | 17.2 | 6.915 | 115.0 | .0388 | .00080 | 360.0 | 40792. |
| 0.00 | 15.4 | 3.591 | 105.0 | .0412 | .00038 | 180.0 | 20396. |
| 0.00 | 12.6 | 1.000 | 108.0 | .0579 | .00010 | 52.0 | 5892. |
| .10 | 18.1 | 9.279 | 130.0 | .0410 | .00118 | 525.0 | 59489. |
| .10 | 17.1 | 6.684 | 125.0 | .0425 | .00085 | 360.0 | 40792. |
| .10 | 15.2 | 3.317 | 110.0 | .0440 | .00037 | 180.0 | 20396. |
| .10 | 12.6 | 1.000 | 120.0 | .0643 | .00011 | 52.0 | 5892. |
| .20 | 18.2 | 9.576 | 150.0 | .0470 | .00139 | 525.0 | 59489. |
| .20 | 17.2 | 6.915 | 140.0 | .0472 | .00094 | 360.0 | 40792. |
| .20 | 15.4 | 3.591 | 125.0 | .0491 | .00044 | 180.0 | 20396. |
| .20 | 12.5 | .947 | 120.0 | .0652 | .00011 | 52.0 | 5892. |
| .30 | 18.2 | 9.576 | 165.0 | .0517 | .00154 | 525.0 | 59489. |
| .30 | 17.1 | 6.684 | 155.0 | .0527 | .00104 | 360.0 | 40792. |
| .30 | 15.3 | 3.452 | 140.0 | .0555 | .00048 | 180.0 | 20396. |
| .30 | 12.5 | .947 | 140.0 | .0761 | .00011 | 52.0 | 5892. |
| .40 | 18.1 | 9.279 | 185.0 | .0584 | .00167 | 525.0 | 59489. |
| .40 | 17.0 | 6.460 | 170.0 | .0583 | .00114 | 360.0 | 40792. |
| .40 | 15.2 | 3.317 | 155.0 | .0620 | .00050 | 180.0 | 20396. |
| .40 | 12.4 | .897 | 150.0 | .0826 | .00012 | 52.0 | 5892. |
| .50 | 18.1 | 9.279 | 210.0 | .0663 | .00192 | 525.0 | 59489. |
| .50 | 17.0 | 6.460 | 190.0 | .0651 | .00123 | 360.0 | 40792. |
| .50 | 15.2 | 3.317 | 175.0 | .0700 | .00058 | 180.0 | 20396. |
| .50 | 12.3 | .848 | 160.0 | .0894 | .00014 | 52.0 | 5892. |

RUN NO. 7

| R/A | E | U | VRMS | TURB | MICRO | Q | RE |
|---|---|---|---|---|---|---|---|
| .60 | 18.0 | 8.989 | 240.0 | .0764 | .00249 | 525.0 | 59489. |
| .60 | 16.9 | 6.241 | 218.0 | .0753 | .00162 | 360.0 | 40792. |
| .60 | 15.1 | 3.186 | 200.0 | .0808 | .00081 | 180.0 | 20396. |
| .60 | 12.3 | .848 | 190.0 | .1062 | .00018 | 52.0 | 5892. |
| .70 | 17.9 | 8.706 | 265.0 | .0849 | .00270 | 525.0 | 59489. |
| .70 | 16.8 | 6.028 | 240.0 | .0836 | .00170 | 360.0 | 40792. |
| .70 | 14.9 | 2.936 | 235.0 | .0968 | .00084 | 180.0 | 20396. |
| .70 | 12.1 | .757 | 220.0 | .1266 | .00019 | 52.0 | 5892. |
| .80 | 17.7 | 8.162 | 295.0 | .0959 | .00272 | 525.0 | 59489. |
| .80 | 16.6 | 5.619 | 260.0 | .0921 | .00174 | 360.0 | 40792. |
| .80 | 14.7 | 2.702 | 275.0 | .1156 | .00091 | 180.0 | 20396. |
| .80 | 11.8 | .635 | 270.0 | .1626 | .00019 | 52.0 | 5892. |
| .85 | 17.4 | 7.394 | 310.0 | .1031 | .00271 | 525.0 | 59489. |
| .85 | 16.3 | 5.045 | 280.0 | .1016 | .00168 | 360.0 | 40792. |
| .85 | 14.5 | 2.482 | 295.0 | .1265 | .00091 | 180.0 | 20396. |
| .85 | 11.6 | .561 | 315.0 | .1958 | .00021 | 52.0 | 5892. |

RUN NO. 8

| R/A | E | U | VRMS | TURB | MICRO | Q | RE |
|---|---|---|---|---|---|---|---|
| 0.00 | 19.0 | 9.885 | 140.0 | .0372 | 0.00000 | 525.0 | 59489. |
| 0.00 | 17.8 | 7.087 | 125.0 | .0361 | 0.00000 | 360.0 | 40792. |
| 0.00 | 15.5 | 3.414 | 130.0 | .0454 | 0.00000 | 180.0 | 20396. |
| .30 | 18.9 | 9.625 | 175.0 | .0468 | 0.00000 | 525.0 | 59489. |
| .30 | 17.6 | 6.686 | 165.0 | .0484 | 0.00000 | 360.0 | 40792. |
| .30 | 15.5 | 3.414 | 160.0 | .0559 | 0.00000 | 180.0 | 20396. |
| .60 | 18.6 | 8.875 | 240.0 | .0655 | .00266 | 525.0 | 59489. |
| .60 | 17.2 | 5.934 | 230.0 | .0696 | .00177 | 360.0 | 40792. |
| .60 | 15.1 | 2.960 | 230.0 | .0836 | .00092 | 180.0 | 20396. |
| .80 | 18.2 | 7.944 | 295.0 | .0829 | .00466 | 525.0 | 59489. |
| .80 | 17.0 | 5.583 | 295.0 | .0907 | .00343 | 360.0 | 40792. |
| .80 | 14.9 | 2.750 | 300.0 | .1112 | .00184 | 180.0 | 20396. |
| .85 | 18.0 | 7.506 | 310.0 | .0883 | .00456 | 525.0 | 59489. |
| .85 | 16.8 | 5.247 | 320.0 | .1000 | .00345 | 360.0 | 40792. |
| .85 | 14.8 | 2.650 | 310.0 | .1161 | .00193 | 180.0 | 20396. |

RUN NO. 9

| R/A | E | U | VRMS | TURB | MICRO | Q | RE |
|---|---|---|---|---|---|---|---|
| -.70 | 16.1 | 8.381 | 160.0 | .0766 | .00177 | 520.0 | 22404. |
| -.50 | 16.2 | 8.791 | 125.0 | .0594 | .00108 | 520.0 | 22404. |
| -.30 | 16.3 | 9.217 | 95.0 | .0448 | .00091 | 520.0 | 22404. |
| -.10 | 16.2 | 8.791 | 76.0 | .0361 | .00061 | 520.0 | 22404. |
| 0.00 | 16.3 | 9.217 | 78.0 | .0367 | .00064 | 520.0 | 22404. |
| .10 | 16.3 | 9.217 | 84.0 | .0396 | .00069 | 520.0 | 22404. |
| .30 | 16.2 | 8.791 | 105.0 | .0499 | .00094 | 520.0 | 22404. |
| .50 | 16.2 | 8.791 | 140.0 | .0665 | .00124 | 520.0 | 22404. |
| .70 | 16.1 | 8.381 | 180.0 | .0862 | .00203 | 520.0 | 22404. |
| .80 | 16.0 | 7.987 | 215.0 | .1038 | .00350 | 520.0 | 22404. |
| .85 | 15.9 | 7.609 | 245.0 | .1193 | .00392 | 520.0 | 22404. |

RUN NO. 9

| R/A | E | U | VRMS | TURB | MICRO | Q | RE |
|---|---|---|---|---|---|---|---|
| -.70 | 15.6 | 6.562 | 195.0 | .0974 | .00163 | 360.0 | 14277. |
| -.50 | 15.7 | 6.897 | 145.0 | .0718 | .00102 | 360.0 | 14277. |
| -.30 | 15.8 | 7.246 | 110.0 | .0540 | .00085 | 360.0 | 14277. |
| -.10 | 15.7 | 6.897 | 90.0 | .0445 | .00054 | 360.0 | 14277. |
| 0.00 | 15.7 | 6.897 | 88.0 | .0436 | .00057 | 360.0 | 14277. |
| .10 | 15.7 | 6.897 | 98.0 | .0485 | .00062 | 360.0 | 14277. |
| .30 | 15.7 | 6.897 | 120.0 | .0594 | .00085 | 360.0 | 14277. |
| .50 | 15.6 | 6.562 | 160.0 | .0799 | .00106 | 360.0 | 14277. |
| .70 | 15.5 | 6.241 | 210.0 | .1058 | .00173 | 360.0 | 14277. |
| .80 | 15.4 | 5.933 | 250.0 | .1271 | .00323 | 360.0 | 14277. |
| .85 | 15.3 | 5.637 | 295.0 | .1513 | .00350 | 360.0 | 14277. |

RUN NO. 9

| R/A | E | U | VRMS | TURB | MICRO | Q | RE |
|---|---|---|---|---|---|---|---|
| -.70 | 14.2 | 3.112 | 210.0 | .1194 | .00083 | 180.0 | 6093. |
| -.50 | 14.2 | 3.112 | 155.0 | .0881 | .00048 | 180.0 | 6093. |
| -.30 | 14.4 | 3.484 | 122.0 | .0680 | .00043 | 180.0 | 6093. |
| -.10 | 14.4 | 3.484 | 100.0 | .0557 | .00031 | 180.0 | 6093. |
| 0.00 | 14.4 | 3.484 | 97.0 | .0541 | .00030 | 180.0 | 6093. |
| .10 | 14.3 | 3.294 | 103.0 | .0580 | .00030 | 180.0 | 6093. |
| .30 | 14.2 | 3.112 | 130.0 | .0739 | .00040 | 180.0 | 6093. |
| .50 | 14.1 | 2.939 | 160.0 | .0919 | .00047 | 180.0 | 6093. |
| .70 | 14.1 | 2.939 | 220.0 | .1264 | .00087 | 180.0 | 6093. |
| .80 | 14.0 | 2.774 | 325.0 | .1887 | .00186 | 180.0 | 6093. |
| .85 | 13.8 | 2.467 | 400.0 | .2371 | .00193 | 180.0 | 6093. |

RUN NO. 10

| R/A | E | U | VRMS | TURB | MICRO | Q | RE |
|---|---|---|---|---|---|---|---|
| 0.00 | 21.7 | 9.030 | 170.0 | .0351 | .00130 | 569.0 | 176687. |
| 0.00 | 20.2 | 6.740 | 165.0 | .0367 | .00097 | 411.0 | 127624. |
| 0.00 | 17.6 | 3.340 | 135.0 | .0371 | .00041 | 207.0 | 64278. |
| 0.00 | 6.9 | 0.000 | 0.0 | 0.0000 | 0.00000 | 0.0 | 0. |
| .50 | 20.5 | 8.350 | 275.0 | .0611 | .00224 | 569.0 | 176687. |
| .50 | 19.0 | 6.180 | 250.0 | .0599 | .00157 | 411.0 | 127624. |
| .50 | 16.9 | 2.990 | 220.0 | .0674 | .00051 | 207.0 | 64278. |
| .50 | 6.9 | 0.000 | 0.0 | 0.0000 | 0.00000 | 0.0 | 0. |
| .85 | 19.0 | 7.090 | 395.0 | .0965 | .00170 | 569.0 | 176687. |
| .85 | 17.7 | 5.230 | 365.0 | .0967 | .00125 | 411.0 | 127624. |
| .85 | 15.4 | 2.480 | 305.0 | .1021 | .00052 | 207.0 | 64278. |
| .85 | 6.9 | 0.000 | 0.0 | 0.0000 | 0.00000 | 0.0 | 0. |

RUN NO.11

| R/A | E | U | VRMS | TURB | MICRO | Q | RE |
|---|---|---|---|---|---|---|---|
| 0.00 | 20.9 | 8.883 | 160.0 | .0342 | .00141 | 546.0 | 140120. |
| 0.00 | 19.7 | 6.807 | 150.0 | .0345 | .00103 | 411.0 | 105475. |
| 0.00 | 17.0 | 3.435 | 125.0 | .0349 | .00045 | 207.0 | 53122. |
| 0.00 | 13.2 | .957 | 100.0 | .0411 | .00009 | 61.0 | 15654. |
| .10 | 21.0 | 9.074 | 175.0 | .0372 | .00157 | 546.0 | 140120. |
| .10 | 19.7 | 6.807 | 160.0 | .0368 | .00112 | 411.0 | 105475. |
| .10 | 17.0 | 3.435 | 140.0 | .0391 | .00050 | 207.0 | 53122. |
| .10 | 13.1 | .919 | 105.0 | .0437 | .00010 | 61.0 | 15654. |
| .20 | 20.9 | 8.883 | 200.0 | .0427 | .00221 | 546.0 | 140120. |
| .20 | 19.6 | 6.651 | 185.0 | .0428 | .00159 | 411.0 | 105475. |
| .20 | 16.8 | 3.247 | 160.0 | .0454 | .00068 | 207.0 | 53122. |
| .20 | 13.0 | .881 | 110.0 | .0464 | .00013 | 61.0 | 15654. |
| .40 | 20.6 | 8.326 | 250.0 | .0544 | .00259 | 546.0 | 140120. |
| .40 | 19.4 | 6.348 | 235.0 | .0551 | .00193 | 411.0 | 105475. |
| .40 | 16.6 | 3.066 | 200.0 | .0578 | .00082 | 207.0 | 53122. |
| .40 | 12.9 | .844 | 135.0 | .0577 | .00016 | 61.0 | 15654. |
| .60 | 20.4 | 7.969 | 330.0 | .0727 | .00299 | 546.0 | 140120. |
| .60 | 19.2 | 6.055 | 305.0 | .0725 | .00208 | 411.0 | 105475. |
| .60 | 16.4 | 2.892 | 245.0 | .0720 | .00090 | 207.0 | 53122. |
| .60 | 12.7 | .774 | 175.0 | .0770 | .00017 | 61.0 | 15654. |
| .80 | 19.8 | 6.965 | 390.0 | .0892 | .00472 | 546.0 | 140120. |
| .80 | 18.6 | 5.234 | 375.0 | .0929 | .00370 | 411.0 | 105475. |
| .80 | 16.1 | 2.645 | 310.0 | .0935 | .00177 | 207.0 | 53122. |
| .80 | 12.5 | .708 | 220.0 | .0996 | .00035 | 61.0 | 15654. |

RUN NO.11

| R/A | E | U | VRMS | TURB | MICRO | Q | RE |
|---|---|---|---|---|---|---|---|
| .85 | 19.7 | 6.807 | 430.0 | .0990 | .00495 | 546.0 | 140120. |
| .85 | 18.5 | 5.105 | 390.0 | .0973 | .00379 | 411.0 | 105475. |
| .85 | 16.0 | 2.566 | 335.0 | .1020 | .00177 | 207.0 | 53122. |
| .85 | 12.5 | .708 | 260.0 | .1177 | .00037 | 61.0 | 15654. |

RUN NO.12

| R/A | E | U | VRMS | TURB | MICRO | Q | RE |
|---|---|---|---|---|---|---|---|
| 0.00 | 20.7 | 9.203 | 153.0 | .0330 | .00141 | 546.0 | 86041. |
| 0.00 | 19.5 | 7.032 | 145.0 | .0337 | .00103 | 411.0 | 64767. |
| 0.00 | 16.9 | 3.619 | 125.0 | .0351 | .00201 | 207.0 | 32619. |
| .40 | 20.4 | 8.621 | 245.0 | .0539 | .00260 | 546.0 | 86041. |
| .40 | 19.3 | 6.710 | 235.0 | .0554 | .00193 | 411.0 | 64767. |
| .40 | 16.4 | 3.135 | 200.0 | .0586 | .00081 | 207.0 | 32619. |
| .50 | 20.2 | 8.247 | 275.0 | .0612 | .00277 | 546.0 | 86041. |
| .50 | 19.1 | 6.399 | 265.0 | .0633 | .00208 | 411.0 | 64767. |
| .50 | 16.4 | 3.135 | 220.0 | .0645 | .00088 | 207.0 | 32619. |
| .80 | 19.5 | 7.032 | 400.0 | .0931 | .00497 | 546.0 | 86041. |
| .80 | 18.2 | 5.125 | 360.0 | .0916 | .00376 | 411.0 | 64767. |
| .80 | 15.8 | 2.617 | 320.0 | .0989 | .00175 | 207.0 | 32619. |
| .85 | 19.3 | 6.710 | 425.0 | .1002 | .00488 | 546.0 | 86041. |
| .85 | 18.1 | 4.995 | 400.0 | .1025 | .00388 | 411.0 | 64767. |
| .85 | 15.7 | 2.537 | 340.0 | .1061 | .00184 | 207.0 | 32619. |

RUN NO. 13

| R/A | E | U | VRMS | TURB | MICRO | Q | RE |
|---|---|---|---|---|---|---|---|
| 0.00 | 23.4 | 9.860 | 170.0 | .0324 | .00168 | 573.0 | 157702. |
| 0.00 | 21.7 | 6.910 | 160.0 | .0338 | .00115 | 399.0 | 109814. |
| 0.00 | 18.9 | 3.720 | 140.0 | .0351 | .00056 | 203.0 | 55870. |
| 0.00 | 7.6 | 0.000 | 0.0 | 0.0000 | 0.00000 | 0.0 | 0. |
| .20 | 22.6 | 9.630 | 200.0 | .0400 | .00247 | 573.0 | 157702. |
| .20 | 20.9 | 6.770 | 185.0 | .0408 | .00168 | 399.0 | 109814. |
| .20 | 18.2 | 3.680 | 160.0 | .0417 | .00082 | 203.0 | 55870. |
| .20 | 7.6 | 0.000 | 0.0 | 0.0000 | 0.00000 | 0.0 | 0. |
| .40 | 22.2 | 9.300 | 245.0 | .0497 | .00281 | 573.0 | 157702. |
| .40 | 20.7 | 6.460 | 230.0 | .0522 | .00195 | 399.0 | 109814. |
| .40 | 17.9 | 3.580 | 210.0 | .0554 | .00099 | 203.0 | 55870. |
| .40 | 7.6 | 0.000 | 0.0 | 0.0000 | 0.00000 | 0.0 | 0. |
| .60 | 22.0 | 8.870 | 300.0 | .0618 | .00514 | 573.0 | 157702. |
| .60 | 20.4 | 6.130 | 295.0 | .0678 | .00381 | 399.0 | 109814. |
| .60 | 17.7 | 3.370 | 250.0 | .0672 | .00197 | 203.0 | 55870. |
| .60 | 7.6 | 0.000 | 0.0 | 0.0000 | 0.00000 | 0.0 | 0. |
| .80 | 21.6 | 8.080 | 395.0 | .0838 | .00548 | 573.0 | 157702. |
| .80 | 19.9 | 5.580 | 370.0 | .0870 | .00422 | 399.0 | 109814. |
| .80 | 17.3 | 3.080 | 325.0 | .0894 | .00224 | 203.0 | 55870. |
| .80 | 7.6 | 0.000 | 0.0 | 0.0000 | 0.00000 | 0.0 | 0. |
| .85 | 21.3 | 7.710 | 410.0 | .0881 | .00545 | 573.0 | 157702. |
| .85 | 19.8 | 5.350 | 410.0 | .0983 | .00419 | 399.0 | 109814. |
| .85 | 17.2 | 3.010 | 345.0 | .0958 | .00234 | 203.0 | 55870. |
| .85 | 7.6 | 0.000 | 0.0 | 0.0000 | 0.00000 | 0.0 | 0. |

RUN NO.14

| R/A | E | U | VRMS | TURB | MICRO | Q | RE |
|---|---|---|---|---|---|---|---|
| 0.00 | 19.4 | 8.752 | 112.0 | .0299 | .00619 | 511.5 | 77573. |
| 0.00 | 18.5 | 6.830 | 100.0 | .0284 | .00492 | 388.8 | 58965. |
| 0.00 | 16.5 | 3.686 | 100.0 | .0335 | .00284 | 205.5 | 31165. |
| .50 | 19.1 | 8.072 | 200.0 | .0545 | .00936 | 511.5 | 77573. |
| .50 | 18.3 | 6.449 | 190.0 | .0549 | .00884 | 388.8 | 58965. |
| .50 | 16.2 | 3.328 | 195.0 | .0671 | .00612 | 205.5 | 31165. |
| .85 | 18.4 | 6.637 | 305.0 | .0874 | .00788 | 511.5 | 77573. |
| .85 | 17.6 | 5.239 | 300.0 | .0915 | .00770 | 388.8 | 58965. |
| .85 | 15.4 | 2.499 | 305.0 | .1136 | .00735 | 205.5 | 31165. |

RUN NO.15

| R/A | E | U | VRMS | TURB | MICRO | Q | RE |
|---|---|---|---|---|---|---|---|
| 0.00 | 23.7 | 9.873 | 170.0 | .0319 | .00775 | 574.0 | 210108. |
| 0.00 | 22.1 | 7.212 | 165.0 | .0338 | .00652 | 402.0 | 147149. |
| 0.00 | 19.2 | 3.760 | 140.0 | .0345 | .00521 | 217.0 | 79431. |
| .40 | 23.4 | 9.327 | 275.0 | .0525 | .00936 | 574.0 | 210108. |
| .40 | 21.8 | 6.778 | 250.0 | .0521 | .00920 | 402.0 | 147149. |
| .40 | 18.9 | 3.489 | 215.0 | .0542 | .00631 | 217.0 | 79431. |
| .80 | 22.5 | 7.821 | 430.0 | .0862 | .00862 | 574.0 | 210108. |
| .80 | 21.0 | 5.712 | 415.0 | .0908 | .00832 | 402.0 | 147149. |
| .80 | 18.2 | 2.911 | 330.0 | .0877 | .00823 | 217.0 | 79431. |
| .85 | 22.3 | 7.512 | 460.0 | .0932 | .00818 | 574.0 | 210108. |
| .85 | 20.8 | 5.466 | 430.0 | .0953 | .00788 | 402.0 | 147149. |
| .85 | 18.0 | 2.759 | 360.0 | .0972 | .00780 | 217.0 | 79431. |

RUN NO.16

| R/A | E | U | VRMS | TURB | MICRO | Q | RE |
|---|---|---|---|---|---|---|---|
| 0.00 | 23.2 | 9.888 | 170.0 | .0328 | .00790 | 574.0 | 163878. |
| 0.00 | 21.6 | 7.156 | 160.0 | .0338 | .00860 | 402.0 | 114772. |
| 0.00 | 18.8 | 3.742 | 140.0 | .0356 | .00550 | 217.0 | 61954. |
| .40 | 22.9 | 9.327 | 260.0 | .0510 | .01015 | 574.0 | 163878. |
| .40 | 21.3 | 6.713 | 250.0 | .0538 | .00949 | 402.0 | 114772. |
| .40 | 18.6 | 3.555 | 210.0 | .0542 | .00935 | 217.0 | 61954. |
| .80 | 22.2 | 8.107 | 430.0 | .0878 | .00951 | 574.0 | 163878. |
| .80 | 20.5 | 5.626 | 400.0 | .0905 | .00883 | 402.0 | 114772. |
| .80 | 17.7 | 2.794 | 325.0 | .0901 | .00845 | 217.0 | 61954. |
| .85 | 21.9 | 7.621 | 445.0 | .0924 | .00883 | 574.0 | 163878. |
| .85 | 20.3 | 5.375 | 420.0 | .0963 | .00836 | 402.0 | 114772. |
| .85 | 17.6 | 2.717 | 370.0 | .1034 | .00768 | 217.0 | 61954. |

RUN NO.17

| R/A | E | U | VRMS | TURB | MICRO | Q | RE |
|---|---|---|---|---|---|---|---|
| -.50 | 24.1 | 21.999 | 210.0 | .0552 | .00398 | 335.8 | 208376. |
| -.50 | 21.0 | 9.062 | 235.0 | .0734 | .00679 | 129.7 | 80483. |
| -.40 | 23.9 | 20.867 | 195.0 | .0517 | .00354 | 335.8 | 208376. |
| -.40 | 20.8 | 7.985 | 225.0 | .0720 | .00700 | 129.7 | 80483. |
| -.20 | 24.2 | 22.583 | 160.0 | .0418 | .00360 | 335.8 | 208376. |
| -.20 | 21.1 | 9.348 | 150.0 | .0465 | .00647 | 129.7 | 80483. |
| 0.00 | 24.3 | 23.180 | 140.0 | .0364 | .00327 | 335.8 | 208376. |
| 0.00 | 21.0 | 9.062 | 130.0 | .0406 | .00551 | 129.7 | 80483. |
| .20 | 24.4 | 23.790 | 160.0 | .0414 | .00380 | 335.8 | 208376. |
| .20 | 20.7 | 8.244 | 150.0 | .0477 | .00530 | 129.7 | 80483. |
| .40 | 24.1 | 21.999 | 195.0 | .0512 | .00373 | 335.8 | 208376. |
| .40 | 20.5 | 7.732 | 200.0 | .0644 | .00617 | 129.7 | 80483. |
| .50 | 24.0 | 21.427 | 205.0 | .0541 | .00387 | 335.8 | 208376. |
| .50 | 20.5 | 7.732 | 225.0 | .0725 | .00634 | 129.7 | 80483. |

RUN NO.19

| R/A | E | U | VRMS | TURB | MICRO | Q | RE |
|---|---|---|---|---|---|---|---|
| .50 | 16.1 | 20.473 | 123.0 | .0387 | .00752 | 322.8 | 71572. |
| .50 | 15.0 | 14.196 | 140.0 | .0493 | .00702 | 220.0 | 48779. |
| .50 | 13.4 | 7.631 | 100.0 | .0429 | .00561 | 117.8 | 26119. |

RUN NO.19

| R/A | E | U | VRMS | TURB | MICRO | Q | RE |
|---|---|---|---|---|---|---|---|
| .50 | 17.3 | 21.191 | 185.0 | .0739 | .00575 | 322.8 | 71572. |
| .50 | 16.3 | 13.958 | 170.0 | .0741 | .00700 | 220.0 | 48779. |
| .50 | 14.9 | 7.259 | 95.0 | .0476 | .00482 | 117.8 | 26119. |

RUN NO. 20

| R/A | E | U | VRMS | TURB | MICRO | Q | RE |
|---|---|---|---|---|---|---|---|
| -.45 | 26.0 | 21.700 | 305.0 | .0512 | .00705 | 335.4 | 245541. |
| -.45 | 23.8 | 14.900 | 270.0 | .0500 | .00758 | 230.0 | 168379. |
| -.45 | 20.5 | 7.600 | 240.0 | .0536 | .00687 | 117.7 | 86166. |
| -.45 | 7.4 | 0.000 | 0.0 | 0.0000 | 0.00000 | 0.0 | 0. |
| -.25 | 26.1 | 22.800 | 240.0 | .0399 | .00690 | 335.4 | 245541. |
| -.25 | 24.0 | 15.600 | 230.0 | .0425 | .00706 | 230.0 | 168379. |
| -.25 | 20.6 | 7.970 | 195.0 | .0433 | .00648 | 117.7 | 86166. |
| -.25 | 7.4 | 0.000 | 0.0 | 0.0000 | 0.00000 | 0.0 | 0. |
| -.05 | 25.6 | 23.400 | 185.0 | .0314 | .00642 | 335.4 | 245541. |
| -.05 | 23.7 | 16.100 | 180.0 | .0341 | .00628 | 230.0 | 168379. |
| -.05 | 20.3 | 8.200 | 143.0 | .0325 | .00591 | 117.7 | 86166. |
| -.05 | 7.4 | 0.000 | 0.0 | 0.0000 | 0.00000 | 0.0 | 0. |
| .05 | 25.5 | 23.400 | 187.0 | .0319 | .00642 | 335.4 | 245541. |
| .05 | 23.5 | 16.100 | 165.0 | .0313 | .00628 | 230.0 | 168379. |
| .05 | 20.1 | 8.200 | 140.0 | .0318 | .00591 | 117.7 | 86166. |
| .05 | 7.4 | 0.000 | 0.0 | 0.0000 | 0.00000 | 0.0 | 0. |
| .15 | 25.6 | 23.200 | 210.0 | .0356 | .00689 | 335.4 | 245541. |
| .15 | 23.7 | 15.900 | 185.0 | .0351 | .00665 | 230.0 | 168379. |
| .15 | 20.3 | 8.120 | 160.0 | .0363 | .00602 | 117.7 | 86166. |
| .15 | 7.4 | 0.000 | 0.0 | 0.0000 | 0.00000 | 0.0 | 0. |
| .35 | 25.3 | 22.600 | 265.0 | .0459 | .00735 | 335.4 | 245541. |
| .35 | 23.2 | 15.500 | 240.0 | .0460 | .00767 | 230.0 | 168379. |
| .35 | 19.9 | 7.920 | 202.0 | .0465 | .00632 | 117.7 | 86166. |
| .35 | 7.4 | 0.000 | 0.0 | 0.0000 | 0.00000 | 0.0 | 0. |

RUN NO. 20

| R/A | E | U | VRMS | TURB | MICRO | Q | RE |
|---|---|---|---|---|---|---|---|
| .55 | 25.0 | 21.300 | 300.0 | .0529 | .01084 | 335.4 | 245541. |
| .55 | 22.8 | 14.600 | 255.0 | .0495 | .01362 | 230.0 | 168379. |
| .55 | 19.6 | 7.480 | 0.0 | 0.0000 | 0.00000 | 117.7 | 86166. |
| .55 | 7.4 | 0.000 | 0.0 | 0.0000 | 0.00000 | 0.0 | 0. |
| .75 | 25.1 | 19.500 | 430.0 | .0750 | .00706 | 335.4 | 245541. |
| .75 | 23.1 | 13.400 | 395.0 | .0765 | .00739 | 230.0 | 168379. |
| .75 | 19.8 | 6.830 | 340.0 | .0790 | .00714 | 117.7 | 86166. |
| .75 | 7.4 | 0.000 | 0.0 | 0.0000 | 0.00000 | 0.0 | 0. |

RUN NO.21

| R/A | E | U | VRMS | TURB | MICRO | Q | RE |
|---|---|---|---|---|---|---|---|
| -.45 | 22.3 | 21.476 | 190.0 | .0477 | .00668 | 325.2 | 98639. |
| -.45 | 21.0 | 15.298 | 197.0 | .0533 | .00811 | 223.8 | 67882. |
| -.45 | 18.7 | 7.813 | 170.0 | .0536 | .00607 | 119.2 | 36155. |
| -.25 | 22.4 | 22.021 | 150.0 | .0374 | .00672 | 325.2 | 98639. |
| -.25 | 21.1 | 15.718 | 140.0 | .0377 | .00722 | 223.8 | 67882. |
| -.25 | 18.8 | 8.062 | 132.0 | .0413 | .00575 | 119.2 | 36155. |
| -.05 | 22.4 | 22.021 | 113.0 | .0282 | .00566 | 325.2 | 98639. |
| -.05 | 21.1 | 15.718 | 116.0 | .0312 | .00578 | 223.8 | 67882. |
| -.05 | 18.9 | 8.318 | 106.0 | .0329 | .00511 | 119.2 | 36155. |
| .05 | 22.3 | 21.476 | 112.0 | .0281 | .00558 | 325.2 | 98639. |
| .05 | 21.1 | 15.718 | 117.0 | .0315 | .00578 | 223.8 | 67882. |
| .05 | 18.9 | 8.318 | 115.0 | .0357 | .00529 | 119.2 | 36155. |
| .25 | 22.3 | 21.476 | 138.0 | .0346 | .00595 | 325.2 | 98639. |
| .25 | 21.0 | 15.298 | 145.0 | .0393 | .00714 | 223.8 | 67882. |
| .25 | 18.9 | 8.318 | 140.0 | .0435 | .00600 | 119.2 | 36155. |
| .45 | 22.3 | 21.476 | 182.0 | .0457 | .00656 | 325.2 | 98639. |
| .45 | 21.0 | 15.298 | 190.0 | .0514 | .00757 | 223.8 | 67882. |
| .45 | 18.8 | 8.062 | 175.0 | .0548 | .00621 | 119.2 | 36155. |
| .65 | 21.9 | 19.400 | 240.0 | .0616 | .00614 | 325.2 | 98639. |
| .65 | 20.7 | 14.093 | 240.0 | .0662 | .00747 | 223.8 | 67882. |
| .65 | 18.6 | 7.569 | 230.0 | .0731 | .00615 | 119.2 | 36155. |

RUN NO.21

| R/A | E | U | VRMS | TURB | MICRO | Q | RE |
|---|---|---|---|---|---|---|---|
| .75 | 21.5 | 17.484 | 255.0 | .0670 | .00633 | 325.2 | 98639. |
| .75 | 20.1 | 11.904 | 255.0 | .0731 | .00656 | 223.8 | 67882. |
| .75 | 18.0 | 6.227 | 220.0 | .0732 | .00493 | 119.2 | 36155. |

RUN NO.22

| R/A | E | U | VRMS | TURB | MICRO | Q | RE |
|---|---|---|---|---|---|---|---|
| -.40 | 23.7 | 22.081 | 260.0 | .0475 | .00662 | 300.0 | 127917. |
| -.40 | 21.2 | 13.561 | 230.0 | .0479 | .00700 | 200.0 | 85278. |
| -.40 | 19.2 | 8.707 | 210.0 | .0494 | .00689 | 119.0 | 50740. |
| -.10 | 24.3 | 24.600 | 170.0 | .0301 | .00577 | 300.0 | 127917. |
| -.10 | 21.9 | 15.648 | 152.0 | .0304 | .00531 | 200.0 | 85278. |
| -.10 | 19.6 | 9.556 | 140.0 | .0321 | .00588 | 119.0 | 50740. |
| .10 | 24.1 | 23.739 | 170.0 | .0304 | .00577 | 300.0 | 127917. |
| .10 | 22.0 | 15.964 | 155.0 | .0309 | .00564 | 200.0 | 85278. |
| .10 | 19.6 | 9.556 | 140.0 | .0321 | .00608 | 119.0 | 50740. |
| .30 | 23.7 | 22.081 | 220.0 | .0401 | .00593 | 300.0 | 127917. |
| .30 | 21.6 | 14.727 | 200.0 | .0407 | .00574 | 200.0 | 85278. |
| .30 | 19.3 | 8.914 | 180.0 | .0421 | .00624 | 119.0 | 50740. |
| .50 | 23.4 | 20.895 | 280.0 | .0519 | .00638 | 300.0 | 127917. |
| .50 | 21.1 | 13.280 | 255.0 | .0534 | .00657 | 200.0 | 85278. |
| .50 | 19.1 | 8.504 | 230.0 | .0545 | .00679 | 119.0 | 50740. |
| .75 | 23.1 | 19.756 | 380.0 | .0715 | .00642 | 300.0 | 127917. |
| .75 | 20.7 | 12.200 | 350.0 | .0751 | .00647 | 200.0 | 85278. |
| .75 | 18.6 | 7.537 | 305.0 | .0748 | .00650 | 119.0 | 50740. |

RUN NO.23

| R/A | E | U | VRMS | TUR3 | MICRO | Q | RE |
|---|---|---|---|---|---|---|---|
| 0.00 | 16.4 | 37.034 | 125.0 | .0543 | .00848 | 464.0 | 50282. |
| .40 | 16.1 | 32.443 | 220.0 | .0984 | .00715 | 464.0 | 50282. |
| .60 | 16.0 | 31.016 | 240.0 | .1084 | .00658 | 464.0 | 50282. |
| 0.00 | 15.4 | 23.462 | 56.0 | .0268 | .00577 | 289.0 | 26540. |
| .40 | 15.2 | 21.296 | 83.0 | .0406 | .00722 | 289.0 | 26540. |
| .60 | 15.1 | 20.273 | 105.0 | .0519 | .00791 | 289.0 | 26540. |
| 0.00 | 14.0 | 11.359 | 67.0 | .0376 | .00385 | 147.2 | 10634. |
| .40 | 13.9 | 10.735 | 108.0 | .0614 | .00721 | 147.2 | 10634. |
| .60 | 13.7 | 9.566 | 135.0 | .0788 | .00778 | 147.2 | 10634. |

Table 6

Energy Spectrum Results and Transformations to Autocorrelations

The table contains a separate computer printout for each spectrum measurement. The information is identified by the following symbols:

R/A - corresponds to r/a in the text, radial position divided by pipe radius.

U - corresponds to $\bar{u}$ in the text, time average velocity in feet per second.

FREQ - frequency in cycles per second.

F(N) x 10000 - normalized spectrum function in seconds times 10,000.

F(N) x 10000 x N**2 - dissipation spectrum function in reciprocal seconds times 10,000 where N is frequency.

E(N) x 10000- spectrum function in square feet per second times 10,000.

DELAY - autocorrelation delay time in seconds.

RU - autocorrelation coefficient corresponding to R(τ) in the text.

MACROSCALE and MICROSCALE are in feet.

RUN NO. 8 AT R/A=0.00, U= 7.09

| FREQ | F(N)X10000 | F(N)X10000XN**2 | E(N)X10000 |
|---|---|---|---|
| 10.00 | 65.72523 | 6572.5 | 4.30565 |
| 12.60 | 120.84590 | 19185.4 | 7.91660 |
| 15.90 | 131.61153 | 33272.7 | 8.62185 |
| 20.00 | 127.66498 | 51065.9 | 8.36331 |
| 25.10 | 149.83247 | 94395.9 | 9.81550 |
| 31.60 | 97.68966 | 97548.9 | 6.39963 |
| 39.80 | 84.03313 | 133111.8 | 5.50500 |
| 50.10 | 71.62707 | 179784.6 | 4.69228 |
| 63.10 | 65.28631 | 259944.6 | 4.27689 |
| 79.40 | 35.39501 | 223142.9 | 2.31872 |
| 100.00 | 30.53277 | 305327.7 | 2.00019 |
| 126.00 | 22.47183 | 356762.8 | 1.47212 |
| 159.00 | 12.85914 | 325092.0 | .84240 |
| 200.00 | 12.64286 | 505714.5 | .82823 |
| 251.00 | 6.00839 | 378534.9 | .39360 |
| 316.00 | 4.10567 | 409976.7 | .26896 |
| 398.00 | 2.24188 | 355124.2 | .14686 |
| 501.00 | 1.13044 | 283741.6 | .07405 |
| 631.00 | .55580 | 221298.9 | .03641 |
| 794.00 | .24639 | 155337.1 | .01614 |
| 1000.00 | .10004 | 100046.6 | .00655 |
| 1260.00 | .02517 | 39972.8 | .00164 |
| 1590.00 | .00699 | 17672.1 | .00045 |
| 2000.00 | .00102 | 4095.0 | .00006 |
| 2510.00 | .00010 | 679.3 | 0.00000 |

| DELAY | RU |
|---|---|
| .00001 | 1.00000 |
| .00010 | .97896 |
| .00020 | .96038 |
| .00030 | .93274 |
| .00040 | .90002 |
| .00050 | .86493 |
| .00060 | .82806 |
| .00100 | .68563 |
| .00150 | .54545 |
| .00200 | .40188 |
| .00250 | .30066 |
| .00300 | .22950 |
| .00350 | .18909 |
| .00400 | .16375 |
| .00450 | .14812 |
| .00500 | .12753 |
| .00600 | .05360 |
| .00700 | -.01918 |
| .01000 | -.11843 |
| .01300 | -.12768 |
| .01600 | -.11142 |
| .01900 | -.11182 |
| .02200 | -.11431 |
| .02500 | -.09678 |
| .02800 | -.06918 |

MACROSCALE = .0151
MICROSCALE = .0098(CURVE FIT)
MICROSCALE = .0093(INTEGRAL)

RUN NO. 8 AT R/A= .50, U= 6.18

| FREQ | F(N)X10000 | F(N)X10000XN**2 | E(N)X10000 |
|---|---|---|---|
| 10.00 | 82.33810 | 8233.8 | 12.32328 |
| 12.60 | 128.43926 | 20391.0 | 19.22309 |
| 15.90 | 172.38191 | 43579.8 | 25.79985 |
| 20.00 | 172.06987 | 68827.9 | 25.75315 |
| 25.10 | 125.77265 | 79238.0 | 18.82399 |
| 31.60 | 117.20701 | 117038.2 | 17.54200 |
| 39.80 | 99.71046 | 157945.3 | 14.92335 |
| 50.10 | 69.83817 | 175294.5 | 10.45245 |
| 63.10 | 60.49494 | 240867.2 | 9.05408 |
| 79.40 | 39.29881 | 247753.8 | 5.88172 |
| 100.00 | 27.97724 | 279772.4 | 4.18726 |
| 126.00 | 18.53205 | 294214.9 | 2.77363 |
| 159.00 | 10.50630 | 265609.8 | 1.57244 |
| 200.00 | 10.17171 | 406868.6 | 1.52236 |
| 251.00 | 5.68522 | 358174.9 | .85088 |
| 316.00 | 3.22158 | 321694.4 | .48216 |
| 398.00 | 1.79887 | 284949.5 | .26923 |
| 501.00 | 1.06987 | 268540.8 | .16012 |
| 631.00 | .41589 | 165591.9 | .06224 |
| 794.00 | .18491 | 116577.1 | .02767 |
| 1000.00 | .07287 | 72870.3 | .01090 |
| 1260.00 | .02250 | 35723.3 | .00336 |
| 1590.00 | .00535 | 13540.3 | .00080 |
| 2000.00 | .00099 | 3997.2 | .00014 |
| 2510.00 | .00009 | 583.5 | .00001 |

| DELAY | RU |
|---|---|
| .00001 | 1.00000 |
| .00010 | .96429 |
| .00020 | .94937 |
| .00030 | .92731 |
| .00040 | .90097 |
| .00050 | .87235 |
| .00060 | .84203 |
| .00100 | .72293 |
| .00150 | .59835 |
| .00200 | .46277 |
| .00250 | .35709 |
| .00300 | .27807 |
| .00350 | .23138 |
| .00400 | .20432 |
| .00450 | .18817 |
| .00500 | .16587 |
| .00600 | .08275 |
| .00700 | .00112 |
| .01000 | -.11840 |
| .01300 | -.13983 |
| .01600 | -.12785 |
| .01900 | -.12970 |
| .02200 | -.13393 |
| .02500 | -.11703 |
| .02800 | -.08665 |

MACROSCALE = .0148
MICROSCALE = .0091(CURVE FIT)
MICROSCALE = .0089(INTEGRAL)

RUN NO. 8 AT R/A= .85, U= 5.25

| FREQ | F(N)X10000 | F(N)X10000XN**2 | E(N)X10000 |
|---|---|---|---|
| 10.00 | 116.57094 | 11657.0 | 32.12986 |
| 12.60 | 124.61486 | 19783.8 | 34.34697 |
| 15.90 | 161.11201 | 40730.7 | 44.40649 |
| 20.00 | 142.24489 | 56897.9 | 39.20624 |
| 25.10 | 129.72352 | 81727.1 | 35.75504 |
| 31.60 | 86.39213 | 86267.7 | 23.81183 |
| 39.80 | 87.23848 | 138189.2 | 24.04510 |
| 50.10 | 69.72652 | 175014.2 | 19.21837 |
| 63.10 | 60.15182 | 239501.1 | 16.57934 |
| 79.40 | 41.49491 | 261598.8 | 11.43703 |
| 100.00 | 31.67789 | 316778.9 | 8.73122 |
| 126.00 | 20.70451 | 328704.9 | 5.70668 |
| 159.00 | 12.56139 | 317564.6 | 3.46223 |
| 200.00 | 11.24771 | 449908.4 | 3.10015 |
| 251.00 | 6.00442 | 378284.5 | 1.65496 |
| 316.00 | 4.00284 | 399707.7 | 1.10328 |
| 398.00 | 1.99490 | 316000.6 | .54984 |
| 501.00 | 1.02912 | 258311.9 | .28365 |
| 631.00 | .53525 | 213117.4 | .14752 |
| 794.00 | .21873 | 137896.9 | .06028 |
| 1000.00 | .08767 | 87676.7 | .02416 |
| 1260.00 | .02596 | 41219.5 | .00715 |
| 1590.00 | .00720 | 18223.3 | .00198 |
| 2000.00 | .00125 | 5008.8 | .00034 |
| 2510.00 | .00017 | 1120.4 | .00004 |

| DELAY | RU |
|---|---|
| .00001 | 1.00000 |
| .00005 | .99693 |
| .00010 | .99235 |
| .00015 | .98502 |
| .00020 | .97514 |
| .00025 | .96321 |
| .00030 | .94964 |
| .00040 | .91931 |
| .00060 | .85197 |
| .00100 | .71572 |
| .00150 | .57383 |
| .00200 | .42570 |
| .00250 | .31570 |
| .00300 | .23687 |
| .00400 | .16918 |
| .00500 | .14284 |
| .00600 | .07025 |
| .00800 | -.02604 |
| .01000 | -.09961 |
| .01200 | -.10071 |
| .01400 | -.10721 |
| .01600 | -.10580 |
| .01800 | -.10405 |
| .02000 | -.12478 |
| .02200 | -.12628 |

MACROSCALE = .0117
MICROSCALE = .0069(CURVE FIT)
MICROSCALE = .0071(INTEGRAL)

RUN NO. 9 AT R/A=0.00, U= 6.90

| FREQ | F(N)X10000 | F(N)X10000XN**2 | E(N)X10000 |
|---|---|---|---|
| 10.00 | 58.90469 | 5890.4 | 5.33115 |
| 12.60 | 77.73997 | 12341.9 | 7.03583 |
| 15.90 | 139.95722 | 35382.5 | 12.66678 |
| 20.00 | 154.21123 | 61684.4 | 13.95684 |
| 25.10 | 152.39178 | 96008.3 | 13.79217 |
| 31.60 | 107.96583 | 107810.3 | 9.77141 |
| 39.80 | 98.61619 | 156211.9 | 8.92522 |
| 50.10 | 78.59081 | 197263.7 | 7.11283 |
| 63.10 | 69.82695 | 278023.6 | 6.31966 |
| 79.40 | 48.00549 | 302643.9 | 4.34472 |
| 100.00 | 36.77313 | 367731.3 | 3.32814 |
| 126.00 | 20.06943 | 318622.3 | 1.81637 |
| 159.00 | 12.95392 | 327488.2 | 1.17239 |
| 200.00 | 9.29458 | 371783.5 | .84120 |
| 251.00 | 4.18523 | 263674.2 | .37878 |
| 316.00 | 2.74298 | 273903.7 | .24825 |
| 398.00 | 1.11956 | 177344.1 | .10132 |
| 501.00 | .35526 | 89170.6 | .03215 |
| 631.00 | .10021 | 39900.5 | .00906 |
| 794.00 | .02342 | 14764.8 | .00211 |
| 1000.00 | .00516 | 5163.9 | .00046 |
| 1260.00 | .00052 | 833.1 | .00004 |
| 1590.00 | .00004 | 109.0 | 0.00000 |

| DELAY | RU |
|---|---|
| .00001 | 1.00000 |
| .00010 | 1.00022 |
| .00020 | .99150 |
| .00030 | .97732 |
| .00040 | .95843 |
| .00050 | .93573 |
| .00060 | .91016 |
| .00100 | .79168 |
| .00150 | .63728 |
| .00200 | .49903 |
| .00250 | .36392 |
| .00300 | .23598 |
| .00350 | .13915 |
| .00400 | .07973 |
| .00450 | .04786 |
| .00500 | .03889 |
| .00600 | .04609 |
| .00700 | .00842 |
| .01000 | -.10021 |
| .01300 | -.15732 |
| .01600 | -.14116 |
| .01900 | -.10873 |
| .02200 | -.10277 |

MACROSCALE = .0151

MICROSCALE = .0134(CURVE FIT)

MICROSCALE = .0133(INTEGRAL)

RUN NO. 9 AT R/A= .50, U= 6.56

| FREQ | F(N)X10000 | F(N)X10000XN**2 | E(N)X10000 |
|---|---|---|---|
| 10.00 | 116.78969 | 11678.9 | 32.08527 |
| 12.60 | 139.80425 | 22195.3 | 38.40799 |
| 15.90 | 235.43534 | 59520.4 | 64.68042 |
| 20.00 | 164.58533 | 65834.1 | 45.21602 |
| 25.10 | 149.19674 | 93995.4 | 40.98836 |
| 31.60 | 109.54938 | 109391.6 | 30.09616 |
| 39.80 | 103.89236 | 164569.6 | 28.54202 |
| 50.10 | 81.68810 | 205037.9 | 22.44192 |
| 63.10 | 65.22222 | 259689.4 | 17.91830 |
| 79.40 | 34.64870 | 218437.9 | 9.51893 |
| 100.00 | 26.62234 | 266223.4 | 7.31387 |
| 126.00 | 17.40023 | 276246.0 | 4.78031 |
| 159.00 | 10.55669 | 266883.7 | 2.90020 |
| 200.00 | 8.76945 | 350778.0 | 2.40920 |
| 251.00 | 4.16880 | 262638.8 | 1.14528 |
| 316.00 | 2.01023 | 200734.3 | .55226 |
| 398.00 | .99283 | 157268.5 | .27275 |
| 501.00 | .37915 | 95169.3 | .10416 |
| 631.00 | .10386 | 41356.9 | .02853 |
| 794.00 | .02884 | 18185.7 | .00792 |
| 1000.00 | .00514 | 5149.8 | .00141 |
| 1260.00 | .00089 | 1424.3 | .00024 |
| 1590.00 | .00007 | 186.4 | .00002 |
| 2000.00 | 0.00000 | 17.6 | 0.00000 |

| DELAY | RU |
|---|---|
| .00001 | 1.00000 |
| .00005 | 1.00314 |
| .00010 | 1.00169 |
| .00015 | .99819 |
| .00020 | .99339 |
| .00025 | .98735 |
| .00030 | .98018 |
| .00040 | .96274 |
| .00060 | .91857 |
| .00100 | .81107 |
| .00150 | .68084 |
| .00200 | .56819 |
| .00250 | .47669 |
| .00300 | .41209 |
| .00400 | .29113 |
| .00500 | .16596 |
| .00600 | .08622 |
| .00800 | -.02053 |
| .01000 | -.09016 |
| .01200 | -.13114 |
| .01400 | -.13548 |
| .01600 | -.13245 |
| .01800 | -.14163 |
| .02000 | -.15159 |

MACROSCALE = .0183
MICROSCALE = .0132(CURVE FIT)
MICROSCALE = .0134(INTEGRAL)

RUN NO. 9 AT R/A= .85, U= 5.64

| FREQ | F(N)X10000 | F(N)X10000XN**2 | E(N)X10000 |
|---|---|---|---|
| 10.00 | 204.35211 | 20435.2 | 148.80419 |
| 12.60 | 215.60705 | 34229.7 | 156.99977 |
| 15.90 | 236.66272 | 59830.7 | 172.33199 |
| 20.00 | 195.12206 | 78048.8 | 142.08310 |
| 25.10 | 165.44198 | 104230.1 | 120.47079 |
| 31.60 | 102.95876 | 102810.4 | 74.97204 |
| 39.80 | 86.77272 | 137451.4 | 63.18577 |
| 50.10 | 67.67455 | 169863.8 | 49.27895 |
| 63.10 | 55.79406 | 222150.1 | 40.62786 |
| 79.40 | 34.82933 | 219576.6 | 25.36186 |
| 100.00 | 27.11050 | 271105.0 | 19.74120 |
| 126.00 | 16.99906 | 269877.1 | 12.37830 |
| 159.00 | 9.05683 | 228965.7 | 6.59496 |
| 200.00 | 8.06290 | 322516.2 | 5.87121 |
| 251.00 | 3.77583 | 237881.3 | 2.74946 |
| 316.00 | 1.79856 | 179597.5 | 1.30967 |
| 398.00 | .78293 | 124020.1 | .57011 |
| 501.00 | .28865 | 72452.4 | .21019 |
| 631.00 | .08603 | 34257.6 | .06265 |
| 794.00 | .02218 | 13984.8 | .01615 |
| 1000.00 | .00517 | 5172.5 | .00376 |
| 1260.00 | .00073 | 1166.5 | .00053 |
| 1590.00 | .00007 | 185.4 | .00005 |
| 2000.00 | 0.00000 | 13.0 | 0.00000 |

| DELAY | RU |
|---|---|
| .00001 | 1.00000 |
| .00010 | 1.00189 |
| .00020 | .99487 |
| .00030 | .98366 |
| .00040 | .96871 |
| .00050 | .95075 |
| .00060 | .93039 |
| .00100 | .83307 |
| .00150 | .70243 |
| .00200 | .57325 |
| .00250 | .45747 |
| .00300 | .37553 |
| .00350 | .32608 |
| .00400 | .29972 |
| .00450 | .28403 |
| .00500 | .26006 |
| .00600 | .17091 |
| .00700 | .08384 |
| .01000 | -.06004 |
| .01300 | -.11202 |
| .01600 | -.12975 |
| .01900 | -.15849 |
| .02200 | -.18616 |
| .02500 | -.18726 |

MACROSCALE = .0172
MICROSCALE = .0124(CURVE FIT)
MICROSCALE = .0122(INTEGRAL)

RUN NO. 9 AT R/A= .85, U= 2.47

| FREQ | F(N)X10000 | F(N)X10000XN**2 | E(N)X10000 |
|---|---|---|---|
| 10.00 | 400.57208 | 40057.2 | 137.38448 |
| 12.60 | 685.19136 | 108780.9 | 235.00055 |
| 15.90 | 502.36885 | 127003.8 | 172.29779 |
| 20.00 | 290.69429 | 116277.7 | 99.69962 |
| 25.10 | 202.83618 | 127788.8 | 69.56686 |
| 31.60 | 94.32283 | 94187.0 | 32.34996 |
| 39.80 | 72.41242 | 114704.1 | 24.83534 |
| 50.10 | 39.41597 | 98934.4 | 13.51852 |
| 63.10 | 25.71582 | 102390.3 | 8.81977 |
| 79.40 | 11.79938 | 74387.5 | 4.04684 |
| 100.00 | 5.11159 | 51115.9 | 1.75312 |
| 126.00 | 1.83076 | 29065.2 | .62789 |
| 159.00 | .60305 | 15245.7 | .20682 |
| 200.00 | .16712 | 6684.9 | .05731 |
| 251.00 | .03125 | 1968.7 | .01071 |
| 316.00 | .00494 | 493.6 | .00169 |
| 398.00 | .00109 | 172.6 | .00037 |
| 501.00 | .00001 | 4.2 | 0.00000 |

| DELAY | RU |
|---|---|
| .00001 | 1.00000 |
| .00040 | .99695 |
| .00080 | .98796 |
| .00120 | .97343 |
| .00200 | .93030 |
| .00250 | .89596 |
| .00300 | .85768 |
| .00350 | .81672 |
| .00400 | .77416 |
| .00500 | .68737 |
| .00600 | .60183 |
| .00700 | .52004 |
| .01000 | .30402 |
| .01300 | .12510 |
| .01600 | -.02710 |
| .01900 | -.15457 |
| .02200 | -.25854 |
| .02500 | -.32766 |

MACROSCALE = .0184
MICROSCALE = .0200(CURVE FIT)
MICROSCALE = .0165(INTEGRAL)

RUN NO. 10 AT R/A=0.00, U= 6.74

| FREQ | F(N)X10000 | F(N)X10000XN**2 | E(N)X10000 |
|---|---|---|---|
| 10.00 | 192.85883 | 19285.8 | 11.80025 |
| 12.60 | 198.34345 | 31489.0 | 12.13583 |
| 15.90 | 249.45677 | 63065.1 | 15.26325 |
| 20.00 | 176.48954 | 70595.8 | 10.79868 |
| 25.10 | 152.70014 | 96202.6 | 9.34310 |
| 31.60 | 93.01904 | 92885.0 | 5.69146 |
| 39.80 | 86.44128 | 136926.4 | 5.28899 |
| 50.10 | 64.67586 | 162337.0 | 3.95725 |
| 63.10 | 54.01849 | 215080.5 | 3.30517 |
| 79.40 | 33.50750 | 211243.3 | 2.05018 |
| 100.00 | 25.90922 | 259092.2 | 1.58528 |
| 126.00 | 16.53144 | 262453.1 | 1.01149 |
| 159.00 | 9.31428 | 235474.4 | .56990 |
| 200.00 | 8.73686 | 349474.4 | .53457 |
| 251.00 | 4.19523 | 264303.7 | .25668 |
| 316.00 | 2.78483 | 278082.8 | .17039 |
| 398.00 | 1.62863 | 257982.8 | .09964 |
| 501.00 | .88554 | 222271.4 | .05418 |
| 631.00 | .42854 | 170628.8 | .02622 |
| 794.00 | .20241 | 127609.3 | .01238 |
| 1000.00 | .06759 | 67595.7 | .00413 |
| 1260.00 | .02043 | 32435.1 | .00125 |
| 1590.00 | .00556 | 14067.9 | .00034 |
| 2000.00 | .00109 | 4383.0 | .00006 |
| 2510.00 | .00031 | 1953.1 | .00001 |
| 3160.00 | .00003 | 358.0 | 0.00000 |

| DELAY | RU |
|---|---|
| .00001 | 1.00000 |
| .00005 | .99280 |
| .00010 | .99040 |
| .00015 | .98649 |
| .00020 | .98122 |
| .00025 | .97439 |
| .00030 | .96608 |
| .00040 | .94437 |
| .00060 | .87521 |
| .00100 | .65891 |
| .00150 | .49490 |
| .00200 | .53975 |
| .00250 | .44988 |
| .00300 | .40251 |
| .00400 | .29652 |
| .00500 | .21687 |
| .00600 | .14106 |
| .00800 | -.00037 |
| .01000 | -.03882 |
| .01200 | -.05809 |
| .01400 | -.08992 |
| .01600 | -.12216 |
| .01800 | -.16514 |
| .02000 | -.17246 |
| .02200 | -.17404 |
| .03100 | -.11886 |

MACROSCALE = .0179

MICROSCALE = .0106(CURVE FIT)

MICROSCALE = .0102(INTEGRAL)

RUN NO. 10 AT R/A= .85, U= 5.23

| FREQ | F(N)X10000 | F(N)X10000XN**2 | E(N)X10000 |
|---|---|---|---|
| 10.00 | 181.96004 | 18196.0 | 42.49358 |
| 12.60 | 200.98446 | 31908.2 | 46.93640 |
| 15.90 | 263.64932 | 66653.1 | 61.57068 |
| 20.00 | 157.65823 | 63063.2 | 36.81831 |
| 25.10 | 161.38784 | 101675.9 | 37.68930 |
| 31.60 | 98.31125 | 98169.6 | 22.95887 |
| 39.80 | 87.04029 | 137875.3 | 20.32673 |
| 50.10 | 65.12404 | 163461.9 | 15.20857 |
| 63.10 | 51.99698 | 207031.6 | 12.14298 |
| 79.40 | 30.62330 | 193060.3 | 7.15153 |
| 100.00 | 26.08876 | 260887.6 | 6.09257 |
| 126.00 | 15.42074 | 244819.7 | 3.60124 |
| 159.00 | 9.84421 | 248871.4 | 2.29894 |
| 200.00 | 8.07365 | 322946.2 | 1.88546 |
| 251.00 | 4.43391 | 279340.9 | 1.03546 |
| 316.00 | 2.94327 | 293904.0 | .68735 |
| 398.00 | 1.87221 | 296566.9 | .43722 |
| 501.00 | .98776 | 247929.7 | .23067 |
| 631.00 | .47185 | 187875.9 | .11019 |
| 794.00 | .23549 | 148461.6 | .05499 |
| 1000.00 | .06569 | 65690.2 | .01534 |
| 1260.00 | .01989 | 31592.9 | .00464 |
| 1590.00 | .00634 | 16033.9 | .00148 |
| 2000.00 | .00111 | 4442.7 | .00025 |
| 2510.00 | .00022 | 1447.9 | .00005 |
| 3160.00 | .00002 | 281.2 | 0.00000 |

| DELAY | RU |
|---|---|
| .00001 | 1.00000 |
| .00010 | 1.02427 |
| .00020 | 1.01382 |
| .00030 | .99661 |
| .00040 | .97240 |
| .00050 | .93988 |
| .00060 | .89839 |
| .00100 | .67863 |
| .00150 | .51537 |
| .00200 | .55961 |
| .00250 | .46798 |
| .00300 | .42073 |
| .00350 | .40642 |
| .00400 | .31274 |
| .00450 | .28944 |
| .00500 | .23060 |
| .00600 | .15192 |
| .00700 | .06993 |
| .01000 | -.04082 |
| .01300 | -.08184 |
| .01600 | -.12894 |
| .01900 | -.18142 |
| .02200 | -.18358 |
| .02500 | -.17087 |
| .02800 | -.16132 |
| .03100 | -.12390 |

MACROSCALE = .0152
MICROSCALE = .0105(CURVE FIT)
MICROSCALE = .0077(INTEGRAL)

RUN NO. 10 AT R/A= .85, U= 2.48

| FREQ | F(N)X10000 | F(N)X10000XN**2 | E(N)X10000 |
|---|---|---|---|
| 10.00 | 198.16807 | 19816.8 | 12.70540 |
| 12.00 | 291.40051 | 41961.6 | 18.68293 |
| 15.90 | 297.72932 | 75268.9 | 19.08870 |
| 20.00 | 182.39575 | 72958.3 | 11.69417 |
| 25.10 | 168.22319 | 105982.2 | 10.78551 |
| 31.60 | 107.78310 | 107627.8 | 6.91043 |
| 39.80 | 93.97873 | 148866.0 | 6.02537 |
| 50.10 | 70.31542 | 176492.4 | 4.50822 |
| 63.10 | 52.24253 | 208009.4 | 3.34949 |
| 79.40 | 34.74684 | 219056.6 | 2.22776 |
| 100.00 | 23.13816 | 231381.6 | 1.48348 |
| 126.00 | 14.35153 | 227845.0 | .92013 |
| 159.00 | 7.37645 | 186484.0 | .47293 |
| 200.00 | 6.33760 | 253504.3 | .40633 |
| 251.00 | 2.42568 | 152820.5 | .15552 |
| 316.00 | 1.20765 | 120591.2 | .07742 |
| 398.00 | .48057 | 76125.0 | .03081 |
| 501.00 | .19904 | 49960.2 | .01276 |
| 631.00 | .06659 | 26515.3 | .00426 |
| 794.00 | .01735 | 10942.1 | .00111 |
| 1000.00 | .00447 | 4474.1 | .00028 |
| 1590.00 | .00006 | 168.7 | 0.00000 |

| DELAY | RU |
|---|---|
| .00001 | 1.00000 |
| .00010 | .97262 |
| .00020 | .96671 |
| .00030 | .95766 |
| .00040 | .94565 |
| .00050 | .93137 |
| .00060 | .91568 |
| .00100 | .84442 |
| .00150 | .73829 |
| .00200 | .63774 |
| .00250 | .54743 |
| .00300 | .46273 |
| .00350 | .38426 |
| .00400 | .31846 |
| .00450 | .26834 |
| .00500 | .23000 |
| .00600 | .17257 |
| .00700 | .13536 |
| .01000 | -.01404 |
| .01300 | -.09525 |
| .01600 | -.15696 |
| .01900 | -.16319 |

MACROSCALE = .0079
MICROSCALE = .0052(CURVE FIT)
MICROSCALE = .0061(INTEGRAL)

RUN NO. 12 AT R/A=0.00, U= 7.01

| FREQ | F(N)X10000 | F(N)X10000XN**2 | E(N)X10000 |
|---|---|---|---|
| 10.00 | 120.70976 | 12070.9 | 6.73656 |
| 12.60 | 143.21526 | 22736.8 | 7.99254 |
| 15.90 | 174.53712 | 44124.7 | 9.74055 |
| 20.00 | 157.83568 | 63134.2 | 8.80848 |
| 25.10 | 177.51851 | 111838.4 | 9.90693 |
| 31.60 | 93.68464 | 93549.7 | 5.22834 |
| 39.80 | 97.89790 | 155074.1 | 5.46347 |
| 50.10 | 65.09316 | 163384.5 | 3.63271 |
| 63.10 | 62.28749 | 248004.5 | 3.47613 |
| 79.40 | 36.19589 | 228191.9 | 2.02001 |
| 100.00 | 27.68567 | 276856.7 | 1.54507 |
| 126.00 | 18.09521 | 287279.6 | 1.00985 |
| 159.00 | 10.97834 | 277543.4 | .61267 |
| 200.00 | 10.03707 | 401483.1 | .56014 |
| 251.00 | 5.14845 | 324357.6 | .28732 |
| 316.00 | 3.21323 | 320861.2 | .17932 |
| 398.00 | 1.74096 | 275775.9 | .09715 |
| 501.00 | .80630 | 202384.2 | .04499 |
| 631.00 | .35816 | 142605.7 | .01998 |
| 794.00 | .16723 | 105427.8 | .00933 |
| 1000.00 | .03989 | 39896.3 | .00222 |
| 1260.00 | .01116 | 17726.6 | .00062 |
| 1590.00 | .00243 | 6161.7 | .00013 |
| 2000.00 | .00041 | 1659.5 | .00002 |
| 2510.00 | .00003 | 198.3 | 0.00000 |

| DELAY | RU |
|---|---|
| .00001 | 1.00000 |
| .00010 | .99641 |
| .00020 | .98316 |
| .00030 | .96272 |
| .00040 | .93735 |
| .00050 | .90882 |
| .00060 | .87815 |
| .00100 | .75646 |
| .00150 | .62791 |
| .00200 | .49155 |
| .00250 | .38692 |
| .00300 | .30897 |
| .00350 | .26163 |
| .00400 | .23254 |
| .00450 | .21404 |
| .00500 | .19003 |
| .00600 | .10437 |
| .00700 | .01919 |
| .01000 | -.11040 |
| .01300 | -.13986 |
| .01600 | -.13377 |
| .01900 | -.13991 |
| .02200 | -.14676 |
| .02500 | -.13056 |
| .02800 | -.09925 |

MACROSCALE = .0182
MICROSCALE = .0115(CURVE FIT)
MICROSCALE = .0109(INTEGRAL)

RUN NO. 12 AT R/A= .85, U= 6.72

| FREQ | F(N)X10000 | F(N)X10000XN**2 | E(N)X10000 |
|---|---|---|---|
| 10.00 | 169.09155 | 16909.1 | 76.66477 |
| 12.60 | 151.60946 | 24069.5 | 68.73853 |
| 15.90 | 204.95763 | 51815.3 | 92.92617 |
| 20.00 | 132.35708 | 52942.8 | 60.00965 |
| 25.10 | 166.46494 | 104874.5 | 75.47389 |
| 31.60 | 78.49571 | 78382.6 | 35.58934 |
| 39.80 | 81.58184 | 129228.9 | 36.98856 |
| 50.10 | 64.80703 | 162666.3 | 29.38300 |
| 63.10 | 52.24901 | 208035.2 | 23.68929 |
| 79.40 | 37.94375 | 239211.1 | 17.20340 |
| 100.00 | 27.51602 | 275160.2 | 12.47555 |
| 126.00 | 17.98433 | 285519.3 | 8.15395 |
| 159.00 | 10.29475 | 260261.5 | 4.66755 |
| 200.00 | 10.15293 | 406117.2 | 4.60325 |
| 251.00 | 5.60227 | 352949.1 | 2.54002 |
| 316.00 | 3.94026 | 393459.1 | 1.78648 |
| 398.00 | 2.19196 | 347216.3 | .99382 |
| 501.00 | 1.29075 | 323981.8 | .58522 |
| 631.00 | .68938 | 274487.1 | .31256 |
| 794.00 | .37201 | 234533.8 | .16867 |
| 1000.00 | .18182 | 181823.5 | .08243 |
| 1260.00 | .08168 | 129681.8 | .03703 |
| 1590.00 | .03261 | 82462.4 | .01478 |
| 2000.00 | .01029 | 41160.7 | .00466 |
| 2510.00 | .00357 | 22502.8 | .00161 |
| 3160.00 | .00072 | 7287.0 | .00033 |
| 3980.00 | .00011 | 1856.1 | .00005 |

| DELAY | RU |
|---|---|
| .00001 | 1.00000 |
| .00005 | 1.00715 |
| .00010 | 1.00116 |
| .00015 | .99123 |
| .00020 | .97885 |
| .00025 | .96494 |
| .00030 | .95013 |
| .00050 | .88397 |
| .00080 | .78969 |
| .00100 | .72206 |
| .00120 | .64624 |
| .00150 | .54189 |
| .00180 | .45781 |
| .00200 | .41658 |
| .00220 | .39131 |
| .00250 | .37347 |
| .00300 | .36812 |
| .00350 | .32994 |
| .00500 | .17802 |
| .00650 | .04799 |
| .00800 | -.01671 |
| .00950 | -.04230 |
| .01100 | -.06055 |
| .01250 | -.07604 |
| .01400 | -.08777 |
| .01550 | -.10580 |
| .01700 | -.13315 |

MACROSCALE = .0170
MICROSCALE = .0084(CURVE FIT)
MICROSCALE = .0074(INTEGRAL)

RUN NO. 12 AT R/A= .85, U= 2.53

| FREQ | F(N)X10000 | F(N)X10000XN**2 | E(N)X10000 |
|---|---|---|---|
| 10.00 | 229.99944 | 22999.9 | 15.46733 |
| 12.60 | 243.27545 | 38622.4 | 16.36014 |
| 15.90 | 299.49244 | 75714.6 | 20.14070 |
| 20.00 | 209.69045 | 83876.1 | 14.10156 |
| 25.10 | 172.70097 | 108803.3 | 11.61404 |
| 31.60 | 112.92235 | 112759.7 | 7.59396 |
| 39.80 | 95.77122 | 151705.4 | 6.44056 |
| 50.10 | 71.65657 | 179858.7 | 4.81886 |
| 63.10 | 57.34653 | 228331.5 | 3.85652 |
| 79.40 | 33.61245 | 211904.9 | 2.26041 |
| 100.00 | 24.44882 | 244488.2 | 1.64416 |
| 126.00 | 12.61708 | 200308.8 | .84849 |
| 159.00 | 6.72501 | 170014.9 | .45225 |
| 200.00 | 4.66581 | 186632.4 | .31377 |
| 251.00 | 1.82973 | 115275.3 | .12304 |
| 316.00 | .89065 | 88936.7 | .05989 |
| 398.00 | .33910 | 53715.7 | .02280 |
| 501.00 | .09864 | 24759.1 | .00663 |
| 631.00 | .02505 | 9977.1 | .00168 |
| 794.00 | .00479 | 3022.3 | .00032 |
| 1000.00 | .00060 | 603.8 | .00004 |
| 1260.00 | .00003 | 53.7 | 0.00000 |

| DELAY | RU |
|---|---|
| .00001 | 1.00000 |
| .00020 | .99692 |
| .00040 | .98043 |
| .00060 | .95503 |
| .00080 | .92344 |
| .00100 | .88782 |
| .00120 | .84920 |
| .00140 | .80840 |
| .00200 | .68696 |
| .00250 | .59285 |
| .00300 | .50568 |
| .00350 | .42720 |
| .00400 | .36325 |
| .00450 | .31474 |
| .00500 | .27516 |
| .00600 | .19772 |
| .00700 | .11548 |
| .01000 | -.03049 |
| .01300 | -.09867 |
| .01600 | -.15554 |
| .01900 | -.19379 |
| .02200 | -.20601 |

MACROSCALE = .0087
MICROSCALE = .0080(CURVE FIT)
MICROSCALE = .0071(INTEGRAL)

RUN NO. 14 AT R/A=0.00, U= 6.83

| FREQ | F(N)X10000 | F(N)X1000)XN**2 | E(N)X10000 |
|---|---|---|---|
| 10.00 | 91.71143 | 9171.1 | 3.45065 |
| 12.60 | 141.94384 | 22535.0 | 5.34065 |
| 15.90 | 225.15076 | 56920.3 | 8.47132 |
| 20.00 | 142.40175 | 56960.7 | 5.35788 |
| 25.10 | 132.65054 | 83571.1 | 4.99099 |
| 31.60 | 92.37172 | 92238.7 | 3.47549 |
| 39.80 | 97.45910 | 154379.1 | 3.66691 |
| 50.10 | 62.39087 | 156601.7 | 2.34746 |
| 63.10 | 55.94545 | 222752.9 | 2.10495 |
| 79.40 | 37.28147 | 235035.8 | 1.40272 |
| 100.00 | 29.08469 | 290846.9 | 1.09431 |
| 126.00 | 17.52937 | 278296.3 | .65954 |
| 159.00 | 10.90278 | 275633.3 | .41021 |
| 200.00 | 12.25905 | 490362.0 | .46124 |
| 251.00 | 5.51593 | 347509.7 | .20753 |
| 316.00 | 4.22337 | 421729.3 | .15890 |
| 398.00 | 2.10947 | 334149.8 | .07936 |
| 501.00 | 1.01940 | 255672.7 | .03835 |
| 631.00 | .57579 | 229257.8 | .02166 |
| 794.00 | .21809 | 137496.1 | .00820 |
| 1000.00 | .08415 | 84156.2 | .00316 |
| 1260.00 | .02510 | 39858.8 | .00094 |
| 1590.00 | .00901 | 22793.8 | .00033 |
| 2000.00 | .00186 | 7451.1 | .00007 |
| 2510.00 | .00041 | 2597.5 | .00001 |

| DELAY | RU |
|---|---|
| .00001 | 1.00000 |
| .00010 | 1.00927 |
| .00020 | .99184 |
| .00030 | .96625 |
| .00040 | .93587 |
| .00050 | .90307 |
| .00060 | .86846 |
| .00100 | .73532 |
| .00150 | .60404 |
| .00200 | .46866 |
| .00250 | .37093 |
| .00300 | .29923 |
| .00350 | .25559 |
| .00400 | .22725 |
| .00450 | .21003 |
| .00500 | .13911 |
| .00600 | .11189 |
| .00700 | .03048 |
| .01000 | -.09276 |
| .01300 | -.12659 |
| .01600 | -.12748 |
| .01900 | -.13939 |
| .02200 | -.15320 |
| .02500 | -.14507 |
| .02800 | -.11797 |

MACROSCALE = .0174
MICROSCALE = .0105(CURVE FIT)
MICROSCALE = .0092(INTEGRAL)

RUN NO. 14 AT R/A=0.00, U= 6.83 (DIRECT)

| FREQ | F(E)X10000 | F(N)X10000XN**2 | E(N)X10000 |
|---|---|---|---|
| 10.00 | 225.40401 | 22540.4 | 8.48085 |
| 12.60 | 248.66306 | 39478.5 | 9.35616 |
| 15.90 | 154.61885 | 39089.1 | 5.81755 |
| 20.00 | 147.52573 | 59010.2 | 5.55067 |
| 25.10 | 170.38439 | 107543.8 | 6.41073 |
| 31.60 | 117.96456 | 117794.6 | 4.43843 |
| 38.90 | 99.24091 | 150172.3 | 3.73395 |
| 50.10 | 99.84965 | 142693.2 | 2.13897 |
| 63.10 | 49.64309 | 197659.4 | 1.86782 |
| 79.40 | 36.69244 | 231322.3 | 1.38055 |
| 100.00 | 24.42980 | 244298.0 | .91917 |
| 126.00 | 15.96719 | 253495.1 | .60076 |
| 159.00 | 9.68727 | 244903.9 | .36448 |
| 200.00 | 8.26234 | 330493.9 | .31087 |
| 251.00 | 4.47909 | 282187.7 | .16852 |
| 316.00 | 2.93806 | 293383.4 | .11054 |
| 398.00 | 1.61938 | 256517.5 | .06092 |
| 501.00 | .84868 | 213021.5 | .03193 |
| 631.00 | .43186 | 171951.1 | .01624 |
| 794.00 | .17049 | 107489.2 | .00641 |
| 1000.00 | .07792 | 77924.1 | .00293 |
| 1260.00 | .02191 | 34793.7 | .00082 |
| 1590.00 | .00619 | 15660.9 | .00023 |
| 2000.00 | .00162 | 6483.4 | .00006 |

| DELAY | RU |
|---|---|
| .00001 | 1.00000 |
| .00010 | .98924 |
| .00020 | .97554 |
| .00030 | .95517 |
| .00040 | .93094 |
| .00050 | .90534 |
| .00060 | .87941 |
| .00100 | .76941 |
| .00150 | .64751 |
| .00200 | .53012 |
| .00250 | .42120 |
| .00300 | .34436 |
| .00350 | .29484 |
| .00400 | .26726 |
| .00450 | .25154 |
| .00500 | .22855 |
| .00600 | .14279 |
| .00700 | .05542 |
| .01000 | -.08731 |
| .01300 | -.13000 |
| .01600 | -.12425 |
| .01900 | -.12532 |
| .02200 | -.13652 |
| .02500 | -.13518 |

MACROSCALE = .0191
MICROSCALE = .0112(CURVE FIT)
MICROSCALE = .0104(INTEGRAL)

RUN NO. 14 AT R/A= .85, U= 6.64

| FREQ | F(N)X10000 | F(N)X10000XN**2 | E(N)X10000 |
|---|---|---|---|
| 10.00 | 172.59107 | 17259.1 | 58.12692 |
| 12.60 | 206.60184 | 32800.1 | 69.58140 |
| 15.90 | 247.01356 | 62447.4 | 83.19166 |
| 20.00 | 158.67075 | 63468.3 | 53.43870 |
| 25.10 | 167.57214 | 105572.1 | 56.43659 |
| 31.60 | 95.56022 | 95422.6 | 32.18371 |
| 39.80 | 83.77723 | 132706.4 | 28.21532 |
| 50.10 | 68.79451 | 172674.9 | 23.16929 |
| 63.10 | 59.71022 | 237742.8 | 20.10979 |
| 79.80 | 37.15600 | 236610.9 | 12.51376 |
| 100.00 | 30.12147 | 301214.7 | 10.14460 |
| 126.00 | 16.41224 | 260560.7 | 5.52747 |
| 159.00 | 9.95728 | 251729.9 | 3.35351 |
| 200.00 | 7.43547 | 297418.9 | 2.50419 |
| 251.00 | 3.81397 | 240284.3 | 1.28450 |
| 316.00 | 2.29938 | 229607.0 | .77440 |
| 398.00 | 1.15194 | 182472.5 | .38796 |
| 501.00 | .46950 | 117846.8 | .15812 |
| 631.00 | .19566 | 77906.7 | .06589 |
| 798.00 | .07942 | 50579.6 | .02675 |
| 1000.00 | .02147 | 21479.8 | .00723 |
| 1260.00 | .00615 | 9764.5 | .00207 |
| 1590.00 | .00202 | 5114.2 | .00068 |
| 2000.00 | .00024 | 980.6 | .00008 |

| DELAY | RU |
|---|---|
| .00001 | 1.00000 |
| .00010 | .97082 |
| .00020 | .96194 |
| .00030 | .94780 |
| .00040 | .92987 |
| .00050 | .90944 |
| .00060 | .88732 |
| .00100 | .78658 |
| .00150 | .65979 |
| .00200 | .53372 |
| .00250 | .41733 |
| .00300 | .33426 |
| .00350 | .28377 |
| .00400 | .25904 |
| .00450 | .24777 |
| .00500 | .22876 |
| .00600 | .14619 |
| .00700 | .06369 |
| .01000 | -.05835 |
| .01300 | -.09742 |
| .01600 | -.11458 |
| .01900 | -.14726 |
| .02200 | -.17507 |
| .02500 | -.17400 |

MACROSCALE = .0186
MICROSCALE = .0118(CURVE FIT)
MICROSCALE = .0124(INTEGRAL)

RUN NO. 14 AT R/A= .85, U= 2.50

| FREQ | F(N)X10000 | F(N)X10000XN**2 | E(N)X10000 |
|---|---|---|---|
| 10.00 | 253.47559 | 25347.5 | 20.44432 |
| 12.60 | 176.93966 | 28090.9 | 14.27124 |
| 15.90 | 313.81220 | 79334.8 | 25.31083 |
| 20.00 | 200.69613 | 80278.4 | 16.18734 |
| 25.10 | 215.53236 | 135787.5 | 17.38397 |
| 31.60 | 109.63284 | 109474.9 | 8.84254 |
| 50.10 | 95.01932 | 238499.4 | 7.66387 |
| 63.10 | 86.56392 | 344663.7 | 6.98189 |
| 79.40 | 57.87407 | 364858.9 | 4.66789 |
| 100.00 | 32.75049 | 327504.9 | 2.64152 |
| 126.00 | 20.32737 | 322717.3 | 1.63952 |
| 159.00 | 12.22344 | 309020.8 | .98589 |
| 200.00 | 5.37143 | 214857.5 | .43323 |
| 251.00 | 3.83326 | 241499.4 | .30917 |
| 316.00 | 1.55357 | 155134.0 | .12530 |
| 398.00 | .50668 | 80261.2 | .04086 |
| 501.00 | .20724 | 52018.8 | .01671 |
| 631.00 | .07397 | 29454.2 | .00596 |
| 798.00 | .03146 | 20038.1 | .00253 |
| 1000.00 | .00897 | 8975.6 | .00072 |
| 1260.00 | .00122 | 1943.0 | .00009 |

| DELAY | RU |
|---|---|
| .00001 | 1.00000 |
| .00020 | 1.02526 |
| .00040 | 1.00248 |
| .00060 | .96830 |
| .00080 | .92626 |
| .00100 | .87885 |
| .00120 | .82785 |
| .00140 | .77507 |
| .00200 | .62019 |
| .00250 | .50173 |
| .00300 | .40401 |
| .00350 | .33758 |
| .00400 | .29567 |
| .00450 | .25882 |
| .00500 | .21503 |
| .00600 | .10660 |
| .00700 | .02277 |
| .01000 | -.06017 |
| .01300 | -.07103 |
| .01600 | -.12571 |
| .01900 | -.17759 |

MACROSCALE = .0076
MICROSCALE = .0070(CURVE FIT)
MICROSCALE = .0054(INTEGRAL)

RUN NO. 15 AT R/A=0.00, U= 7.21

| FREQ | F(N)X10000 | F(N)X10000XN**2 | E(N)X10000 |
|---|---|---|---|
| 10.00 | 22.88963 | 2288.9 | 1.35938 |
| 12.60 | 65.52540 | 10402.8 | 3.89146 |
| 15.90 | 284.48134 | 71919.7 | 16.89498 |
| 20.00 | 158.87590 | 63550.3 | 9.43543 |
| 25.10 | 150.67520 | 94926.8 | 8.94840 |
| 31.60 | 116.71303 | 116544.9 | 6.93143 |
| 39.80 | 100.31339 | 158900.4 | 5.95748 |
| 50.10 | 66.50851 | 166937.0 | 3.94985 |
| 63.10 | 52.51848 | 209108.1 | 3.11900 |
| 79.40 | 34.99777 | 220638.5 | 2.07847 |
| 100.00 | 23.99686 | 239968.6 | 1.42514 |
| 126.00 | 15.38099 | 244188.5 | .91345 |
| 159.00 | 9.90306 | 250359.3 | .58813 |
| 200.00 | 9.32157 | 372863.0 | .55359 |
| 251.00 | 5.50674 | 346930.3 | .32703 |
| 316.00 | 3.85766 | 385211.1 | .22910 |
| 398.00 | 2.43370 | 385508.1 | .14453 |
| 501.00 | 1.34275 | 337034.0 | .07974 |
| 631.00 | .82775 | 329580.8 | .04915 |
| 798.00 | .42675 | 271760.7 | .02534 |
| 1000.00 | .21168 | 211680.3 | .01257 |
| 1260.00 | .07089 | 112553.1 | .00421 |
| 1590.00 | .03338 | 84405.8 | .00198 |
| 2000.00 | .01059 | 42387.7 | .00062 |
| 2510.00 | .00283 | 17868.6 | .00016 |
| 3160.00 | .00075 | 7493.5 | .00004 |
| 3980.00 | .00016 | 2570.8 | 0.00000 |

| DELAY | RU |
|---|---|
| .00001 | 1.00000 |
| .00010 | 1.04120 |
| .00020 | 1.01689 |
| .00030 | .98598 |
| .00040 | .95172 |
| .00050 | .91597 |
| .00060 | .88321 |
| .00100 | .76311 |
| .00150 | .59874 |
| .00200 | .48487 |
| .00250 | .43941 |
| .00300 | .42326 |
| .00350 | .37757 |
| .00400 | .30030 |
| .00450 | .23968 |
| .00500 | .20584 |
| .00600 | .10001 |
| .00700 | .02522 |
| .01000 | -.10188 |
| .01300 | -.12492 |
| .01600 | -.16408 |
| .01900 | -.19856 |
| .02200 | -.19350 |
| .02500 | -.16508 |
| .02800 | -.13683 |
| .03400 | -.05318 |
| .03700 | -.01996 |

MACROSCALE = .0201
MICROSCALE = .0110(CURVE FIT)
MICROSCALE = .0078(INTEGRAL)

RUN NO. 15 AT R/A= .85, U= 7.51

| FREQ | F(N)X10000 | F(N)X10000XN**2 | E(N)X10000 |
|---|---|---|---|
| 10.00 | 22.91575 | 2291.5 | 11.22653 |
| 12.60 | 51.07280 | 8108.3 | 25.02081 |
| 15.90 | 254.03991 | 64223.8 | 124.45537 |
| 20.00 | 134.30980 | 53723.9 | 65.79901 |
| 25.10 | 126.75351 | 79855.9 | 62.09715 |
| 31.60 | 108.35122 | 108195.1 | 53.08178 |
| 39.80 | 88.62367 | 140383.4 | 43.41716 |
| 50.10 | 62.35793 | 156519.0 | 30.54945 |
| 63.10 | 55.91592 | 222635.3 | 27.39347 |
| 79.40 | 35.03771 | 220890.3 | 17.16514 |
| 100.00 | 24.02424 | 240242.4 | 11.76959 |
| 126.00 | 16.44222 | 261036.7 | 8.05512 |
| 159.00 | 10.56431 | 267076.4 | 5.17550 |
| 200.00 | 11.81108 | 472443.2 | 5.78630 |
| 251.00 | 6.39380 | 402816.2 | 3.13235 |
| 316.00 | 4.22114 | 421506.6 | 2.06795 |
| 398.00 | 2.78831 | 441679.8 | 1.36600 |
| 501.00 | 1.86061 | 467015.3 | .91152 |
| 631.00 | 1.19333 | 475138.0 | .58461 |
| 794.00 | .66756 | 420859.6 | .32704 |
| 1000.00 | .41536 | 415366.9 | .20349 |
| 1260.00 | .18664 | 296313.9 | .09143 |
| 1590.00 | .10012 | 253131.3 | .04905 |
| 2000.00 | .04243 | 169744.2 | .02078 |
| 2510.00 | .01741 | 109687.2 | .00852 |
| 3160.00 | .00676 | 67519.1 | .00331 |
| 3980.00 | .00186 | 29484.8 | .00091 |
| 5010.00 | .00050 | 12758.8 | .00024 |
| 6310.00 | .00012 | 4814.7 | .00005 |

| DELAY | RU |
|---|---|
| .00001 | 1.00000 |
| .00010 | .95719 |
| .00020 | .92047 |
| .00030 | .87760 |
| .00040 | .83373 |
| .00050 | .79448 |
| .00060 | .76035 |
| .00100 | .60561 |
| .00150 | .45654 |
| .00200 | .40068 |
| .00250 | .38186 |
| .00300 | .31636 |
| .00350 | .24203 |
| .00400 | .20555 |
| .00450 | .15426 |
| .00500 | .09126 |
| .00600 | .02863 |
| .00700 | -.02994 |
| .01000 | -.07882 |
| .01300 | -.11765 |
| .01600 | -.14830 |
| .01900 | -.13390 |
| .02200 | -.11678 |
| .02500 | -.09442 |
| .02800 | -.06962 |
| .03100 | -.05636 |
| .03400 | -.04108 |
| .03700 | -.02532 |
| .04000 | -.01031 |

MACROSCALE = .0157
MICROSCALE = .0084(CURVE FIT)
MICROSCALE = .0057(INTEGRAL)

RUN NO. 15 AT R/A= .85, U= 2.76

| FREQ | F(N)X10000 | F(N)X10000XN**2 | E(N)X10000 |
|---|---|---|---|
| 10.00 | 26.20263 | 2620.2 | 1.88579 |
| 12.60 | 78.73141 | 12499.4 | 5.66628 |
| 15.90 | 304.89127 | 77079.5 | 21.94298 |
| 20.00 | 196.91652 | 78766.6 | 14.17205 |
| 25.10 | 170.09635 | 107162.4 | 12.24181 |
| 31.60 | 120.73603 | 120562.1 | 8.68935 |
| 39.80 | 102.42782 | 162249.7 | 7.37171 |
| 50.10 | 81.54906 | 204688.9 | 5.86907 |
| 63.10 | 57.02943 | 227068.9 | 4.10440 |
| 79.40 | 38.00382 | 239589.8 | 2.73513 |
| 100.00 | 27.92986 | 279298.6 | 2.01010 |
| 126.00 | 15.79771 | 250804.4 | 1.13695 |
| 159.00 | 8.92108 | 225533.9 | .64204 |
| 200.00 | 8.23477 | 329390.8 | .59265 |
| 251.00 | 3.13427 | 197462.4 | .22557 |
| 316.00 | 1.96267 | 195984.8 | .14125 |
| 398.00 | .92296 | 146201.9 | .06642 |
| 501.00 | .44691 | 112177.2 | .03216 |
| 631.00 | .14951 | 59529.9 | .01076 |
| 794.00 | .05235 | 33009.1 | .00376 |
| 1000.00 | .01484 | 14843.5 | .00106 |
| 1260.00 | .00318 | 5061.3 | .00022 |
| 1590.00 | .00076 | 1921.6 | .00005 |
| 2000.00 | .00011 | 476.5 | 0.00000 |

| DELAY | RU |
|---|---|
| .00001 | 1.00000 |
| .00010 | .96097 |
| .00020 | .95318 |
| .00030 | .94119 |
| .00040 | .92589 |
| .00050 | .90805 |
| .00060 | .88834 |
| .00100 | .79684 |
| .00150 | .67632 |
| .00200 | .55296 |
| .00250 | .43760 |
| .00300 | .35249 |
| .00350 | .29862 |
| .00400 | .26918 |
| .00600 | .13192 |
| .00800 | -.00429 |
| .01000 | -.11028 |
| .01400 | -.15220 |
| .01800 | -.15623 |
| .02200 | -.18659 |
| .02600 | -.17618 |
| .03000 | -.12727 |
| .03400 | -.08004 |
| .03800 | -.03134 |

MACROSCALE = .0074
MICROSCALE = .0050(CURVE FIT)
MICROSCALE = .0055(INTEGRAL)

RUN NO. 15 AT R/A= .85, U= 5.46(PDM)

| FREQ | F(N)X10000 | F(N)X1000)XN**2 | E(N)X10000 |
|---|---|---|---|
| 10.00 | 352.31104 | 35281.1 | 95.52416 |
| 12.60 | 241.27367 | 38304.6 | 65.32523 |
| 15.90 | 178.72518 | 45183.5 | 48.39013 |
| 20.00 | 170.90156 | 68360.6 | 46.27187 |
| 25.10 | 152.07121 | 95806.3 | 41.17352 |
| 31.60 | 107.12952 | 106975.2 | 29.00549 |
| 39.80 | 78.54662 | 124420.9 | 21.26662 |
| 50.10 | 63.20320 | 158640.6 | 17.11236 |
| 63.10 | 38.13117 | 151823.4 | 10.32407 |
| 79.40 | 29.35737 | 185079.4 | 7.94855 |
| 100.00 | 21.32357 | 218235.7 | 5.90876 |
| 126.00 | 12.93766 | 205398.4 | 3.50289 |
| 159.00 | 12.93449 | 326996.9 | 3.50203 |
| 200.00 | 8.02485 | 320994.0 | 2.17274 |
| 251.00 | 4.46557 | 281335.4 | 1.20906 |
| 316.00 | 3.20838 | 320376.3 | .86867 |
| 398.00 | 1.86577 | 295546.6 | .50516 |
| 501.00 | 1.14513 | 287430.7 | .31004 |
| 631.00 | .66068 | 263058.9 | .17888 |
| 794.00 | .31061 | 195824.0 | .08410 |
| 1000.00 | .15301 | 153011.0 | .04142 |
| 1260.00 | .05184 | 82304.2 | .01403 |
| 1590.00 | .02066 | 52255.6 | .00559 |
| 2000.00 | .00607 | 24290.6 | .00164 |
| 2500.00 | .00177 | 11123.6 | .00048 |

| DELAY | RU |
|---|---|
| .00001 | 1.00000 |
| .00010 | 1.01154 |
| .00020 | .99135 |
| .00030 | .96353 |
| .00040 | .93363 |
| .00050 | .90398 |
| .00060 | .87398 |
| .00100 | .76279 |
| .00150 | .65591 |
| .00200 | .54033 |
| .00250 | .45409 |
| .00300 | .38894 |
| .00350 | .34860 |
| .00400 | .32093 |
| .00450 | .30128 |
| .00500 | .27657 |
| .00600 | .19687 |
| .00700 | .11566 |
| .01000 | -.03332 |
| .01300 | -.09893 |
| .01600 | -.12277 |
| .01900 | -.14536 |
| .02200 | -.16484 |
| .02500 | -.16354 |
| .02800 | -.14388 |

MACROSCALE = .0166
MICROSCALE = .0084(CURVE FIT)
MICROSCALE = .0068(INTEGRAL)

RUN NO. 15 AT R/A= .85, U= 2.76(PDM)

| FREQ | F(N)X10000 | F(N)X1000)XN**2 | E(N)X10000 |
|---|---|---|---|
| 10.00 | 449.82068 | 44982.0 | 32.37353 |
| 12.60 | 310.12080 | 49234.7 | 22.31935 |
| 15.90 | 144.93656 | 36641.4 | 10.43106 |
| 20.00 | 198.73486 | 79493.9 | 14.30292 |
| 25.10 | 179.32843 | 112978.7 | 12.90624 |
| 31.60 | 104.78571 | 104634.8 | 7.54141 |
| 39.80 | 84.91000 | 134500.8 | 6.11096 |
| 50.10 | 64.02369 | 160700.1 | 4.60777 |
| 63.10 | 41.22034 | 164123.3 | 2.96662 |
| 79.40 | 32.56919 | 205327.9 | 2.34400 |
| 100.00 | 24.05969 | 240596.9 | 1.73157 |
| 126.00 | 13.27863 | 210811.5 | .95566 |
| 159.00 | 11.19286 | 282966.7 | .80554 |
| 200.00 | 5.38817 | 215527.0 | .38778 |
| 251.00 | 2.81938 | 177623.8 | .20291 |
| 316.00 | 1.58269 | 158041.7 | .11390 |
| 398.00 | .68785 | 108958.5 | .04950 |
| 501.00 | .29786 | 74763.8 | .02143 |
| 631.00 | .09872 | 39307.1 | .00710 |
| 794.00 | .03040 | 19168.3 | .00218 |
| 1000.00 | .00869 | 8694.4 | .00062 |

| DELAY | RU |
|---|---|
| .00001 | 1.00000 |
| .00010 | .99462 |
| .00020 | .98863 |
| .00030 | .97808 |
| .00040 | .96424 |
| .00050 | .94758 |
| .00060 | .92888 |
| .00100 | .84416 |
| .00150 | .73536 |
| .00200 | .63319 |
| .00250 | .54575 |
| .00300 | .46398 |
| .00350 | .38949 |
| .00400 | .32816 |
| .00450 | .28381 |
| .00500 | .25071 |
| .00600 | .19860 |
| .00700 | .15770 |
| .01000 | -.00096 |
| .01300 | -.08863 |
| .01600 | -.14297 |

MACROSCALE = .0090
MICROSCALE = .0061(CURVE FIT)
MICROSCALE = .0063(INTEGRAL)

RUN NO. 17 AT R/A=0.00, U= 9.06

| FREQ | F(N)X10000 | F(N)X1000)XN**2 | E(N)X10000 |
|---|---|---|---|
| 10.00 | 60.85260 | 6085.2 | 8.23355 |
| 12.60 | 62.43830 | 9912.7 | 8.44810 |
| 15.90 | 130.27763 | 32935.4 | 17.62699 |
| 20.00 | 75.84274 | 30337.0 | 10.26177 |
| 25.10 | 83.63168 | 52688.7 | 11.31564 |
| 31.60 | 65.49854 | 65404.2 | 8.86217 |
| 39.80 | 59.11614 | 93642.3 | 7.99861 |
| 50.10 | 53.87980 | 135238.8 | 7.29011 |
| 63.10 | 52.54750 | 209223.6 | 7.10985 |
| 79.40 | 39.34590 | 248050.7 | 5.32363 |
| 100.00 | 33.29529 | 332952.9 | 4.50496 |
| 126.00 | 25.48235 | 404557.8 | 3.44784 |
| 159.00 | 14.83234 | 374976.5 | 2.00686 |
| 200.00 | 13.96706 | 558682.4 | 1.88978 |
| 251.00 | 8.52612 | 537154.1 | 1.15361 |
| 316.00 | 6.35352 | 634438.0 | .85965 |
| 398.00 | 4.17589 | 661478.8 | .56501 |
| 501.00 | 2.51878 | 632217.4 | .34079 |
| 631.00 | 1.70669 | 679538.1 | .23092 |
| 794.00 | 1.06920 | 674063.5 | .14466 |
| 1000.00 | .62784 | 627848.0 | .08494 |
| 1260.00 | .28224 | 448099.5 | .03818 |
| 1590.00 | .14449 | 365291.9 | .01955 |
| 2000.00 | .05782 | 231286.6 | .00782 |
| 2510.00 | .02468 | 155545.1 | .00334 |
| 3160.00 | .00857 | 85629.1 | .00116 |
| 3980.00 | .00426 | 67497.1 | .00057 |
| 5010.00 | .00243 | 61099.8 | .00032 |

| DELAY | RU |
|---|---|
| .00001 | 1.00000 |
| .00005 | .99151 |
| .00010 | .97213 |
| .00015 | .94546 |
| .00020 | .91560 |
| .00025 | .88435 |
| .00030 | .85160 |
| .00050 | .72765 |
| .00080 | .57577 |
| .00100 | .46900 |
| .00120 | .39627 |
| .00150 | .34215 |
| .00180 | .32646 |
| .00200 | .30502 |
| .00220 | .27024 |
| .00250 | .20453 |
| .00300 | .13728 |
| .00350 | .09114 |
| .00500 | -.00490 |
| .00650 | -.03122 |
| .00800 | -.05058 |
| .00950 | -.05453 |
| .01100 | -.04731 |
| .01250 | -.05645 |
| .01400 | -.07252 |
| .01550 | -.07412 |
| .01700 | -.07016 |
| .01850 | -.07026 |

MACROSCALE = .0123

MICROSCALE = .0086(CURVE FIT)

MICROSCALE = .0057(INTEGRAL)

RUN NO. 17 AT R/A=0.00, U= 15.80

| FREQ | F(N)X10000 | F(N)X10000XN**2 | E(N)X10000 |
|---|---|---|---|
| 10.00 | 35.94802 | 3594.8 | 13.30180 |
| 12.60 | 33.42881 | 5307.1 | 12.36962 |
| 15.90 | 82.21873 | 20785.7 | 30.42330 |
| 20.00 | 43.83109 | 17532.4 | 16.21877 |
| 25.10 | 48.92371 | 30822.4 | 18.10318 |
| 31.60 | 33.09201 | 33044.3 | 12.24500 |
| 39.80 | 34.49374 | 54639.4 | 12.76368 |
| 50.10 | 37.03048 | 92946.8 | 13.70235 |
| 63.10 | 33.57490 | 133682.1 | 12.42368 |
| 79.40 | 31.87804 | 200970.6 | 11.79579 |
| 100.00 | 27.43578 | 274357.8 | 10.15203 |
| 126.00 | 21.60817 | 343051.4 | 7.99565 |
| 159.00 | 14.69958 | 371620.1 | 5.43927 |
| 200.00 | 16.19976 | 647990.6 | 5.99438 |
| 251.00 | 10.93325 | 688805.9 | 4.04562 |
| 316.00 | 8.30471 | 829275.9 | 3.07298 |
| 398.00 | 6.09996 | 966258.3 | 2.25716 |
| 501.00 | 3.91238 | 982012.2 | 1.44769 |
| 631.00 | 2.53818 | 1010604.3 | .93919 |
| 798.00 | 1.82538 | 1162410.2 | .67544 |
| 1000.00 | 1.36974 | 1369743.7 | .50684 |
| 1260.00 | .87904 | 1395575.9 | .32527 |
| 1590.00 | .57540 | 1454678.8 | .21291 |
| 2000.00 | .35815 | 1432602.7 | .13252 |
| 2510.00 | .22021 | 1387376.0 | .08148 |
| 3160.00 | .11181 | 1116547.9 | .04137 |
| 3980.00 | .07773 | 1231290.6 | .02876 |
| 5010.00 | .09724 | 2440753.7 | .03598 |
| 6310.00 | .01058 | 421502.0 | .00391 |
| 7940.00 | .00185 | 116639.5 | .00068 |

| DELAY | RU |
|---|---|
| .00001 | 1.00000 |
| .00005 | .95912 |
| .00010 | .88242 |
| .00015 | .83000 |
| .00020 | .78355 |
| .00025 | .72751 |
| .00030 | .68147 |
| .00050 | .55471 |
| .00080 | .35468 |
| .00100 | .24186 |
| .00120 | .15626 |
| .00150 | .11643 |
| .00180 | .13971 |
| .00200 | .15026 |
| .00220 | .13786 |
| .00250 | .08587 |
| .00300 | .05993 |
| .00350 | .05418 |
| .00500 | -.02271 |
| .00650 | -.05112 |
| .00800 | -.03936 |
| .00950 | -.02012 |
| .01100 | -.01904 |
| .01250 | -.03314 |
| .01400 | -.04396 |
| .01550 | -.04095 |
| .01700 | -.03192 |
| .01850 | -.02971 |
| .02000 | -.03682 |
| .02150 | -.04367 |

MACROSCALE = .0132
MICROSCALE = .0076(CURVE FIT)
MICROSCALE = .0037(INTEGRAL)

RUN NO. 17 AT R/A=0.00, U= 23.40

| FREQ | F(N)X10000 | F(N)X10000XN**2 | E(N)X10000 |
|---|---|---|---|
| 10.00 | 2.08882 | 208.8 | 1.51543 |
| 12.60 | 5.46363 | 867.4 | 3.96384 |
| 15.90 | 24.53849 | 6203.5 | 17.80255 |
| 20.00 | 26.47631 | 10590.5 | 19.20843 |
| 25.10 | 25.21442 | 15885.3 | 18.29294 |
| 31.60 | 23.37625 | 23342.5 | 16.95935 |
| 39.80 | 21.01522 | 33288.9 | 15.24644 |
| 50.10 | 20.88106 | 52411.6 | 15.14910 |
| 63.10 | 21.32469 | 84906.6 | 15.47096 |
| 79.40 | 18.01485 | 113572.1 | 13.06968 |
| 100.00 | 17.57975 | 175797.5 | 12.75402 |
| 126.00 | 14.82566 | 235372.1 | 10.75594 |
| 159.00 | 10.36782 | 262109.0 | 7.52180 |
| 200.00 | 13.61044 | 544417.8 | 9.87431 |
| 251.00 | 8.19577 | 516341.7 | 5.94599 |
| 316.00 | 7.64170 | 763069.7 | 5.54401 |
| 398.00 | 5.81351 | 920884.2 | 4.21767 |
| 501.00 | 4.23997 | 1064238.3 | 3.07608 |
| 631.00 | 3.70136 | 1473740.9 | 2.68532 |
| 794.00 | 2.62774 | 1656526.3 | 1.90641 |
| 1000.00 | 2.33737 | 2337377.8 | 1.69575 |
| 1260.00 | 1.56247 | 2480579.1 | 1.13356 |
| 1590.00 | 1.36338 | 3446783.4 | .98913 |
| 2000.00 | 1.06001 | 4240056.0 | .76903 |
| 2510.00 | .81029 | 5104969.0 | .58786 |
| 3160.00 | .52431 | 5235618.5 | .38038 |
| 3980.00 | .31637 | 5011509.4 | .22952 |
| 5010.00 | .13179 | 3308073.9 | .09561 |
| 6310.00 | .04129 | 1644155.6 | .02995 |
| 7940.00 | .01600 | 1008713.8 | .01160 |

| DELAY | RU |
|---|---|
| .00001 | 1.00000 |
| .00005 | .88661 |
| .00010 | .67032 |
| .00015 | .56775 |
| .00020 | .52742 |
| .00025 | .44919 |
| .00030 | .40369 |
| .00050 | .31202 |
| .00080 | .17099 |
| .00100 | .10814 |
| .00120 | .05903 |
| .00150 | .03645 |
| .00180 | .04944 |
| .00200 | .05794 |
| .00220 | .05190 |
| .00250 | .02445 |
| .00300 | .01232 |
| .00350 | .01093 |
| .00500 | -.02393 |
| .00650 | -.03643 |
| .00800 | -.03077 |
| .00950 | -.02139 |
| .01100 | -.01986 |
| .01250 | -.02527 |
| .01400 | -.02955 |
| .01550 | -.02729 |
| .01700 | -.02142 |
| .01850 | -.01796 |
| .02000 | -.01908 |
| .02150 | -.02088 |

MACROSCALE = .0104
MICROSCALE = .0077(CURVE FIT)
MICROSCALE = .0034(INTEGRAL)

RUN NO. 18 AT R/A= .5-1, U= 21.40

| FREQ | F(N)X10000 | F(N)X10000XN**2 | E(N)X10000 |
|---|---|---|---|
| 10.00 | 51.94576 | 5194.5 | 0.00000 |
| 12.60 | 77.89236 | 12366.1 | 0.00000 |
| 15.90 | 253.94148 | 64198.9 | 0.00000 |
| 20.00 | 134.70107 | 53880.4 | 0.00000 |
| 25.10 | 87.27894 | 54986.6 | 0.00000 |
| 31.60 | 58.17053 | 58086.7 | 0.00000 |
| 39.80 | 43.63783 | 69124.0 | 0.00000 |
| 50.10 | 40.46120 | 101558.0 | 0.00000 |
| 63.10 | 33.69204 | 134148.5 | 0.00000 |
| 79.40 | 22.50233 | 141862.8 | 0.00000 |
| 100.00 | 17.97792 | 179779.2 | 0.00000 |
| 126.00 | 14.89568 | 236483.8 | 0.00000 |
| 159.00 | 11.07954 | 280101.9 | 0.00000 |
| 200.00 | 11.55627 | 462251.0 | 0.00000 |
| 251.00 | 7.69737 | 484942.1 | 0.00000 |
| 316.00 | 6.67904 | 666943.0 | 0.00000 |
| 398.00 | 4.38984 | 695369.3 | 0.00000 |
| 501.00 | 3.20292 | 803937.2 | 0.00000 |
| 631.00 | 2.08498 | 830161.0 | 0.00000 |
| 794.00 | 1.17232 | 739072.7 | 0.00000 |
| 1000.00 | 1.10702 | 1107028.4 | 0.00000 |
| 1260.00 | .67043 | 1064374.9 | 0.00000 |
| 1590.00 | .55922 | 1413780.3 | 0.00000 |
| 2000.00 | .36904 | 1476192.4 | 0.00000 |
| 2510.00 | .23978 | 1510651.6 | 0.00000 |
| 3160.00 | .12432 | 1241488.6 | 0.00000 |
| 3980.00 | .10457 | 1656575.8 | 0.00000 |
| 5010.00 | .07416 | 1861509.1 | 0.00000 |
| 6310.00 | .01021 | 406548.1 | 0.00000 |
| 7940.00 | .00118 | 74909.7 | 0.00000 |

| DELAY | RU |
|---|---|
| .00001 | 1.00000 |
| .00005 | .95207 |
| .00010 | .87770 |
| .00015 | .83237 |
| .00020 | .79985 |
| .00025 | .75655 |
| .00030 | .72367 |
| .00050 | .63509 |
| .00080 | .48696 |
| .00100 | .40333 |
| .00120 | .34029 |
| .00150 | .31022 |
| .00180 | .32309 |
| .00200 | .32622 |
| .00220 | .31261 |
| .00250 | .27117 |
| .00300 | .24222 |
| .00350 | .22303 |
| .00500 | .12370 |
| .00650 | .05358 |
| .00800 | .01807 |
| .00950 | .00023 |
| .01100 | -.02028 |
| .01250 | -.05031 |
| .01400 | -.08220 |
| .01550 | -.10531 |
| .01700 | -.11682 |
| .01850 | -.12170 |
| .02000 | -.12529 |
| .02150 | -.12758 |

MACROSCALE = .0390

MICROSCALE = .0111(CURVE FIT)

MICROSCALE = .0052(INTEGRAL)

RUN NO. 18 AT R/A= .52, U= 21.40

| FREQ | F(N)X10000 | F(N)X10000XN**2 | E(N)X10000 |
|---|---|---|---|
| 10.00 | 55.25930 | 5525.9 | 0.00000 |
| 12.60 | 86.67020 | 13759.7 | 0.00000 |
| 15.90 | 180.83752 | 45717.5 | 0.00000 |
| 20.00 | 125.28810 | 50115.2 | 0.00000 |
| 25.10 | 84.59757 | 53297.3 | 0.00000 |
| 31.60 | 61.88113 | 61792.0 | 0.00000 |
| 39.80 | 43.32130 | 69414.6 | 0.00000 |
| 50.10 | 39.21817 | 98437.9 | 0.00000 |
| 63.10 | 34.84566 | 138741.8 | 0.00000 |
| 79.40 | 24.27368 | 153030.0 | 0.00000 |
| 100.00 | 20.00389 | 200038.9 | 0.00000 |
| 126.00 | 15.16439 | 240749.9 | 0.00000 |
| 159.00 | 11.95170 | 302151.1 | 0.00000 |
| 200.00 | 14.97241 | 598896.6 | 0.00000 |
| 251.00 | 9.35115 | 589132.0 | 0.00000 |
| 316.00 | 7.75133 | 774016.9 | 0.00000 |
| 398.00 | 4.59788 | 728323.7 | 0.00000 |
| 501.00 | 3.77042 | 946381.0 | 0.00000 |
| 631.00 | 2.57058 | 1023505.2 | 0.00000 |
| 794.00 | 1.36304 | 859315.6 | 0.00000 |
| 1000.00 | .88101 | 881010.3 | 0.00000 |
| 1260.00 | .47742 | 757965.6 | 0.00000 |
| 1590.00 | .34850 | 881068.0 | 0.00000 |
| 2000.00 | .23915 | 956636.0 | 0.00000 |
| 2510.00 | .17075 | 1075769.4 | 0.00000 |
| 3160.00 | .10497 | 1048249.7 | 0.00000 |
| 3980.00 | .04985 | 789706.8 | 0.00000 |
| 5010.00 | .05596 | 1404747.6 | 0.00000 |
| 6310.00 | .01047 | 416897.5 | 0.00000 |
| 7940.00 | .00139 | 88182.4 | 0.00000 |

| DELAY | RU |
|---|---|
| .00001 | 1.00000 |
| .00005 | .98073 |
| .00010 | .92318 |
| .00015 | .88463 |
| .00020 | .85250 |
| .00025 | .81003 |
| .00030 | .77299 |
| .00050 | .64965 |
| .00080 | .46653 |
| .00100 | .37562 |
| .00120 | .31411 |
| .00150 | .28553 |
| .00180 | .29602 |
| .00200 | .29928 |
| .00220 | .28710 |
| .00250 | .24621 |
| .00300 | .21684 |
| .00350 | .20086 |
| .00500 | .10448 |
| .00650 | .03791 |
| .00800 | .00510 |
| .00950 | -.00970 |
| .01100 | -.02728 |
| .01250 | -.05397 |
| .01400 | -.08256 |
| .01550 | -.10237 |
| .01700 | -.11101 |
| .01850 | -.11334 |
| .02000 | -.11487 |
| .02150 | -.11545 |

MACROSCALE = .0360

MICROSCALE = .0124(CURVE FIT)

MICROSCALE = .0060(INTEGRAL)

RUN NO. 18 AT R/A= .53, U= 21.40

| FREQ | F(N)X10000 | F(N)X10000XN**2 | E(N)X10000 |
|---|---|---|---|
| 10.00 | 36.15089 | 3615.0 | 0.00000 |
| 12.60 | 38.59147 | 6126.7 | 0.00000 |
| 15.90 | 91.61521 | 23161.2 | 0.00000 |
| 20.00 | 44.07845 | 17631.3 | 0.00000 |
| 25.10 | 57.74144 | 36377.6 | 0.00000 |
| 31.60 | 40.43293 | 40424.6 | 0.00000 |
| 39.80 | 34.68840 | 54947.8 | 0.00000 |
| 50.10 | 25.41294 | 63786.7 | 0.00000 |
| 63.10 | 26.42212 | 105202.5 | 0.00000 |
| 79.40 | 19.21475 | 121136.7 | 0.00000 |
| 100.00 | 15.83483 | 158348.3 | 0.00000 |
| 126.00 | 13.34918 | 211931.6 | 0.00000 |
| 159.00 | 10.06136 | 254361.3 | 0.00000 |
| 200.00 | 12.68345 | 507338.0 | 0.00000 |
| 251.00 | 9.36848 | 590223.7 | 0.00000 |
| 316.00 | 8.83563 | 882291.2 | 0.00000 |
| 398.00 | 5.80727 | 919896.1 | 0.00000 |
| 501.00 | 5.60487 | 1406827.9 | 0.00000 |
| 631.00 | 4.21944 | 1680018.6 | 0.00000 |
| 794.00 | 3.10230 | 1955804.1 | 0.00000 |
| 1000.00 | 2.64083 | 2640837.2 | 0.00000 |
| 1260.00 | 1.42409 | 2260885.9 | 0.00000 |
| 1590.00 | .82008 | 2073254.2 | 0.00000 |
| 2000.00 | .39708 | 1588357.8 | 0.00000 |
| 2510.00 | .28028 | 1765806.9 | 0.00000 |
| 3160.00 | .11642 | 1162592.8 | 0.00000 |
| 3980.00 | .08233 | 1304267.4 | 0.00000 |
| 5010.00 | .06379 | 1601252.7 | 0.00000 |
| 6310.00 | .00413 | 164800.1 | 0.00000 |
| 7940.00 | .00186 | 117297.7 | 0.00000 |

| DELAY | RU |
|---|---|
| .00001 | 1.00000 |
| .00005 | .95235 |
| .00010 | .84967 |
| .00015 | .76270 |
| .00020 | .68589 |
| .00025 | .59483 |
| .00030 | .52017 |
| .00050 | .37447 |
| .00080 | .23774 |
| .00100 | .19319 |
| .00120 | .15480 |
| .00150 | .13855 |
| .00180 | .13966 |
| .00200 | .14220 |
| .00220 | .13807 |
| .00250 | .10861 |
| .00300 | .09473 |
| .00350 | .08450 |
| .00500 | .02982 |
| .00650 | -.00489 |
| .00800 | -.01780 |
| .00950 | -.02033 |
| .01100 | -.02577 |
| .01250 | -.03645 |
| .01400 | -.04688 |
| .01550 | -.05141 |
| .01700 | -.05075 |
| .01850 | -.04847 |
| .02000 | -.04735 |
| .02150 | -.04649 |

MACROSCALE = .0179
MICROSCALE = .0083(CURVE FIT)
MICROSCALE = .0050(INTEGRAL)

RUN NO. 19 AT R/A= .51, U= 20.50

| FREQ | F(N)X10000 | F(N)X10000XN**2 | E(N)X10000 |
|---|---|---|---|
| 10.00 | 33.45995 | 3345.9 | 21.05983 |
| 12.60 | 28.47485 | 4520.6 | 17.92219 |
| 15.90 | 89.39916 | 22601.0 | 56.26820 |
| 20.00 | 66.04292 | 26417.1 | 41.56769 |
| 25.10 | 55.21975 | 34788.9 | 34.75554 |
| 31.60 | 44.94643 | 44881.7 | 28.28947 |
| 39.80 | 44.31260 | 70192.9 | 27.89054 |
| 50.10 | 35.11273 | 88133.3 | 22.10010 |
| 63.10 | 37.73828 | 150259.1 | 23.75263 |
| 79.80 | 28.45380 | 181194.9 | 17.90894 |
| 100.00 | 22.90022 | 229002.2 | 14.41349 |
| 126.00 | 16.91204 | 268495.5 | 10.64451 |
| 159.00 | 13.19789 | 333655.9 | 8.30680 |
| 200.00 | 15.01524 | 600609.6 | 9.45065 |
| 251.00 | 11.78230 | 742296.8 | 7.41583 |
| 316.00 | 10.64433 | 1062901.0 | 6.69959 |
| 398.00 | 7.93834 | 1257465.6 | 4.99642 |
| 501.00 | 3.91504 | 982681.2 | 2.46414 |
| 631.00 | 2.77701 | 1105699.5 | 1.74786 |
| 794.00 | 1.95042 | 1229621.0 | 1.22760 |
| 1000.00 | 1.35316 | 1353160.5 | .85168 |
| 1260.00 | .70340 | 1116730.7 | .44272 |
| 1590.00 | .38726 | 979045.1 | .24374 |
| 2000.00 | .20579 | 823199.9 | .12953 |
| 2510.00 | .12510 | 788178.2 | .07874 |
| 3160.00 | .06642 | 663257.5 | .04180 |
| 3980.00 | .04349 | 689025.7 | .02737 |
| 5010.00 | .03458 | 868033.3 | .02176 |
| 6310.00 | .00611 | 243499.7 | .00384 |
| 7940.00 | .00087 | 55391.0 | .00055 |

| DELAY | RU |
|---|---|
| .00001 | 1.00000 |
| .00005 | .97171 |
| .00010 | .91614 |
| .00015 | .86607 |
| .00020 | .81609 |
| .00025 | .75695 |
| .00030 | .70315 |
| .00050 | .54703 |
| .00080 | .34409 |
| .00100 | .25183 |
| .00120 | .18942 |
| .00150 | .16328 |
| .00180 | .17344 |
| .00200 | .17708 |
| .00220 | .16653 |
| .00250 | .12556 |
| .00300 | .10113 |
| .00350 | .08929 |
| .00500 | .01104 |
| .00650 | -.03179 |
| .00800 | -.03995 |
| .00950 | -.03327 |
| .01100 | -.03334 |
| .01250 | -.04399 |
| .01400 | -.05616 |
| .01550 | -.06039 |
| .01700 | -.05753 |
| .01850 | -.05405 |
| .02000 | -.05429 |
| .02150 | -.05568 |

MACROSCALE = .0206
MICROSCALE = .0104(CURVE FIT)
MICROSCALE = .0063(INTEGRAL)

RUN NO. 19 AT R/A= .52, U= 20.50

| FREQ | F(N)X10000 | F(N)X10000XN**2 | E(N)X10000 |
|---|---|---|---|
| 10.00 | 14.26673 | 1426.6 | 13.81385 |
| 12.60 | 18.80233 | 2985.0 | 18.20547 |
| 15.90 | 44.63629 | 11284.5 | 43.21935 |
| 20.00 | 33.55574 | 13422.2 | 32.49055 |
| 25.10 | 37.45449 | 23596.7 | 36.26553 |
| 31.60 | 31.64587 | 31600.3 | 30.64131 |
| 39.80 | 29.26022 | 46349.3 | 28.33139 |
| 50.10 | 28.34940 | 71157.2 | 27.44948 |
| 63.10 | 27.71916 | 110366.8 | 26.83924 |
| 79.40 | 21.35742 | 134644.8 | 20.67945 |
| 100.00 | 21.00399 | 210039.9 | 20.33724 |
| 126.00 | 17.44883 | 277017.7 | 16.89493 |
| 159.00 | 13.00488 | 328776.4 | 12.59205 |
| 200.00 | 15.49182 | 619673.1 | 15.00005 |
| 251.00 | 13.21286 | 832423.7 | 12.79343 |
| 316.00 | 11.46486 | 1144835.9 | 11.10092 |
| 398.00 | 9.94708 | 1575657.6 | 9.63132 |
| 501.00 | 6.03403 | 1514549.5 | 5.84249 |
| 631.00 | 3.76981 | 1500993.6 | 3.65014 |
| 794.00 | 2.12568 | 1340109.0 | 2.05820 |
| 1000.00 | 1.79322 | 1793226.0 | 1.73630 |
| 1260.00 | .95669 | 1518849.3 | .92632 |
| 1590.00 | .52841 | 1335883.9 | .51164 |
| 2000.00 | .26873 | 1074931.4 | .26020 |
| 2510.00 | .16858 | 1062132.5 | .16323 |
| 3160.00 | .10127 | 1011336.3 | .09806 |
| 3980.00 | .06268 | 992903.8 | .06069 |
| 5010.00 | .05825 | 1462236.0 | .05640 |
| 6310.00 | .00630 | 251228.5 | .00610 |
| 7940.00 | .00072 | 45559.0 | .00069 |

| DELAY | RU |
|---|---|
| .00001 | 1.00000 |
| .00005 | .96171 |
| .00010 | .88725 |
| .00015 | .82312 |
| .00020 | .76018 |
| .00025 | .68544 |
| .00030 | .61869 |
| .00050 | .43634 |
| .00080 | .21754 |
| .00100 | .13035 |
| .00120 | .07802 |
| .00150 | .06835 |
| .00180 | .07985 |
| .00200 | .08055 |
| .00220 | .07104 |
| .00250 | .04081 |
| .00300 | .03418 |
| .00350 | .02589 |
| .00500 | -.01567 |
| .00650 | -.03605 |
| .00800 | -.03690 |
| .00950 | -.03033 |
| .01100 | -.02826 |
| .01250 | -.03197 |
| .01400 | -.03586 |
| .01550 | -.03516 |
| .01700 | -.03126 |
| .01850 | -.02795 |
| .02000 | -.02723 |
| .02150 | -.02726 |

MACROSCALE = .0127
MICROSCALE = .0091(CURVE FIT)
MICROSCALE = .0054(INTEGRAL)

RUN NO. 19 AT R/A= .53, U= 21.20

| FREQ | F(N)X10000 | F(N)X1000)XN**2 | E(N)X10000 |
|---|---|---|---|
| 10.00 | 5.78118 | 578.1 | 13.92229 |
| 12.60 | 7.34457 | 1166.0 | 17.68725 |
| 15.90 | 15.32446 | 3874.1 | 36.90448 |
| 20.00 | 11.01398 | 4405.5 | 26.52395 |
| 25.10 | 12.29366 | 7745.1 | 29.60569 |
| 31.60 | 12.03835 | 12021.0 | 28.99084 |
| 39.80 | 12.20430 | 19332.1 | 29.39050 |
| 50.10 | 13.08346 | 32839.6 | 31.50770 |
| 63.10 | 18.19463 | 72443.9 | 43.81644 |
| 79.40 | 15.87184 | 100061.8 | 38.22269 |
| 100.00 | 17.60038 | 176003.8 | 42.38537 |
| 126.00 | 16.99246 | 269772.3 | 40.92137 |
| 159.00 | 12.82889 | 324327.3 | 30.89464 |
| 200.00 | 15.93642 | 637457.1 | 38.37822 |
| 251.00 | 12.63492 | 796012.6 | 30.42750 |
| 316.00 | 9.93399 | 991969.2 | 23.92312 |
| 398.00 | 7.49523 | 1187275.2 | 18.05008 |
| 501.00 | 5.68489 | 1426914.2 | 13.69040 |
| 631.00 | 5.69060 | 2265778.2 | 13.70416 |
| 794.00 | 3.88177 | 2447209.8 | 9.34811 |
| 1000.00 | 2.82941 | 2829417.0 | 6.81382 |
| 1260.00 | 1.64297 | 2608390.4 | 3.95662 |
| 1590.00 | 1.10986 | 2805854.0 | 2.67278 |
| 2000.00 | .54221 | 2168852.0 | 1.30576 |
| 2510.00 | .29157 | 1836934.1 | .70216 |
| 3160.00 | .15234 | 1521283.0 | .36688 |
| 3980.00 | .13039 | 2065463.4 | .31401 |
| 5010.00 | .11483 | 2882287.1 | .27653 |
| 6310.00 | .00684 | 272596.9 | .01648 |
| 7940.00 | .00242 | 153126.9 | .00584 |

| DELAY | RU |
|---|---|
| .00001 | 1.00000 |
| .00005 | .93978 |
| .00010 | .81773 |
| .00015 | .71996 |
| .00020 | .62837 |
| .00025 | .52392 |
| .00030 | .43869 |
| .00050 | .26221 |
| .00080 | .08507 |
| .00100 | .02865 |
| .00120 | -.01360 |
| .00150 | -.02807 |
| .00180 | -.01990 |
| .00200 | -.01098 |
| .00220 | -.00864 |
| .00250 | -.03256 |
| .00300 | -.03559 |
| .00350 | -.02470 |
| .00500 | -.03323 |
| .00650 | -.02837 |
| .00800 | -.01654 |
| .00950 | -.00667 |
| .01100 | -.00627 |
| .01250 | -.01072 |
| .01400 | -.01286 |
| .01550 | -.00941 |
| .01700 | -.00517 |
| .01850 | -.00462 |
| .02000 | -.00809 |
| .02200 | -.01091 |

MACROSCALE = .0072

MICROSCALE = .0076(CURVE FIT)

MICROSCALE = .0042(INTEGRAL)

RUN NO. 20 AT R/A=0.00, U= 23.40

| FREQ | F(N)X10000 | F(N)X10000XN**2 | E(N)X10000 |
|---|---|---|---|
| 10.00 | 4.70954 | 470.9 | 2.47818 |
| 12.60 | 10.28738 | 1633.2 | 5.41327 |
| 15.90 | 50.50350 | 12767.7 | 26.57520 |
| 20.00 | 31.08334 | 12433.3 | 16.35621 |
| 25.10 | 37.51175 | 23632.7 | 19.73887 |
| 31.60 | 35.87235 | 35820.7 | 18.87621 |
| 39.80 | 33.11493 | 52455.3 | 17.42524 |
| 50.10 | 33.35683 | 83725.9 | 17.55253 |
| 63.10 | 37.23277 | 148246.3 | 19.59207 |
| 79.40 | 26.68345 | 168222.1 | 14.04097 |
| 100.00 | 25.51648 | 255164.8 | 13.42690 |
| 126.00 | 17.42718 | 276674.0 | 9.17027 |
| 159.00 | 13.29954 | 336225.7 | 6.99828 |
| 200.00 | 16.50259 | 660103.9 | 8.68375 |
| 251.00 | 11.10547 | 699656.0 | 5.84375 |
| 316.00 | 9.72301 | 970901.3 | 5.11630 |
| 398.00 | 6.42261 | 1017368.4 | 3.37961 |
| 501.00 | 5.03864 | 1264705.2 | 2.65136 |
| 631.00 | 3.52070 | 1401807.7 | 1.85261 |
| 794.00 | 2.08369 | 1313635.2 | 1.09645 |
| 1000.00 | 1.77280 | 1772809.5 | .93286 |
| 1260.00 | .93986 | 1492132.6 | .49456 |
| 1590.00 | .70823 | 1790497.2 | .37267 |
| 2000.00 | .40777 | 1631088.8 | .21457 |
| 2510.00 | .25618 | 1613986.3 | .13480 |
| 3160.00 | .14647 | 1462616.3 | .07707 |
| 3980.00 | .08607 | 1363409.5 | .04529 |
| 5010.00 | .04889 | 1227161.6 | .02572 |
| 6310.00 | .02583 | 1028600.2 | .01359 |
| 7940.00 | .01163 | 733739.3 | .00612 |

| DELAY | RU |
|---|---|
| .00001 | 1.00000 |
| .00005 | .95664 |
| .00010 | .86660 |
| .00015 | .80176 |
| .00020 | .74444 |
| .00025 | .67544 |
| .00030 | .61871 |
| .00050 | .47353 |
| .00080 | .27753 |
| .00100 | .18541 |
| .00120 | .11976 |
| .00150 | .09306 |
| .00180 | .10683 |
| .00200 | .11136 |
| .00220 | .10022 |
| .00250 | .05902 |
| .00300 | .03834 |
| .00350 | .02744 |
| .00500 | -.03900 |
| .00650 | -.06672 |
| .00800 | -.05929 |
| .00950 | -.04025 |
| .01100 | -.03100 |
| .01250 | -.03380 |
| .01400 | -.03790 |
| .01550 | -.03458 |
| .01700 | -.02648 |
| .01850 | -.02136 |
| .02000 | -.02267 |
| .02150 | -.02599 |

MACROSCALE = .0164
MICROSCALE = .0103(CURVE FIT)
MICROSCALE = .0052(INTEGRAL)

RUN NO. 20 AT R/A= .75, U= 19.50

| FREQ | F(N)X10000 | F(N)X10000XN**2 | E(N)X10000 |
|---|---|---|---|
| 10.00 | 9.99797 | 999.7 | 21.38473 |
| 12.60 | 33.28650 | 5284.5 | 71.19670 |
| 15.90 | 139.42215 | 35247.3 | 298.21090 |
| 20.00 | 85.48834 | 34195.3 | 182.85155 |
| 25.10 | 84.11995 | 52996.4 | 179.92469 |
| 31.60 | 86.64642 | 86521.6 | 185.32856 |
| 39.80 | 67.85524 | 107485.4 | 145.13601 |
| 50.10 | 47.40429 | 118985.2 | 101.39334 |
| 63.10 | 40.52701 | 161362.7 | 86.68348 |
| 79.40 | 28.90142 | 182205.0 | 61.81744 |
| 100.00 | 25.65358 | 256535.8 | 54.87062 |
| 126.00 | 17.48662 | 277617.6 | 37.40224 |
| 159.00 | 12.20222 | 308484.5 | 26.09941 |
| 200.00 | 12.78789 | 511515.8 | 27.35211 |
| 251.00 | 8.08446 | 509329.2 | 17.29190 |
| 316.00 | 6.73997 | 673026.6 | 14.41616 |
| 398.00 | 4.75390 | 753036.9 | 10.16814 |
| 501.00 | 3.42257 | 859069.3 | 7.32056 |
| 631.00 | 2.33670 | 930384.5 | 4.99799 |
| 794.00 | 1.38295 | 871864.1 | 2.95800 |
| 1000.00 | 1.05213 | 1052137.4 | 2.25042 |
| 1260.00 | .61582 | 977677.6 | 1.31718 |
| 1590.00 | .44567 | 1126714.9 | .95326 |
| 2000.00 | .24091 | 963641.4 | .51528 |
| 2510.00 | .15858 | 999126.8 | .33920 |
| 3160.00 | .08275 | 826322.0 | .17699 |
| 3980.00 | .04447 | 704434.3 | .09511 |
| 5010.00 | .02507 | 629400.3 | .05363 |
| 6310.00 | .01339 | 533139.1 | .02864 |
| 7940.00 | .00544 | 343333.2 | .01164 |

| DELAY | RU |
|---|---|
| .00001 | 1.00000 |
| .00005 | .96916 |
| .00010 | .91424 |
| .00015 | .87207 |
| .00020 | .83519 |
| .00025 | .79042 |
| .00030 | .75264 |
| .00050 | .64598 |
| .00080 | .47839 |
| .00100 | .38513 |
| .00120 | .31411 |
| .00150 | .27610 |
| .00180 | .28575 |
| .00200 | .28821 |
| .00220 | .27264 |
| .00250 | .22240 |
| .00300 | .18228 |
| .00350 | .15850 |
| .00500 | .03868 |
| .00650 | -.03329 |
| .00800 | -.05622 |
| .00950 | -.05761 |
| .01100 | -.06540 |
| .01250 | -.08454 |
| .01400 | -.10198 |
| .01550 | -.10529 |
| .01700 | -.09615 |
| .01850 | -.08495 |
| .02000 | -.07871 |
| .02150 | -.07484 |

MACROSCALE = .0275
MICROSCALE = .0108(CURVE FIT)
MICROSCALE = .0058(INTEGRAL)

RUN NO. 20 AT R/A= .75, U= 6.83

| FREQ | F(N)X10000 | F(N)X10000XN**2 | E(N)X10000 |
|---|---|---|---|
| 10.00 | 22.17544 | 2217.5 | 6.45606 |
| 12.60 | 54.24187 | 8611.4 | 15.79175 |
| 15.90 | 182.98066 | 46259.3 | 53.27221 |
| 20.00 | 142.64373 | 57057.4 | 41.52869 |
| 25.10 | 116.88730 | 73640.1 | 34.03007 |
| 31.60 | 94.00866 | 93873.2 | 27.36928 |
| 39.80 | 71.40011 | 113100.6 | 20.78712 |
| 50.10 | 61.88568 | 155333.6 | 18.01713 |
| 63.10 | 55.84091 | 222336.7 | 16.25728 |
| 79.40 | 37.21180 | 234596.6 | 10.83368 |
| 100.00 | 29.03034 | 290303.4 | 8.45177 |
| 126.00 | 19.78836 | 314160.0 | 5.76110 |
| 159.00 | 11.93202 | 301653.6 | 3.47384 |
| 200.00 | 12.54395 | 501758.3 | 3.65199 |
| 251.00 | 6.79054 | 427811.0 | 1.97697 |
| 316.00 | 5.29663 | 528900.2 | 1.54203 |
| 398.00 | 3.49873 | 554213.2 | 1.01860 |
| 501.00 | 2.07610 | 521103.3 | .60442 |
| 631.00 | 1.26737 | 504620.3 | .36897 |
| 794.00 | .66905 | 421797.4 | .19478 |
| 1000.00 | .44114 | 441140.4 | .12843 |
| 1260.00 | .20825 | 330631.9 | .06063 |
| 1590.00 | .10633 | 268838.1 | .03095 |
| 2000.00 | .03805 | 152227.9 | .01107 |
| 2510.00 | .01384 | 87240.7 | .00403 |
| 3160.00 | .00403 | 40336.1 | .00117 |
| 3980.00 | .00104 | 16562.9 | .00030 |
| 5010.00 | .00029 | 7287.1 | .00008 |
| 6310.00 | .00007 | 2942.8 | .00002 |

| DELAY | RU |
|---|---|
| .00001 | 1.00000 |
| .00005 | 1.00476 |
| .00010 | .99097 |
| .00015 | .97141 |
| .00020 | .95006 |
| .00025 | .92689 |
| .00030 | .90078 |
| .00050 | .80168 |
| .00080 | .66473 |
| .00100 | .57030 |
| .00120 | .50394 |
| .00150 | .45375 |
| .00180 | .43770 |
| .00200 | .41783 |
| .00220 | .38485 |
| .00250 | .32194 |
| .00300 | .25315 |
| .00350 | .20079 |
| .00500 | .06635 |
| .00650 | -.00823 |
| .00800 | -.05652 |
| .00950 | -.07180 |
| .01100 | -.07390 |
| .01250 | -.09498 |
| .01400 | -.12294 |
| .01550 | -.13479 |
| .01700 | -.13639 |
| .01850 | -.13445 |
| .02000 | -.12620 |

MACROSCALE = .0130

MICROSCALE = .0075(CURVE FIT)

MICROSCALE = .0052(INTEGRAL)

RUN NO. 21 AT R/A= .05, U= 15.70

| FREQ | F(N)X10000 | F(N)X10000XN**2 | E(N)X10000 |
|---|---|---|---|
| 10.00 | 8.35997 | 835.9 | 2.04467 |
| 12.60 | 19.20974 | 3049.7 | 4.69831 |
| 15.90 | 74.39066 | 18806.7 | 18.19444 |
| 20.00 | 48.55558 | 19422.2 | 11.87570 |
| 25.10 | 49.86679 | 31416.5 | 12.19640 |
| 31.60 | 45.59155 | 45525.8 | 11.15076 |
| 39.80 | 48.77763 | 77265.7 | 11.93001 |
| 50.10 | 38.29430 | 96119.0 | 9.36600 |
| 63.10 | 37.67286 | 149998.6 | 9.21401 |
| 79.40 | 34.35488 | 216585.5 | 8.40250 |
| 100.00 | 28.55857 | 285585.7 | 6.98484 |
| 126.00 | 19.46678 | 309054.6 | 4.76118 |
| 159.00 | 14.75618 | 373051.2 | 3.60906 |
| 200.00 | 17.33370 | 693348.1 | 4.23947 |
| 251.00 | 11.04276 | 695705.0 | 2.70083 |
| 316.00 | 9.63744 | 962356.3 | 2.35712 |
| 398.00 | 6.74607 | 1068605.2 | 1.64995 |
| 501.00 | 4.97651 | 1249109.3 | 1.21715 |
| 631.00 | 3.34880 | 1333362.2 | .81904 |
| 794.00 | 1.78552 | 1125658.1 | .43670 |
| 1000.00 | 1.12090 | 1120908.4 | .27415 |
| 1260.00 | .62597 | 993792.9 | .15310 |
| 1590.00 | .36451 | 921528.4 | .08915 |
| 2000.00 | .14975 | 599016.5 | .03662 |
| 2510.00 | .07136 | 449628.0 | .01745 |
| 3160.00 | .02984 | 298067.3 | .00730 |
| 3980.00 | .01544 | 244661.8 | .00377 |
| 5010.00 | .00619 | 155612.5 | .00151 |
| 6310.00 | .00234 | 93460.4 | .00057 |
| 7940.00 | .00053 | 33487.8 | .00012 |

| DELAY | RU |
|---|---|
| .00001 | 1.00000 |
| .00005 | .98784 |
| .00010 | .94720 |
| .00015 | .90039 |
| .00020 | .85096 |
| .00025 | .79446 |
| .00030 | .74148 |
| .00050 | .57972 |
| .00080 | .35476 |
| .00100 | .24765 |
| .00120 | .17593 |
| .00150 | .14545 |
| .00180 | .15739 |
| .00200 | .16060 |
| .00220 | .14741 |
| .00250 | .10123 |
| .00300 | .07158 |
| .00350 | .05814 |
| .00500 | -.02663 |
| .00650 | -.06363 |
| .00800 | -.05955 |
| .00950 | -.04307 |
| .01100 | -.03964 |
| .01250 | -.04947 |
| .01400 | -.05805 |
| .01550 | -.05478 |
| .01700 | -.04443 |
| .01850 | -.03759 |
| .02000 | -.03851 |
| .02150 | -.04115 |

MACROSCALE = .0141
MICROSCALE = .0086(CURVE FIT)
MICROSCALE = .0063(INTEGRAL)

RUN NO. 21 AT R/A= .75, U= 17.40

| FREQ | F(N)X10000 | F(N)X10000XN**2 | E(N)X10000 |
|---|---|---|---|
| 10.00 | 12.80912 | 1280.9 | 17.40874 |
| 12.60 | 34.54301 | 5484.0 | 46.94705 |
| 15.90 | 152.20001 | 38477.6 | 206.85345 |
| 20.00 | 109.52519 | 43810.0 | 148.85454 |
| 25.10 | 96.43591 | 60755.5 | 131.06504 |
| 31.60 | 77.08950 | 76978.4 | 104.77154 |
| 39.80 | 69.30339 | 109779.3 | 94.18952 |
| 50.10 | 52.06876 | 130693.1 | 70.76612 |
| 63.10 | 38.58653 | 153636.5 | 52.44255 |
| 79.40 | 27.81189 | 175336.1 | 37.79885 |
| 100.00 | 21.69711 | 216971.1 | 29.48832 |
| 126.00 | 14.99728 | 238096.9 | 20.38265 |
| 159.00 | 10.79527 | 272915.2 | 14.67174 |
| 200.00 | 13.16912 | 526765.0 | 17.89802 |
| 251.00 | 8.53366 | 537629.4 | 11.59801 |
| 316.00 | 6.99439 | 698432.4 | 9.50601 |
| 398.00 | 5.14782 | 815435.7 | 6.99635 |
| 501.00 | 3.78085 | 948999.4 | 5.13852 |
| 631.00 | 2.76786 | 1102054.1 | 3.76177 |
| 794.00 | 1.50970 | 951769.2 | 2.05181 |
| 1000.00 | 1.12373 | 1123731.3 | 1.52725 |
| 1260.00 | .56260 | 893192.2 | .76463 |
| 1590.00 | .34340 | 868152.7 | .46671 |
| 2000.00 | .16731 | 669251.5 | .22739 |
| 2510.00 | .09030 | 568912.1 | .12272 |
| 3160.00 | .04218 | 421208.8 | .05732 |
| 3980.00 | .02075 | 328814.7 | .02821 |
| 5010.00 | .01147 | 288072.8 | .01559 |
| 6310.00 | .00499 | 198941.0 | .00679 |
| 7940.00 | .00203 | 128265.6 | .00276 |

| DELAY | RU |
|---|---|
| .00001 | 1.00000 |
| .00005 | .94495 |
| .00010 | .90506 |
| .00015 | .86491 |
| .00020 | .82488 |
| .00025 | .77871 |
| .00030 | .73689 |
| .00050 | .61986 |
| .00080 | .46156 |
| .00100 | .38484 |
| .00120 | .32957 |
| .00150 | .30133 |
| .00180 | .30413 |
| .00200 | .30255 |
| .00220 | .28827 |
| .00250 | .24548 |
| .00300 | .20931 |
| .00350 | .18196 |
| .00500 | .06388 |
| .00650 | -.01604 |
| .00800 | -.05089 |
| .00950 | -.05960 |
| .01100 | -.06745 |
| .01250 | -.08406 |
| .01400 | -.10271 |
| .01550 | -.11210 |
| .01700 | -.10941 |
| .01850 | -.10035 |
| .02000 | -.09206 |
| .02150 | -.08592 |

MACROSCALE = .0258
MICROSCALE = .0095(CURVE FIT)
MICROSCALE = .0066(INTEGRAL)

RUN NO. 21 AT R/A= .75, U= 6.23

| FREQ | F(N)X10000 | F(N)X1000)XN**2 | E(N)X10000 |
|---|---|---|---|
| 10.00 | 11.93109 | 1193.1 | 2.48129 |
| 12.60 | 43.79402 | 6952.7 | 9.10779 |
| 15.90 | 169.59451 | 42875.1 | 35.27037 |
| 20.00 | 102.93047 | 41172.1 | 21.40632 |
| 25.10 | 124.77040 | 78606.5 | 25.94835 |
| 31.60 | 102.59331 | 102445.5 | 21.33621 |
| 39.80 | 68.65045 | 108745.0 | 14.27715 |
| 50.10 | 47.89526 | 120217.5 | 9.96072 |
| 63.10 | 55.04109 | 219152.1 | 11.44683 |
| 79.40 | 36.67881 | 231236.4 | 7.62804 |
| 100.00 | 30.37502 | 303750.2 | 6.31705 |
| 126.00 | 21.82698 | 346525.1 | 4.53933 |
| 159.00 | 12.44025 | 314501.9 | 2.58718 |
| 200.00 | 14.35344 | 574137.9 | 2.98506 |
| 251.00 | 8.74224 | 550770.1 | 1.81811 |
| 316.00 | 5.94007 | 593151.7 | 1.23534 |
| 398.00 | 3.92376 | 621539.7 | .81602 |
| 501.00 | 2.38021 | 597437.4 | .49501 |
| 631.00 | 1.45019 | 577412.8 | .30159 |
| 794.00 | .65712 | 414275.1 | .13666 |
| 1000.00 | .38583 | 385838.1 | .08024 |
| 1260.00 | .15158 | 240654.6 | .03152 |
| 1590.00 | .05793 | 146457.1 | .01204 |
| 2000.00 | .01984 | 79364.0 | .00412 |
| 2510.00 | .00570 | 35937.1 | .00118 |
| 3160.00 | .00131 | 13128.4 | .00027 |
| 3980.00 | .00024 | 3837.8 | .00005 |

| DELAY | RU |
|---|---|
| .00001 | 1.00000 |
| .00005 | .98987 |
| .00010 | .98208 |
| .00015 | .96506 |
| .00020 | .94359 |
| .00025 | .91974 |
| .00030 | .89452 |
| .00050 | .78792 |
| .00080 | .66159 |
| .00100 | .58286 |
| .00120 | .49585 |
| .00150 | .38878 |
| .00180 | .31051 |
| .00200 | .27287 |
| .00220 | .25280 |
| .00250 | .23888 |
| .00300 | .24116 |
| .00350 | .21318 |
| .00500 | .09540 |
| .00650 | -.00384 |
| .00800 | -.04683 |
| .00950 | -.06130 |
| .01100 | -.07509 |
| .01250 | -.08939 |
| .01400 | -.09950 |
| .01550 | -.11184 |
| .01700 | -.12993 |

MACROSCALE = .0111
MICROSCALE = .0055(CURVE FIT)
MICROSCALE = .0052(INTEGRAL)

Table 7

Autocorrelation Results and Transformations to Energy Spectra

The table contains a separate computer printout for each autocorrelation measurement. The information is identified by the following symbols:

R/A - corresponds to r/a in the text, radial position divided by pipe radius.

U - corresponds to $\bar{u}$ in the text, time average velocity in feet per second.

DELAY - autocorrelation delay time in seconds.

RU - autocorrelation coefficient corresponding to $R(\tau)$ in the text.

FREQ - frequency in cycles per second.

F(N) x 10000 - normalized spectrum function in seconds times 10,000.

RUN 40. 8 AT R/A= .50, U= 6.18

| DELAY | RU |
|---|---|
| 0.0000 | 1.00000 |
| .00011 | . 94 7 |
| .00022 | .98461 |
| .00033 | .97435 |
| .00045 | .94358 |
| .00056 | .93333 |
| .00067 | .90256 |
| .00078 | .81025 |
| .00090 | .76923 |
| .00146 | .56410 |
| .00202 | .41025 |
| .00146 | .27692 |
| .00315 | .20512 |
| .00371 | .12307 |
| .00427 | .02051 |
| .00461 | 0.00000 |
| .00540 | -.04102 |
| .00653 | -.08205 |
| .00765 | -.11282 |
| .0087 | -.12307 |
| .00990 | -.13333 |
| .01103 | -.12307 |
| .01216 | -.12307 |
| .01328 | -.11282 |
| .01441 | -.10256 |
| .01554 | -.09230 |
| .01666 | -.08205 |
| .01779 | -.06153 |
| .01891 | -.04102 |
| .02004 | -.01025 |

SCALE= .01134 MICROSCALE= .01186

| FREQ | F(N)X10000 |
|---|---|
| 3.18 | 22.81768 |
| 6.36 | 27.65778 |
| 15.92 | 56.18201 |
| 31.84 | 102.52800 |
| 63.69 | 63.27113 |
| 111.46 | 31.40732 |
| 159.23 | 16.71740 |
| 238.85 | 9.18042 |
| 318.47 | 7.31705 |
| 477.70 | -.82315 |
| 636.94 | -.92925 |
| 1114.64 | -.62786 |
| 1592.35 | .68456 |

RUN NO. 8 AT R/A= .85, U= 5.24

| DELAY | RU |
|---|---|
| 0.00000 | 1.00000 |
| .00011 | .99487 |
| .00022 | .98461 |
| .00033 | .97435 |
| .00045 | .94358 |
| .00056 | .92307 |
| .00067 | .88205 |
| .00078 | .81025 |
| .00090 | .77948 |
| .00101 | .74871 |
| .00112 | .70769 |
| .00123 | .66666 |
| .00180 | .52307 |
| .00236 | .35897 |
| .00292 | .23589 |
| .00349 | .14358 |
| .00405 | .07179 |
| .00461 | .02051 |
| .00472 | 0.00000 |
| .00518 | -.04102 |
| .00574 | -.07179 |
| .00686 | -.09230 |
| .00799 | -.09230 |
| .00912 | -.10256 |
| .01024 | -.10256 |
| .01137 | -.10256 |
| .01250 | -.09230 |
| .01362 | -.08205 |
| .01475 | -.08205 |
| .01587 | -.07179 |
| .01700 | -.07179 |
| .01813 | -.05128 |
| .01925 | -.03076 |
| .02038 | -.02051 |
| .02150 | 0.00000 |

SCALE= .01060 MICROSCALE= .01041

| FREQ | F(N)X10000 |
|---|---|
| 3.18 | 33.37815 |
| 6.36 | 37.67717 |
| 15.92 | 62.64044 |
| 31.84 | 100.67005 |
| 63.69 | 67.19976 |
| 111.46 | 33.96793 |
| 159.23 | 14.58581 |
| 238.85 | 7.33656 |
| 318.47 | 2.70840 |
| 477.70 | 1.13075 |
| 636.94 | .35402 |
| 1114.64 | -.19632 |
| 1592.35 | .06431 |

RUN NO. 9 AT R/A=0.00, U= 6.90

| DELAY | RU |
|---|---|
| 0.00000 | 1.00000 |
| .00011 | .98979 |
| .00022 | .96938 |
| .00033 | .94387 |
| .00045 | .89795 |
| .00056 | .83673 |
| .00078 | .78571 |
| .00135 | .57142 |
| .00191 | .40816 |
| .00247 | .23469 |
| .00304 | .13265 |
| .00360 | .06122 |
| .00416 | .01020 |
| .00427 | 0.00000 |
| .00529 | -.07142 |
| .00698 | -.13265 |
| .00810 | -.15306 |
| .01036 | -.15306 |
| .01148 | -.15306 |
| .01373 | -.12244 |
| .01599 | -.07142 |
| .01711 | -.04081 |
| .01936 | -.02040 |
| .02162 | 0.00000 |

SCALE= .01194 MICROSCALE= .00986

| FREQ | F(N)X10000 |
|---|---|
| 3.18 | 7.57120 |
| 6.36 | 12.37380 |
| 15.92 | 41.23183 |
| 31.84 | 94.00151 |
| 63.69 | 69.19437 |
| 111.46 | 36.40084 |
| 159.23 | 19.37071 |
| 238.85 | 7.93749 |
| 318.47 | 2.91388 |
| 477.70 | 1.31898 |
| 636.94 | .75748 |
| 1114.64 | .14621 |
| 1592.35 | -.07332 |

RUN NO. 9 AT R/A= .50, U= 6.56

| DELAY | RU |
|---|---|
| 0.00000 | 1.00000 |
| .00011 | .98984 |
| .00022 | .98984 |
| .00033 | .97461 |
| .00045 | .95431 |
| .00056 | .91370 |
| .00067 | .86294 |
| .00078 | .82233 |
| .00090 | .80203 |
| .00101 | .76142 |
| .00112 | .74111 |
| .00123 | .70050 |
| .00180 | .54822 |
| .00236 | .38578 |
| .00292 | .26395 |
| .00349 | .14213 |
| .00405 | .07106 |
| .00461 | .01015 |
| .00472 | 0.00000 |
| .00518 | -.03045 |
| .00630 | -.10152 |
| .00743 | -.12182 |
| .00855 | -.15228 |
| .01081 | -.15228 |
| .01418 | -.11167 |
| .01644 | -.04060 |
| .01981 | 0.00000 |

SCALE= .01366 MICROSCALE= .01297

| FREQ | F(N)X10000 |
|---|---|
| 3.18 | 28.25462 |
| 6.36 | 32.56619 |
| 15.92 | 58.47484 |
| 31.84 | 105.34320 |
| 63.69 | 73.19704 |
| 111.46 | 34.60122 |
| 159.23 | 16.30173 |
| 238.85 | 4.71520 |
| 318.47 | 2.67220 |
| 477.70 | .71172 |
| 636.94 | .23742 |
| 1114.64 | -.10598 |
| 1592.35 | -.14010 |

RUN NO. 9 AT R/A= .85, U= 5.64

| DELAY | RU |
|---|---|
| 0.00000 | 1.00000 |
| .00011 | .98984 |
| .00022 | .97969 |
| .00033 | .96954 |
| .00045 | .92893 |
| .00056 | .91370 |
| .00112 | .76142 |
| .00168 | .58883 |
| .00225 | .45685 |
| .00281 | .29441 |
| .00337 | .23350 |
| .00394 | .12182 |
| .00450 | .04060 |
| .00484 | 0.00000 |
| .00596 | -.08121 |
| .00765 | -.12182 |
| .00878 | -.15228 |
| .01103 | -.13197 |
| .01328 | -.13197 |
| .01610 | -.09137 |
| .01891 | -.06091 |
| .02173 | -.01015 |
| .01328 | 0.00000 |

SCALE= .01242 MICROSCALE= .01072

| FREQ | F(N)X10000 |
|---|---|
| 3.18 | 47.86440 |
| 6.36 | 50.01080 |
| 15.92 | 63.63255 |
| 31.84 | 94.98555 |
| 63.69 | 87.49672 |
| 111.46 | 30.79003 |
| 159.23 | 9.60233 |
| 238.85 | 2.76928 |
| 318.47 | .10869 |
| 477.70 | -1.18262 |
| 636.94 | -.15387 |
| 1114.64 | .77276 |
| 1592.35 | -.43834 |

RUN NO. 9 AT R/A= .85, U= 2.47

| DELAY | RU |
|---|---|
| 0.00000 | 1.00000 |
| .00011 | 1.00000 |
| .00033 | .99487 |
| .00056 | .98974 |
| .00078 | .98461 |
| .00112 | .97435 |
| .00135 | .94358 |
| .00168 | .92307 |
| .00225 | .85128 |
| .00281 | .76923 |
| .00337 | .69743 |
| .00394 | .58461 |
| .00450 | .48205 |
| .00506 | .38974 |
| .00619 | .20512 |
| .00731 | .06153 |
| .00788 | 0.00000 |
| .00822 | -.03076 |
| .00878 | -.08205 |
| .00934 | -.13333 |
| .01047 | -.21538 |
| .01159 | -.24615 |
| .01272 | -.33846 |
| .01385 | -.30769 |
| .01666 | -.27692 |
| .01948 | -.26666 |
| .02229 | -.18461 |
| .02511 | -.11282 |
| .02792 | -.05128 |
| .03074 | -.03076 |
| .03355 | 0.00000 |

SCALE= .01091 MICROSCALE= .01492

| FREQ | F(N)X10000 |
|---|---|
| 3.18 | 15.75390 |
| 6.36 | 46.67622 |
| 15.92 | 193.03502 |
| 31.84 | 237.79104 |
| 63.69 | 50.85975 |
| 111.46 | 5.53605 |
| 159.23 | -1.68314 |
| 238.85 | .45721 |
| 318.47 | -.10299 |
| 477.70 | .11877 |
| 636.94 | -.10215 |
| 1114.64 | .01324 |
| 1592.35 | -.01429 |

RUN NO. 10 AT R/A=0.00, U= 6.74

| DELAY | RU |
|---|---|
| 0.00000 | 1.00000 |
| .00005 | 1.00000 |
| .00016 | .98974 |
| .00028 | .92307 |
| .00039 | .88205 |
| .00050 | .84102 |
| .00061 | .81025 |
| .00095 | .67692 |
| .00152 | .51282 |
| .00208 | .37948 |
| .00264 | .25641 |
| .00320 | .20512 |
| .00377 | .14358 |
| .00433 | .09230 |
| .00489 | .04102 |
| .00546 | .01025 |
| .00557 | 0.00000 |
| .00602 | -.03076 |
| .00715 | -.09230 |
| .00827 | -.12307 |
| .01052 | -.14358 |
| .01165 | -.13333 |
| .01390 | -.11282 |
| .01728 | -.07179 |
| .01953 | -.04102 |
| .02179 | -.02051 |
| .02516 | 0.00000 |

SCALE= .01301 MICROSCALE= .00831

| FREQ | F(N)X10000 |
|---|---|
| 3.18 | 19.66430 |
| 6.36 | 25.65000 |
| 15.92 | 59.53093 |
| 31.84 | 105.29313 |
| 63.69 | 61.58561 |
| 111.46 | 25.65636 |
| 159.23 | 17.91933 |
| 238.85 | 8.82299 |
| 318.47 | 4.05303 |
| 477.70 | 1.89653 |
| 636.94 | .87246 |
| 1114.64 | .26748 |
| 1592.35 | .06286 |

RUN NO. 10 AT R/A= .85, U= 5.23

| DELAY | RU |
|---|---|
| 0.00000 | 1.00000 |
| .00005 | .99492 |
| .00011 | .97969 |
| .00022 | .94416 |
| .00033 | .89340 |
| .00045 | .83248 |
| .00056 | .76142 |
| .00112 | .57868 |
| .00168 | .37563 |
| .00225 | .30456 |
| .00281 | .24365 |
| .00337 | .17258 |
| .00394 | .10152 |
| .00450 | .03045 |
| .00495 | 0.00000 |
| .00506 | -.01015 |
| .00563 | -.04060 |
| .00675 | -.07106 |
| .00788 | -.11167 |
| .01013 | -.11167 |
| .01238 | -.10152 |
| .01351 | -.10152 |
| .01576 | -.06091 |
| .01801 | -.03045 |
| .01914 | -.02030 |
| .02139 | -.01015 |
| .02252 | 0.00000 |

SCALE= .00910 MICROSCALE= .00601

| FREQ | F(N)X10000 |
|---|---|
| 3.18 | 24.49020 |
| 6.36 | 28.33410 |
| 15.92 | 50.97548 |
| 31.84 | 88.42736 |
| 63.69 | 58.82678 |
| 111.46 | 27.53574 |
| 159.23 | 15.43766 |
| 238.85 | 9.61485 |
| 318.47 | 7.24590 |
| 477.70 | 1.66635 |
| 636.94 | 1.39469 |
| 1114.64 | .35995 |
| 1592.35 | -.02993 |

RUN NO. 12 AT R/A=0.00, U= 7.01

| DELAY | RU |
|---|---|
| 0.00000 | 1.00000 |
| .00011 | .99489 |
| .00022 | .97959 |
| .00033 | .95918 |
| .00045 | .91836 |
| .00056 | .88775 |
| .00067 | .84693 |
| .00123 | .60204 |
| .00180 | .42857 |
| .00236 | .30612 |
| .00292 | .22448 |
| .00349 | .13265 |
| .00405 | .07142 |
| .00461 | .05102 |
| .00518 | 0.00000 |
| .00574 | -.04081 |
| .00686 | -.07142 |
| .00799 | -.09183 |
| .00912 | -.10204 |
| .01024 | -.10204 |
| .01137 | -.10204 |
| .01362 | -.10204 |
| .01475 | -.06122 |
| .01587 | -.03061 |
| .01700 | -.02040 |
| .01813 | -.01020 |
| .01925 | 0.00000 |

SCALE= .01331 MICROSCALE= .01200

| FREQ | F(N)X10000 |
|---|---|
| 11.14 | 48.45026 |
| 15.92 | 57.88931 |
| 31.84 | 89.21534 |
| 63.69 | 65.37825 |
| 111.46 | 35.24638 |
| 159.23 | 17.14400 |
| 238.85 | 9.38327 |
| 318.47 | 4.34227 |
| 477.70 | 1.19365 |
| 636.94 | .36982 |
| 1114.64 | -.05836 |
| 1592.35 | .06329 |
| 2388.53 | .00389 |

RUN NO. 12 AT R/A= .85, U= 5.00

| DELAY | RU |
|---|---|
| 0.00000 | 1.00000 |
| .00011 | .97938 |
| .00022 | .94329 |
| .00033 | .82474 |
| .00090 | .60824 |
| .00146 | .43298 |
| .00202 | .27835 |
| .00259 | .17525 |
| .00315 | .10309 |
| .00371 | .04123 |
| .00427 | 0.00000 |
| .00484 | -.02061 |
| .00540 | -.06185 |
| .00653 | -.06185 |
| .00765 | -.07216 |
| .00990 | -.09278 |
| .01216 | -.10309 |
| .01441 | -.08247 |
| .01666 | -.03092 |
| .01891 | -.02061 |
| .02117 | 0.00000 |

SCALE= .00737 MICROSCALE= .00407

| FREQ | F(N)X10000 |
|---|---|
| 11.14 | 30.23681 |
| 15.92 | 41.19511 |
| 31.84 | 74.57083 |
| 63.69 | 52.29754 |
| 111.46 | 33.51682 |
| 159.23 | 17.06900 |
| 238.85 | 8.21281 |
| 318.47 | 4.23612 |
| 477.70 | 1.65668 |
| 636.94 | .99072 |
| 1114.64 | -.17233 |
| 1592.35 | -.57261 |
| 2388.53 | -.53163 |

# APPENDIX IV

## CALIBRATION FACTORS

1. Frequency Response of Ampex 601-2 Recorder

Table 8 shows the three frequency response determinations for three different adjustments of the recorder equalization circuits.

2. Peak Gain Factors for Band Pass Filter

Table 9 shows the peak gain factor for each band corresponding to the band center frequency.

3. Hot-Film Probe Calibration Coefficients

The coefficients A, B, and c of equation 96 are shown in Table 10. The standard deviation of $E^2$ about the least square best fit is shown for each run.

Table 8

Ampex 601-2 Recorder Frequency Response

The responses below are overall playback to input ratios:

| Frequency | Runs 8,9,10,12,14 | | Runs 17,18,19 | Runs 15,20,21 |
|---|---|---|---|---|
| cps | Channel I | Channel II | Channel I | Channel I |
| 10 | 0.056 | 0.021 | 0.055 | 0.16 |
| 15 | 0.277 | 0.238 | 0.215 | 0.28 |
| 20 | 0.624 | 0.434 | 0.492 | 0.63 |
| 30 | 0.827 | 0.842 | 0.659 | 0.76 |
| 40 | 0.900 | 0.921 | 0.790 | 0.85 |
| 50 | 0.967 | 0.895 | 0.856 | 0.91 |
| 60 | 0.935 | 0.895 | 0.856 | 0.89 |
| 70 | 0.967 | 0.947 | | |
| 80 | 1.000 | 1.000 | 0.905 | 0.94 |
| 90 | 1.000 | 1.000 | | |
| 100 | 1.000 | 1.000 | 0.935 | 0.96 |
| 200 | 1.000 | 0.975 | 0.988 | 0.97 |
| 300 | 1.000 | 1.000 | 0.996 | 0.97 |
| 400 | 1.000 | 0.975 | 1.000 | 0.97 |
| 600 | 1.032 | 0.975 | 1.000 | 0.99 |
| 800 | 1.032 | 0.947 | 1.032 | 1.05 |
| 1000 | 1.068 | 0.921 | 1.028 | 1.06 |
| 1500 | 1.068 | 0.816 | 1.032 | 1.12 |
| 2000 | 1.100 | 0.711 | 1.022 | 1.16 |
| 3000 | 1.032 | 0.487 | 0.878 | 1.19 |
| 4000 | 0.900 | 0.238 | 0.593 | 1.17 |
| 6000 | 0.677 | 0.164 | 0.300 | 1.12 |
| 8000 | 0.434 | | 0.254 | 1.08 |
| 10000 | | | 0.246 | 0.88 |

Table 9

Peak Gain Factors for the Band Pass Filter*

| Band Center Frequency cps | Band Gain Ratio | Band Width | |
|---|---|---|---|
| | | Low Frequency cps | High Frequency cps |
| 10.0 | 2.70 | 8.91 | 11.2 |
| 12.6 | 3.22 | 11.2 | 14.1 |
| 15.9 | 2.82 | 14.1 | 17.8 |
| 20.0 | 3.42 | 17.8 | 22.4 |
| 25.1 | 3.32 | 22.4 | 28.2 |
| 31.6 | 3.82 | 28.2 | 35.5 |
| 39.8 | 3.98 | 35.5 | 44.8 |
| 50.1 | 4.26 | 44.8 | 56.2 |
| 63.1 | 4.23 | 56.2 | 70.8 |
| 79.4 | 4.41 | 70.8 | 89.1 |
| 100 | 3.80 | 89.1 | 112 |
| 126 | 4.35 | 112 | 141 |
| 159 | 4.78 | 141 | 178 |
| 200 | 3.72 | 178 | 224 |
| 251 | 4.53 | 224 | 282 |
| 316 | 4.10 | 282 | 355 |
| 398 | 4.51 | 355 | 448 |
| 501 | 4.26 | 448 | 562 |
| 631 | 4.02 | 562 | 708 |
| 794 | 4.37 | 708 | 891 |
| 1000 | 4.00 | 891 | 1120 |
| 1260 | 4.31 | 1120 | 1410 |
| 1590 | 3.80 | 1410 | 1780 |
| 2000 | 4.16 | 1780 | 2240 |
| 2510 | 4.00 | 2240 | 2820 |
| 3160 | 4.07 | 2820 | 3550 |
| 3980 | 4.05 | 3550 | 4480 |
| 5010 | 3.90 | 4480 | 5620 |
| 6310 | 3.53 | 5620 | 7080 |
| 7940 | 4.19 | 7080 | 8910 |
| 10000 | 3.40 | 8910 | 11200 |
| 12600 | 3.62 | 11200 | 14100 |
| 15900 | 2.76 | 14100 | 17800 |
| 20000 | 3.10 | 17800 | 22400 |

* Measurements of T. B. Watson (97), who designed and built the instrument.

Table 10

Hot-Film Probe Calibrations

The best fit to the equation $E^2 = A+B(\bar{u})^c$, is given for each run. Runs 13 and 20 are not included because a different calibration was used at each radial position.

| Run No. | Data Points | A | B | c | Std. Dev. about $E^2$ |
|---|---|---|---|---|---|
| 1 | 90 | 48.63 | 161.08 | 0.50 | 3.8 |
| 2* | 48 | 55.62 | 154.02 | 0.50 | 5.0 |
| | 96 | 54.29 | 158.47 | 0.50 | 4.6 |
| 3 | 90 | 45.30 | 121.93 | 0.50 | 1.7 |
| 4 | 80 | 42.11 | 115.22 | 0.50 | 3.4 |
| 6 | 25 | 44.60 | 110.72 | 0.50 | 3.1 |
| 7 | 50 | 43.22 | 116.63 | 0.40 | 2.9 |
| 8 | 20 | 43.42 | 113.27 | 0.45 | 3.0 |
| 9 | 44 | 35.26 | 118.34 | 0.30 | 3.0 |
| 10 | 12 | 47.81 | 130.09 | 0.50 | 2.0 |
| 11 | 35 | 48.32 | 130.37 | 0.50 | 2.5 |
| 12 | 20 | 45.30 | 126.30 | 0.50 | 3.4 |
| 14 | 12 | 53.41 | 121.66 | 0.45 | 3.0 |
| 15 | 16 | 57.40 | 160.49 | 0.50 | 6.7 |
| 16 | 16 | 58.00 | 152.72 | 0.50 | 2.9 |
| 17 | 21 | 56.90 | 177.59 | 0.35 | 5.4 |
| 19**(fresh) | 4 | 54.70 | 45.20 | 0.50 | 0.9 |
| 19(degraded) | 4 | 52.13 | 84.88 | 0.35 | 1.5 |
| 21 | 32 | 53.60 | 130.10 | 0.40 | 5.4 |
| 22 | 24 | 42.79 | 110.43 | 0.50 | 6.6 |

* The calibration for the first six points is different from the calibration for the last twelve.

** The calibrations were different for fresh and degraded solutions.

# APPENDIX V

## CALCULATION PROCEDURES

### 1. Turbulence Intensity

#### 1.1. Longitudinal intensity

The calibration of the hot-film probe has been described in Appendix II. The least squares regression involved was straight-forward. The calculation of turbulence intensity was simply an arithmetic computation following equation 79. Since many measurements were made, the repetitive calculations were done using the IBM 1620-II computer.

#### 1.2. Radial and tangential intensity and Reynolds stress

The calculation of radial and tangential turbulence intensities and Reynolds stresses from the V-probe measurements were complicated by the large distance (0.06 inches) between centers of the two films of the V. It was necessary to plot rms voltage versus r/a using radial positions at the center of each film. From these plots, readings corresponding to the same position were determined for each section of the V-probe. The dc voltage for a film at an angle $\theta$ to a steady velocity, $\bar{u}$, is:

$$E^2 = A + B\,(\bar{u} \sin \theta)^c$$

$$\text{or} \quad E^2 = A + B'\,(\bar{u})^c$$

The instantaneous voltage (dc plus fluctuating) for a film at an angle $\theta$ of 45° to the flow is:

$$(E')^2 = A + B'\,(\bar{u} + u' + v')^c$$

where u' and v' are longitudinal and transverse fluctuating velocity components, respectively. Analogous to equation 79, the rms voltage may be approximately linearly related to the root-mean-square of the sum

of u' and v':

$$\langle E' \rangle_+^2 = \left(\frac{\partial E}{\partial \bar{u}}\right)_+^2 \left(\overline{(u')^2} + \overline{(v')^2} + 2\overline{u'v'}\right)$$

For a film at an angle of -45° to the flow:

$$(E')^2 = A + B' (\bar{u} + u' - v')^c$$

$$\langle E' \rangle_-^2 = \left(\frac{\partial E}{\partial \bar{u}}\right)_-^2 \left(\overline{(u')^2} + \overline{(v')^2} - 2\,\overline{u'v'}\right)$$

Subtracting, the relation used to calculate the Reynolds stress $\overline{u'v'}$ was obtained:

$$\overline{u'v'} = 1/4 \langle E' \rangle_+^2 / \left(\frac{\partial E}{\partial \bar{u}}\right)_+^2 - 1/4 \langle E' \rangle_-^2 / \left(\frac{\partial E}{\partial \bar{u}}\right)_-^2$$

Using values for $\langle u' \rangle$ determined with a standard film probe, the values of $\langle v' \rangle$ were then calculated:

$$\langle v' \rangle = \left(\langle E' \rangle_+^2 / \left(\frac{\partial E}{\partial \bar{u}}\right)_+^2 - \overline{(u')^2} - 2\,\overline{u'v'}\right)^{1/2}$$

2. Velocity Profiles

The calculation of velocity profiles from impact tube data has been described by Hershey (33).

3. Energy Spectra

The reduction of the band pass filter data to energy spectra was done as follows:

(1) rms voltages obtained from each band were divided by the recorder frequency response factor and the band gain factor.

(2) Each corrected value was then squared and the sum of these squares was obtained.

(3) Each corrected value from (1) was divided by the band frequency width and by the sum of the squares to yield the value of F(n) for the band center frequency, n.

4. Autocorrelation and Macroscale

The autocorrelation calculations were as follows:

(1) Each delay time was found by dividing the micrometer movement by the factor, 8.88 inches per second, obtained from the calibration with a 100 cps signal.

(2) Each value of autocorrelation measured by the DISA correlator was normalized by dividing by the peak value at a time delay of zero. This peak value was usually about 0.98 - 0.99.

(3) The calculation of macroscale was simply a numerical integration of the autocorrelation function up to the first zero correlation coefficient using the trapezoidal rule.

5. Dissipation Spectra and Microscale

The dissipation spectra were determined by multiplying each spectrum value by the corresponding frequency squared. The value of the microscale was determined using equation 64. The numerical integration of the dissipation spectrum was done using the trapezoidal rule since the points were so close together. Some of the dissipation spectra levels were not insignificant at the highest measured frequency, but the errors introduced are less than 10 per cent for the 1-inch pipe data and negligible for the 2-inch pipe data.

6. Fourier Transformations

The Fourier transformations of energy spectra to autocorrelations and vice-versa were both done in the same manner. Equations 61 were used for the calculation, involving a numerical integration of the function times a cosine function. The greatest difficulties were experienced in obtaining from the spectra autocorrelations which did not oscillate at long delay times and in obtaining from the autocorrelations energy spectra

that did not oscillate at high frequencies. The best results were obtained by least square fitting of short intervals of the function to be integrated with a second degree power series, then integrating analytically. This eliminated the oscillation in the autocorrelations transformed from energy spectra and extended the transformed spectra to higher frequencies. The smoothing introduced by using least square fits for sections of the functions apparently eliminated noise caused by random errors in the individual points.

# APPENDIX VI

## MATERIALS

The solvents and polymers used in this investigation, their properties, and suppliers are as follows:

Benzene. Specific gravity range 0.882 - 0.886; maximum boiling range 1°C, including 80.1°C; acid wash color-0-1; acidity-negative; doctor test-sweet; corrosion - 16 maximum; sulfur as $H_2S/SO_2$ negative; thiophene free; solidification point - 4.85°C maximum; purchased from Independent Petrochemical Corp., St. Louis, Missouri.

Cyclohexane. Purity (wt. per cent cyclohexane) 99.0 per cent minimum; impurities-non-volatiles, water, benzene 0.1 per cent maximum; maximum boiling range 0.4°C, including 80.7°C; specific gravity range 0.780-0.784 at 15.5°C; purchased from G.S. Robins Co., St. Louis, Missouri.

Toluene. Purity (wt per cent toluene) 99.5 per cent minimum; impurities-heptane isomers 0.5 per cent maximum; maximum boiling range 1°C, including 110.6°C, specific gravity between 0.869 and 0.873 at 15.5°C; nitration grade; purchased from G.S. Robins Co., St. Louis, Missouri.

Polyisobutylene (PIB) L-80. Enjay MM Vistanex; grade L-80; lot B40828; code 230; molecular weight approximately 720,000, distribution unknown; produced by a low temperature Friedel-Craft reaction; catalyst-free with trace amounts of butylated hydroxytoluene and sodium stearate; color, slightly yellow; donated by Humble Oil and Refining Co., Baton Rouge, Louisiana.

Polyisobutylene (PIB) L-200. Enjay HM Vistanex; grade L-200; lot B31006; code 054; viscosity average molecular weight 4,000,000-4,700,000; distribution unknown; exact production method and catalyst content unknown

to author; color, white; donated by Humble Oil and Refining Co., Baton Rouge, Louisiana.

Polymethylmethacrylate (PMMA) G. Procured in the form of 1/4-inch plexiglas sheet with molecular weight approximately 1,500,000, distribution unknown; donated by Rohm and Haas Co., Philadelphia, Pennsylvania.

Polymethylmethacrylate (PMMA) V-100. Rohm and Haas Plexiglas V-100 molding powder; molecular weight approximately 110,000; donated by Rohm and Haas Co., Philadelphia, Pennsylvania.

Table 11 shows the solutions made from these materials and their properties.

Table 11

Solution Compositions and Properties

| Run No. | Solvent | Solute | Per Cent Solute by Weight | Fluid Temp. °C | Density g/cc | Viscosity cp |
|---|---|---|---|---|---|---|
| 1; 2; 15; 20 | toluene | none | | 30 | 0.856 | 0.518 |
| 3; 22 | cyclohexane | none | | 25 | 0.775 | 0.889 |
| 4 | cyclohexane | PIB L-80 | 0.05 | 25 | 0.775 | 0.998 |
| 6 | cyclohexane | PIB L-80 | 0.1 | 25 | 0.775 | 1.120 |
| 7; 8 | cyclohexane | PIB L-80 | 0.3 | 25 | 0.775 | 1.673 |
| 9 | cyclohexane | PIB L-80 | 1.0 | 25 | 0.775 | See below* |
| 10 | benzene | none | | 24 | 0.874 | 0.610 |
| 11 | benzene | PIB L-80 | 0.25 | 24 | 0.874 | 0.739 |
| 12 | benzene | PIB L-80 | 0.85 | 24 | 0.874 | 1.203 |
| 13 | toluene | PMMA-G | 0.25 | 30 | 0.856 | 0.689 |
| 14 | toluene | PMMA-G | 0.9 | 30 | 0.856 | 1.313 |
| 16 | toluene | PMMA V-100 | 0.95 | 30 | 0.856 | 0.664 |
| 17 | toluene | PIB L-200 | 0.05 | 30 | 0.856 | 0.611 |
| 18 | toluene | PIB L-200 | 0.1 | 30 | 0.856 | 0.658 |
| 19 | toluene | PIB L-200 | 0.42 | 30 | 0.856 | See below** |
| 21 | toluene | PMMA-G | 0.82 | 30 | 0.856 | 1.33 |
| 23 | cyclohexane | PIB L-200 | 0.38 | 25 | 0.775 | See below*** |

* 1.0 per cent PIB L-80 in cyclohexane was non-Newtonian. Its flow equation was:

$$D\Delta P/4L = 0.122\ (8V/D)^{0.8882} \text{ in dynes/cm}^2.$$

** 0.42 per cent PIB L-200 in toluene:

$$D\Delta P/4L = 0.024\ (8V/D)^{0.956} \text{ in dynes/cm}^2.$$

***0.38 per cent PIB L-200 in cyclohexane:

$$D\Delta P/4L = 0.083\ (8V/D)^{0.884} \text{ in dynes/cm}^2.$$

# APPENDIX VII

## NON-NEWTONIAN TECHNOLOGY

A short summary of non-Newtonian rheological relationships is included to supplement the discussion in the literature review of previous investigations of drag reduction, most of which used non-Newtonian polymer solutions. Any fluid is non-Newtonian if its behavior deviates from the constant viscosity laminar flow equation:

$$\tau = \mu\left(\frac{du}{dr}\right)$$

For laminar flow in circular ducts, this equation becomes:

$$(D\triangle P/4L) = \mu(8U/D)$$

The non-Newtonian deviations from these equations are of many different types, but the most widely used model to describe non-Newtonian behavior is the Ostwald-deWaele or power law equation:

$$\tau = K\left(\frac{du}{dr}\right)^{n}$$

Even more general is the equation of Rabinowitsch (75) and Mooney (64) for laminar flow through round tubes:

$$\tau_w = (D\triangle P/4L) = K'(8U/D)^{n'}$$

where $\tau_w$ is the shear stress at the wall, D the tube diameter, $\triangle P/L$ the pressure gradient, U the space average velocity, and $K'$ and $n'$ rheological parameters.

The Rabinowitsch and Mooney equation is a rigorous mathematical relation independent of any assumptions about fluid behavior and constancy of $K'$ or $n'$. The only assumptions in the derivation were no slip at the tube wall and purely viscous behavior. For the special

case of a power law fluid K and K' are simply related:

$$K' = ((3n' + 1)/4n')^{n'}K$$

$$\text{where} \quad n' = d(\log \tau_w)/d(\log 8U/D)$$

For a power law fluid, n' = n.

By assuming the same form as equation 16, a "power law" Reynolds number may be defined for power law fluids:

$$\text{let} \quad f = 16/Re^\circ = (D\triangle P/4L)/(\rho U^2/2gc)$$

By substituting the power law relation for $D\triangle P/4L = K((3n + 1)/4n)^n(8U/D)^n$, the following form of the Reynolds number is derived:

$$Re^\circ = 8D^nU^{2-n}\rho/K(6 + 2/n)^n$$

The Metzner and Reed (61) Reynolds number is a generalization of the power law Reynolds number using the Rabinowitsch and Mooney relation:

$$Re' = D^{n'}U^{2-n'}\rho/g_cK'8^{n'-1}$$

The relation between $u^+$ and the power law $y^+$ (equation 13) used by Wells (98) to correlate turbulent velocity profiles may be derived from the universal velocity profile (equation 8) as follows:

$$u^+ = u/u^* = A + B \ln(y\rho u^*/\mu_w)$$

where $\mu_w$ is the apparent wall viscosity. For a boundary layer thickness of $\delta$:

$$\tau_w = K(u_\delta/\delta)^n$$

$$\text{so} \quad \mu_w = \tau_w(\delta/u_\delta) = \tau_w^{(n-1)/n}K^{1/n}$$

Since $u^* = \sqrt{\tau_w/\rho}$, the velocity profile equation becomes:

$$u^+ = A + (B/n) \ln(y^n\rho(u^*)^{2-n}/K)$$

In Wells derivation, A included the terms $2/k - (1/k)\ln(4.6/k)$ and B was $1/k$, where k was the mixing length constant.

The derivation of the friction factor correlation (equation 22) used by Clapp (9) involved the integration of the power law universal velocity profile. From the relations above, it is evident that the generalized Reynolds number of Metzner and Reed could be used in place of the power law Reynolds number in Clapp's friction factor equation.

# ABBREVIATIONS AND NOMENCLATURE

| Symbol | Explanation |
|---|---|
| a | radial tube dimension |
| a' | constant used in Gill and Scher velocity profile equation |
| $a^+$ | dimensionless tube radius, $au^*/\nu$ |
| A | constant in universal velocity profile equation and in King's Law equation |
| b | constant in von Karman velocity profile equation |
| B | constant in King's Law equation |
| c | variable used in Gill and Scher velocity profile equation or exponent in King's Law equation |
| cc | cubic centimeters |
| cm | centimeters |
| cp | centipoise |
| d | variable used in Gill and Scher equation |
| dl | deciliter |
| D | tube diameter |
| exp | a power of e |
| E | anemometer bridge voltage |
| E' | fluctuating anemometer bridge voltage |
| $\langle E' \rangle$ | root-mean-square fluctuating bridge voltage |
| $E_x(k)$ | one-dimensional energy spectrum function |
| f | Fanning friction factor |
| fps | feet per second |
| ft | feet |
| $f(\delta)$ | axial space correlation function |
| $f_1$ | friction factor on extension of laminar line |

| Symbol | Explanation |
|---|---|
| $f_{pv}$ | friction factor for purely viscous fluid |
| $f_o^{II}, g_o^{II}$ | second derivative of correlation function at $\delta = 0$ |
| $F_x(k)$ | normalized one-dimensional energy spectrum |
| g | grams |
| $g_c$ | gravitational constant |
| gpm | gallons per minute |
| $g(\delta)$ | transverse space correlation function |
| G | correction function in Bogue's velocity profile equation and shear rigidity modulus |
| $h(\delta), k(\delta), q(\delta)$ | triple correlation functions (page 35) |
| i | anemometer probe current |
| k | mixing length constant or wave number or triple correlation |
| $k_k$ | Kolmogoroff characteristic wave number |
| K | constant in power law equation |
| K' | constant in Rabinowitsch equation |
| $\ell$ | Prandtl mixing length or liters |
| log | base ten logarithm |
| ln | natural logarithm |
| L | tube length or macroscale |
| Ly | transverse macroscale of turbulence |
| mm | millimeters |
| mps | meters per second |
| n | exponent in power law equation or an adjustable constant in Pai velocity profile equation or frequency in energy spectrum |
| n' | exponent in Rabinowitsch equation |
| Nu | Nusselt number |
| p' | fluctuating pressure |
| $\bar{p}$ | time average pressure |

| Symbol | Explanation |
|---|---|
| P | isotropic pressure |
| PIB | polyisobutylene |
| PMMA | polymethyl methacrylate |
| ppm | pounds per minute |
| $P_{ii}$ | deviatoric normal stress in i direction |
| q | turbulent kinetic energy |
| Q | flow rate |
| r | distance from tube center |
| rms | root-mean-square |
| R | anemometer probe resistance |
| $R_o$ | anemometer probe resistance at fluid temperature |
| Re | Reynolds number |
| Re' | generalized Reynolds number |
| $Re^o$ | power law Reynolds number |
| $Re_L$ | macroscale Reynolds number |
| $Re_\lambda$ | microscale Reynolds number |
| $R_{ij}$ | double correlation tensor |
| $R(\tau)$ | autocorrelation function |
| s | shear as dz'/dr |
| $s_g$ | recoverable or elastic shear |
| $s_\mu$ | non-recoverable or viscous shear |
| t | time |
| $T_{ijk}$ | triple correlation tensor |
| T(k) | spectral energy transfer function |
| $u_i$ | velocity in i direction |
| $\bar{u}$ | time average velocity in the axial direction |
| $\bar{u}_c$ | average velocity at tube center |

| Symbol | Explanation |
|---|---|
| $\bar{u}_{max}$ | maximum average velocity |
| $\bar{u}_{\delta}$ | average velocity at $\delta$ distance from wall |
| $u^*$ | friction velocity, $\sqrt{\tau_w/\rho}$ |
| $u^+$ | dimensionless velocity, $\bar{u}/u^*$ |
| $u'$ | fluctuating velocity in axial direction |
| $\bar{v}$ | time average radial velocity |
| $v'$ | fluctuating velocity in the radial or transverse direction |
| $\bar{w}$ | time average tangential veloctiy |
| $w'$ | fluctuating tangential velocity |
| $<u'>,<v'>,<w'>$ | rms fluctuating velocities |
| $W$ | rate of turbulent energy dissipation |
| $W_s$ | solvent energy dissipation rate |
| $y$ | distance from tube wall or coordinate transverse to flow direction |
| $y^+$ | dimensionless distance from tube wall, $y\ u^*/\nu$ |
| $z$ | distance in axial direction |
| $z'$ | deformation in z direction |
| $\alpha$ | constant in Pao energy transfer function |
| $\beta$ | ratio of Eulerian and Lagrangian length scales |
| $\delta$ | laminar boundary layer thickness or space correlation distance |
| $\Delta$ | increment operator |
| $\gamma$ | exponent in Shaver friction factor correlation |
| $\theta$ | tangential angle |
| $\lambda_f$ or $\lambda$ | axial microscale |
| $\lambda_g$ | transverse microscale |
| $\mu$ | viscosity |
| $\mu_o$ | zero shear rate viscosity |

| Symbol | Explanation |
|---|---|
| $\mu_s$ | solvent viscosity |
| $\mu_w$ | apparent wall viscosity |
| $\nu$ | kinematic viscosity |
| $\rho$ | fluid density |
| $\rho'$ | fluctuating density |
| $\bar{\rho}$ | time average density |
| $\tau$ | autocorrelation delay time or shear stress |
| $\tau_w$ | wall shear stress |
| $\tau_{ij}$ | shear stress on the i surface in the j direction |
| $\tau_{1/2}$ | wall shear stress where $\mu = \mu_o/2$ |
| $\phi$ | variable in Gill and Scher velocity profile equation |
| $\omega$ | frequency in radians/second |

## ACKNOWLEDGEMENTS

The author wishes to thank Dr. Jaques L. Zakin, who conceived the investigation of turbulence in polymer solutions using hot-film anemometry, for his guidance, help, and inspiration during this investigation.

He is grateful for the financial support of the National Science Foundation.

Professor A. V. Kilpatrick and Shop Instructor L. N. Anderson of the Mechanical Engineering Department are thanked for their help and advice during the construction of the apparatus.

The other students involved in the experimental work are thanked for their cooperation and assistance. Dr. H. C. Hershey, who carried the burden of design and construction of the pipe flow unit and made a comprehensive study of the polymer-solvent properties affecting drag reduction, was a partner in this project and contributed his special abilities in many areas of this investigation. Mr. J. M. Rodriguez spent many hours helping the author obtain hot-film anemometry data, friction factor data, velocity profiles, viscometry and normal stress data. Miss L. Y. Chou made the viscosity and intrinsic viscosity measurements using the Ubbelohde viscometer. The normal stress apparatus was constructed by Mr. C. D. Green, and he obtained some of the data used in this thesis.

The financial support for the experimental work involved was contributed by the Petroleum Research Fund, administered by the American Chemical Society; National Science Foundation; Socony Mobil Company; and the National Aeronautics and Space Administration. Materials and

equipment were contributed by the Humble Oil and Refining Company, Dow Chemical Company, and Rohm and Haas Company.

The University of Missouri at Rolla provided an explosion-proof laboratory equipped with utilities for this investigation.

# VITA

Gary Kent Patterson, son of Efton William and Freda Patterson, was born on December 10, 1939, in Springfield, Missouri.

He attended elementary schools in Carthage, Ozark, Doolittle, and Rolla, Missouri. He graduated from Rolla High School in June, 1956. He received the Bachelor of Science in Chemical Engineering from the University of Missouri School of Mines and Metallurgy in June, 1960, and the Master of Science in Engineering from the University of Michigan in June, 1961.

He was employed the summer of 1959 by the Procter and Gamble Manufacturing Company as a Trainee; the summer of 1960 by the Columbia-Southern Chemical Company as a Development Engineer; and from October, 1961, to August, 1963, by the Esso Research Laboratories, Humble Oil and Refining Company, as a Research Engineer.

On June 3, 1960, he married Miss Barbara Ruth Lay of Rolla, Missouri. A son was born on August 7, 1965.

In September, 1963, he entered the Graduate School of the University of Missouri at Rolla, doing graduate work to the present time as a National Science Foundation Fellow. He was a half-time Assistant Instructor of Physical Chemistry during the academic year 1964-65.

# BIBLIOGRAPHY


1. Astarita, G., I/EC Fund., 4, 354, August 1965.

1a. Baker, W. O., and Heiss, T. H., Bell Telephone Tech. J. , 31, 306 (1952).

2. Baldwin, L. V., and Walsh, T. J., A.I.Ch.E. J., 7, 53 (1961).

3. Betchov, R., J. of Fluid Mech., 3, 205 (1958).

4. Bogue, D. C., Ph.D. Thesis, University of Delaware, Newark, 1961.

5. Brodnyan, J. G., Gaskins, F. H., and Philippoff, W., Trans. Soc. Rheol., 1, 109 (1957).

6. Bull, M. K., A. A. S. U. Report 234, University of Southampton, Hamshire, England (1963).

7. Bunch, D., Ph.D. Thesis, University of Missouri at Rolla, 1964.

8. Chang, I. C., M.S. Thesis, University of Missouri at Rolla, 1965.

9. Clapp, R. M., Intern. Devel. in Heat Transfer, III, A.S.M.E., New York, 652 (1961).

10. Corcoran, W. H., Opfell, J. B. and Sage, B. H., Momentum Transfer in Fluids, 83, Acad. Press, New York, (1956).

10a. Corino, E. R., and Brodkey, R. S., Ohio State University Res. Fou Report, Project 1191, Report 3, N.S.F. Grant G-14807, March 1965.

11. Corrsin, S., and Uberoi, M. S., N.A.C.A. T.N. 1865 (1949).

12. Deissler, R. G., Trans. A.S.M.E., 73, 101 (1957).

13. Dexter, F. D., Miller, J. C., Philippoff, W., Trans. Soc. Rheol., 5, 193 (1961).

14. Dodge, D. W., Ph.D. Thesis, University of Delaware, Newark, 1957.

15. Eagleson, P. S., Huval, D. J., and Perkins, F. E., M.I.T. Hydro. Lab. Tech. Report No. 46 (1961).

16. Eagleson, P. S., and Perkins, F. E., I.A.H.R. 9th Convention, Belgrade (1961).

17. Eissenberg, D. M., A.I.Ch.E. J., 10, 403 (1964).

18. Ernst, W. D., Ling-Tempco-Vought Research Center Report No. 0-7100/5R-14 (1965).

19. Fabula, A. G., 4th Intern. Congr. on Rheol., Brown University, Prov., R. I., August 1963.

20. Favre, A., Gaviglio, J., Dumas, R., Translation in N.A.C.A. T.M. 1370 (1955).

21. Flory, P. J , Principles of Polymer Chemistry, Cornell University Press, Ithaca, N. Y. (1953).

22. Gardner, S., Report submitted to Office of Naval Research by T.R.G., Inc., on Contract Nonr-3208(00) (1963).

23. Gibson, A. H , Phil. Mag., 15, 637 (1933).

24. Gibson, M. M., J. of Fluid Mech., 15, 161 (1963).

25. Gibson, C. H. and Schwarz, W. H., J. Fluid Mech., 16, 365 (1963).

26. Gill, W. N., and Scher, M., A.I.Ch.E. J. 7, 61 (1961).

27. Goldstein, S., Proc. Roy. Soc., A159, 473 (1937).

28. Goldstein, S., Modern Development in Fluid Dynamics, 2, 355, Oxford University Press, New York, (1938).

29. Grant, H. P., and Kronauer, R. E., Review Paper in Symp. on Measurement in Unsteady Flow, A.S.M.E. Hyd. Div. Conf., Worcester, Mass., May 1962.

30. Grant, H. L., Stewart, R. W. Moilliet, A., J. of Fluid Mech., 12, 241 (1962).

31. Green, C. D., M.S. Thesis, University of Missouri at Rolla, 1965.

32. Heisenberg, W., Z. Physik, 124, 628 (1948).

33. Hershey, H. C., Ph.D. Thesis, University of Missouri at Rolla, 1965.

34. Hinze, J. O., Turbulence, McGraw-Hill, New York (1959).

35. Houghton, W. T., M.S. Thesis, University of Delaware, Newark, 1961.

36. Hoyt, J. W., and Fabula, A. G., ONR-Skipsmodelltanken, Fifth Sym. on Naval Hydrodynamics, Bergen, Norway, September 1964.

37. Karman, T. von, N.A.C.A. T.M. 611 (1931).

38. Karman, T. von, and Howarth, L., Proc. of Royal Society, A164, 192 (1938).

39. Kim, W. J , and Manning, F. S., A.I.Ch.E. J., 10, 747 (1964).

40. Knudsen, J. G., and Katz, D. L., Fluid Dynamics and Heat Transfer, 156, McGraw-Hill, New York (1958).

41. ibid., 159.

42. ibid., 172.

43. Kolmogoroff, A. N., Comptes rendus (Doklady) de 1' Academiedes sciences de 1' U. R. S. S., 30, 301 (1941) as translated in Friedlander, S. K., and Topper, L., Turbulence, Interscience, London (1961).

44. Kotaka, T., Kurata, M., and Tamura, M., J. Appl. Phys., 30, 1705 (1959).

45. Kovasznay, L. S. G., J. Aeronaut. Sci., 15, 745 (1948).

46. Laufer, J., N.A.C.A. T.R. 1053 (1951).

47. Laufer, J., N.A.C.A. T.R. 1174 (1953).

48. Lawrence, J. C., I.S.A. J., December 1953.

49. Lawrence, J. C., and Landes, L. G., N.A.C.A. T.N. 2843 (1952).

50. Lee, J., and Brodkey, R. S., A.I.Ch.E. J., 10, 187 (1964).

51. Levick, V. G., Physico-Chemical Hydrodynamics, Prentice-Hall, Englewood Cliffs, N. J. (1962).

52. Lin, C. C., Statistical Theories of Turbulence, Princeton University Press, 1961.

53. Lin, C. C., Quart. of Applied Math., 10, 295 (1963).

54. Lindgren, E. R., Tech. Report No. 1, Bureau of Ships Gen. Hydro. Res. Prog. S-R009 01 01, Res. Contr. Nonr 2595(05), 1965.

55. Lindgren, E. R., Tech. Report No. 2, Bureau of Ships Gen. Hydro. Res. Prog. S-R009 01 01, Res. Contr. Nonr 2595(05), 1965.

56. Ling, S. C., Ph.D. Thesis, Iowa State University, Ames, 1955.

57. Ling, S. C., Trans. A.S.M.E., D, J. Basic Engr., 629, September 1960.

58. Martin, G. Q., and Johanson, L. N., A.I.Ch.E. J., 11, 30 (1965).

59. Meter, D. M., Ph.D. Thesis, University of Wisconsin, Madison, 1963.

60. Meter, D. M., A.I.Ch.E. J., 10, 879 (1964).

61. Metzner, A. B., and Reed, J. C., A.I.Ch.E. J., 1, 434 (1955).

62. Metzner, A. B., Houghton, W. T., Sailor, R. A., and White, J. L., Trans. Soc. Rheol., 5, 133 (1961).

63. Mickelson, W. R., N.A.C.A. T.N. 3570 (1955).

64. Mooney, M., J. Rheol., 2, 210 (1931).

65. Nikuradse, J., N.A.C.A. T.M. 1292 (1950).

66. Obukhoff, A. M , Review by Lin, C. C., and Reid, W. H., in Handbuch der Physik, VIII/2, 471 (1963).

67. Ossofsky, E., Rev. Sci. Inst., 19, 881 (1948).

68. Pai, S. J , J. Appl. Mech., 20, 109 (1953).

69. Pao, Y. H., Boeing Flight Sciences Lab. Report No. 90, August 1964.

70. Park, M. G., M. Ch. E. Thesis, University of Delaware, Newark, 1964.

71. Philippoff, W., Trans. Soc. Rheol., I, 95 (1957).

71a. Philippoff, W., Trans. Soc. Rheol., V, 163 (1961).

72. Philippoff, W., Brodnyan, J. G., and Gaskins, F. H., J. Appl. Phys., 28, 1118 (1957).

73. Prandtl, L., N.A.C.A. T.M. 720 (1933).

74. Prandtl, L., N.A.C.A. T.M. 1231 (1949).

75. Rabinowitsch, B. Z., Z. Physik. Chem., A145, 1 (1929).

75a. Reid, W. H., and Lin, C. C., Handbuch der Physic, VIII/2, 471 (1963).

76. Reynolds, O., Trans. Roy. Soc. (London), 174A, 935 (1883).

77. Ripken, J. F., and Pilch, M., Tech. Paper No. 42, Series B, University of Minnesota, St. Anthony Falls Hyd. Lab., Office of Naval Res. Contract Nonr 710 (49), April 1963.

78. Rodriguez, J. M., M.S. Thesis, University of Missouri at Rolla, 1966.

79. Rosler, R. S., and Bankoff, S. G., A.I.Ch.E. J., 9, 672 (1963).

80. Ross, D., N.O.R.D. Report No. 7958246, Penn. St. University, College Park (1952).

80a. Rouse, P. E., and Sittel, K., J. Applied Physics, 24, 690 (1953).

81. Sandborn, V. A., N.A.C.A. T.N. 3266 (1955).

82. Savins, J. G., J. of the Inst. of Pet., 47, 329 (1961).

83. Savins, G., Presented at A.I.Ch.E. National Meeting, Houston, Texas, December 1963, and Soc. Pet. Eng. J., 4, 203 (1964)

84. Savins, J. G., A.I.Ch.E. J., 11, 673 (1965).

85. Shaver, R. G., Sc.D. Thesis, M.I.T., Cambridge, Mass., 1957.

86. Shertzer, C. R., and Metzner, A. B., Conf. on Advances in Polymer Science and Tech., May 1963.

87. Shertzer, C. R., M. Ch. E. Thesis, University of Delaware, Newark, 1964.

88. Stanton, T. E. and Pannell, J. R., Trans. Roy. Soc., London, 214A, 199 (1914).

89. Stewart, R. W., and Townsend, A. A., Phil. Trans. Royal Soc., London, A243, 359 (1951).

90. Tanenbaum, B. S., Physics of Fluids, 3, 529 (1960).

91. Tao, F., Ph.D. Thesis, University of Missouri at Rolla, 1964.

92. Taylor, G. I., Proc. Royal Soc., A157, 421 (1935).

93. Taylor, G. I., Proc. Royal Soc., A159, 496 (1937).

94. Taylor, G. I., Proc. Royal Soc., A164, 476 (1938).

95. Toms, B. A., Proceedings Intern. Rheol. Congr., Holland (1948), North Holland Publishing Co., Amsterdam (1949).

96. Uberoi, M. S., and Corrsin, S., N.A.C.A. T.R. 1142 (1953).

97. Watson, T. B., M.S. Thesis, University of Missouri at Rolla, 1965.

98. Wells, C. S., Jr., "On the Turbulent Shear Flow of an Elastico-Viscous Fluid", Preprint of paper presented to A.I.A.A. Aerospace Sciences Meeting, New York, January 1964.

99. Weske, J. R., N.A.C.A. T.N. 881 (1943).

100. Willmarth, W. W., and Wooldridge, C. E., J. Fluid Mech., 14, 187 (1962).

101. Willmarth, W. W., and Wooldridge, C. E., AGARD Rep., 456 (1963).

102. Zimm, B. H., J. Chem. Phys., 24, 269 (1956).